THESIS ON NATURAL AND EXACT SCIENCES B157

Studies of CD44 Hyaluronan Binding Domain as Novel Angiogenesis Inhibitor

TAAVI PÄLL

TUT
PRESS

TALLINN UNIVERSITY OF TECHNOLOGY
Faculty of Science
Department of Gene Technology

Dissertation was accepted for the defence of the degree of Doctor of Philosophy in Gene Technology on May 09, 2013.

Supervisor: **Prof. Priit Kogerman**, PhD
Department of Gene Technology,
Tallinn University of Technology, Tallinn, Estonia

Advisor: **Assistant prof. Andres Valkna**, PhD
Department of Gene Technology,
Tallinn University of Technology, Tallinn, Estonia

Opponents: **Prof. Lena Claesson-Welsh**, PhD, Department of Immunology, Genetics and Pathology, Uppsala University, Sweden
Dr. **Alar Aints**, MD/PhD, Department of Hematology and Oncology, University of Tartu, Estonia

Defence of the thesis: August 14, 2013

Declaration:
Hereby I declare that this doctoral thesis, my original investigation and achievement, submitted for the doctoral degree at Tallinn University of Technology has not been submitted for any academic degree.

/Taavi Päll/

European Union
European Social Fund
Investing in your future

ISSN 1406-4723
ISBN 978-9949-23-513-1 (publication)
ISBN 978-9949-23-514-8 (PDF)

LOODUS- JA TÄPPISTEADUSED B157

CD44 hüaluroonhapet siduv domään kui uudne angiogeneesi inhibiitor

TAAVI PÄLL

TTÜ KIRJASTUS

CONTENTS

INTRODUCTION

Solid tumors depend in their expansion on angiogenesis to meet metabolic needs and to invade surrounding tissues. Angiogenesis is the process of blood vessel growth from existing vasculature. In tissue microenvironment, angiogenesis is controlled by the balance of pro- and antiangiogenic factors. To induce angiogenesis in nearby blood vessels, tumor cells start to secrete various angiogenic factors that stimulate endothelial cells to proliferate. Proangiogenic molecules could be growth factors or proteinases that degrade extracellular matrix, controlling endothelial quiescence. However, angiogenesis process also releases antiangiogenic factors to tip the balance back. Importantly, such antiangiogenic factors could be expressed by tumor cells themselves because of the selective advantage in other stages of tumor development. The idea that HA receptor CD44 might inhibit angiogenesis was based on the findings by P. Kogerman et al. (Kogerman et al., 1997a). They found that mouse fibrosarcoma cells overexpressing human CD44 showed prolonged latency for subcutaneous growth in mice compared to parental cells. Later analysis of large tumors showed that introduced exogenous CD44 expression was downregulated. These findings lead to the hypothesis that tumor angiogenesis might be affected, and fitted with the concept that solid tumors are dependent on angiogenesis to expand over 1 millimeter size. Given that CD44 overexpression on the tumor cell surface can inhibit tumor growth, we hypothesized that a purified recombinant CD44 HABD might as well serve as angiogenesis inhibitor and may thereby block tumor growth.

ORIGINAL PUBLICATIONS

I **Päll T.**, Gad A., Kasak L., Drews M., Strömblad S., Kogerman P. (2004) Recombinant CD44-HABD is a novel and potent direct angiogenesis inhibitor enforcing endothelial cell-specific growth inhibition independently of hyaluronic acid binding.
Oncogene 23: 7874–7881.

II **Päll T.**, Pink A., Kasak L., Turkina M., Anderson W., Valkna A., Kogerman P. (2011) Soluble CD44 Interacts with Intermediate Filament Protein Vimentin on Endothelial Cell Surface.
PLoS ONE 6(12): e29305. doi:10.1371/journal.pone.0029305.

MANUSCIPT Pink A., Kallastu A., **Päll T.**, Turkina M., Školnaja M., Kogerman P., Valkna A. (2013) Purification, characterization and plasma half-life of PEGylated soluble recombinant non-HA-binding CD44.

PATENT Kogerman P., **Päll T.**, Strömblad S. (2010) Drug for treating states related to the inhibition of angiogenesis and/or endothelial cell proliferation. US Patent No: 8,192,744.

ABBREVIATIONS

aa, amino acid
bFGF, basic fibroblast growth factor
CAM, chorioallantoic membrane
CD44s, standard CD44
CD44v, variant CD44 isoform
CRC, colorectal cancer
EC, endothelial cells
ECM, extracellular matrix
EGFR, epidermal growth factor receptor
ELISA, enzyme-linked immuno sorbent assay
FACS, fluorescence activated cell sorter
FN, fibronectin
GF, gel filtration
GSK-3β, glycogen synthase kinase 3β
GST, glutathione S-transferase
HA, hyaluronan, hyaluronic acid
HABD, hyaluronan binding domain
HIF1α, hypoxia-inducible factor 1α
HUVEC, human umbilical vein endothelial cells
IEC, ion exchange chromatography
IF, intermediate filaments
ip, intraperitoneal
KO, knockout
LPS, lipopolysaccharide
MALDI-TOF MS, matrix-assisted laser desorption ionization time of flight mass spectrometry
MLEC, mouse lung endothelial cells
MMP, matrix metalloproteinase
mTOR, mammalian target of rapamycin
PAI-1, plasminogen activator inhibitor 1
PI3K, phosphatidylinositol-3 kinase
PFS, progression free survival
PKC, protein kinase C
PLGF, placenta growth factor

ROS, reactive oxygen species
RTKI, receptor tyrosine kinase inhibitor
sc, subcutaneous
sCD44, soluble CD44
TGF-α, transforming growth factor α
TGF-β, transforming growth factor β
ULF, unit-length filament
VEGF, vascular endothelial growth factor
VEGFR, vascular endothelial growth factor receptor
wt, wild type

REVIEW OF THE LITERATURE

1 Angiogenesis introduction

The vascular system is essential for supplying tissues with oxygen and nutrients, and disposing of metabolic waste products. Blood and lymphatic vessels are necessary for body's immune surveillance. Vascular lumen is ensheathed by endothelial cell (EC) layer. Depending on the vessel type, ECs can be covered by mural cells – either pericytes or smooth muscle cells. Endothelial and mural cells are surrounded by common basement membrane. In an adult organism, the growth of new blood vessels is tightly controlled by a balance between angiogenic and angiostatic factors, and physiologically, most of the time ECs reside in quiescence. Maintenance of endothelial quiescence and survival is controlled by mural cells. The new blood vessels can grow either by vasculogenesis or angiogenesis. Vasculogenesis takes place during embryonic development, whereas further expansion and reorganization of embryonic vasculature occurs by angiogenesis (Figure 1). Angiogenesis is the process of blood vessel growth by sprouting from preexisting vessels.

Angiogenic signal leading to blood vessel destabilization and subsequent sprouting can be elicited by tissue hypoxia, or factors released by tumor or inflammatory cells. Key regulator of blood vessel growth and maintenance is VEGF-A which signals through its tyrosine kinase receptor VEGFR2 (Carmeliet and Jain, 2011). The various steps of angiogenesis include increase in vessel permeability and dissolution of basement membrane by activated ECs, deposition of provisional extracellular matrix (ECM), and subsequent tissue invasion involving EC migration. Cell adhesion to the ECM proteins is mediated by integrin receptors. Integrins direct the ECM signals to the dynamic multiprotein complexes – focal adhesions, that are linked to the actin cytoskeleton (Geiger et al., 2009). In addition to actin microfilaments, focal adhesion dynamics involves the intermediate filament (IF) and microtubule cytoskeletons (Avraamides et al., 2008, Burgstaller et al., 2010).

1.1 Angiogenesis in pathological conditions and antiangiogenesis paradigm in cancer treatment

Under physiological conditions, new blood vessels grow during tissue regeneration, hair growth, exercise, and in the endometrium. Angiogenesis is also involved in development of various pathological conditions, including tumor growth, metastasis,

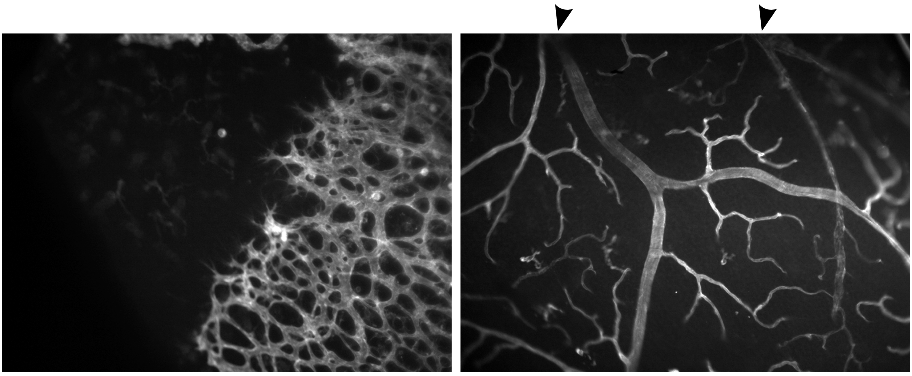

Figure 1 Retinal vascular development. Retinas were prepared from 3-day old pups (*left*) or from 6-week old adult mice (*right*). Blood vessels were stained using *Griffonia simplicifolia* isolectin B4 conjugated Alexa Fluor 488 fluorochrome. *Left*, growing blood vessels of primary vascular plexus, a network of homogeneously sized primitive blood vessels. Note the endothelial tip cells at the front of growing vasculature. *Right*, pruned mature retinal vasculature. Arrowheads indicate putative arterial and venous compartments – arterioles are thin and venules are broader. Retina preparation and staining was performed by Marianna Školnaja, microscopy and image preparation by Taavi Päll.

diabetic retinopathy, wet age-related macular degeneration, rheumatoid arthritis and psoriasis. Excessive angiogenesis occurs when diseased cells produce abnormal amounts of angiogenic growth factors, outbalancing the effects of natural angiogenesis inhibitors. New blood vessels nourish diseased tissues, subvert normal tissues, and in the case of cancer, allow cancer cells to metastasize.

The process of cancer metastasis is dependent on angiogenesis in its two steps – first, migration from primary tumor and second, colonization. In the absence of angiogenesis, micrometastases appear unable to grow over millimeter size and remain dormant (Holmgren et al., 1995, O'Reilly et al., 1996). Cancer cells begin to promote angiogenesis early in tumorigenesis – this tumor "angiogenic switch" is turned on by production of angiogenic factors like VEGF, bFGF and TGF-α (Bergers and Benjamin, 2003). The angiogenic switch involves also downregulation of endogenous angiogenesis suppressor proteins, such as thrombospondin-1. Characteristically, tumor blood vessels are morphologically immature, tortuous, leaky, contain "blind" ends and are not properly covered by pericytes.

1.2 Antiangiogenesis drugs

Angiogenesis inhibitors, targeted to block new blood vessel development, are used to treat pathological conditions associated with excessive blood vessel growth. Currently, angiogenesis inhibitors that are already available or in the late stage of clinical development fall under three main classes: a) monoclonal antibodies, b) small molecule inhibitors of growth factor receptors and c) inhibitors of mTOR.

Antibodies directed against angiogenic growth factors or their receptors block growth factor–receptor interaction and thereby cause blockage of proangiogenic signaling. Examples of such inhibitors are *bevacizumab* (Avastin, Genentech) (Hurwitz et al., 2004, Yang et al., 2003) and *cetuximab* (Erbitux; ImClone, Eli Lilly)(Perrotte et al., 1999, Pueyo et al., 2010). Bevacizumab is VEGF neutralizing antibody and cetuximab targets and inhibits EGFR which is receptor for angiogenic growth factor TGF-α.

Small molecule inhibitors of receptor tyrosine kinases block angiogenic growth factor receptor activation. Examples of such inhibitors are *erlotinib* (Tarceva; Genentech) (Pore et al., 2006, Tabernero, 2007), *sorafenib* (Nexavar; Bayer, Onyx) (Escudier, 2007) and *sunitinib* (Sutent; Pfizer) (Ebos et al., 2009, Motzer et al., 2007). Novel small molecule angiogenesis inhibitor, approved for medullary thyroid carcinoma treatment, is *cabozantinib*, that targets c-MET receptor tyrosine kinase and VEGFR2 (Cometriq, Exelixis).

MTOR inhibitors, such as *everolimus* (Afinitor; Novartis) (Mabuchi et al., 2007) and *temsirolimus* (Torisel; Wyeth) (Del Bufalo et al., 2006, Frost et al., 2004) target directly or indirectly, tumor-activated, EC metabolic signaling and survival pathways. PI3K-Akt pathway activated mTOR regulates protein synthesis by phosphorylating its downstream effectors ribosomal p70 S6 kinase and eukaryote initiation factor 4E binding protein 1.

Examples of angiogenesis inhibitors in other diseases, like wet age-related macular degeneration are *ranibizumab* (Rosenfeld et al., 2006) (Lucentis; Genentech), a Fab fragment of bevacizumab, and *pegaptanib* (Gragoudas et al., 2004) (Macugen; OSI Eyetech, Pfizer), a pegylated oligonucleotide (aptamer) which binds and blocks VEGF-165.

In oncology most antiangiogenic drugs are concentrated on a few targets, mainly blocking VEGF/VEGFR signaling. Remarkably, approximately 70 VEGF-pathway targeting projects are currently in clinical development (Booth, 2012). To successfully reach market, these drug candidates should be superior to eg. bevacizumab or sorafenib in many parameters, including efficacy, side effects or cost. Considering that compounds in development have already active comparator drug in class, higher bar for approval and other drugs in use already ahead, this could be difficult to achieve. Such overcrowding also may limit recources available to less studied novel targets, and in the longer perspective suggests that resources are wasted by pharmaceutical industry.

On the flip side, this concentration indicates also the urgent need for new drugs against novel targets advanced into preclinical development (Booth, 2012). These new targets should preferably have well characterized biology to mitigate investment risks for biotech venture capital to move forward into clinical development with novel biology.

1.3 Mechanisms of tumor resistance to antiangiogenic (anti-VEGF) therapy

Antiangiogenesis therapy with bevacizumab provides significant benefit with at least increased PFS for metastatic colorectal cancer (CRC) patients (Hurwitz et al., 2004), advanced nonsquamous non-small cell lung cancer (Johnson et al., 2004), metastatic renal cancer (Yang et al., 2003), and recurrent glioblastoma (Friedman et al., 2009, Vredenburgh et al., 2007). However, in November-2011, US Food and Drug Administration revoked its initial accelerated bevacizumab approval for treating metastatic HER2-negative breast cancer, as follow-up studies did not confirm sufficiently significant clinical benefit (FDA, 2011, Miller et al., 2005, Schneider et al., 2008).

When used in combination treatment, bevacizumab significantly increases the efficacy (in the sense of response rate) of chemotherapy, which could be attributed to "normalization" of tumor vasculature and resulting improved drug delivery into tumor tissue (Dings et al., 2007). Suggesting that tumor vascularisation is one factor that mediates cancer drug resistance. Likewise, in antiangiogenesis therapy specifically, drug resistance is a problem – while some patients have noticeable responses and live longer, the overall response rate in patients is still roughly 30%, suggesting that the whole patient population might have limited clinical benefit (Sennino and McDonald, 2012).

There are several mechanisms of intrinsic or acquired resistance to antiangiogenic therapies (Loges et al., 2010). Tumor cells can *amplify proangiogenic gene loci* in their genomes. VEGF-A gene locus amplification associating with poor prognosis has reported in 3-6% CRCs (Vlajnic et al., 2011) and in ∼64%(!) osteosarcomas (Yang et al., 2011). In osteosarcomas, VEGF-A amplification correlated with increased microvascular density in tumor samples and reduced disease free survival of patients (Yang et al., 2011). Breast cancer ECOG2100 trial concluded that VEGF-A amplification was associated with poor outcomes – it was found that paclitaxel with bevacizumab combination treatment increased PFS compared to paclitaxel alone only in patients without VEGF-A gene amplification (Schneider et al., 2013). This suggest that such proangiogenic growth factor gene amplification clearly has negative contribution to the efficacy of anti-angiogenesis therapy.

Tumors escape from antiangiogenesis therapies can arise by *preexistence or activation of alternative angiogenic pathways*. It was found, that in mouse tumor models, anti-VEGFR2 monotherapy when used alone, induces compensatory proangiogenic gene expression. Whereas, simultaneous treatment using anti-PLGF Ab and anti-VEGFR2 enhances therapeutic effect and does not induce angiogenesis rescue as anti-VEGFR2 therapy alone (Fischer et al., 2007). Anti-PLGF treatment in this setting affects tumor microenvironment by suppressing proangiogenic macrophage recruitment. Other growth factors or angiogenic signaling pathways involved in resistance to anti-VEGF therapies are bFGF (Casanovas et al., 2005), PDGF (Pietras et al., 2008), angiopoietin-Tie2 (Xu et al., 2009), DLL4-Notch (Li et al., 2011, 2007) and EphB4-EphrinB2 (Li et al., 2011). In glioblastoma model and patients the resistance to bevacizumab treatment is mediated by the upregulation of receptor tyrosine kinase c-MET protein and activity which is suppressed by VEGF-VEGFR2 complex (Jahangiri et al., 2013, Lu et al., 2012). This mechanism is different from hypoxia-mediated resistance to bevacizumab treatment in glioblastoma (Keunen et al., 2011).

Mobilization of macrophages and vascular progenitor cells from the bone marrow via SDF-1–CXCR4 signaling is another mechanism that contributes to restoration of tumor proangiogenic microenvironment. Such signaling is elicited by mesenchymal stem cells or cancer-associated fibroblasts (Xu et al., 2009). Alternatively, tumor recruitment of proangiogenic blood-borne $Gr1^{+}CD11b^{+}$ myeloid cells can be mediated by G-CSF, VEGF-A or Bv8 (Christoffersson et al., 2012, Hiratsuka et al., 2011, Shojaei et al., 2009, 2007). Invading $Gr1^{+}CD11b^{+}$ cells produce

MMP-9 that promotes tumor angiogenesis (Christoffersson et al., 2012, Yang et al., 2004).

At some stage, tumor cells can also do without induction of angiogenesis, just by growing along preexisting blood vessels, a process called *vessel co-option*, which can take place in well vascularised tissues like lungs and brain (Leenders et al., 2004, Pezzella et al., 1997). It is found that mature blood vessels are more resistant to anti-VEGF therapy, and *increased pericyte coverage* of tumor associated blood vessels makes them less susceptible to anti-VEGF treatment (Helfrich et al., 2010). Pericytes supply ECs with VEGF which might be unaccessible to its targeting drug, also ECs in mature vessels express very low levels of VEGFR2, which makes them insensitive to specific RTKI. Typically, tumors contain morphologically different types of blood vessels. In this morphological space, low VEGFR2-expressing later-stage vessels define anti-VEGF refractory population (Sitohy et al., 2011).

Angiogenesis inhibition and collapse of tumor vascular network creates a hypoxic milieu in tumor microenvironment, which tumor cells might overcome by acquisition of *enhanced capability to invade* – bevacizumab treatment induced hypoxia activates HIF1α-dependent transcription, leading to invasive phenotype in glioblastoma cells (Keunen et al., 2011).

2 CD44 and its physiological functions

CD44 glycoprotein is a type I membrane glycoprotein. It functions as a receptor for hyaluronan (HA), a glucosaminoglycan abundantly present in ECM of embryonic and adult tissues. HA-binding function of CD44 is mediated via its N-terminal domain which contains a single Link module (Banerji et al., 2007, Teriete et al., 2004).

CD44 is expressed on many cell types, including lymphocytes and ECs, and has multiple alternatively spliced isoforms that contain variant exons in its membrane proximal region. CD44 molecules with combinations from ten (designated v1-v10) alternatively spliced variant exons in its extracellular domain are called variant CD44 (CD44v) and CD44 molecule without any of the variant exons is called the standard CD44 (CD44s). In physiology, cell surface CD44 functions as a lymphocyte homing receptor (Bonder et al., 2006, Hollingsworth et al., 2007, Khan et al., 2004, McDonald et al., 2008, Rouschop et al., 2005), mediates cell adhesion to HA, cell migration and HA metabolism. In addition to HA-mediated interactions, N-glycosylation of CD44 provides binding sites for E-selectin and contributes to homing function of hematopoietic progenitor cells into bone marrow sinusoids (Avigdor et al., 2004, Dimitroff et al., 2001), and neutrophils homing into inflammatory site (Katayama et al., 2005). Notably, these CD44-mediated processes are triggered by SDF-1 or G-CSF (Avigdor et al., 2004, Katayama et al., 2005), the same cytokines which tumors use to recruit proangiogenic myeloid cells. Further, CD44 mediates HA retention on the EC surface and this function is in large part regulated by cytokine activation. HA binding can be tuned by N-glycosylation – de-glycosylation of CD44, which is in turn regulated by cytokines (Ariel et al., 2000, English et al., 1998). TNF-α induced HA-binding ability of CD44 and by this determined EC surface HA level. Interactions between CD44 and HA are sufficient to support rolling adhesions on ECs under physiological laminar flow conditions (Nandi et al., 2000).

In normal physiology, *Cd44* KO mice have no obvious developmental phenotypes, but display changes in inflammatory reactions (Protin et al., 1999, Schmits et al., 1997). *Cd44* KO in mouse models of ischemia, atherosclerosis and arthritis confirm CD44 functions in leukocyte recruitment (Cuff et al., 2001, Hutás et al., 2008, Rouschop et al., 2005).

CD44 contributes to keratinocyte functions and normal epidermal physiology. CD44 knockdown by antisense expression in mouse skin causes abnormal HA accumulation with changes in skin elasticity, reduces keratinocyte proliferation in response to phorbol ester stimulation, and slows down wound healing (Kaya et al., 1997). These defects could be attributed to HA accumulation, as hyaluronidase treatment seemed to rescue skin elasticity and high HA concentrations suppressed keratinocyte proliferation in culture (Kaya et al., 1997). Likewise, complete *Cd44* KOs show several skin-related defects, such as decrease in epidermal differentiation and epidermal thickness, reduced number of proliferating cells in the skin and delayed epidermal barrier recovery after its disruption (Bourguignon et al., 2006). However, in contrast to skin-specific CD44 antisense, in complete *Cd44* KOs skin HA content appears reduced and interestingly, also skin cholesterol level (Bourguignon et al., 2006). Nevertheless, a further analysis of *Cd44* KOs revealed a temporarily reduced expression at E17.5 of tight junction proteins Claudin-1, Claudin-4, ZO-1 and polarity complex protein Par3, which together contributed to defective epidermal barrier function at this stage (Kirschner et al., 2011). These data suggest that CD44, additionally to its other known functions, like leukocyte rolling, is implicated in tight junction formation and maintenance.

2.1 The role of CD44 in cancer

CD44 has significant role in tumor malignancy, mainly as a metastasis promoting molecule. Variant CD44 isoform expression in tumor cells was shown to be sufficient to establish metastatic behavior (Günthert et al., 1991). Human standard CD44 overexpression in nonmetastatic mouse fibrosarcoma cells induced spontaneous lung metastases (Kogerman et al., 1997a,b). Clinically, high tumor CD44 expression correlates with metastases and poor survival in renal cell carcinoma patients (Lim et al., 2008). In contrast, reduced CD44s expression in prostate cancer patients predicted poor prognosis (Noordzij et al., 1997). High CD44s expression was a negative prognostic marker in patients with resected NSCLC and correlated with more advanced regional lymph node metastasis (Ko et al., 2011). CD44s expression was associated with overall survival in colon adenocarcinomas, being high in more aggressive carcinomas (Visca et al., 2002).

Experimentally, the CD44s role in colon cancer development is underpinned by findings that CD44 gene is regulated by WNT/β-catenin pathway. In a *Apc* mutant-mouse model of colon carcinogenesis, CD44 is overexpressed all-over the intestinal polyps compared to restricted expression in intestinal crypts of normal intestine. Knockout of *Tcf7l2* (formerly *Tcf4*), a β-catenin-associated transcription factor, completely abrogates CD44 expression in intestinal epithelium (Wielenga et al., 1999). Deletion of CD44 in $Apc^{Min/+}$ mice caused almost 50% reduction in the number of intestinal adenomas. This reduction was primarily caused by a decrease in the formation of aberrant crypts, as the number of apoptotic epithelial cells at the base of the crypt was significantly increased, whereas adenoma growth was not affected (Zeilstra et al., 2008). However, earlier study by another group did not find a significant difference in intestinal polyps in $Apc^{Min/+}$ mice (Weber et al., 2002).

Additionally, WNT/β-catenin regulation of CD44 seems to be also implicated in development of type II diabetes. In gene expression-based genome-wide association study CD44 was the top match and highly significantly associated with development of this disease (Kodama et al., 2012). Intriguingly, Tcf7l2 was among other significant matches. Together, data from spontaneous tumorigenesis models suggest that CD44 expression affects tumor cell survival in tissue microenvironment or colonization, not later outgrowth. Accordingly, metastases, but not primary tumor incidence, were affected by CD44-deficiency in two other spontaneous tumorigenesis models – breast cancer and sarcoma (Lopez et al., 2005, Weber et al., 2002). *Apc*$^{Min/+}$ intestinal tumors are benign and nonmetastatic, so only the primary tumor incidence is affected (Zeilstra et al., 2008).

In humans, development of liver metastasis causes most of CRC-related deaths. CD44 expressed on CRC cells might be functionally linked to these events, when normally, during liver inflammation, CD44 mediates neutrophil homing into HA-rich liver sinusoids (McDonald et al., 2008). Widely expressed secreted phosphoprotein 1/SPP1 (Osteopontin) is considered as CD44 ligand, although this interaction could not be verified *in vitro* (Smith et al., 1999, Weber et al., 1996). SPP1 enhances CRC metastasis formation and its targeting by antisense oligonucleotides was transiently effective in suppressing CRC liver metastases in a rat model (Uhlmann et al., 2011). Vice versa, suppression of CD44s by antisense blocked metastatic colon cancer cell line LS174T adhesion *in vitro* to HA and SPP1, and completely abolished LS147T liver metastases in a mouse model (Harada et al., 2001). In RAW264.7 murine leukemia cells and HepG2 liver carcinoma cells, SPP1 increases plasma membrane CD44 expression and cell adhesion by binding to its αvβ3-integrin receptor (Gao et al., 2003, Marroquin et al., 2004). Given the widespread SPP1 expression, this signaling is also feasible for other tumor or normal cell types.

Consistently, in *trp53+/tm1* sarcoma tumor model, CD44-deficient mice had significantly less osteosarcoma metastases, whereas no difference in primary tumor incidence was observed (Weber et al., 2002). Osteosarcomas in *trp53+/tm1* mice show prominent CD44 expression (Weber et al., 2002). This is in agreement with the finding that p53 directly suppresses CD44 gene expression, which leads to a inhibition of EGF signaling and increased tumor cell apoptosis (Godar and Weinberg, 2008), as CD44 is a constitutive coreceptor for Erbb2 and Erbb3 (Sherman et al., 2000, Wobus et al., 2002). In a model of spontaneous metastatic mammary cancer, MMTV-PyV-mT mice develop metastases with 100% penetrance and primary breast lesions show strong expression of CD44 throughout the tumor epithelium of large tumors. However, quite contrary to intestinal tumor and sarcoma model, metastasis formation in MMTV-PyV-mT mice was markedly enhanced in *Cd44* KO background (Lopez et al., 2005). In breast cancer cells, CD44-mediated HA-adhesion is thought to suppress the dissemination, as *in vitro* experiment using CD44-expressing breast cancer cell lines showed that they failed to invade HA-containing collagen matrix (Lopez et al., 2005).

2.2 The role of CD44 in vascular permeability and angiogenesis

The endothelial cells of neo-vessels in *Cd44* KO mice display an absence of cellular ruffling, often irregular surface and appear in some places very thin or flattened (Cao et al., 2006). Accordingly, *Cd44* KO mice show significantly increased dermal microvascular permeability in response to challenge with vasoactive substances, like histamine and LPS, compared to their wt counterparts. Additionally, *Cd44* KO endothelial monolayers display a reduced baseline barrier strength and reduced levels of adherens junction protein VE-cadherin along with increased amounts of phosphorylated, i.e. targeted for degradation, β-catenin (Flynn et al., 2013). Consistent with impaired barrier function, *Cd44* KO ECs showed increased MMP expression. One mechanism by which VE-cadherin homotypic adhesion regulates EC tight junctions (TJ) is via upregulation of TJ adhesive protein claudin-5 by inducing AKT phosphorylation of FoxO1 and consecutive release of FoxO1-Tcf7l2-β-catenin-inhibitory complex from claudin-5 promoter (Taddei et al., 2008). However, EC tight junction protein levels in *Cd44* KO ECs, including claudin-5, appeared comparable to wt (Flynn et al., 2013), therefore indicating another underlying cause of reduced barrier function. Further, (Flynn et al., 2013) suggest considerable phenotypic overlap between *Cd44* KO and PECAM-1-null mice and cells, supported by reduced level of PECAM-1 expression in *Cd44* KO mice.

Reconstitution of mouse CD44 or PECAM-1 in *Cd44* KO ECs was able to restore barrier function and CD44 expression rescued PECAM-1, suggesting that CD44 regulates vascular permeability and integrity through a PECAM-1 dependent mechanism (Flynn et al., 2013). PECAM-1 is a homotypic cell-cell adhesion molecule involved in EC migration and angiogenesis (Cao et al., 2002, DeLisser et al., 1997). These functions are related to PECAM-1 employment as a component of EC adherens junctions. Activation of MAPK/ERK by PECAM-1 via recruitment of protein-tyrosine phosphatase SHP-2 facilitates EC migration and is involved in organization of capillary networks during early stages of angiogenesis (Jackson et al., 1997, Wu and Sheibani, 2003). However, the exact mechanism how CD44 regulates PECAM-1 expression is not clear.

Additionally, CD44/c-Met interaction plays role in EC barrier function – c-Met ligand HGF enhances endothelial barrier via c-Met activation of Rac1. The role of the CD44 in this set is to function as a co-receptor for c-Met to recruit a Rac1 activator Tiam1. CD44 silencing in this situation disrupts HGF-induced enhancement of endothelial layer resistance (Singleton et al., 2007). Interestingly, it was found that in the *Cd44* KO mice and in human liver hepatocellular carcinoma cells, the c-Met co-receptor function of CD44 is taken over by ICAM-1, which helps to explain the absence of *c-Met* KO-like phenotype (Olaku et al., 2011).

CD44 has a role in tumor angiogenesis, supported by several independent findings. Cell surface CD44 expression was elevated in renal cell carcinoma blood vessels and CD44 isoforms were induced in cultured HUVEC by bFGF (Griffioen et al., 1997). *Cd44* KO mice showed reduced vascularisation of B16 melanoma cells-containing Matrigel plugs compared to wt counterparts and reduced growth of sc implanted B16 melanoma cell and ID8-VEGF ovarian tumor cell xenografts (Cao et al., 2006). ECs were mainly affected since wt bone-marrow transplantation to *Cd44* KO mice could not rescue B16 melanoma containing Matrigel plug vascularisation (Cao et al., 2006).

2.3 Soluble CD44 physiological concentration in serum and its increase in response to immune cell activity

In addition to cell surface expression, CD44 can be expressed as an alternatively spliced soluble isoform (Yu and Toole, 1996). However, the major source of soluble CD44 (sCD44) is proteolytic release of membrane CD44 by matrix proteases (Murakami et al., 2003, Nagano et al., 2004, Okamoto et al., 1999). It is proposed that sCD44 is not directly released into circulation, but accumulates first in the pericellular or extracellular matrix as a consequence of constitutive shedding. Lymph and serum sCD44 levels increase through its release from matrix-embedded pool and this is associated with excessive matrix reorganization during different pathological conditions, including cancer (Cichy et al., 2002). For example, in colon cancer patients serum sCD44 levels decreased after surgical resection of tumors (Guo et al., 1994). Nevertheless, matrix-embedded sCD44-hypothesis is in contrast with *in vivo* and *in vitro* findings, showing negative correlation between cell-surface CD44 and serum CD44 levels, suggesting direct release instead (Katoh et al., 1994, Rouschop et al., 2005).

The ectodomain shedding is not unique to CD44. During inflammation, many of the cell surface receptors, including E-selectin, ICAM-1 and ERBB2, become cleaved off from cell surface to regulate tumor cell migration or effective leukocyte homing (Garton et al., 2006). However, sCD44 generation can occur specifically and is not on par with many other cell surface molecules released by shedding. In renal transplantation patients, sCD44 is elevated in background of sICAM-1 and sIL-2R, and potentially can serve as a prognostic marker for transplant rejection (Rouschop et al., 2005). Proteases responsible for shedding CD44 in tumor cell models are predominantly ADAM10 and MT1-MMP, which are also involved in cleaving off other cell surface molecules (Garton et al., 2006, Kajita et al., 2001, Mori et al., 2002, Nagano et al., 2004, Stoeck et al., 2006, Takamune et al., 2007).

The shedding has clear impact on cell adhesion – in a mouse model of rheumatoid arthritis antibody-induced CD44 shedding reduces leukocytes adhesion to HA and joint inflammation (Mikecz et al., 1999). However, the further physiological role of the released sCD44 is unclear. Because sCD44 retains its HA-binding ability, it is proposed that it may function as an antagonist to membrane CD44 and be a decoy receptor (Katoh et al., 1994). Experimentally, this is shown in cancer cells – its overexpression in cancer cells blocks HA-mediated functions (Ahrens et al., 2001, Subramaniam et al., 2007).

Soluble CD44 may have also role in HA metabolism and excretion (clearance), as increased CD44 shedding and serum levels correlated with decreased serum HA (Mikecz et al., 1999). In macrophages, sCD44 might be directly involved in regulation of proinflammatory cytokine release in site of infection. Wild type serum, but not *Cd44* KO serum, suppressed elevated TNF-α production in response to LPS in *Cd44* KO macrophages. *Cd44* KO mice display increased TNF-α production in peritoneal lavage fluid, but not in serum, when they were intraperitoneally challenged with *E. coli*. Although, this TNF-α phenotype could not be rescued by direct supplementation of KO serum with recombinant soluble CD44-Rg protein, the simplest explanation is still the presence of sCD44 in wt serum (van der Windt et al., 2010).

Based on several studies, average physiologic sCD44 serum concentration in healthy persons (persons not having cancer diagnosed) is 347 ng/ml (95% CI 153-541 ng/ml) (BenderMedSystems, 2012, Lockhart et al., 1999, Loeffler-Ragg et al., 2011, Mäenpää et al., 2000, Mayer et al., 2008, Niitsu and Iijima, 2002). Given that the size of sCD44 molecule is between 30-120 kD, these levels correspond roughly to 3-14 nM concentration. In mice, serum concentration of sCD44 is in average $\sim$2.2 μg/ml (Katoh et al., 1994, Mikecz et al., 1999).

Interestingly, immunocompromised BALB/c.Xid and CB17.SCID mice display a significantly reduced serum sCD44 levels, whereas MLR/lpr mice carrying lymphoproliferative mutation have significantly higher serum sCD44, underscoring its lymphocytic or immune-related origin (Katoh et al., 1994). However, serum concentrations of sCD44 for Balbc/nude mice, widely used model for human tumor xenograft or angiogenesis studies, are not available.

Elevated serum sCD44 or sCD44v6 was predictor of poor outcome in non-Hodgkin's lymphoma or breast cancer patients, respectively (Lockhart et al., 1999, Mayer et al., 2008, Ristamäki et al., 1994); in addition, increased sCD44 was found in the saliva of head and neck squamous cell carcinoma patients (Franzmann et al., 2007). Circulatory sCD44 was significantly elevated also in patients with advanced gastric (24 nM) or colon cancer (31 nM) versus normal individuals ($\sim$3 nM) (Guo et al., 1994). Importantly, this study showed that circulating CD44 levels declined after tumor was surgically removed (Guo et al., 1994). Recent gene expression-based genome-wide association study identified that CD44 is pathogenetically implicated in the development of adipose tissue inflammation, insulin resistance and type II diabetes (Kodama et al., 2012). Soluble CD44 serum levels in human subjects showed positive correlation with increased glycated hemoglobin and insulin resistance index, markers for reduced glycemic control. In contrast with some cancers, in this study sCD44 levels ranged between 50-350 ng/ml, suggesting that in persons with reduced glycemic control the sCD44 levels don't increase severalfold and remain within normal boundaries.

2.4 CD44 HABD and its structure

Cell surface CD44 binding to HA is mediated by its amino-terminal domain which contains the Link module. The Link module is approximately 100 aa long conserved structure consisting of two alpha helices and two triple-stranded antiparallel beta sheets, which are interconnected by two disulphide bridges (Kohda et al., 1996). In addition to Link module, the CD44 HABD has an additional lobe consisting of four beta strands formed by the aa residues flanking the core link module (Banerji et al., 2007, Teriete et al., 2004). This enlarged structure is further stabilized by an additional disulphide bridge between flanking regions. Together, the CD44 HABD structure consists aa 21-169 according to human protein.

However, the Link module is absolutely sufficient for the HA-binding function of CD44 and its flanking regions don't directly contribute to the HA binding (Banerji et al., 2007). The critical residues in the human CD44 HA-binding surface, that are directly involved in binding, are Arg41, Tyr42, Arg78 and Tyr79 (Bajorath et al., 1998, Banerji et al., 2007). As can be seen, these aa belong to two Arg-Tyr clusters that together form the HA binding surface. Mutations in either of these clusters abolishes HA binding.

CD44 is a glycoprotein and is mainly O-glycosylated by its alternatively spliced exons. However, it contains also five N-glycosylation sites within its HABD – Asn25, Asn57, Asn100, Asn110, Asn120. Glycosylation at two sites, Asn25 and Asn125, within HABD is involved in regulation of HA binding – high glycosylation at these sites blocks HA binding completely, intermediate levels make binding inducible and complete removal of glycosylation grants constitutive HA binding (English et al., 1998, Lesley et al., 1995). Nevertheless, *in vitro* experiments show that bacterially expressed recombinant human CD44 HABD containing aa 20-178 binds HA comparably to glycosylated CD44-Rg fusion protein (Teriete et al., 2004).

3 Vimentin and its functions

Vimentin intermediate filaments (IF) function as cell supporting framework. Intermediate filament-based cytoskeleton links extracellular matrix with nuclear membrane and provides a cell with stiffness to resist tensile and shear stress (Eckes et al., 1998, Wang and Stamenović, 2000). Vimentin IF form a cage-like structure enclosing the nucleus. Vimentin is highly expressed in vertebrates during development and in adult organism in cells of mesenchymal origin. However, vimentin (*Vim*) KO mice develop normally (Colucci-Guyon et al., 1994). In physiology, vimentin deficient mice have defects in vascular function, manifested by reduced flow-induced dilatation of arteries, which is caused by decreased nitric oxide production and elevated endothelin (Henrion et al., 1997, Terzi et al., 1997). Imbalance and impaired release of vasodilator and vasoconstrictor agents in *Vim* KO mice might be caused by loss of its functions in intracellular vesicular transport.

Vimentin is an important mediator of vesicular transport, it associates prominently with synaptobrevin/VAMP/syntaxin complex protein SNAP23 which directs and facilitates the fusion of transport vesicle with target membrane (Faigle et al., 2000). Vimentin also binds directly to adaptor complex AP-3 $\beta3$ subunit (Styers et al., 2004). Importantly, vimentin is involved in recycling of $\beta1$ integrin in migrating cells. Vimentin traps $\beta1$ integrin-containing vesicles in cytoplasm and they can be released for recycling to the plasma membrane following serine phosphorylation of vimentin N-terminal domain by an atypical PKC (PKCε). Mutation of PKCε phosphorylation sites in vimentin or PKC inhibition leads to the intracellular accumulation of PKCε/integrin positive vesicles and inhibition of directional migration (Ivaska et al., 2005).

Vimentin role in targeting cell adhesion proteins to plasma membrane is further underscored by lymphocyte–endothelial adhesion and homing defect in *Vim* KO mice (Nieminen et al., 2006). Aberrant leukocyte homing could be attributed to the reduced levels of EC surface ICAM-1 and VCAM-1 cell adhesion molecules in a vasculature of KO mice and reduced β1-integrin in lymphocytes (Nieminen et al., 2006).

Vimentin is implicated in regulation of cell polarity in epithelial cells and ECs, by stabilizing polarity-complex protein scribbled homolog (Drosophila) (Phua et al., 2009). Therefore, it was proposed that perinuclear vimentin IF cage is necessary for proper front-rear polarization, similar to microtubules (Burgstaller et al., 2010, Pegtel et al., 2007). In addition to scribbled, cell polarity regulatory complex contains disc large and lethal giant larvae and is important regulator of apical-basal polarization in epithelial cells or front-rear polarization in migrating cells. Vimentin binding increases scribbled stability by protecting it from proteasomal degradation. Silencing of either scribbled or vimentin in MDCK cells resulted in random alignment of *in vitro* wound invading cells and reduced ability for directional movement (Phua et al., 2009).

3.1 Cell surface vimentin is involved in lymphocyte activation

The functional role of vimentin in cell surface receptor trafficking and in secretory pathway may also provide the mechanism of vimentin transport to the plasma membrane and into ECM. Intriguingly, it was found that macrophages secrete phosphorylated vimentin and its secretion is regulated by inflammatory cytokines (Mor-Vaknin et al., 2003). Recently, the same group reported that vimentin interacts with p47phox on the surface of activated macrophages (Mor-Vaknin et al., 2013). P47phox is subunit of NADPH oxidase, an enzyme involved in ROS production. Interestingly, vimentin seemed to interfere with ROS production, as bacterial killing *in vivo* was more effective in *Vim* KO mice and p47phox cell-surface localization upon activation was not influenced by the absence of vimentin. Together suggesting that vimentin regulates p47phox activity but not its localization.

Additionally, cell surface vimentin is a specific marker for Sézary syndrome T-cell lymphoma and this is linked to the lymphocyte activation status, as its extracellular expression is induced during normal T lymphocyte activation (Huet et al., 2006). Identified extracellular ligands for vimentin include phospholipase A2 in apoptotic T-cells (Boilard et al., 2003) and vitronectin in complex with PAI-1 on activated platelets (Podor et al., 2002). Importantly, vimentin is identified as possible antiangiogenesis target overexpressed on tumor endothelium *in vivo* and as such was directly usable as antiangiogenesis therapy target. Anti-vimentin antibody treatment was able to significantly inhibit tumor growth and vascular density (van Beijnum et al., 2006).

3.2 Vimentin is anchored to integrin containing EC adhesions disassembled during angiogenic switch

Vimentin KOs displayed elevated leukocyte extravasation as a result of compromised endothelial-cell layer and markable blood vessel leakiness, suggesting that vimentin has important role in vascular integrity (Nieminen et al., 2006). In primary microvascular ECs approximately 60-70% of focal adhesions associate with vimentin IF (Gonzales et al., 2001). Association of vimentin IF with $\beta 3$-integrin containing focal adhesions improves significantly EC resistance to shear stress (Bhattacharya et al., 2009). In stably adherent ECs, vimentin cage is anchored to hemidesmosome-like stable matrix adhesions (Homan et al., 1998). These adhesions are based on laminin receptor $\alpha 6\beta 4$ integrin and are anchored to the vimentin IF via versatile cytoskeletal cross-linking protein, plectin. Plectin is a large > 500-kD protein with characteristically dumbbell-like shape – its globular end domains are separated by an elongated rod domain. The $\beta 4$ integrin is localized to epithelial hemidesmosome-like stable adhesions in ECs, whereas its expression is lost in cultured ECs. The $\alpha 6\beta 4$ integrin plays an essential structural role in type I hemidesmosomes of stratified epithelial cells by connecting basement membrane to keratin IFs. It has been proposed, that the endothelial function of $\alpha 6\beta 4$ integrin may be analogous to its function in epithelial cells or tumors (Nikolopoulos et al., 2004). During angiogenesis, the $\alpha 6\beta 4$ integrin may confer a promigratory phenotype in response to angiogenic stimuli and in mature vasculature it may contribute to stable adhesion of endothelial cells to BM.

Stable adhesions are disassembled in angiogenic vasculature allowing cells to migrate and invade the surrounding ECM (Nikolopoulos et al., 2004). This is achieved by phosphorylation of the signaling portion of the long cytoplasmic tail of $\beta4$ integrin adjacent to its plectin binding site and results in destabilization of $\beta4$–plectin–vimentin IF interaction which is necessary for EC migration. Plectin binding site in $\beta4$ integrin is critical for vimentin IF recruitment into sites of $\alpha6\beta4$ matrix adhesions in ECs (Homan et al., 2002). Endothelial-specific deletion of the $\beta4$ integrin signaling portion causes reduced EC migration resulting in defective angiogenesis (Nikolopoulos et al., 2004). In contrast to downregulation in angiogenic vasculature, $\beta4$ integrin expression is elevated in carcinoma. In fibroblasts and cancer cells, the $\alpha6\beta4$ integrin mediates invasion through the PI3K signaling pathway and through cross-talk with the ERBB2 and c-MET tyrosine kinase receptors (Gambaletta et al., 2000, Shaw et al., 1997, Trusolino et al., 2001). Notably, $\beta4$ integrin expression was also significantly downregulated in vimentin-silenced breast cancer cells, suggesting that they belong to the common functional complex (Vuoriluoto et al., 2011).

Given that vimentin is involved on ROS generation, it's intriguing that vimentin–plectin interaction is also sensitive to redox environment of the cytoplasm. While plectin binding to $\beta4$ integrin is mediated via its N-terminal part, then vimentin-binding site of plectin is located in its C-terminal domain. Vimentin binds plectin through its rod-domain 1B. The vimentin binding region of plectin contains four cysteine residues the redox status of which modifies its vimentin binding affinity (Spurny et al., 2007). When Plectin vimentin binding region was chemically reduced or critical cysteine was mutated to serine, plectin bound to vimentin with three times higher affinity than in its nonreduced form, probably due to a more relaxed conformation (Spurny et al., 2007).

AIMS OF THE STUDY

Current study was undertaken to test the hypothesis that CD44 hyaluronan receptor has antiangiogenic function in tumor microenvironment. To elucidate this, we posed three main objectives:

1. Generate soluble recombinant CD44-HABD proteins.
2. Test CD44-HABD as potential antiangiogenesis agent in angiogenesis assays.
3. Test if exogenous CD44-HABD inhibits tumor xenograft growth in mice.

MATERIALS AND METHODS

Detailed description of materials and methods is provided in the publications of this thesis. Briefly, the following methods were used in the present study:

1. Cell culture and transfection (Publication I, II).
2. Recombinant protein expression and purification (Publication I, II, Manuscript).
3. ELISA, HA binding assay (Publication I, II).
4. Cell migration and proliferation assays (Publication I).
5. Cell cycle analysis of BrdU-labeled cells by FACS (Publication I).
6. Chick CAM angiogenesis assay (Publication I).
7. Chick aorta fragment 3D culture angiogenesis assay (Patent).
8. Mouse tumor xenograft assay (Publication I, Patent).
9. GST pull-down, immunoprecipitation and cell surface biotinylation (Publication II).
10. Isothermal titration calorimetry and surface plasmon resonance (Publication II).
11. Radioligand saturation binding and displacement assays (Publication II, Patent).
12. Internalization assay, confocal immunofluorescence microscopy and image analysis (Publication II).
13. Isolation of mouse lung endothelial cells (Publication II).
14. Statistical analysis (Publication I, II, Manuscript).
15. MALDI-TOF MS (Publication II).

RESULTS AND DISCUSSION

Given that CD44 overexpression on the tumor cell surface can inhibit tumor growth, we hypothesized that a purified recombinant CD44 HABD might serve as an angiogenesis inhibitor and may thereby block tumor growth. The original hypothesis was that HA-rich coat that surrounds tumors inhibits the growth of surrounding blood vessels into tumor. CD44 overexpression on tumor cells tethers HA to plasma membrane and stabilizes HA-containing ECM. Surplus of soluble HA binding proteins might display similar stabilizing effect. It has been shown that high molecular weight HA has antimitogenic effect to ECs, whereas, in contrast, oligomeric HA fragments stimulate angiogenesis (Deed et al., 1997, Slevin et al., 1998, 2002). Therefore, another alternative was that high tumor CD44 might compete for angiogenic HA fragments, and soluble HA binding protein can be used as a decoy receptor.

1 Design and purification of CD44-HABD and CD44-3MUT recombinant proteins (Publication I, Manuscript, Patent)

We proposed a mechanism of possible angiogenesis inhibition that was based on HA-binding property of CD44 that we set out to test. To this objective, we constructed and purified human CD44-HABD as GST fusion protein. In addition to WT recombinant CD44-HABD, we produced non-HA-binding mutants which contained mutations in aa Arg41 and in Arg78-Tyr79 to use them as negative controls. First, Arg78 and Tyr79 were substituted by serines and Arg41 was substituted by alanine. We termed the CD44-HABD construct containing mutations in all these three sites as CD44-3MUT. The obtained recombinant CD44-HABD proteins contained aa 21-132 from human protein. Compared to the extended structure of HABD of CD44, these proteins lack the flanking region (Figure 2)(Teriete et al., 2004).

The CD44 region spanning the Link domain (aa 32-120) which was shown to be minimally sufficient for ligand binding was included into our CD44-HABD protein (Peach et al., 1993). However, this was not entirely deliberate decision to omit CD44 HABD flanking region – at the time when our recombinant proteins were designed the structure of CD44 HABD was not yet resolved. As a consequence, the absence of C-terminal extension remained naked the N-terminal $\beta 0$-sheet, formed

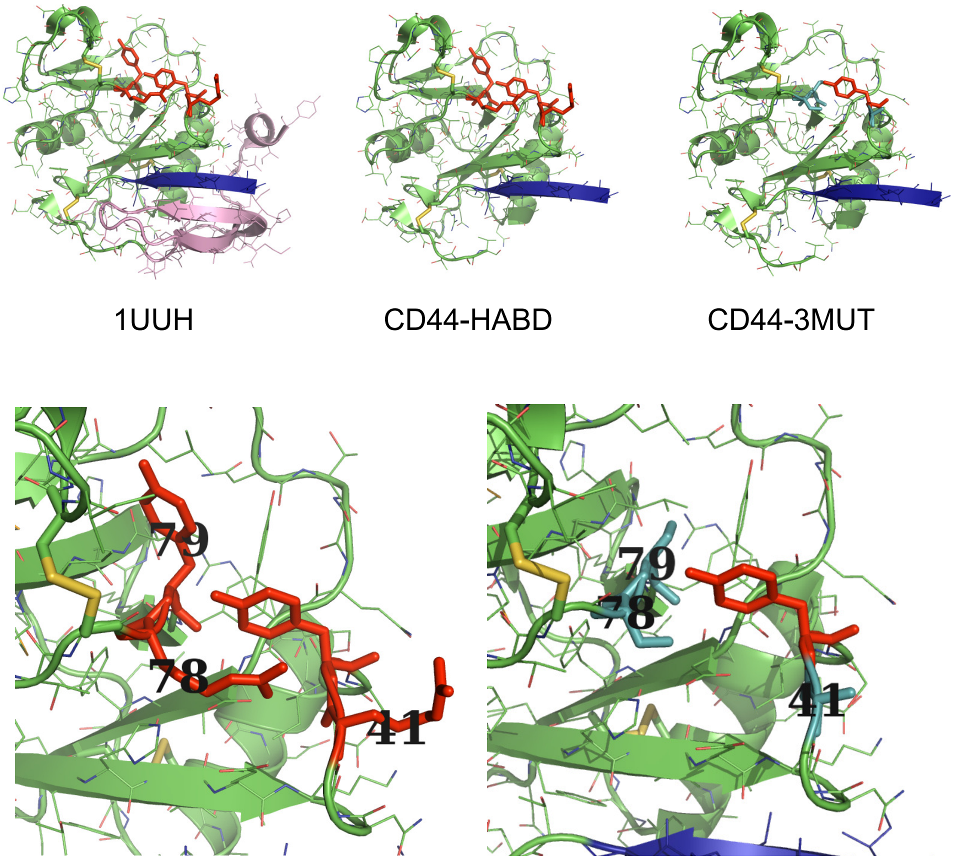

Figure 2 The structure of human CD44 HABD (Teriete et al., 2004). CD44-HABD$^{21\text{-}132}$ (upper middle) and CD44-3MUT$^{21\text{-}132}$ (upper right) protein models, based on human CD44 HABD$^{20\text{-}178}$ X-ray diffraction structure (PDB ID: 1UUH; upper left). Compared to CD44-HABD and -3MUT, complete CD44 HABD contains flanking region (pink) not directly involved in HA binding. Original CD44-HABD constructs contained β0-sheet (blue), which was removed from later constructs to improve recombinant protein solubility. Lower left, two arginine-tyrosine clusters form HA binding site (red). Residues Arg41, Arg78 and Tyr79 were mutated in CD44-3MUT protein (lower right, teal). Disulfide bonds are shown as yellow sticks.

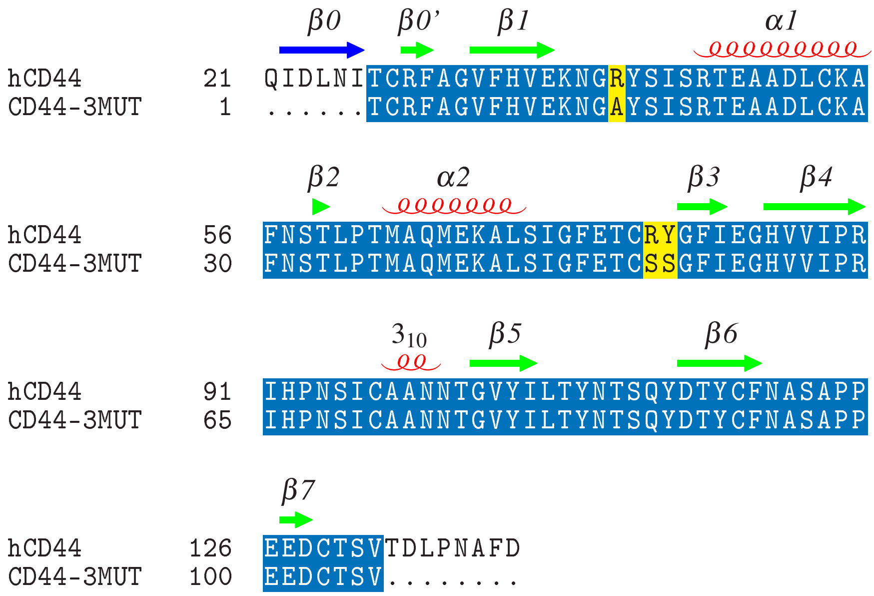

Figure 3 CD44 3MUT protein sequence alignment with human CD44. CD44 3MUT is a fragment from human CD44 hyaluronan binding domain encompassing aa 27-132 (*blue*) with three point mutations: R41A, R78S, Y79S (*yellow*). These mutations completely disrupt CD44 binding to hyaluronan. β0-sheet (*blue right arrow*) was removed to improve protein solubility (see Figure 2). Secondary structure elements are based on crystal structure of CD44 HABD, 1UUH (Teriete et al., 2004). *Right arrows*, β-structures. *Helices*, α-helices and 3_{10}-helix.

by aa directly after the signal peptide. Nevertheless, we were able to purify GST-tagged bacterially expressed CD44-HABD proteins from soluble fraction using simple one step affinity purification protocol, although most of the protein appeared in inclusion bodies. However, β0-sheet contributed to protein aggregation and significantly affected the solubility of purified proteins. Therefore, we subsequently removed six N-terminal aa, contributing to β0-sheet, from untagged CD44-3MUT and in further experiments, eg. pegylation, we used this N-terminally truncated version (Figure 3, Manuscript).

All successful attempts to purify CD44-HABD are based on method published by Banerji et al. (Banerji et al., 1998, Teriete et al., 2004). Our initial attempts to purify untagged CD44-HABD or CD44-3MUT were based on this protocol, but we were unable to fully refold the protein. It has been shown that high molecular weight contaminants could affect protein refolding efficiency and yield (Ouellette et al., 2003). To ensure the removal of such contaminants, we included an additional IEC step under denaturing conditions before refolding into our purification protocol. We found that, although most of the CD44-3MUT protein resulted in flow through fraction after IEC (Manuscript, Figure 2), the IEC inclusion resulted in improved protein yield. This was mainly caused by reduced aggregation of CD44-3MUT. Flow through fraction contained beside CD44-3MUT also considerable amount of contaminating *E. coli* proteins, suggesting that the purity was not increased during this step. While IEC step does not enrich CD44-3MUT from bacterial lysate, we propose that it still eliminates some of the contaminants interfering with folding. Using this protocol, final protein yield for CD44-3MUT was 1-1.3 mg/g of wet bacterial mass. The molecular weight of untagged CD44-3MUT with/without N-terminal β0-sheet was 12.3/11.5 kD, respectively, and for CD44-HABD 12.8 kD. Based on HA binding assay, Banerji et al. reported the failure of proper refolding of the version of CD44 HABD containing residues 20-120 (Banerji et al., 1998). However, we found that our version of the WT CD44-HABD GST fusion protein retained its HA binding property in a modified ELISA assay and in a functional assay, where CD44-HABD was able to inhibit EC migration towards HA (Publication I, Figure 1). Additionally, we found that hyaluronidase treatment reduced CD44-HABD binding sites in ECs, while such treatment had no effect on CD44-3MUT binding to ECs (Patent, Figure 12B,C). Together, these data confirm that the residues 21-132 are sufficient for proper folding and functionality of CD44-HABD. Given that R41A mutation does not cause distortion in human CD44 HABD structure (Banerji et al., 2007) and also other mutated aa (Arg78 and Tyr79) are similarly solvent exposed, we believe that CD44-3MUT assumes structure close to its WT counterpart.

2 Angiogenesis inhibition by soluble CD44-HABD and CD44-3MUT (Publication I, Patent)

First, we tested the possible antiangiogenic effect of CD44 in the chick embryo chorioallantoic membrane (CAM) angiogenesis assay. Chorioallanois is a highly vascularised extraembyonic tissue of the developing embryo that starts to arise at day 7 after start of incubation. At day 10 CAM has completely superseded by yolk sac membrane and can be used to test angiogenic or antiangiogenic substances. We used VEGF, bFGF or TGF-α soaked filter disks to induce angiogenesis in 10 day old CAMs. Test protein solutions were applied topically to filter disks once a day and we used GST as nonspecific protein control. Three days later we dissected filter disks and surrounding CAM tissue and quantitated angiogenesis by counting blood vessel branch points below filter area. We found that CD44-HABD GST fusion protein suppressed angiogenic response induced by different growth factors (Publication I, Figure 2). To our great surprise, non-HA-binding CD44-3MUT GST fusion protein appeared equally effective in angiogenesis inhibition. We concluded from these experiments that CD44 HABD may inhibit angiogenesis induced by different proangiogenic factors. More importantly, these results suggested that CD44 HABD can block angiogenesis independently of its HA-binding property.

In a further series of experiments, to confirm antiangiogenic properties of untagged version of CD44-3MUT, we decided to use *ex vivo* chick aortic fragment angiogenesis assay. This assay is a modification of rat or mouse aortic arch fragment *ex vivo* assays. Here, aortic fragments were prepared from 14 day old chick embryos and implanted into type I collagen gels. In postnatal angiogenesis, blood vessels invade connective tissue matrix mainly comprised of type I collagen, the major extracellular protein found in mammals. In chick aortic fragment cultures, new vessels outgrowth is complete after 48 hours, whereas from mouse or rat aortic fragments the vessel outgrowth takes 7 days. Neovessel outgrowth from aortic fragments in our assay was strongly dependent on VEGF – uninduced fragments mostly did not produce any outgrowth – 20-30% the number of vessels per fragment compared to VEGF-stimulated fragments. We found that, the presence of 10 μg/ml CD44-3MUT inhibited mean vessel length in VEGF-induced chick aortic arch cultures comparably to 10 μg/ml Avastin (Patent, Figure 10). Avastin was used as a positive control compound. In another independent series of chick aortic fragment assays ($N = 7$), we tested CD44-3MUT in concentrations 2.3, 12.7 and 63.5 μg/ml (0.2 nM, 1 μM and 5 μM, respectively; mean vessel length μm ±SE, uninduced 107.9 ±38.7, and VEGF-induced fragments treated with PBS 261.7 ±11.5, GST 257.9 ±10.9, CD44-3MUT 2.3 μg/ml 209.1 ±7.4, CD44-3MUT 12.7 μg/ml 194.7 ±4.4, CD44-3MUT 63.5 μg/ml 192 ±7.3, fumagillin 1 nM 203.3 ±8.5; one-way ANOVA, $F(8,47) = 10.52$, $p < 0.0001$) and found concentration dependent trend with mean efficacies comparable to 10 μg/ml Avastin (0.14 nM as monomeric), here we used also 1 nM fumagillin as a positive control (Wally Anderson, unpublished results). In these experiments, fumagillin effect was comparable to Avastin. Fumagillin is a natural antibiotic produced by *Aspergillus fumigatus* that has strong antiangiogenic effect *in vitro* and *in vivo*; its synthetic analogue TNP-470 slow release formulation is currently in preclinical development (Benny et al., 2008). Together, we like to state that Avastin and Fumagillin define maximum inhibitory effect in this assay. Chick aortic arches are derived from growing embryos and contain proliferating cells. While this might cause occasional vessel outgrowth in uninduced cultures, then VEGF-stimulation always unleashes this intrinsic growth potential. The extra VEGF-simulated growth, which is sensitive to our treatments, is 20-25% on top of the background. Nevertheless, proliferating ECs are characteristic to tumor microenvironment and this model might quite properly simulate the real life situation before start of treatment.

Our approach of using soluble fragments of ECM receptors to suppress angiogenesis and choice of chick CAM model stemmed from study showing that MMP-2 is recruited to angiogenic blood vessels via binding to $\alpha v\beta 3$ integrin (Brooks et al., 1996). They found that by blocking MMP-2 binding to this integrin, using soluble recombinant MMP-2 hemopexin domain, also inhibited angiogenesis in chick CAM and melanoma xenograft growth in mice (Brooks et al., 1998). ECM enforces growth control over embedded cells. Consequently, processes like blood vessel growth and tumor cell invasion in three-dimensional ECM is dependent on pericellular proteolysis mediated by MMP-s. It has been shown that CD44 is a cell surface docking receptor for MMP-9 (Yu and Stamenkovic, 1999, 2000). MMP-9 is released for example by tissue invading macrophages or by tumor cells and is involved in proteolytic activation of latent TGF-β. MMP-2 and MMP-9 activity is necessary for EC migration (Koivunen et al., 1999). Based on chick CAM assay results, suggesting that HA binding function is not necessary for soluble CD44 fragments to inhibit angiogenesis, we hypothesized alternatively that soluble CD44 HABD fragments could disrupt cell surface localization of MMP-9 and therefore hamper tissue invasion of ECs. Indeed, we found that CD44-HABD bound MMP-9. Importantly, MMP-9 binding was lost in its HA-binding site mutants CD44-3MUT, CD44-HABD^{R41A} or CD44-HABD^{R78SY79S}. Furthermore, CD44-HABD MMP-9 binding was disrupted by addition of HA into pull-down reaction (Wally Anderson, Anne Pink, unpublished results). Together, these results suggest that MMP-9 binds to HA-binding region of CD44. Nevertheless, as mutant CD44-HABD proteins does not bind MMP-9, these results rule out that disruption of MMP-9 localization or activity by soluble CD44 is responsible for angiogenesis inhibition observed in our assays. Consistent with this, study of Chun et al. (2004), directly addressing the role of collagenolytic activity in angiogenesis, found that type I collagen aortic fragment cultures derived from MMP-9 or Cd44 KO mice showed normal vessel outgrowth, suggesting that their function was not important for EC collagen invasion (Chun et al., 2004). Instead, it was found that MT1-MMP, a metalloproteinase originally thought to be involved only in activation of MMP-2 or MMP-9, itself is important for invasion of type I collagen matrices (Chun et al., 2004, Hotary et al., 2003). Interestingly, MT1-MMP is one of the enzymes directly involved in CD44 shedding (Kajita et al., 2001).

3 Tumor xenograft growth inhibition (Publication I, Patent)

According to antiangiogenesis cancer treatment paradigm all solid tumors need to induce angiogenesis to grow over millimeter size. Therefore, we tested whether our recombinant proteins could also inhibit tumor growth in mouse sc xenograft model. For this purpose, first, we used BxPC-3 pancreatic human adenocarcinoma or SMMU-1 melanoma cells xenografted sc onto backs of nude mice. When the tumors appeared as palpable nodules, BxPC-3 tumor carrying mice started to receive 20 μg of GST fused CD44-HABD, GST-CD44-3MUT or GST alone by sc injections every second day into a region proximal to the tumor. BxPC-3 cells gave rise to relatively slow-growing tumors. We found that after 52 days after start of experiment, when the mice were sacrificed, in GST-CD44-HABD or GST-CD44-3MUT treated mice tumors were approximately 60-70% smaller than in GST treated controls. Then we performed the same experiment using the more aggressive human SMMU-1 melanoma cell line and observed a significant inhibition of tumor growth by approximately 50% by GST-CD44-HABD or GST-CD44-3MUT sc treatment every second day at 50 μg dose (Publication I, Figure 5 and 6).

To assess whether angiogenesis was affected, we analyzed vascular density in SMMU-1 tumor sections by counting PECAM-1 (CD31)-positive blood vessels. We found that GST-CD44-HABD or GST-CD44-3MUT treated tumors showed reduced blood vessel density compared to GST control treatment (Publication I, Figure 6d). These results suggest that GST-CD44-HABD as well as the GST-CD44-3MUT inhibited tumor-induced angiogenesis. Therefore, consistent with antiangiogenesis paradigm, the observed reduced tumor growth may have caused by suppressed angiogenesis.

In a liver cancer model, administration of 10 μg dose of CD44-3MUT three times a week decreased human Hep3B tumor cells xenograft growth. We also found that CD44-3MUT effect on tumor growth is dose-dependent. Administering of CD44-3MUT in doses 2, 10 or 50 μg/mouse (0.1-2.5 mg/kg) inhibited tumor growth in a dose-dependent manner, where 2 μg/mouse treatment was not effective (Patent, Figure 8). Taken into account that CD44-3MUT is a relatively small $\sim$12-kD protein with rapid clearance (see Manuscript), we also used constant drug administration via ip implanted micro-osmotic pump. Such administration allows more uniform release of CD44-3MUT over time and may improve its antiangiogenic and anti-tumor efficacy. To this end we found that CD44-3MUT administration to mice carrying Hep3B sc xenografts using micro-osmotic pumps, with calculated dose of 1 μg/mouse/day, inhibited tumor growth more effectively than the same dose administrated via ip injections (Patent, Figure 9). Importantly, in this model CD44-3MUT dosing 10 μg (0.5 mg/kg) ip three times a week was able to inhibit tumor growth comparably to Bevacizumab in dose 100 μg (5 mg/kg) ip two times a week (Patent, Figure 11).

Subsequent analysis of Hep3B tumor xenografts for vascular density revealed no significant differences between control and CD44-3MUT treatments, whereas Bevacizumab treatment resulted in less vascularized tumors (Riin Saarmäe, unpublished results). Notably, characteristic features of Bevacizumab treated tumors were macroscopically pale appearance and, histologically, blood vessels had enlarged lumens. Such large blood vessels are shown to be resistant to anti-VEGF treatment (Li et al., 2011). The inconsistency between different tumor models in reduction of vascular density in response to CD44-HABD or CD44-3MUT treatment could be explained by different sensitivity of tumor cells to hypoxic conditions. SMMU-1 melanoma cells were probably less sensitive and expanded relatively better even when blood vessel growth was suppressed. Whereas, Hep3B cells are probably more stringently controlled by hypoxia in tumor microenvironment and therefore in Hep3B tumors blood vessel density remained constant. Alternatively, CD44-3MUT might have direct effect *in vivo* on Hep3B cells, however, CD44-3MUT binding to Hep3B cells was non saturable and had low affinity (see section 4).

Taken together, our results show that CD44-3MUT inhibits growth of various human tumor models xenografted into athymic nude mice, including SMMU-1 melanoma, BxPC-3 pancreatic adenocarcinoma and Hep3B hepatic adenocarcinoma.

4 Endothelial cell binding and growth inhibition (Publication I, Patent)

Angiogenesis is a complex process and its steps include dissolving of basement membrane and tissue invasion, latter involving migration and proliferation. Our results show that CD44 takes part in EC migration primarily via its HA binding property (Publication I, Figure 1C) and soluble CD44-HABD R41A does not affect HA-stimulated EC migration. Additionally, we could not detect that our recombinant CD44-HABD binds MMP-9 (see section 2), suggesting that putative CD44-MMP-9 invasion mechanism of pericellular proteolysis was not affected (we did not test MT1-MMP interaction, though). Based on these arguments we proposed that CD44-HABD or CD44-3MUT elicit their effect by direct binding to cells. This is contrasted to indirect effects by blocking CD44 binding sites in ECM or disrupting CD44–MMP-9 interaction. To this end we estimated dissociation constants (Kd) and maximum number of binding sites (Bmax) from saturation binding experiments with ^{125}I-labeled CD44-3MUT for a number of cell lines (Table 1). Rationale for choosing CD44-3MUT was to eliminate HA binding to measure other putative interactions. We found that ^{125}I-CD44-3MUT binds with comparable affinity to most of our tested cell lines with Kd between 100-200 nM. Three cell lines differed in our sample, Ramos lymphoma cells bound CD44-3MUT with highest affinity, in contrast binding to MCF7 breast carcinoma cells was saturable but low affinity and binding to Hep3B cells remained practically unsaturated. We concluded from these results that there is a specific binding site for CD44-3MUT on the surface of cells of different origin.

Next we tested if GST-CD44-HABD proteins might affect endothelial cell proliferation. To this end, HUVEC and CPAE endothelial cells, as well as various other primary and tumor cells were grown in the presence of GST, GST-CD44-HABD or GST-CD44-3MUT. We found that HUVEC and CPAE cells exposed to GST-HABD or GST-3MUT for 48 h displayed a markedly reduced amount of cells in cell cycle S-phase as compared to GST-treated control cells (Publication I, Figure 3). We also evaluated whether the effect of our CD44 proteins is dose dependent, first, in MTT assay, which measures cell number and, secondly, by measuring the number of S-phase cells. GST-fused proteins showed clear concentration-dependent effect on CPAE cells in MTT assay (Publication I, Figure 4). By using CPAE cells we observed that also GST had some growth inhibitory effect

Table 1 ^{125}I-CD44-3MUT cellular binding (Patent, Table 1).

Cells	Kd, nM	Bmax, fmol/cell	N^a	Cells origin
Ramos	54 ±22[b]	0.0198 ±0.0054	2	Human Burkitt's lymphoma
Raji	140 ±9	0.0175 ±6.2E-5	2	Human Burkitt's lymphoma
THP-1	93 ±19	0.0226 ±0.0133	5	Human Myelocytic leukemia
HUVEC	146 ±72	0.028 ±0.019	15	Human umbilical vein ECs
PC-3	171 ±62	0.0192 ±0.0023	2	Human prostate adenocarcinoma
COS-1	176 ±74	0.0305 ±0.021	5	Green monkey kidney fibroblasts
CPAE	185	0.08	1	Cow pulmonary artery ECs
MCF7	422 ±379	0.095 ±0.097	2	Human breast adenocarcinoma
Hep3B	966 ±764	0.265 ±0.19	4	Human hepatocellular carcinoma

[a]number of experiments.
[b]values shown as mean ±SD.

at higher concentrations, although much smaller compared to GST-CD44-HABD or GST-CD44-3MUT. This effect was probably caused by endotoxins in our protein samples. HUVEC tolerated without significant growth inhibition much higher amounts of bacterial LPS than endotoxins measured in our bacterial recombinant CD44-3MUT preparations. However, unlike HUVEC, CPAE cells were sensitive to LPS (Lagle Kasak, unpublished results). Therefore, we confirmed the growth inhibitory effect of CD44-3MUT in HUVEC model, using concentration range 0.1-10 μM and found up to 40% reduction in number of S-phase cells (Patent, Figure 15). Notably, we did not observed increased apoptosis within the treated cell populations, which indicated that the primary effect on HUVEC growth was because of reduced cell proliferation.

In contrast, GST-CD44-HABD or GST-CD44-3MUT had no significant effect on cell proliferation of other untransformed cells including normal human dermal fibroblasts (NHDF), human embryonic kidney cells (HEK-293) and tumor cells of various origins – MCF7 breast carcinoma cells, SMMU-1 melanoma cells, U373MG glioblastoma cells, BxPC-3 pancreatic carcinoma cells. These data suggested that cell growth inhibitory effect by CD44-HABD is specific to ECs.

Taken together, these data indicate that CD44-HABD and CD44-3MUT directly inhibit endothelial cell proliferation and thus act as direct angiogenesis inhibitors. Regarding cell cycle control mechanism affected, we found that cyclin D1 upregulation was suppressed and delayed after release from serum starvation in synchronised HUVEC population treated with CD44-3MUT or CD44-HABD. Further, we found that cyclin D1 levels could be rescued by inhibition of GSK-3β by using either LiCl or specific inhibitor SB216763 (Wally Anderson and Taavi Päll, unpublished results). GSK-3β is a serine-threonine protein kinase, that plays an important role in the control of cyclin D1 expression level by regulating its transcription and protein degradation. Cyclin D1 is expressed in response to many mitogenic signals and triggers in cells G0→G1 entry. The cyclin D1 mRNA level increases greatly following mitogenic stimulation and both mRNA and protein levels of cyclin D1 are under stringent regulation after induction. Possible mechanisms for cyclin D1 inhibition by soluble CD44-3MUT include either interference of growth factor receptor signaling or with cell adhesion, possibly by disrupting receptor complexes. CD44 is involved in EGFR (ErbB family), VEGFR2 and c-Met signaling, in all these cases functioning as a co-receptor (Sherman et al., 2000, Singleton et al., 2007, Tremmel et al., 2009).

We tested CD44-3MUT binding to recombinant VEGFR1 and VEGFR2 in a *in vitro* assay. However, we found that CD44-3MUT does not bind to these receptors, therefore ruling out that CD44-3MUT functions as antagonist to VEGF signaling (Patent, Figure 13). Additionally, it has been shown that CD44 complex formation with VEGFR2 and c-Met is dependent on CD44 variant exon 6, which lies outside of CD44 HABD (Singleton et al., 2007, Tremmel et al., 2009).

High molecular weight HA inhibits cyclin D1 expression and proliferation in vascular smooth muscle cells (Cuff et al., 2001, Kothapalli et al., 2007), whereas such native HA has been shown to induce CD44 clustering (Yang et al., 2012). Also in angiogenic signaling, high molecular weight HA shows inhibitory effect on early-response gene upregulation, whereas HA oligomers were stimulatory (Deed et al., 1997). However, the mechanism by which HA binding to CD44 regulates cell cycle proteins is not clear. Probably, it's still related to receptor tyrosine kinase signaling, where CD44 functions as a coreceptor. To fit CD44-3MUT mediated EC growth inhibition into this context, we should assume that CD44-3MUT induces membrane CD44 clustering similarly to high molecular weight HA, rather than breaking it apart.

5 CD44 interaction with vimentin on endothelial cells (Publication II)

Based on our findings that CD44-HABD and CD44-3MUT bind to ECs and exert direct effect on EC proliferation, we proposed that CD44 HABD could bind additionally to a different ligand than HA. To catch this putative EC target of CD44-3MUT we used GST pull-down from HUVEC lysate. When we identified the 50–60-kD protein consistently co-precipitating with GST-CD44-3MUT by MALDI-TOF-MS fingerprinting, we found intermediate filament protein vimentin. Vimentin is considered as a common contaminant in mass spectrometry analyses. Nevertheless, vimentin band persisted in CD44-3MUT pull-downs. Therefore, we decided to verify this interaction, further motivated by Mor-Vaknin et al., 2003 publication which showed that vimentin can be secreted by activated macrophages. To confirm CD44-HABD binding to vimentin, we performed pull-down assay using purified vimentin and found that both CD44-HABD and CD44-3MUT bind vimentin directly (Publication II, Figure 1). To test full-length CD44 and vimentin association, we co-immunoprecipitated endogenous CD44–vimentin complex from HUVEC lysate and this complex was also present when both proteins were overexpressed in vimentin nonexpressing MCF7 cells.

Several independent findings make CD44–vimentin interaction spaciotemporally possible. *First*, number of reports show that CD44 and vimentin are both present in membrane lipid rafts in different cell models (Oliferenko et al., 1999, Runembert et al., 2002, Thankamony and Knudson, 2006); *second*, CD44 and vimentin localize to clathrin independent carrier vesicles (Howes et al., 2010), which contain, among others, already known vimentin cargo integrin $\beta 1$.

Cell surface vimentin is a well-known phenomenon without any known function – when we overexpressed vimentin in MCF7 cells, it was biochemically detectable on the surface of living cells (Publication II, Figure S1). Naturally, HUVEC with high endogenous vimentin level express it in the cell surface. When serum starved HUVEC were induced with VEGF, CD44-3MUT could pull-down extracellular vimentin (Publication II, Figure 3). The latter is directly related to another our finding that CD44-3MUT binding to HUVEC increased in response to growth factor stimulation. Thus, our results are consistent with findings showing that vimentin is detected on the surface of malignant lymphocytes, activated macrophages and platelets (Huet et al., 2006, Mor-Vaknin et al., 2003, Podor et al., 2002). Vimentin provides bacterial binding sites on the surface of human brain endothelial cells

(Zou et al., 2006). Importantly, vimentin is expressed on the surface of angiogenic blood vessels, as it is induced in tumor vasculature and is accessible to antibody treatment (van Beijnum et al., 2006). Physiological relevance of the interaction is further suggested, by our findings that vimentin provides specific cell surface binding site for CD44-3MUT (Publication II, Figure 3), along with the fact that soluble CD44 is present in circulation in considerable amount.

Using vimentin deletion mutants we mapped CD44 HABD binding site to the vimentin head domain (Publication II, Figure 2). *In vitro* dissociation constant using full length vimentin was in 12–74 nM range measured by two different methods (Publication II, Table 1 and 2). Isothermal titration calorimetry showed 12–37 nM Kd in solution, which was 2–5 times higher, than affinity obtained by surface plasmon resonance. Such difference between these methods can be explained either by limited dynamics of the immobilized vimentin or by sterical interferences in the SPR chip environment. Importantly, stoichiometry of the CD44-3MUT:vimentin complex was approximately 1:8. This is consistent with the vimentin filament structure and our finding that CD44 binds to vimentin head domain. Vimentin head-domain is essential for filament formation, as "head-less" vimentin does not oligomerize beyond dimer (Chernyatina et al., 2012). Head-domain interactions include ankyrin binding at the plasma membrane (Aziz et al., 2010, Georgatos et al., 1985).

Vimentin IF model seems to imply that some of the head domains stick out beyond filament or ULF surface. Vimentin forms a nonpolar 32-meric unit-length filaments consisting of 16 dimers or 8 tetramers (Sokolova et al., 2006). The stoichiometry of 6–10 moles of vimentin per one mole CD44-3MUT probably reflects the number of head domains available on the ULF surface. The exact model of vimentin binding by CD44 or whether its binding site coincides with the HA binding surface is not known. However, our data show that in CD44 molecule intact HA binding site is not necessary for vimentin binding.

6 Endocytosis of CD44-HABD and CD44-3MUT by endothelial cells (Publication II)

Plasma membrane CD44 is largely endocytosed via clathrin independent carriers in migrating fibroblasts (Howes et al., 2010). Accordingly, based on or finding that vimentin provides specific binding site for CD44-3MUT on ECs, we decided to test whether CD44-3MUT becomes endocytosed. We incubated HUVEC with CD44-3MUT for 30 min to allow internalization and detected endocytosed protein using mouse monoclonal antibody raised against CD44-3MUT (Publication II, Figure S2). We found that CD44-3MUT was indeed endocytosed and displayed a vesicular localization pattern in the cytoplasm of ECs. Next, we used CD44-HABD and CD44-3MUT directly conjugated to Alexa Fluor fluorochrome to track their endocytosis. Fluorescence-conjugated CD44-HABD and CD44-3MUT were endocytosed and distributed in HUVEC cytoplasm similarly to each other, localized to vesicles with pattern similar to unlabeled CD44-3MUT. Co-staining with endocytosis marker showed that freshly endocytosed CD44-3MUT was targeted mostly to EEA1-positive early endosomes – 10 min after start of incubation 30% of the EEA1-positive vesicles were CD44-3MUT-positive, but EEA1 colocalization waned rapidly and 20 min later only 10% EEA1 vesicles colocalized with CD44-3MUT. However, 90 min after CD44-3MUT pulse cells were essentially free of detectable CD44-3MUT (Taavi Päll, unpublished results). The fate of endocytosed CD44-3MUT was probably lysosomal degradation. However, we could not observe accumulation or colocalization of CD44-3MUT in CD63-positive late endosomal compartment or in the juxtanuclear area, corresponding to trans-Golgi network. This is compatible also with rapid recycling back to the plasma membrane from early endosomes, but then we should probably see the fluorescent signal to persist much longer.

HUVEC express vimentin at high level and endocytosed CD44-3MUT-containing vesicles were surrounded by a dense network of vimentin IF. However, we did not observe extensive colocalization of CD44-3MUT with vimentin filaments. Cytoplasmic vimentin is present in different forms – long filaments, short squiggles or particles. Filaments are mainly concentrated around nucleus, in cell trailing edge and tail. Squiggles are located near filament tips at the lamellipodium border and vimentin particles localize in lamellipodium (Prahlad et al., 1998). The nature of directly membranes-associated or -embedded vimentin is not known. Based on fluorescence microscopy data, we suggest that its not filamentous, but rather dimers-tetramers.

To test directly whether vimentin mediates CD44-3MUT internalization, first we isolated lung endothelial cells from wt or *Vim* KO mice. Initially, we also attempted to suppress vimentin expression in HUVEC using siRNA. Nevertheless, due to very high expression and/or functional significance, vimentin silencing caused apoptosis and was overall not effective. Characterization of isolated MLEC for EC-specific cell surface markers by flow cytometry showed that PECAM-1 and CD44 were expressed on *Vim* KO MLEC at levels comparable to wt cells. However, we found that ICAM-2 expression was reduced on *Vim* KO MLEC compared to wt cells. Previously, it has been shown reduced ICAM-1 and VCAM-1 in isolated mouse skin ECs (Nieminen et al., 2006). Together, these data indicate defective plasma membrane trafficking of adhesion receptors in *Vim* KOs. Specific defect in receptor-mediated endocytosis can be ruled out, as *Vim* KO cells show normal transferrin receptor level and distribution (Faigle et al., 2000, Styers et al., 2004). Nevertheless, our endocytosis assays using fluorescence-labeled CD44-3MUT showed that, while wt MLEC endocytosed CD44-3MUT comparably to HUVEC after 30 min uptake, CD44-3MUT uptake by MLECs isolated from *Vim* KO mice was clearly reduced (Publication II, Figure 6). Together our data demonstrate that CD44-3MUT is endocytosed following binding to plasma membrane and localizes transiently to early endosomes, whereas CD44-3MUT EC uptake is covered by the presence of vimentin.

CONCLUSIONS

1. Human recombinant CD44 HABD and its non-hyaluronan binding triple-mutant can be efficiently expressed and purified from bacterial system.
2. CD44-HABD and CD44-3MUT inhibit angiogenesis in chick CAM and aortic fragment models.
3. antiangiogenesis effect of CD44-HABD and CD44-3MUT is independent of hyaluronan binding function.
4. CD44-HABD and CD44-3MUT inhibit human tumor xenograft growth in mice, showing that this is also independent of hyaluronan binding function.
5. Tumor growth inhibition associated with reduced vascular density, suggesting that the effect is caused by suppressed angiogenesis.
6. antiangiogenic effect of CD44-HABD and CD44-3MUT is caused by inhibition of EC proliferation.
7. CD44-HABD and CD44-3MUT bind directly to EC and are endocytosed.
8. Vimentin binds and mediates endocytosis of CD44-HABD and CD44-3MUT.

REFERENCES

Ahrens, T., J. P. Sleeman, C. M. Schempp, N. Howells, M. Hofmann, H. Ponta, P. Herrlich, and J. C. Simon (2001). Soluble CD44 inhibits melanoma tumor growth by blocking cell surface CD44 binding to hyaluronic acid. *Oncogene 20*(26), 3399–408.

Ariel, A., O. Lider, A. Brill, L. Cahalon, N. Savion, D. Varon, and R. Hershkoviz (2000). Induction of interactions between CD44 and hyaluronic acid by a short exposure of human T cells to diverse pro-inflammatory mediators. *Immunology 100*(3), 345–51.

Avigdor, A., P. Goichberg, S. Shivtiel, A. Dar, A. Peled, S. Samira, O. Kollet, R. Hershkoviz, R. Alon, I. Hardan, H. Ben-Hur, D. Naor, A. Nagler, and T. Lapidot (2004). CD44 and hyaluronic acid cooperate with SDF-1 in the trafficking of human CD34+ stem/progenitor cells to bone marrow. *Blood 103*(8), 2981–9.

Avraamides, C. J., B. Garmy-Susini, and J. A. Varner (2008). Integrins in angiogenesis and lymphangiogenesis. *Nat Rev Cancer 8*(8), 604–17.

Aziz, A., J. F. Hess, M. S. Budamagunta, J. C. Voss, and P. G. Fitzgerald (2010). Site-directed spin labeling and electron paramagnetic resonance determination of vimentin head domain structure. *J Biol Chem 285*(20), 15278–85.

Bajorath, J., B. Greenfield, S. Munro, A. Day, and A. Aruffo (1998). Identification of CD44 residues important for hyaluronan binding and delineation of the binding site. *J Biol Chem 273*(1), 338–343.

Banerji, S., A. Day, J. Kahmann, and D. Jackson (1998). Characterization of a functional hyaluronan-binding domain from the human CD44 molecule expressed in Escherichia coli. *Protein Expr Purif 14*(3), 371–381.

Banerji, S., A. J. Wright, M. Noble, D. J. Mahoney, I. D. Campbell, A. J. Day, and D. G. Jackson (2007). Structures of the Cd44-hyaluronan complex provide insight into a fundamental carbohydrate-protein interaction. *Nat Struct Mol Biol 14*(3), 234–9.

BenderMedSystems (2012). *Human sCD44std Platinum ELISA*. Campus Vienna Biocenter 2, 1030 Vienna, Austria: Bender MedSystems GmbH. 09.07.12 (25).

Benny, O., O. Fainaru, A. Adini, F. Cassiola, L. Bazinet, I. Adini, E. Pravda, Y. Nahmias, S. Koirala, G. Corfas, R. J. D'Amato, and J. Folkman (2008). An orally delivered small-molecule formulation with antiangiogenic and anticancer activity. *Nat Biotechnol 26*(7), 799–807.

Bergers, G. and L. E. Benjamin (2003). Tumorigenesis and the angiogenic switch.

Nat Rev Cancer 3(6), 401–10.

Bhattacharya, R., A. M. Gonzalez, P. J. DeBiase, H. E. Trejo, R. D. Goldman, F. W. Flitney, and J. C. R. Jones (2009). Recruitment of vimentin to the cell surface by $\beta 3$ integrin and plectin mediates adhesion strength. *J Cell Sci 122*(9), 1390–1400.

Boilard, E., S. G. Bourgoin, C. Bernatchez, and M. E. Surette (2003). Identification of an autoantigen on the surface of apoptotic human T cells as a new protein interacting with inflammatory group IIA phospholipase A2. *Blood 102*(8), 2901–9.

Bonder, C. S., S. R. Clark, M. U. Norman, P. Johnson, and P. Kubes (2006). Use of CD44 by CD4+ Th1 and Th2 lymphocytes to roll and adhere. *Blood 107*(12), 4798–806.

Booth, B. (2012). Cancer Drug Targets: The March of the Lemmings.

Bourguignon, L. Y. W., M. Ramez, E. Gilad, P. A. Singleton, M.-Q. Man, D. A. Crumrine, P. M. Elias, and K. R. Feingold (2006). Hyaluronan-CD44 interaction stimulates keratinocyte differentiation, lamellar body formation/secretion, and permeability barrier homeostasis. *J Invest Dermatol 126*(6), 1356–65.

Brooks, P. C., S. Silletti, T. L. von Schalscha, M. Friedlander, and D. A. Cheresh (1998). Disruption of angiogenesis by PEX, a noncatalytic metalloproteinase fragment with integrin binding activity. *Cell 92*(3), 391–400.

Brooks, P. C., S. Strömblad, L. C. Sanders, T. L. von Schalscha, R. T. Aimes, W. G. Stetler-Stevenson, J. P. Quigley, and D. A. Cheresh (1996). Localization of matrix metalloproteinase MMP-2 to the surface of invasive cells by interaction with integrin αvβ3. *Cell 85*(5), 683–93.

Burgstaller, G., M. Gregor, L. Winter, and G. Wiche (2010). Keeping the vimentin network under control: cell-matrix adhesion-associated plectin 1f affects cell shape and polarity of fibroblasts. *Mol Biol Cell 21*(19), 3362–75.

Cao, G., C. D. O'Brien, Z. Zhou, S. M. Sanders, J. N. Greenbaum, A. Makrigiannakis, and H. M. DeLisser (2002). Involvement of human PECAM-1 in angiogenesis and in vitro endothelial cell migration. *Am J Physiol Cell Physiol 282*(5), C1181–90.

Cao, G., R. C. Savani, M. Fehrenbach, C. Lyons, L. Zhang, G. Coukos, and H. M. Delisser (2006). Involvement of endothelial CD44 during in vivo angiogenesis. *Am J Pathol 169*(1), 325–36.

Carmeliet, P. and R. K. Jain (2011). Molecular mechanisms and clinical applications of angiogenesis. *Nature 473*(7347), 298–307.

Casanovas, O., D. J. Hicklin, G. Bergers, and D. Hanahan (2005). Drug resistance by evasion of antiangiogenic targeting of VEGF signaling in late-stage pancreatic islet tumors. *Cancer Cell 8*(4), 299–309.

Chernyatina, A. A., S. Nicolet, U. Aebi, H. Herrmann, and S. V. Strelkov (2012). Atomic structure of the vimentin central Îś-helical domain and its implications for intermediate filament assembly. *Proc Natl Acad Sci U S A 109*(34), 13620–5.

Christoffersson, G., E. Vågesjö, J. Vandooren, M. Lidén, S. Massena, R. B. Reinert, M. Brissova, A. C. Powers, G. Opdenakker, and M. Phillipson (2012). VEGF-A recruits a proangiogenic MMP-9-delivering neutrophil subset that induces angiogenesis in transplanted hypoxic tissue. *Blood 120*(23), 4653–62.

Chun, T.-H., F. Sabeh, I. Ota, H. Murphy, K. T. McDonagh, K. Holmbeck, H. Birkedal-Hansen, E. D. Allen, and S. J. Weiss (2004). MT1-MMP-dependent neovessel formation within the confines of the three-dimensional extracellular matrix. *J Cell Biol 167*(4), 757–67.

Cichy, J., R. Bals, J. Potempa, A. Mani, and E. Puré (2002). Proteinase-mediated release of epithelial cell-associated CD44. Extracellular CD44 complexes with components of cellular matrices. *J Biol Chem 277*(46), 44440–7.

Colucci-Guyon, E., M. Portier, I. Dunia, D. Paulin, S. Pournin, and C. Babinet (1994). Mice lacking vimentin develop and reproduce without an obvious phenotype. *Cell 79*(4), 679–694.

Cuff, C. A., D. Kothapalli, I. Azonobi, S. Chun, Y. Zhang, R. Belkin, C. Yeh, A. Secreto, R. K. Assoian, D. J. Rader, and E. Puré (2001). The adhesion receptor CD44 promotes atherosclerosis by mediating inflammatory cell recruitment and vascular cell activation. *J Clin Invest 108*(7), 1031–40.

Deed, R., P. Rooney, P. Kumar, J. D. Norton, J. Smith, A. J. Freemont, and S. Kumar (1997). Early-response gene signalling is induced by angiogenic oligosaccharides of hyaluronan in endothelial cells. Inhibition by non-angiogenic, high-molecular-weight hyaluronan. *Int J Cancer 71*(2), 251–6.

Del Bufalo, D., L. Ciuffreda, D. Trisciuoglio, M. Desideri, F. Cognetti, G. Zupi, and M. Milella (2006). Antiangiogenic potential of the Mammalian target of rapamycin inhibitor temsirolimus. *Cancer Res 66*(11), 5549–54.

DeLisser, H. M., M. Christofidou-Solomidou, R. M. Strieter, M. D. Burdick, C. S. Robinson, R. S. Wexler, J. S. Kerr, C. Garlanda, J. R. Merwin, J. A. Madri, and S. M. Albelda (1997). Involvement of endothelial PECAM-1/CD31 in angiogenesis. *Am J Pathol 151*(3), 671–7.

Dimitroff, C. J., J. Y. Lee, S. Rafii, R. C. Fuhlbrigge, and R. Sackstein (2001).

CD44 is a major E-selectin ligand on human hematopoietic progenitor cells. *J Cell Biol 153*(6), 1277–86.

Dings, R. P. M., M. Loren, H. Heun, E. McNiel, A. W. Griffioen, K. H. Mayo, and R. J. Griffin (2007). Scheduling of radiation with angiogenesis inhibitors anginex and Avastin improves therapeutic outcome via vessel normalization. *Clin Cancer Res 13*(11), 3395–402.

Ebos, J. M. L., C. R. Lee, W. Cruz-Munoz, G. A. Bjarnason, J. G. Christensen, and R. S. Kerbel (2009). Accelerated metastasis after short-term treatment with a potent inhibitor of tumor angiogenesis. *Cancer Cell 15*(3), 232–9.

Eckes, B., D. Dogic, E. Colucci-Guyon, N. Wang, A. Maniotis, D. Ingber, A. Merckling, F. Langa, M. Aumailley, A. Delouvée, V. Koteliansky, C. Babinet, and T. Krieg (1998). Impaired mechanical stability, migration and contractile capacity in vimentin-deficient fibroblasts. *J Cell Sci 111*, 1897–907.

English, N. M., J. F. Lesley, and R. Hyman (1998). Site-specific de-N-glycosylation of CD44 can activate hyaluronan binding, and CD44 activation states show distinct threshold densities for hyaluronan binding. *Cancer Res 58*(16), 3736–42.

Escudier, B. (2007). Advanced renal cell carcinoma: current and emerging management strategies. *Drugs 67*(9), 1257–64.

Faigle, W., E. Colucci-Guyon, D. Louvard, S. Amigorena, and T. Galli (2000). Vimentin filaments in fibroblasts are a reservoir for SNAP23, a component of the membrane fusion machinery. *Mol Biol Cell 11*(10), 3485–94.

FDA (2011). Proposal to Withdraw Approval for the Breast Cancer Indication for AVASTIN (Bevacizumab).

Fischer, C., B. Jonckx, M. Mazzone, S. Zacchigna, S. Loges, L. Pattarini, E. Chorianopoulos, L. Liesenborghs, M. Koch, M. De Mol, M. Autiero, S. Wyns, S. Plaisance, L. Moons, N. van Rooijen, M. Giacca, J.-M. Stassen, M. Dewerchin, D. Collen, and P. Carmeliet (2007). Anti-PlGF inhibits growth of VEGF(R)-inhibitor-resistant tumors without affecting healthy vessels. *Cell 131*(3), 463–75.

Flynn, K. M., M. Michaud, S. Canosa, and J. A. Madri (2013). CD44 regulates vascular endothelial barrier integrity via a PECAM-1 dependent mechanism. *Angiogenesis*, doi:10.1007/s10456–013–9346–9.

Franzmann, E. J., E. P. Reategui, F. Pedroso, F. G. Pernas, B. M. Karakullukcu, K. L. Carraway, K. Hamilton, R. Singal, and W. J. Goodwin (2007). Soluble CD44 is a potential marker for the early detection of head and neck cancer.

Cancer Epidemiol Biomarkers Prev 16(7), 1348–55.

Friedman, H. S., M. D. Prados, P. Y. Wen, T. Mikkelsen, D. Schiff, L. E. Abrey, W. K. A. Yung, N. Paleologos, M. K. Nicholas, R. Jensen, J. Vredenburgh, J. Huang, M. Zheng, and T. Cloughesy (2009). Bevacizumab alone and in combination with irinotecan in recurrent glioblastoma. *J Clin Oncol 27*(28), 4733–40.

Frost, P., F. Moatamed, B. Hoang, Y. Shi, J. Gera, H. Yan, P. Frost, J. Gibbons, and A. Lichtenstein (2004). In vivo antitumor effects of the mTOR inhibitor CCI-779 against human multiple myeloma cells in a xenograft model. *Blood 104*(13), 4181–7.

Gambaletta, D., A. Marchetti, L. Benedetti, A. M. Mercurio, A. Sacchi, and R. Falcioni (2000). Cooperative signaling between $\alpha(6)\beta(4)$ integrin and ErbB-2 receptor is required to promote phosphatidylinositol 3-kinase-dependent invasion. *J Biol Chem 275*(14), 10604–10.

Gao, C., H. Guo, L. Downey, C. Marroquin, J. Wei, and P. C. Kuo (2003). Osteopontin-dependent CD44v6 expression and cell adhesion in HepG2 cells. *Carcinogenesis 24*(12), 1871–8.

Garton, K. J., P. J. Gough, and E. W. Raines (2006). Emerging roles for ectodomain shedding in the regulation of inflammatory responses. *J Leukoc Biol 79*(6), 1105–16.

Geiger, B., J. P. Spatz, and A. D. Bershadsky (2009). Environmental sensing through focal adhesions. *Nat Rev Mol Cell Biol 10*(1), 21–33.

Georgatos, S. D., D. C. Weaver, and V. T. Marchesi (1985). Site specificity in vimentin-membrane interactions: intermediate filament subunits associate with the plasma membrane via their head domains. *J Cell Biol 100*(6), 1962–7.

Godar, S. and R. A. Weinberg (2008). Filling the mosaic of p53 actions: p53 represses RHAMM expression. *Cell Cycle 7*(22), 3479.

Gonzales, M., B. Weksler, D. Tsuruta, R. D. Goldman, K. J. Yoon, S. B. Hopkinson, F. W. Flitney, and J. C. Jones (2001). Structure and function of a vimentin-associated matrix adhesion in endothelial cells. *Mol Biol Cell 12*(1), 85–100.

Gragoudas, E. S., A. P. Adamis, E. T. J. Cunningham, M. Feinsod, and D. R. Guyer (2004). Pegaptanib for neovascular age-related macular degeneration. *N Engl J Med 351*(27), 2805–16.

Griffioen, A. W., M. J. Coenen, C. A. Damen, S. M. Hellwig, D. H. van Weering, W. Vooys, G. H. Blijham, and G. Groenewegen (1997). CD44 is involved in tumor angiogenesis; an activation antigen on human endothelial cells. *Blood 90*(3), 1150–9.

Günthert, U., M. Hofmann, W. Rudy, S. Reber, M. Zöller, I. Haussmann, S. Matzku, A. Wenzel, H. Ponta, and P. Herrlich (1991). A new variant of glycoprotein CD44 confers metastatic potential to rat carcinoma cells. *Cell 65*(1), 13–24.

Guo, Y. J., G. Liu, X. Wang, D. Jin, M. Wu, J. Ma, and M. S. Sy (1994). Potential use of soluble CD44 in serum as indicator of tumor burden and metastasis in patients with gastric or colon cancer. *Cancer Res 54*(2), 422–6.

Harada, N., T. Mizoi, M. Kinouchi, K. Hoshi, S. Ishii, K. Shiiba, I. Sasaki, and S. Matsuno (2001). Introduction of antisense CD44S CDNA down-regulates expression of overall CD44 isoforms and inhibits tumor growth and metastasis in highly metastatic colon carcinoma cells. *Int J Cancer 91*(1), 67–75.

Helfrich, I., I. Scheffrahn, S. Bartling, J. Weis, V. von Felbert, M. Middleton, M. Kato, S. Ergün, and D. Schadendorf (2010). Resistance to antiangiogenic therapy is directed by vascular phenotype, vessel stabilization, and maturation in malignant melanoma. *J Exp Med 207*(3), 491–503.

Henrion, D., F. Terzi, K. Matrougui, M. Duriez, C. M. Boulanger, E. Colucci-Guyon, C. Babinet, P. Briand, G. Friedlander, P. Poitevin, and B. I. Lévy (1997). Impaired flow-induced dilation in mesenteric resistance arteries from mice lacking vimentin. *J Clin Invest 100*(11), 2909–14.

Hiratsuka, S., D. G. Duda, Y. Huang, S. Goel, T. Sugiyama, T. Nagasawa, D. Fukumura, and R. K. Jain (2011). C-X-C receptor type 4 promotes metastasis by activating p38 mitogen-activated protein kinase in myeloid differentiation antigen (Gr-1)-positive cells. *Proc Natl Acad Sci U S A 108*(1), 302–7.

Hollingsworth, J. W., Z. Li, D. M. Brass, S. Garantziotis, S. H. Timberlake, A. Kim, I. Hossain, R. C. Savani, and D. A. Schwartz (2007). CD44 regulates macrophage recruitment to the lung in lipopolysaccharide-induced airway disease. *Am J Respir Cell Mol Biol 37*(2), 248–53.

Holmgren, L., M. S. O'Reilly, and J. Folkman (1995). Dormancy of micrometastases: balanced proliferation and apoptosis in the presence of angiogenesis suppression. *Nat Med 1*(2), 149–53.

Homan, S. M., R. Martinez, A. Benware, and S. E. LaFlamme (2002). Regulation of the association of $\alpha 6 \beta 4$ with vimentin intermediate filaments in endothelial cells. *Exp Cell Res 281*(1), 107–114.

Homan, S. M., A. M. Mercurio, and S. E. LaFlamme (1998). Endothelial cells assemble two distinct $\alpha 6 \beta 4$-containing vimentin-associated structures: roles for ligand binding and the $\beta 4$ cytoplasmic tail. *J Cell Sci 111*, 2717–28.

Hotary, K. B., E. D. Allen, P. C. Brooks, N. S. Datta, M. W. Long, and S. J. Weiss (2003). Membrane type I matrix metalloproteinase usurps tumor growth control imposed by the three-dimensional extracellular matrix. *Cell 114*(1), 33–45.

Howes, M. T., M. Kirkham, J. Riches, K. Cortese, P. J. Walser, F. Simpson, M. M. Hill, A. Jones, R. Lundmark, M. R. Lindsay, D. J. Hernandez-Deviez, G. Hadzic, A. McCluskey, R. Bashir, L. Liu, P. Pilch, H. McMahon, P. J. Robinson, J. F. Hancock, S. Mayor, and R. G. Parton (2010). Clathrin-independent carriers form a high capacity endocytic sorting system at the leading edge of migrating cells. *J Cell Biol 190*(4), 675–91.

Huet, D., M. Bagot, D. Loyaux, J. Capdevielle, L. Conraux, P. Ferrara, A. Bensussan, and A. Marie-Cardine (2006). SC5 mAb represents a unique tool for the detection of extracellular vimentin as a specific marker of Sezary cells. *J Immunol 176*(1), 652–9.

Hurwitz, H., L. Fehrenbacher, W. Novotny, T. Cartwright, J. Hainsworth, W. Heim, J. Berlin, A. Baron, S. Griffing, E. Holmgren, N. Ferrara, G. Fyfe, B. Rogers, R. Ross, and F. Kabbinavar (2004). Bevacizumab plus irinotecan, fluorouracil, and leucovorin for metastatic colorectal cancer. *N Engl J Med 350*(23), 2335–42.

Hutás, G., E. Bajnok, I. Gál, A. Finnegan, T. T. Glant, and K. Mikecz (2008). CD44-specific antibody treatment and CD44 deficiency exert distinct effects on leukocyte recruitment in experimental arthritis. *Blood 112*(13), 4999–5006.

Ivaska, J., K. Vuoriluoto, T. Huovinen, I. Izawa, M. Inagaki, and P. J. Parker (2005). PKC epsilon-mediated phosphorylation of vimentin controls integrin recycling and motility. *EMBO J 24*(22), 3834–3845.

Jackson, D. E., C. M. Ward, R. Wang, and P. J. Newman (1997). The protein-tyrosine phosphatase SHP-2 binds platelet/endothelial cell adhesion molecule-1 (PECAM-1) and forms a distinct signaling complex during platelet aggregation. Evidence for a mechanistic link between PECAM-1- and integrin-mediated cellular signaling. *J Biol Chem 272*(11), 6986–93.

Jahangiri, A., M. De Lay, L. M. Miller, W. S. Carbonell, Y.-L. Hu, K. Lu, M. W. Tom, J. Paquette, T. A. Tokuyasu, S. Tsao, R. Marshall, A. Perry, K. M. Bjorgan, M. M. Chaumeil, S. M. Ronen, G. Bergers, and M. K. Aghi (2013). Gene expression profile identifies tyrosine kinase c-Met as a targetable mediator of antiangiogenic therapy resistance. *Clin Cancer Res 19*(7), 1773–83.

Johnson, D. H., L. Fehrenbacher, W. F. Novotny, R. S. Herbst, J. J. Nemunaitis, D. M. Jablons, C. J. Langer, R. F. r. DeVore, J. Gaudreault, L. A. Damico, E. Holmgren, and F. Kabbinavar (2004). Randomized phase II trial comparing bevacizumab plus carboplatin and paclitaxel with carboplatin and paclitaxel alone in previously untreated locally advanced or metastatic non-small-cell lung cancer. *J Clin Oncol 22*(11), 2184–91.

Kajita, M., Y. Itoh, T. Chiba, H. Mori, A. Okada, H. Kinoh, and M. Seiki (2001). Membrane-type 1 matrix metalloproteinase cleaves CD44 and promotes cell migration. *J Cell Biol 153*(5), 893–904.

Katayama, Y., A. Hidalgo, J. Chang, A. Peired, and P. S. Frenette (2005). CD44 is a physiological E-selectin ligand on neutrophils. *J Exp Med 201*(8), 1183–9.

Katoh, S., J. B. McCarthy, and P. W. Kincade (1994). Characterization of soluble CD44 in the circulation of mice. Levels are affected by immune activity and tumor growth. *J Immunol 153*(8), 3440–9.

Kaya, G., I. Rodriguez, J. L. Jorcano, P. Vassalli, and I. Stamenkovic (1997). Selective suppression of CD44 in keratinocytes of mice bearing an antisense CD44 transgene driven by a tissue-specific promoter disrupts hyaluronate metabolism in the skin and impairs keratinocyte proliferation. *Genes Dev 11*(8), 996–1007.

Keunen, O., M. Johansson, A. Oudin, M. Sanzey, S. A. A. Rahim, F. Fack, F. Thorsen, T. Taxt, M. Bartos, R. Jirik, H. Miletic, J. Wang, D. Stieber, L. Stuhr, I. Moen, C. B. Rygh, R. Bjerkvig, and S. P. Niclou (2011). Anti-VEGF treatment reduces blood supply and increases tumor cell invasion in glioblastoma. *Proc Natl Acad Sci U S A 108*(9), 3749–54.

Khan, A. I., S. M. Kerfoot, B. Heit, L. Liu, G. Andonegui, B. Ruffell, P. Johnson, and P. Kubes (2004). Role of CD44 and hyaluronan in neutrophil recruitment. *J Immunol 173*(12), 7594–601.

Kirschner, N., M. Haftek, C. M. Niessen, M. J. Behne, M. Furuse, I. Moll, and J. M. Brandner (2011). CD44 regulates tight-junction assembly and barrier function. *J Invest Dermatol 131*(4), 932–43.

Ko, Y. H., H. S. Won, E. K. Jeon, S. H. Hong, S. Y. Roh, Y. S. Hong, J. H. Byun, C.-K. Jung, and J. H. Kang (2011). Prognostic significance of CD44s expression in resected non-small cell lung cancer. *BMC Cancer 11*, 340.

Kodama, K., M. Horikoshi, K. Toda, S. Yamada, K. Hara, J. Irie, M. Sirota, A. A. Morgan, R. Chen, H. Ohtsu, S. Maeda, T. Kadowaki, and A. J. Butte (2012). Expression-based genome-wide association study links the receptor CD44 in adipose tissue with type 2 diabetes. *Proc Natl Acad Sci U S A 109*(18), 7049–54.

Kogerman, P., M. S. Sy, and L. A. Culp (1997a). Counter-selection for overexpressed human CD44s in primary tumors versus lung metastases in a mouse fibrosarcoma model. *Oncogene 15*(12), 1407–16.

Kogerman, P., M. S. Sy, and L. A. Culp (1997b). Overexpressed human CD44s promotes lung colonization during micrometastasis of murine fibrosarcoma cells: facilitated retention in the lung vasculature. *Proc Natl Acad Sci U S A 94*(24), 13233–8.

Kohda, D., C. J. Morton, A. A. Parkar, H. Hatanaka, F. M. Inagaki, I. D. Campbell, and A. J. Day (1996). Solution structure of the link module: a hyaluronan-binding domain involved in extracellular matrix stability and cell migration. *Cell 86*(5), 767–75.

Koivunen, E., W. Arap, H. Valtanen, A. Rainisalo, O. P. Medina, P. Heikkilä, C. Kantor, C. G. Gahmberg, T. Salo, Y. T. Konttinen, T. Sorsa, E. Ruoslahti, and R. Pasqualini (1999). Tumor targeting with a selective gelatinase inhibitor. *Nat Biotechnol 17*(8), 768–74.

Kothapalli, D., L. Zhao, E. A. Hawthorne, Y. Cheng, E. Lee, E. PurÃl', and R. K. Assoian (2007). Hyaluronan and CD44 antagonize mitogen-dependent cyclin D1 expression in mesenchymal cells. *J Cell Biol 176*(4), 535–44.

Leenders, W. P. J., B. Küsters, K. Verrijp, C. Maass, P. Wesseling, A. Heerschap, D. Ruiter, A. Ryan, and R. de Waal (2004). Antiangiogenic therapy of cerebral melanoma metastases results in sustained tumor progression via vessel co-option. *Clin Cancer Res 10*(18 Pt 1), 6222–30.

Lesley, J., N. English, A. Perschl, J. Gregoroff, and R. Hyman (1995). Variant cell lines selected for alterations in the function of the hyaluronan receptor CD44 show differences in glycosylation. *J Exp Med 182*(2), 431–7.

Li, J.-L., R. C. A. Sainson, C. E. Oon, H. Turley, R. Leek, H. Sheldon, E. Bridges, W. Shi, C. Snell, E. T. Bowden, H. Wu, P. S. Chowdhury, A. J. Russell, C. P. Montgomery, R. Poulsom, and A. L. Harris (2011). DLL4-Notch signaling mediates tumor resistance to anti-VEGF therapy in vivo. *Cancer Res 71*(18), 6073–83.

Li, J.-L., R. C. A. Sainson, W. Shi, R. Leek, L. S. Harrington, M. Preusser, S. Biswas, H. Turley, E. Heikamp, J. A. Hainfellner, and A. L. Harris (2007). Delta-like 4 Notch ligand regulates tumor angiogenesis, improves tumor vascular function, and promotes tumor growth in vivo. *Cancer Res 67*(23), 11244–53.

Lim, S., A. Young, G. Paner, and M. Amin (2008). Prognostic role of CD44 cell adhesion molecule expression in primary and metastatic renal cell carcinoma: a clinicopathologic study of 125 cases. *Virchows Arch 452*(1), 49–55.

Lockhart, M. S., C. Waldner, C. Mongini, M. J. Gravisaco, S. Casanova, E. Alvarez, and S. Hajos (1999). Evaluation of soluble CD44 in patients with breast and colorectal carcinomas and non-Hodgkin's lymphoma. *Oncol Rep 6*(5), 1129–33.

Loeffler-Ragg, J., U. Germing, W. R. Sperr, H. Herrmann, H. Zwierzina, P. Valent, H. Ulmer, and R. Stauder (2011). Serum CD44 levels predict survival in patients with low-risk myelodysplastic syndromes. *Crit Rev Oncol Hematol 78*(2), 150–61.

Loges, S., T. Schmidt, and P. Carmeliet (2010). Mechanisms of resistance to anti-angiogenic therapy and development of third-generation anti-angiogenic drug candidates. *Genes Cancer 1*(1), 12–25.

Lopez, J. I., T. D. Camenisch, M. V. Stevens, B. J. Sands, J. McDonald, and J. A. Schroeder (2005). CD44 attenuates metastatic invasion during breast cancer progression. *Cancer Res 65*(15), 6755–63.

Lu, K. V., J. P. Chang, C. A. Parachoniak, M. M. Pandika, M. K. Aghi, D. Meyronet, N. Isachenko, S. D. Fouse, J. J. Phillips, D. A. Cheresh, M. Park, and G. Bergers (2012). VEGF inhibits tumor cell invasion and mesenchymal transition through a MET/VEGFR2 complex. *Cancer Cell 22*(1), 21–35.

Mabuchi, S., D. A. Altomare, D. C. Connolly, A. Klein-Szanto, S. Litwin, M. K. Hoelzle, H. H. Hensley, T. C. Hamilton, and J. R. Testa (2007). RAD001 (Everolimus) delays tumor onset and progression in a transgenic mouse model of ovarian cancer. *Cancer Res 67*(6), 2408–13.

Mäenpää, H., R. Ristamäki, J. Virtamo, K. Franssila, D. Albanes, and H. Joensuu (2000). Serum CD44 levels preceding the diagnosis of non-Hodgkin's lymphoma. *Leuk Lymphoma 37*(5-6), 585–92.

Marroquin, C. E., L. Downey, H. Guo, and P. C. Kuo (2004). Osteopontin increases CD44 expression and cell adhesion in RAW 264.7 murine leukemia cells. *Immunol Lett 95*(1), 109–12.

Mayer, S., A. zur Hausen, D. O. Watermann, S. Stamm, M. Jäger, G. Gitsch, and E. Stickeler (2008). Increased soluble CD44 concentrations are associated with larger tumor size and lymph node metastasis in breast cancer patients. *J Cancer Res Clin Oncol 134*(11), 1229–35.

McDonald, B., E. F. McAvoy, F. Lam, V. Gill, C. de la Motte, R. C. Savani, and P. Kubes (2008). Interaction of CD44 and hyaluronan is the dominant mechanism for neutrophil sequestration in inflamed liver sinusoids. *J Exp Med 205*(4), 915–27.

Mikecz, K., K. Dennis, M. Shi, and J. H. Kim (1999). Modulation of hyaluronan receptor (CD44) function in vivo in a murine model of rheumatoid arthritis. *Arthritis Rheum 42*(4), 659–68.

Miller, K. D., L. I. Chap, F. A. Holmes, M. A. Cobleigh, P. K. Marcom, L. Fehrenbacher, M. Dickler, B. A. Overmoyer, J. D. Reimann, A. P. Sing, V. Langmuir, and H. S. Rugo (2005). Randomized phase III trial of capecitabine compared with bevacizumab plus capecitabine in patients with previously treated metastatic breast cancer. *J Clin Oncol 23*(4), 792–9.

Mor-Vaknin, N., M. Legendre, Y. Yu, C. H. C. Serezani, S. K. Garg, A. Jatzek, M. D. Swanson, M. J. Gonzalez-Hernandez, S. Teitz-Tennenbaum, A. Punturieri, N. C. Engleberg, R. Banerjee, M. Peters-Golden, J. Y. Kao, and D. M. Markovitz (2013). Murine colitis is mediated by vimentin. *Sci Rep 3*, 1045.

Mor-Vaknin, N., A. Punturieri, K. Sitwala, and D. M. Markovitz (2003). Vimentin is secreted by activated macrophages. *Nat Cell Biol 5*(1), 59–63.

Mori, H., T. Tomari, N. Koshikawa, M. Kajita, Y. Itoh, H. Sato, H. Tojo, I. Yana, and M. Seiki (2002). CD44 directs membrane-type 1 matrix metalloproteinase to lamellipodia by associating with its hemopexin-like domain. *EMBO J 21*(15), 3949–59.

Motzer, R. J., T. E. Hutson, P. Tomczak, M. D. Michaelson, R. M. Bukowski, O. Rixe, S. Oudard, S. Negrier, C. Szczylik, S. T. Kim, I. Chen, P. W. Bycott, C. M. Baum, and R. A. Figlin (2007). Sunitinib versus interferon alfa in metastatic renal-cell carcinoma. *N Engl J Med 356*(2), 115–24.

Murakami, D., I. Okamoto, O. Nagano, Y. Kawano, T. Tomita, T. Iwatsubo, B. De Strooper, E. Yumoto, and H. Saya (2003). Presenilin-dependent γ-secretase activity mediates the intramembranous cleavage of CD44. *Oncogene 22*(10), 1511–6.

Nagano, O., D. Murakami, D. Hartmann, B. De Strooper, P. Saftig, T. Iwatsubo, M. Nakajima, M. Shinohara, and H. Saya (2004). Cell-matrix interaction via CD44 is independently regulated by different metalloproteinases activated in response to extracellular Ca(2+) influx and PKC activation. *J Cell Biol 165*(6), 893–902.

Nandi, A., P. Estess, and M. H. Siegelman (2000). Hyaluronan anchoring and regulation on the surface of vascular endothelial cells is mediated through the functionally active form of CD44. *J Biol Chem 275*(20), 14939–48.

Nieminen, M., T. Henttinen, M. Merinen, F. Marttila-Ichihara, J. E. Eriksson, and S. Jalkanen (2006). Vimentin function in lymphocyte adhesion and transcellular migration. *Nat Cell Biol 8*(2), 156–62.

Niitsu, N. and K. Iijima (2002). High serum soluble CD44 is correlated with a poor outcome of aggressive non-Hodgkin's lymphoma. *Leuk Res 26*(3), 241–8.

Nikolopoulos, S. N., P. Blaikie, T. Yoshioka, W. Guo, and F. G. Giancotti (2004). Integrin $\beta 4$ signaling promotes tumor angiogenesis. *Cancer Cell 6*(5), 471–83.

Noordzij, M., G. van Steenbrugge, N. Verkaik, F. Schröder, and T. van der Kwast (1997). The prognostic value of CD44 isoforms in prostate cancer patients treated by radical prostatectomy. *Clin Cancer Res 3*(5), 805–815.

Okamoto, I., Y. Kawano, H. Tsuiki, J. Sasaki, M. Nakao, M. Matsumoto, M. Suga, M. Ando, M. Nakajima, and H. Saya (1999). CD44 cleavage induced by a membrane-associated metalloprotease plays a critical role in tumor cell migration. *Oncogene 18*(7), 1435–46.

Olaku, V., A. Matzke, C. Mitchell, S. Hasenauer, A. Sakkaravarthi, G. Pace, H. Ponta, and V. Orian-Rousseau (2011). c-Met recruits ICAM-1 as a coreceptor to compensate for the loss of CD44 in Cd44 null mice. *Mol Biol Cell 22*(15), 2777–86.

Oliferenko, S., K. Paiha, T. Harder, V. Gerke, C. Schwärzler, H. Schwarz, H. Beug, U. Günthert, and L. A. Huber (1999). Analysis of CD44-containing lipid rafts: Recruitment of annexin II and stabilization by the actin cytoskeleton. *J Cell Biol 146*(4), 843–54.

O'Reilly, M. S., L. Holmgren, C. Chen, and J. Folkman (1996). Angiostatin induces and sustains dormancy of human primary tumors in mice. *Nat Med 2*(6), 689–92.

Ouellette, T., S. Destrau, T. Ouellette, J. Zhu, J. M. Roach, J. D. Coffman, T. Hecht, J. E. Lynch, and S. L. Giardina (2003). Production and purification of refolded recombinant human IL-7 from inclusion bodies. *Protein Expr Purif 30*(2), 156–66.

Peach, R. J., D. Hollenbaugh, I. Stamenkovic, and A. Aruffo (1993). Identification of hyaluronic acid binding sites in the extracellular domain of CD44. *J Cell Biol 122*(1), 257–64.

Pegtel, D. M., S. I. J. Ellenbroek, A. E. E. Mertens, R. A. van der Kammen, J. de Rooij, and J. G. Collard (2007). The Par-Tiam1 complex controls persistent migration by stabilizing microtubule-dependent front-rear polarity. *Curr Biol 17*(19), 1623–34.

Perrotte, P., T. Matsumoto, K. Inoue, H. Kuniyasu, B. Y. Eve, D. J. Hicklin, R. Radinsky, and C. P. Dinney (1999). Anti-epidermal growth factor receptor antibody C225 inhibits angiogenesis in human transitional cell carcinoma growing orthotopically in nude mice. *Clin Cancer Res 5*(2), 257–65.

Pezzella, F., U. Pastorino, E. Tagliabue, S. Andreola, G. Sozzi, G. Gasparini,

S. Menard, K. C. Gatter, A. L. Harris, S. Fox, M. Buyse, S. Pilotti, M. Pierotti, and F. Rilke (1997). Non-small-cell lung carcinoma tumor growth without morphological evidence of neo-angiogenesis. *Am J Pathol 151*(5), 1417–23.

Phua, D. C. Y., P. O. Humbert, and W. Hunziker (2009). Vimentin regulates scribble activity by protecting it from proteasomal degradation. *Mol Biol Cell 20*(12), 2841–55.

Pietras, K., J. Pahler, G. Bergers, and D. Hanahan (2008). Functions of paracrine PDGF signaling in the proangiogenic tumor stroma revealed by pharmacological targeting. *PLoS Med 5*(1), e19.

Podor, T. J., D. Singh, P. Chindemi, D. M. Foulon, R. McKelvie, J. I. Weitz, R. Austin, G. Boudreau, and R. Davies (2002). Vimentin exposed on activated platelets and platelet microparticles localizes vitronectin and plasminogen activator inhibitor complexes on their surface. *J Biol Chem 277*(9), 7529–39.

Pore, N., Z. Jiang, A. Gupta, G. Cerniglia, G. D. Kao, and A. Maity (2006). EGFR tyrosine kinase inhibitors decrease VEGF expression by both hypoxia-inducible factor (HIF)-1-independent and HIF-1-dependent mechanisms. *Cancer Res 66*(6), 3197–204.

Prahlad, V., M. Yoon, R. D. Moir, R. D. Vale, and R. D. Goldman (1998). Rapid movements of vimentin on microtubule tracks: kinesin-dependent assembly of intermediate filament networks. *J Cell Biol 143*(1), 159–70.

Protin, U., T. Schweighoffer, W. Jochum, and F. Hilberg (1999). CD44-deficient mice develop normally with changes in subpopulations and recirculation of lymphocyte subsets. *J Immunol 163*(9), 4917–23.

Pueyo, G., R. Mesia, A. Figueras, A. Lozano, M. Baro, S. Vazquez, G. Capella, and J. Balart (2010). Cetuximab may inhibit tumor growth and angiogenesis induced by ionizing radiation: a preclinical rationale for maintenance treatment after radiotherapy. *Oncologist 15*(9), 976–86.

Ristamäki, R., H. Joensuu, M. Salmi, and S. Jalkanen (1994). Serum CD44 in malignant lymphoma: an association with treatment response. *Blood 84*(1), 238–43.

Rosenfeld, P. J., D. M. Brown, J. S. Heier, D. S. Boyer, P. K. Kaiser, C. Y. Chung, and R. Y. Kim (2006). Ranibizumab for neovascular age-related macular degeneration. *N Engl J Med 355*(14), 1419–31.

Rouschop, K. M. A., J. J. T. H. Roelofs, N. Claessen, P. da Costa Martins, J.-J. Zwaginga, S. T. Pals, J. J. Weening, and S. Florquin (2005). Protection against renal ischemia reperfusion injury by CD44 disruption. *J Am Soc Nephrol 16*(7), 2034–43.

Rouschop, K. M. A., J. J. T. H. Roelofs, A. T. Rowshani, J. C. Leemans, T. van der Poll, I. J. M. Ten Berge, J. J. Weening, and S. Florquin (2005). Pre-transplant plasma and cellular levels of CD44 correlate with acute renal allograft rejection. *Nephrol Dial Transplant 20*(10), 2248–54.

Runembert, I., G. Queffeulou, P. Federici, F. Vrtovsnik, E. Colucci-Guyon, C. Babinet, P. Briand, G. Trugnan, G. Friedlander, and F. Terzi (2002). Vimentin affects localization and activity of sodium-glucose cotransporter SGLT1 in membrane rafts. *J Cell Sci 115*(Pt 4), 713–24.

Schmits, R., J. Filmus, N. Gerwin, G. Senaldi, F. Kiefer, T. Kundig, A. Wakeham, A. Shahinian, C. Catzavelos, J. Rak, C. Furlonger, A. Zakarian, J. J. Simard, P. S. Ohashi, C. J. Paige, J. C. Gutierrez-Ramos, and T. W. Mak (1997). CD44 regulates hematopoietic progenitor distribution, granuloma formation, and tumorigenicity. *Blood 90*(6), 2217–33.

Schneider, B. P., R. J. Gray, M. Radovich, F. Shen, G. Vance, L. Li, G. Jiang, K. D. Miller, J. R. Gralow, M. N. Dickler, M. A. Cobleigh, E. A. Perez, T. N. Shenkier, K. Vang Nielsen, S. Müller, A. Thor, G. W. J. Sledge, J. A. Sparano, N. E. Davidson, and S. S. Badve (2013). Prognostic and Predictive Value of Tumor Vascular Endothelial Growth Factor Gene Amplification in Metastatic Breast Cancer Treated with Paclitaxel with and without Bevacizumab; Results from ECOG 2100 Trial. *Clin Cancer Res 19*(5), 1281–9.

Schneider, B. P., M. Wang, M. Radovich, G. W. Sledge, S. Badve, A. Thor, D. A. Flockhart, B. Hancock, N. Davidson, J. Gralow, M. Dickler, E. A. Perez, M. Cobleigh, T. Shenkier, S. Edgerton, and K. D. Miller (2008). Association of vascular endothelial growth factor and vascular endothelial growth factor receptor-2 genetic polymorphisms with outcome in a trial of paclitaxel compared with paclitaxel plus bevacizumab in advanced breast cancer: ECOG 2100. *J Clin Oncol 26*(28), 4672–8.

Sennino, B. and D. M. McDonald (2012). Controlling escape from angiogenesis inhibitors. *Nat Rev Cancer 12*(10), 699–709.

Shaw, L. M., I. Rabinovitz, H. H. Wang, A. Toker, and A. M. Mercurio (1997). Activation of phosphoinositide 3-OH kinase by the $\alpha6\beta4$ integrin promotes carcinoma invasion. *Cell 91*(7), 949–60.

Sherman, L. S., T. A. Rizvi, S. Karyala, and N. Ratner (2000). CD44 enhances neuregulin signaling by Schwann cells. *J Cell Biol 150*(5), 1071–84.

Shojaei, F., X. Wu, X. Qu, M. Kowanetz, L. Yu, M. Tan, Y. G. Meng, and N. Ferrara

(2009). G-CSF-initiated myeloid cell mobilization and angiogenesis mediate tumor refractoriness to anti-VEGF therapy in mouse models. *Proc Natl Acad Sci U S A 106*(16), 6742–7.

Shojaei, F., X. Wu, C. Zhong, L. Yu, X.-H. Liang, J. Yao, D. Blanchard, C. Bais, F. V. Peale, N. van Bruggen, C. Ho, J. Ross, M. Tan, R. A. D. Carano, Y. G. Meng, and N. Ferrara (2007). Bv8 regulates myeloid-cell-dependent tumour angiogenesis. *Nature 450*(7171), 825–31.

Singleton, P. A., R. Salgia, L. Moreno-Vinasco, J. Moitra, S. Sammani, T. Mirzapoiazova, and J. G. N. Garcia (2007). CD44 regulates hepatocyte growth factor-mediated vascular integrity. Role of c-Met, Tiam1/Rac1, dynamin 2, and cortactin. *J Biol Chem 282*(42), 30643–57.

Sitohy, B., J. A. Nagy, S.-C. S. Jaminet, and H. F. Dvorak (2011). Tumor-surrogate blood vessel subtypes exhibit differential susceptibility to anti-VEGF therapy. *Cancer Res 71*(22), 7021–8.

Slevin, M., J. Krupinski, S. Kumar, and J. Gaffney (1998). Angiogenic oligosaccharides of hyaluronan induce protein tyrosine kinase activity in endothelial cells and activate a cytoplasmic signal transduction pathway resulting in proliferation. *Lab Invest 78*(8), 987–1003.

Slevin, M., S. Kumar, and J. Gaffney (2002). Angiogenic oligosaccharides of hyaluronan induce multiple signaling pathways affecting vascular endothelial cell mitogenic and wound healing responses. *J Biol Chem 277*(43), 41046–59.

Smith, L. L., B. W. Greenfield, A. Aruffo, and C. M. Giachelli (1999). CD44 is not an adhesive receptor for osteopontin. *J Cell Biochem 73*(1), 20–30.

Sokolova, A. V., L. Kreplak, T. Wedig, N. Mücke, D. I. Svergun, H. Herrmann, U. Aebi, and S. V. Strelkov (2006). Monitoring intermediate filament assembly by small-angle x-ray scattering reveals the molecular architecture of assembly intermediates. *Proc Natl Acad Sci U S A 103*(44), 16206–11.

Spurny, R., K. Abdoulrahman, L. Janda, D. Rünzler, G. Köhler, M. J. Castañón, and G. Wiche (2007). Oxidation and nitrosylation of cysteines proximal to the intermediate filament (IF)-binding site of plectin: effects on structure and vimentin binding and involvement in IF collapse. *J Biol Chem 282*(11), 8175–87.

Stoeck, A., S. Keller, S. Riedle, M. P. Sanderson, S. Runz, F. Le Naour, P. Gutwein, A. Ludwig, E. Rubinstein, and P. Altevogt (2006). A role for exosomes in the constitutive and stimulus-induced ectodomain cleavage of L1 and CD44. *Biochem J 393*(Pt 3), 609–18.

Styers, M. L., G. Salazar, R. Love, A. A. Peden, A. P. Kowalczyk, and V. Faundez (2004). The endo-lysosomal sorting machinery interacts with the intermediate filament cytoskeleton. *Mol Biol Cell 15*(12), 5369–82.

Subramaniam, V., H. Gardner, and S. Jothy (2007). Soluble CD44 secretion contributes to the acquisition of aggressive tumor phenotype in human colon cancer cells. *Exp Mol Pathol 83*(3), 341–6.

Tabernero, J. (2007). The role of VEGF and EGFR inhibition: implications for combining anti-VEGF and anti-EGFR agents. *Mol Cancer Res 5*(3), 203–20.

Taddei, A., C. Giampietro, A. Conti, F. Orsenigo, F. Breviario, V. Pirazzoli, M. Potente, C. Daly, S. Dimmeler, and E. Dejana (2008). Endothelial adherens junctions control tight junctions by VE-cadherin-mediated upregulation of claudin-5. *Nat Cell Biol 10*(8), 923–34.

Takamune, Y., T. Ikebe, O. Nagano, H. Nakayama, K. Ota, T. Obayashi, H. Saya, and M. Shinohara (2007). ADAM-17 associated with CD44 cleavage and metastasis in oral squamous cell carcinoma. *Virchows Arch 450*(2), 169–77.

Teriete, P., S. Banerji, M. Noble, C. D. Blundell, A. J. Wright, A. R. Pickford, E. Lowe, D. J. Mahoney, M. I. Tammi, J. D. Kahmann, I. D. Campbell, A. J. Day, and D. G. Jackson (2004). Structure of the regulatory hyaluronan binding domain in the inflammatory leukocyte homing receptor CD44. *Mol Cell 13*(4), 483–96.

Terzi, F., D. Henrion, E. Colucci-Guyon, P. Federici, C. Babinet, B. I. Levy, P. Briand, and G. Friedlander (1997). Reduction of renal mass is lethal in mice lacking vimentin. Role of endothelin-nitric oxide imbalance. *J Clin Invest 100*(6), 1520–8.

Thankamony, S. P. and W. Knudson (2006). Acylation of CD44 and its association with lipid rafts are required for receptor and hyaluronan endocytosis. *J Biol Chem 281*(45), 34601–9.

Tremmel, M., A. Matzke, I. Albrecht, A. M. Laib, V. Olaku, K. Ballmer-Hofer, G. Christofori, M. Héroult, H. G. Augustin, H. Ponta, and V. Orian-Rousseau (2009). A CD44v6 peptide reveals a role of CD44 in VEGFR-2 signaling and angiogenesis. *Blood 114*(25), 5236–44.

Trusolino, L., A. Bertotti, and P. M. Comoglio (2001). A signaling adapter function for $\alpha 6 \beta 4$ integrin in the control of HGF-dependent invasive growth. *Cell 107*(5), 643–54.

Uhlmann, M. E., R. B. Georges, A. Boleij, E. Eyol, A. Kubarenko, H. Adwan, and M. R. Berger (2011). Influence of osteopontin expression on the metastatic growth of CC531 rat colorectal carcinoma cells in rat liver. *Cancer Gene Ther 18*(11), 795–805.

van Beijnum, J. R., R. P. Dings, E. van der Linden, B. M. M. Zwaans, F. C. S. Ramaekers, K. H. Mayo, and A. W. Griffioen (2006). Gene expression of tumor angiogenesis dissected: specific targeting of colon cancer angiogenic vasculature. *Blood 108*(7), 2339–48.

van der Windt, G. J. W., C. van 't Veer, S. Florquin, and T. van der Poll (2010). CD44 deficiency is associated with enhanced Escherichia coli-induced proinflammatory cytokine and chemokine release by peritoneal macrophages. *Infect Immun 78*(1), 115–24.

Visca, P., F. Del Nonno, C. Botti, F. Marandino, V. Sebastiani, U. Di Tondo, R. P. Donnorso, G. Trombetta, S. Filippi, and P. L. Alo (2002). Role and prognostic significance of CD44s expression in colorectal cancer. *Anticancer Res 22*(5), 2671–5.

Vlajnic, T., M. C. Andreozzi, S. Schneider, L. Tornillo, E. Karamitopoulou, A. Lugli, C. Ruiz, I. Zlobec, and L. Terracciano (2011). VEGFA gene locus (6p12) amplification identifies a small but highly aggressive subgroup of colorectal cancer [corrected] patients. *Mod Pathol 24*(10), 1404–12.

Vredenburgh, J. J., A. Desjardins, J. E. n. Herndon, J. Marcello, D. A. Reardon, J. A. Quinn, J. N. Rich, S. Sathornsumetee, S. Gururangan, J. Sampson, M. Wagner, L. Bailey, D. D. Bigner, A. H. Friedman, and H. S. Friedman (2007). Bevacizumab plus irinotecan in recurrent glioblastoma multiforme. *J Clin Oncol 25*(30), 4722–9.

Vuoriluoto, K., H. Haugen, S. Kiviluoto, J.-P. Mpindi, J. Nevo, C. Gjerdrum, C. Tiron, J. B. Lorens, and J. Ivaska (2011). Vimentin regulates EMT induction by Slug and oncogenic H-Ras and migration by governing Axl expression in breast cancer. *Oncogene 30*(12), 1436–48.

Wang, N. and D. Stamenović (2000). Contribution of intermediate filaments to cell stiffness, stiffening, and growth. *Am J Physiol Cell Physiol 279*(1), C188–94.

Weber, G. F., S. Ashkar, M. J. Glimcher, and H. Cantor (1996). Receptor-ligand interaction between CD44 and osteopontin (Eta-1). *Science 271*(5248), 509–12.

Weber, G. F., R. T. Bronson, J. Ilagan, H. Cantor, R. Schmits, and T. W. Mak (2002). Absence of the CD44 gene prevents sarcoma metastasis. *Cancer Res 62*(8), 2281–6.

Wielenga, V. J., R. Smits, V. Korinek, L. Smit, M. Kielman, R. Fodde, H. Clevers, and S. T. Pals (1999). Expression of CD44 in Apc and Tcf mutant mice implies regulation by the WNT pathway. *Am J Pathol 154*(2), 515–23.

Wobus, M., R. Rangwala, I. Sheyn, R. Hennigan, B. Coila, E. E. Lower, R. S. Yassin, and L. S. Sherman (2002). CD44 associates with EGFR and erbB2 in metastasizing mammary carcinoma cells. *Appl Immunohistochem Mol Morphol 10*(1), 34–9.

Wu, J. and N. Sheibani (2003). Modulation of VE-cadherin and PECAM-1 mediated cell-cell adhesions by mitogen-activated protein kinases. *J Cell Biochem 90*(1), 121–37.

Xu, L., D. G. Duda, E. di Tomaso, M. Ancukiewicz, D. C. Chung, G. Y. Lauwers, R. Samuel, P. Shellito, B. G. Czito, P.-C. Lin, M. Poleski, R. Bentley, J. W. Clark, C. G. Willett, and R. K. Jain (2009). Direct evidence that bevacizumab, an anti-VEGF antibody, up-regulates SDF1α, CXCR4, CXCL6, and neuropilin 1 in tumors from patients with rectal cancer. *Cancer Res 69*(20), 7905–10.

Yang, C., M. Cao, H. Liu, Y. He, J. Xu, Y. Du, Y. Liu, W. Wang, L. Cui, J. Hu, and F. Gao (2012). The high and low molecular weight forms of hyaluronan have distinct effects on CD44 clustering. *J Biol Chem 287*(51), 43094–107.

Yang, J., D. Yang, Y. Sun, B. Sun, G. Wang, J. C. Trent, D. M. Araujo, K. Chen, and W. Zhang (2011). Genetic amplification of the vascular endothelial growth factor (VEGF) pathway genes, including VEGFA, in human osteosarcoma. *Cancer 117*(21), 4925–38.

Yang, J. C., L. Haworth, R. M. Sherry, P. Hwu, D. J. Schwartzentruber, S. L. Topalian, S. M. Steinberg, H. X. Chen, and S. A. Rosenberg (2003). A randomized trial of bevacizumab, an anti-vascular endothelial growth factor antibody, for metastatic renal cancer. *N Engl J Med 349*(5), 427–34.

Yang, L., L. M. DeBusk, K. Fukuda, B. Fingleton, B. Green-Jarvis, Y. Shyr, L. M. Matrisian, D. P. Carbone, and P. C. Lin (2004). Expansion of myeloid immune suppressor Gr+CD11b+ cells in tumor-bearing host directly promotes tumor angiogenesis. *Cancer Cell 6*(4), 409–21.

Yu, Q. and I. Stamenkovic (1999). Localization of matrix metalloproteinase 9 to the cell surface provides a mechanism for CD44-mediated tumor invasion. *Genes Dev 13*(1), 35–48.

Yu, Q. and I. Stamenkovic (2000). Cell surface-localized matrix metalloproteinase-9 proteolytically activates TGF-β and promotes tumor invasion and angiogenesis. *Genes Dev 14*(2), 163–76.

Yu, Q. and B. P. Toole (1996). A new alternatively spliced exon between v9 and v10 provides a molecular basis for synthesis of soluble CD44. *J Biol*

Chem 271(34), 20603–7.

Zeilstra, J., S. P. J. Joosten, M. Dokter, E. Verwiel, M. Spaargaren, and S. T. Pals (2008). Deletion of the WNT target and cancer stem cell marker CD44 in Apc(Min/+) mice attenuates intestinal tumorigenesis. *Cancer Res 68*(10), 3655–61.

Zou, Y., L. He, and S.-H. Huang (2006). Identification of a surface protein on human brain microvascular endothelial cells as vimentin interacting with Escherichia coli invasion protein IbeA. *Biochem Biophys Res Commun 351*(3), 625–30.

PUBLICATION I

Päll T., Gad A., Kasak L., Drews M., Strömblad S., Kogerman P. (2004) Recombinant CD44-HABD is a novel and potent direct angiogenesis inhibitor enforcing endothelial cell-specific growth inhibition independently of hyaluronic acid binding. Oncogene 23: 7874–7881

Oncogene (2004) 23, 7874–7881

www.nature.com/onc

Recombinant CD44-HABD is a novel and potent direct angiogenesis inhibitor enforcing endothelial cell-specific growth inhibition independently of hyaluronic acid binding

Taavi Päll[1,2,3], Annica Gad[1], Lagle Kasak[2], Monika Drews[2], Staffan Strömblad[1] and Priit Kogerman*[,2,3]

[1]*Department of Laboratory Medicine, Karolinska Institutet, Huddinge University Hospital F 46, Huddinge, 141 86 Huddinge, Sweden;* [2]*Laboratory of Molecular Genetics, National Institute of Chemical Physics and Biophysics, 12618 Tallinn, Estonia;* [3]*Department of Gene Technology, Tallinn University of Technology, 19086 Tallinn, Estonia*

CD44 is the main cellular receptor for hyaluronic acid (HA). We previously found that overexpression of CD44 inhibited tumor growth of mouse fibrosarcoma cells in mice. Here, we show that soluble recombinant CD44 HA-binding domain (CD44-HABD) acts directly onto endothelial cells by inhibiting endothelial cell proliferation in a cell-specific manner. Consequently, soluble recombinant CD44-HABD also blocked angiogenesis *in vivo* in chick and mouse, and thereby inhibited tumor growth of various origins at very low doses (0.25 mg/kg × day). The antiangiogenic effect of CD44 is independent of its HA-binding capacity, since mutants deficient in HA binding still maintain their antiangiogenic and antiproliferative properties. Recombinant CD44-HABD represents a novel class of angiogenesis inhibitors based on a cell-surface receptor.
Oncogene (2004) **23,** 7874–7881. doi:10.1038/sj.onc.1208083
Published online 13 September 2004

Keywords: CD44; angiogenesis; hyaluronic acid

Introduction

CD44 is a transmembrane receptor for hyaluronic acid (HA) (Aruffo *et al*., 1990) that is functional in HA metabolism (Culty *et al*., 1992; Kaya *et al*., 1997), cell migration (Thomas *et al*., 1992) and cell adhesion (Lesley *et al*., 1993). The highly conserved link module located in the amino-terminal portion of the extracellular domain mediates CD44 binding to HA. CD44 displays a complex pattern of alternative splicing within its extracellular domain, and the genomic structure of the CD44 gene reveals the presence of 10 alternatively spliced exons (Screaton *et al*., 1992). Alternatively spliced CD44 variant isoforms have been reported to confer a metastatic phenotype to tumor cells (Gunthert *et al*., 1991; Arch *et al*., 1992). We previously found that the CD44 standard isoform induced metastatic capacity of mouse fibrosarcoma cells while it inhibited subcutaneous tumor growth in mice (Kogerman *et al*., 1997). Mouse fibrosarcoma cells overexpressing the human CD44 standard isoform showed prolonged latency time for growth in mice compared to parental cells, and the transgene CD44 expression was downregulated once subcutaneous tumors were established. Moreover, tumorigenicity studies with SV40 large T-transformed CD44-negative fibroblasts showed that reintroduction of the CD44 standard isoform into these cells significantly reduced subcutaneous tumor growth in mice (Schmits *et al*., 1997).

The formation of solid tumors is dependent on the formation of new blood vessels by angiogenesis (Hanahan and Folkman, 1996). A switch to an angiogenic phenotype is one of the critical steps in the development of a malignant tumor phenotype and is dependent on the balance between pro- and anti-angiogenic factors in the tumor microenvironment. Several endogenous angiogenesis inhibitors have been described, including endostatin (a fragment of collagen type XVIII) (O'Reilly *et al*., 1997), angiostatin (a fragment of plasminogen) (O'Reilly *et al*., 1994), thrombospondin (Guo *et al*., 1997), antithrombin (O'Reilly *et al*., 1999), and pigment epithelium-derived factor (Stellmach *et al*., 2001). There are two types of angiogenesis inhibitors: direct inhibitors acting directly onto vascular cells and indirect inhibitors acting on neighboring cells or factors in the surrounding that would otherwise stimulate angiogenesis (Kerbel and Folkman, 2002).

CD44 has been suggested to promote tumor angiogenesis and growth by mediating localization of matrix metalloprotease-9 (MMP-9) to the tumor cell surface (Yu and Stamenkovic, 1999, 2000), since overexpression in tumor cells of a naturally occurring soluble CD44 isoform disrupted the localization of MMP-9 to the tumor cell surface and inhibited tumor growth and invasion (Yu and Stamenkovic, 1999, 2000). The resulting tumors were also less vascularized, suggesting that the tumor growth inhibition might be related to an

*Correspondence: P Kogerman, Laboratory of Molecular Genetics, National Institute of Chemical Physics and Biophysics, Akadeemia 23, 12618 Tallinn, Estonia. E-mail: priit@kbfi.ee
Received 7 April 2004; revised 3 August 2004; accepted 4 August 2004; published online 13 September 2004

inhibition of tumor angiogenesis (Yu and Stamenkovic, 1999, 2000).

Given that CD44 overexpression on the tumor cell surface can inhibit tumor growth, we hypothesized that a purified recombinant CD44-HABD might serve as an angiogenesis inhibitor and may thereby block tumor growth. Furthermore, as CD44 is the main cellular receptor for HA, we wanted to test whether the potential effects on angiogenesis and tumor growth could be dependent on the HA-binding properties of CD44. Therefore, we produced recombinant CD44-HABD and various non-HA-binding mutants thereof and tested them in various models of cell proliferation, angiogenesis and tumor growth.

We report here that soluble CD44-HABD inhibits tumor growth and angiogenesis. The observed tumor growth- and angiogenesis-inhibiting effect of CD44-HABD is independent of HA binding since a non-HA-binding mutant was equally effective. Furthermore, CD44-HABD blocked cell proliferation in an endothelial cell-specific manner and showed no effect on proliferation of tumor cells or untransformed epithelial or fibroblast cells. Therefore, recombinant CD44-HABD represents a new type of direct angiogenesis inhibitor based on a cell surface receptor.

Results

Recombinant CD44-HABD binds to HA and inhibits HA-induced endothelial cell migration

The HA-binding domain is the most evolutionary conserved region in the extracellular part of the CD44 receptor, with human and avian CD44 showing a 78% amino acid (aa) similarity and a 57% amino acid (aa) identity within aa 21–133 (Figure 1a). To test if CD44-HABD might inhibit tumor growth and angiogenesis, we created recombinant bacterial glutathione S-transferase (GST) fusion proteins of CD44-HABD (GST-HABD). We also generated three mutants of human CD44-HABD GST-fusion proteins at positions that have previously been demonstrated or predicted to make CD44 defective in HA binding (Bajorath *et al*., 1998): GST-HABD^{R41A} (GST-R41A), GST-HABD^{R78SY79S} (GST-R78SY79S), and the triple mutant GST-HABD^{R41AR78SY79S} (GST-3MUT) (the numbers correspond to aa positions in full-length human CD44). To test the HA-binding capacity of the recombinant GST-HABD proteins, we performed a modified ELISA assay with immobilized HA. In this assay, wild-type CD44 fusion proteins were bound to HA in a concentration-dependent manner while the mutant protein did not display any binding significantly higher than the background even at high concentrations (Figure 1b). Given that CD44 mediates cell migration on HA (Thomas *et al*., 1992), we then tested the effect of soluble CD44-HABD proteins on cell migration. We found that wild-type GST-HABD but not the GST-R41A non-HA-binding mutant inhibited HA-induced human aortic endothelial cell (HAEC) migration (Figure 1c). This effect on cell migration was specific for HA-mediated migration, since migration towards collagen type I was not inhibited (data not shown). Furthermore, preincubation of endothelial cells with an antibody that specifically blocks CD44 binding to HA (GKW.A3; (Guo *et al*., 1994)) also inhibited their migration towards HA (Figure 1c). This demonstrates that while wild-type CD44-HABD binds to HA and inhibits HA-induced cell migration, all the mutants were deficient in these capacities.

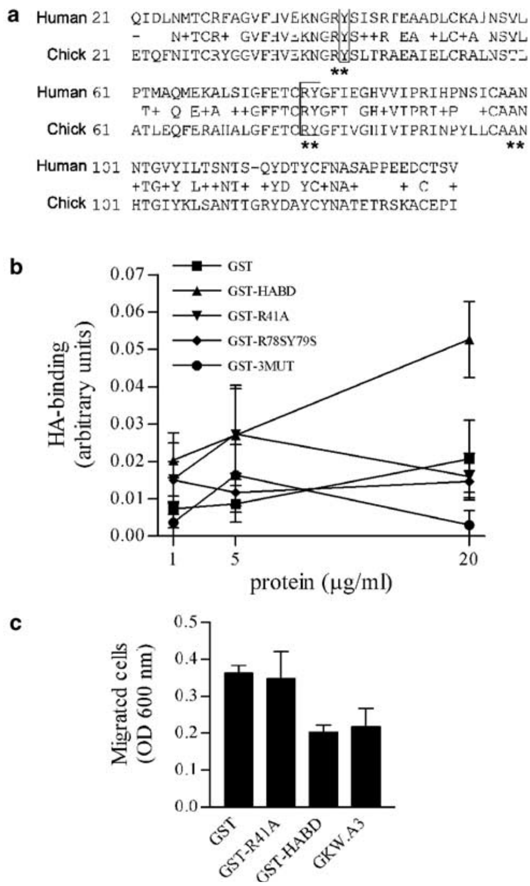

Figure 1 Properties of recombinant CD44-HABD. (**a**) Amino acid alignment of human and chick CD44-HABD demonstrates a high degree of sequence conservation during evolution; identical aa residues are shown in the middle and conservative replacements are indicated (+). Amino acid residues involved in HA-binding are indicated with asterisks and residues mutated in this study are boxed. (**b**) GST-HABD, but not GST-3MUT or GST control bound to immobilized HA in a modified ELISA assay. (**c**) GST-HABD inhibits HA-induced human aortic endothelial cell migration, whereas GST-R41A non-HA-binding mutant had no effect. GKW.A3, a monoclonal antibody to CD44 that blocks CD44 binding to HA, also blocks HAEC haptotaxis towards HA. Error bars in (**b**) and (**c**) indicate s.e.

Recombinant CD44-HABD proteins inhibit angiogenesis in the chick chorio-allantoic membrane

To test the effect of CD44-HABD on angiogenesis, we used a chick chorio-allantoic membrane (CAM) angiogenesis assay (Brooks *et al*., 1999). We induced angiogenesis in 10-day-old chick embryo CAMs by the use of filter discs saturated with 100 ng/ml VEGF, 1 μg/ml bFGF or 200 ng/ml TGFα. Growth factor-saturated filter discs were then treated by daily topical addition of 10 μg of GST-HABD, GST-3MUT, GST or vehicle alone. After 3 days, we dissected the filter discs with the surrounding CAM and analysed for angiogenesis by quantifying the number of blood vessel branch points under the filter disc area. Angiogenesis was induced to a similar degree by all three growth factors (Figure 2). Importantly, the angiogenic effects of VEGF, bFGF and TGFα were completely abolished by GST-HABD or GST-3MUT but not by GST or PBS treatment (Figure 2a–f). In addition, treatment with a GST-HABD^{R41A} gave a similar inhibition (data not shown). Therefore, recombinant CD44-HABD blocked angiogenesis that was induced by three distinct angiogenic factors, indicating that CD44-HABD may inhibit angiogenesis regardless of the route of induction. Furthermore, surprisingly, this inhibition of angiogenesis by recombinant CD44 was independent of HA binding since the non-HA-binding mutants were as effective in blocking angiogenesis as wild-type CD44-HABD.

CD44-HABD specifically blocks endothelial cell proliferation

Angiogenesis is a complex process involving cell proliferation, invasion and cell motility. CD44-mediated migration of endothelial cells towards HA is dependent on its HA-binding properties (Figure 1c). To analyse if CD44-HABD could execute a direct effect on vascular endothelial cells, we tested if CD44-HABD could directly bind to endothelial cells. Therefore, we labeled GST-HABD, GST-3MUT or GST protein alone with Alexa488 fluorochrome and tested binding of these proteins to different endothelial and non-endothelial cell lines. Flow cytometry analysis showed that GST-HABD and GST-3MUT proteins but not GST protein bound to CPAE endothelial cells but not to COS-1 kidney fibroblasts (data not shown), suggesting that the CD44-HABD may bind directly to a putative receptor present on endothelial cells.

Therefore, we tested if recombinant CD44-HABD proteins might affect endothelial cell proliferation. To this end, HUVEC and CPAE endothelial cells, as well as various other primary and tumor cells were grown in the

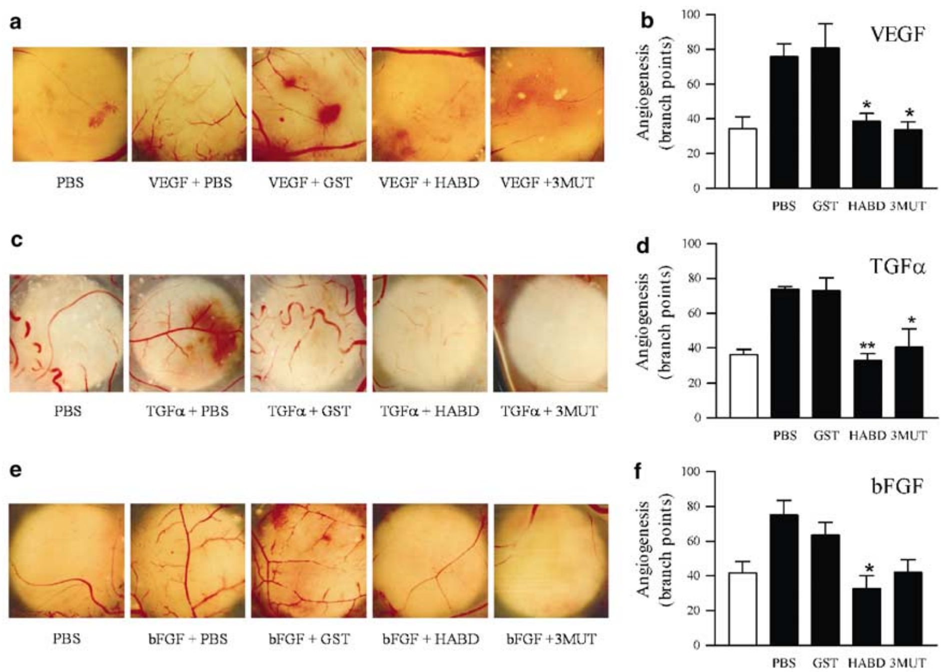

Figure 2 Recombinant CD44-HABD blocks angiogenesis *in vivo*. (**a**, **c** and **e**) Filter discs and associated CAM from representative angiogenesis experiments where angiogenesis was induced with VEGF (**a**), TGFα (**c**) or bFGF (**e**). (**b**, **d** and **f**) Angiogenesis was assessed as the number of blood vessel branch points within the CAM area directly under the filter discs ($n = 6$ for each experiment). Filter discs were soaked with PBS only (empty bars) or with the respective growth factor (filled bars). Data in (**b**, **d** and **f**) represent the average effects on angiogenesis of at least three independent experiments $\pm$s.e. Abbreviations: HABD, GST-HABD; 3MUT, GST-3MUT. $^{*}P<0.05$; $^{**}P<0.01$

presence of GST, GST-HABD or GST-3MUT. HUVEC and CPAE cells exposed to GST-HABD or GST-3MUT for 48 h displayed a markedly reduced amount of cells in S phase as compared to control-treated cells (Figure 3a and b), indicating that CD44-HABD directly inhibits endothelial cell proliferation and thus acts as a direct angiogenesis inhibitor. By contrast, CD44-HABD had no significant effect on cell proliferation of other untransformed cells of mesodermal (NHDF; Figure 3) or epithelial (HEK-293; Figure 3) origin or on tumor cells of various origins (MCF-7 breast carcinoma cells, SMMU-1 melanoma cells, U373MG glioblastoma cells, BxPC-3 pancreatic carcinoma cells; Figure 3). This suggests that cell growth inhibition by CD44-HABD is endothelial cell specific. However, we did not detect any increase in apoptosis within the treated cell populations (data not shown), indicating that the primary effect on endothelial cells may be on cell proliferation.

To test if the effect on the endothelial cells was dose-dependent, we performed a dose–response analysis on CPAE cells using an MTT assay followed by spectrophotometric detection. As shown in Figure 4, both WT (GST-HABD) and 3MUT (GST-3MUT) versions of CD44-HABD inhibited the proliferation of CPAE cells at concentrations starting from 0.5 to 1 μg/ml. At the highest concentration used (10 μg/ml), GST control protein also has a slight effect on cell proliferation but this effect was much weaker than that seen with CD44-HABD proteins. These data indicate that recombinant CD44-HABD proteins inhibit the proliferation of endothelial cells in a dose-dependent manner.

Recombinant CD44-HABD inhibits tumor growth and angiogenesis at low doses independent of HA binding

Given that CD44-HABD inhibits both angiogenesis in the chick CAM and endothelial cell proliferation, we wanted to test if our recombinant proteins could also inhibit tumor growth. For this purpose, we injected 1×10^6 BxPC-3 pancreatic human adenocarcinoma or SMMU-1 melanoma cells subcutaneously (s.c.) onto the backs of nude mice. When the tumors appeared as palpable nodules, mice received GST-HABD, GST-3MUT or GST by s.c. injections every second day into a region proximal to the tumor. BxPC-3 cells gave rise to slow-growing tumors. The GST-treated controls reached an average weight of 0.267 ± 0.042 g ($n = 6$) on day 52 when the mice were killed (Figure 5a–c). However, treatment of the mice with 0.25 mg/kg day GST-HABD or GST-3MUT protein significantly inhibited BxPC-3 tumor growth and reduced the average tumor weight by approximately 60% (0.108 ± 0.028 g; $P = 0.0159$; $n = 6$) and 70% (0.085 ± 0.017 g; $P = 0.0076$; $n = 5$), respectively (Figure 5b). We then performed the same experiment using the more aggressive SMMU-1 melanoma cell line and again observed a significant inhibition of tumor growth by approximately 50% by both GST-HABD and GST-3MUT treatment (average tumor weight after sacrifice after 16 days was 0.81 ± 0.061 g ($P = 0.0015$; $n = 8$) and 0.746 ± 0.132 g ($P = 0.0014$; $n = 7$), respectively), as compared to GST-treated controls (1.559 ± 0.124 g; $n = 8$) (Figure 6a–c).

Next, we analysed mouse subcutaneous SMMU-1 and BxPC-3 tumors for blood vessel density by counting PECAM-1 (CD31)-positive blood vessels. GST-HABD or GST-3MUT treatment significantly reduced blood vessel density in SMMU-1 tumors compared to GST-control treatment (Figure 6d), indicating that CD44-HABD as well as the GST-3MUT also blocked tumor-induced angiogenesis. Similar results were also obtained with BxPC-3 tumors (data not shown). Given that inhibition of angiogenesis is known to suppress tumor growth (Holmgren *et al*., 1995; O'Reilly *et al*., 1997, 1996; Parangi *et al*., 1996), and that we found CD44-HABD to block angiogenesis directly (Figure 2),

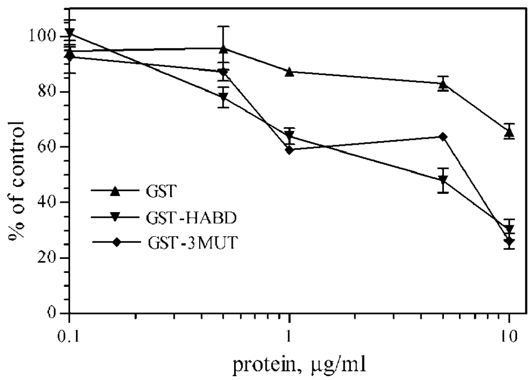

Figure 4 Endothelial cell growth inhibition by CD44-HABD is concentration dependent. Exponentially growing CPAE cells were treated with indicated amounts of GST-HABD, GST-3MUT or GST for 48 h and the effect on cell proliferation was measured by MTT assay. The plot represents the average percentage of triplicate wells (mean $\pm$ s.e.) normalized to vechicle-treated controls

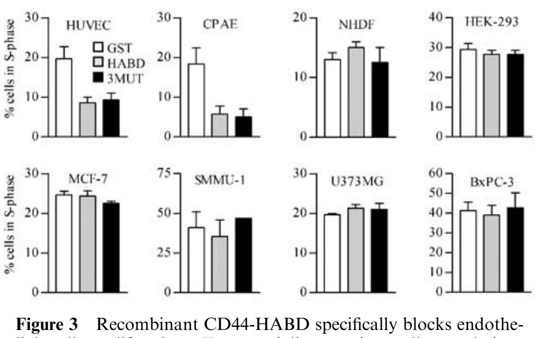

Figure 3 Recombinant CD44-HABD specifically blocks endothelial cell proliferation. Exponentially growing cell populations were treated with GST, GST-HABD or GST-3MUT for 48 h. Cells were incubated with BrdU and their cell cycle distributions were determined by flow cytometry analysis of BrdU and PI content as described in Materials and methods. Bars represent the proportion of cells in S phase of endothelial cells; HUVEC and CPAE primary human dermal fibroblasts, NHDF epithelial embryonic kidney cells, HEK-293 and different tumor cells; MCF-7 breast carcinoma, SMMU-1 melanoma, U373MG glioblastoma and BxPC-3 pancreatic adenocarcinoma. The data represent the mean of three experiments $\pm$ s.e.

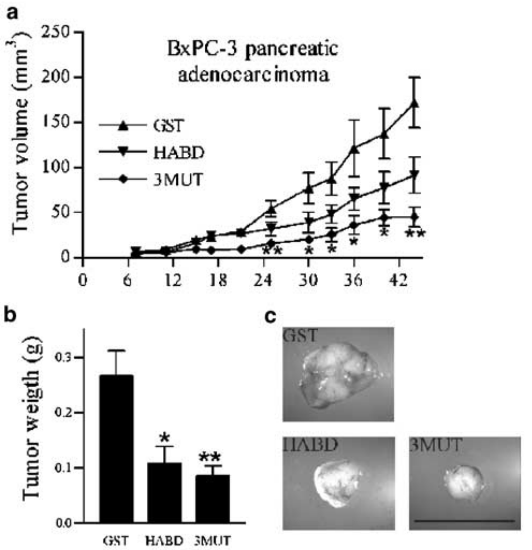

Figure 5 CD44-HABD fusion proteins inhibit pancreatic adenocarcinoma growth *in vivo*. (**a**) Growth curves of s.c. BxPC-3 pancreatic adenocarcinoma tumors in nude mice treated with GST-HABD, GST-3MUT or GST control. (**b**) Average BxPC-3 tumor weights at the end of the experiment ($n = 5$–6). (**c**) Pictures of representative BxPC-3 tumors from GST, GST-HABD and GST-3MUT-treated mice. Abbreviations: HABD, GST-HABD; 3MUT, GST-3MUT. Values in graphs and bars represent mean±s.e. *$P<0.05$; **$P<0.01$. Scale bar, 1 cm

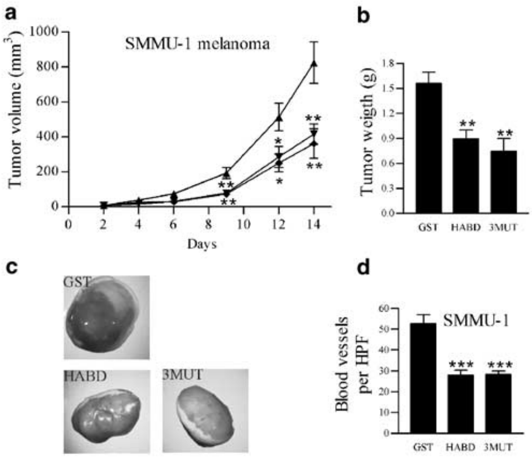

Figure 6 CD44-HABD fusion proteins inhibit melanoma growth *in vivo*. (**a**) Growth curves of s.c. SMMU-1 melanoma tumors in nude mice treated with GST-HABD, GST-3MUT or GST control (Labeling is the same as in Figure 5). (**b**) Average SMMU-1 tumor weights at the end of the experiment, day 16 ($n = 6$–8). (**c**) Pictures of representative SMMU-1 tumors from GST, GST-HABD and GST-3MUT treated mice. (**d**) Quantification of blood vessel density determined as PECAM-1 (CD31) immunoreactive blood vessels per high-power field (HPF; magnification, ×200) as described in Materials and methods. Abbreviations: HABD, GST-HABD; 3MUT, GST-3MUT. Values in graphs and bars represent mean±s.e. *$P<0.05$; **$P<0.01$; ***$P<0.001$

the tumor growth inhibition by CD44-HABD proteins is likely to be caused by the inhibition of angiogenesis.

Discussion

In this study, we describe a novel type of angiogenesis inhibitor, a domain of the cell surface receptor CD44 (CD44-HABD). CD44-HABD blocked angiogenesis in chick CAM induced by various growth factors. CD44-HABD acted directly on endothelial cells and blocked their cell proliferation, indicating that CD44-HABD may act as a direct angiogenesis inhibitor. Surprisingly, the inhibition of endothelial cell proliferation and angiogenesis by CD44-HABD was independent of HA binding, since CD44-HABD non-HA-binding mutant maintained the antiproliferative and antiangiogenic properties. Finally, treatment of mice with soluble CD44-HABD proteins significantly suppressed *in vivo* growth of different tumors and inhibited tumor vascularization. While inhibition of tumor angiogenesis by CD44-HABD is the most likely explanation for our results, alternative explanations cannot be excluded. For instance, CD44-HABD might prevent cell–cell contact of tumor cells precluding the development of a solid mass or it might alter the expression of stromal factors essential for tumor growth. Whatever the mechanism, the observed inhibition of tumor growth opens up the possibility that CD44-HABD may be developed into a drug for treatment of human cancer. Of course, much work remains to be carried out to test that possibility. As a first task, sufficient quantities of CD44 must be obtained to develop an intravenous injection protocol for this protein.

Recent reports show that CD44 extracellular domain can be released from the cell surface by proteolytic cleavage and incorporated into extracellular matrices (ECM) (Okamoto *et al*., 1999; Cichy *et al*., 2002; Okamoto *et al*., 2002). Possible functions for soluble CD44 in ECM include organization of the matrix and the anchoring of growth factors to the ECM. Soluble CD44 levels are elevated in the blood during inflammation and CD44 proteolytic cleavage is enhanced in multiple tumors (Katoh *et al*., 1994; Okamoto *et al*., 2002). In previous studies, disruption of tumor cell adhesion to HA by overexpression of soluble CD44 isoforms in tumor cells inhibited HA-induced melanoma cell proliferation and tumor growth in mice (Ahrens *et al*., 2001). Furthermore, the metastatic capability of murine mammary carcinoma cells was inhibited by overexpression of CD44, these tumors could not be established in the secondary site and instead underwent apoptosis (Yu *et al*., 1997). In both these cases, soluble CD44 acted by inhibiting binding of HA to cell surface CD44. The CD44 to HA interaction also plays a role in endothelial cell proliferation as antibodies against CD44 blocked a mitogenic response to HA in these cells (Lokeshwar *et al*., 1996; Trochon *et al*., 1996; Savani et al., 2001) and CD44 expression was upregulated only in proliferating endothelial cells (Griffioen et al., 1997).

In our experiments, however, inhibition of endothelial cell proliferation and angiogenesis by CD44-HABD was independent of HA binding, since CD44-HABD non-HA-binding mutants were equally effective in blocking endothelial cell proliferation. CD44-HABD bound to the cell surface of endothelial cells, suggesting that CD44-HABD may target a specific cell surface receptor. This receptor may be specific for endothelial cells or may interfere with a signaling pathway required specifically for endothelial cell proliferation. Naturally, identification of this putative receptor and its signaling mechanisms will be of great interest.

A number of CD44-binding proteins other than HA have been described, including HGF, bFGF, fibronectin, osteopontin, selectins, erbB2 and erbB3 (Jalkanen and Jalkanen, 1992; Bennett et al., 1995; Weber et al., 1996; van der Voort et al., 1999; Sherman et al., 2000; Dimitroff et al., 2001). However, the binding of these proteins is dependent on various post-translational modifications of CD44 at alternative exons that are not present in our recombinant fusion proteins. The effects of endogenous CD44-HABD on angiogenesis and tumor growth might instead be caused by enzymes that are responsible for CD44 shedding. CD44-cleaving proteins belong to serine protease and metalloproteinase families; one enzyme that can digest CD44 is MT1-MMP (Kajita et al., 2001). However, MT1-MMP binds to the CD44 stem region and the CD44 HA-binding domain is not involved in this interaction (Mori et al., 2002). Another interesting binding partner for CD44 is MMP-9; CD44 serves as a cell surface docking receptor for this protease (Yu and Stamenkovic, 1999). MMP-9 is implicated in angiogenesis by releasing VEGF from extracellular matrix deposits during ECM proteolysis (Bergers et al., 2000). A role for CD44 in angiogenesis has been suggested to be related to its capacity to bind MMP-9 (Yu and Stamenkovic, 2000) and the binding of MMP-9 to CD44 seems to be dependent on CD44 clustering by HA (Yu and Stamenkovic, 1999). However, our preliminary results suggest that CD44-HABD^{R41AR78SY79S} non-HA-binding mutant cannot bind MMP-9 (Päll et al., unpublished). Furthermore, the observed inhibition of endothelial cell proliferation by CD44-HABD might not be explained by blocking MMP-9 binding to CD44, since MMP-9 is affecting angiogenesis by ECM proteolysis (Bergers et al., 2000), while no evidence is present for MMP-9-mediated direct effect on cell proliferation. Therefore, it is unlikely that the effects of CD44-HABD in angiogenesis are dependent on MMP-9 binding. An intriguing possibility is that CD44 HABD and its mutants may bind to other carbohydrates, for example, to sialyl Lewis X-containing saccharides implicated in angiogenesis. The structure of the CD44 link domain HA-binding surface corresponds closely to the Sialyl Lewis-X-binding site of E-selectin (Kohda et al., 1996; Bajorath et al., 1998). The Sialyl Lewis-X-binding surface in E-selectin is smaller than the HA-binding surface in CD44. Mutations introduced into CD44 HABD to abolish HA binding may not overlap with putative binding site for Sialyl Lewis-X (Nguyen et al., 1993; Koch et al., 1995; Bajorath et al., 1998). It will therefore be interesting to assess whether CD44 protein can bind to Sialyl Lewis-X or similar molecules and if this binding might be responsible for the observed inhibition of angiogenesis.

One possible explanation for the novel properties of recombinant CD44 proteins may be the lack of posttranslational modifications in our bacterially expressed proteins in contrast to proteins expressed in mammalian systems. CD44-HABD contains five putative N-linked glycosylation sites (Bartolazzi et al., 1996). Therefore, we cannot exclude the possibility that novel binding site(s), masked by glycosylation in endogenous CD44, may become available in recombinant CD44-HABD and be responsible for the observed effects on angiogenesis. Taken together, our results suggest that HA-independent inhibition of endothelial cell proliferation by CD44-HABD is a novel mechanism for direct inhibition of angiogenesis. Therefore, new drugs based on CD44 sequences may be effective in treating human angiogenesis-dependent diseases such as cancer.

Materials and methods

Cell lines and cell culture

SMMU-1 melanoma cells (Guo et al., 1994), normal human dermal fibroblasts (NHDF; Clonetics, San Diego, CA, USA), HEK-293 epithelial human embryonic kidney cells, MCF-7 human breast carcinoma cells, U373MG glioblastoma cells (ATCC, Manassas, VA, USA) were grown in DMEM with 10% FCS. Human pancreatic adenocarcinoma cells (BxPC-3; ATCC) were grown in RPMI 1640 with 10% FCS. Primary human umbilical vein endothelial cells (HUVEC) were grown in M199 with 20% FCS, 4 mM L-glutamine, 0.9 mg/ml heparin and 30 μg/ml endothelial cell growth supplement (Upstate Biotechnology, Lake Placid, NY, USA). Cow pulmonary endothelial cells (CPAE; ATCC) were grown in MEM (25 mM HEPES) with 20% FCS, 2 mM L-glutamine and nonessential aa. Human aortic endothelial cells (HAEC) were obtained from Clonetics and grown according to the manufacturer's specifications.

Construction and purification of the human CD44-HABD as a GST fusion protein

Human CD44 standard isoform cDNA (Aruffo et al., 1990) was used to amplify the HA-binding domain, covering aa 21–132. The resulting PCR amplification product was cloned into a pGEX-KG vector (Guan and Dixon, 1991). Generation of HABD non-HA-binding mutants was performed by means of the QuickChange site-directed mutagenesis kit (Stratagene, La Jolla, CA, USA). Mutagenic oligo pairs R41A (5′-GAGAA AAATGGTGCCTACAGCATCTCTCGG-3′, 5′-AGATGCT GTAGGCACCATTTTTCTCCACG-3′) and R78SY79S (5′-GACCTGCAGCTCTGGGTTCATAG-3′, 5′-ATGAACCCA GAGCTGCAGGTCTC-3′) were used for introduction of R41A and/or R78SY79S mutations, respectively, into human CD44-HABD. Wild-type or mutant (R41A, R78SY79S or R41AR78SY79S) glutathione *S*-transferase CD44-HABD (GST-HABD) expression constructs were transformed into *Escherichia coli* BL21(DE3)pLysS strain. Protein expression was induced at 25°C with 0.5 mM IPTG at $OD_{600} = 0.7$ for

2.5 h and soluble recombinant proteins were purified using Glutathione Sepharose 4B beads (Amersham Biosciences AB, Uppsala, Sweden) according to the manufacturer's instructions.

Hyaluronic acid binding assay

High molecular weight HA at 1 mg/ml (Sigma) in PBS was used to coat Maxisorp (Nunc, Rochester, NY, USA) plates overnight at room temperature (RT). Wells were washed with PBS and blocked with 2% BSA for 2 h at RT. Purified proteins diluted in PBS were added to the wells and incubated for 1 h at RT. After three washes with PBS-0.1% Tween-20, the wells were incubated with mouse anti-GST antibody B-14 (Santa Cruz Biotechnology, Santa Cruz, CA, USA) for 1 h at RT before further washing and 1 h incubation at RT with horseradish peroxidase-conjugated goat anti-mouse secondary antibody (Jackson Immunoresearch, West Grove, PA, USA). HA binding was visualized by OPD chromogenic substrate (Sigma) and the absorbance was measured spectrophotometrically at 450 nm.

Cell migration assay

Migration assays were performed in Transwell migration chambers (pore size 8 μm; Costar, London, UK) essentially as described (Zhang *et al*., 2002). The lower compartment of the chambers contained 1 μg/ml high molecular weight HA (Sigma). Test proteins were added to the upper compartment at a final concentration of 10 μg/ml. For antibody inhibition assay, cells were preincubated for 30 min on ice with 10 μg/ml anti-CD44 mAb GKW.A3. Cells were added to the upper compartment of the Transwell chamber and allowed to migrate for 2 h. After the careful removal of all remaining cells in the upper chamber, the migrated cells were fixed and stained with 0.5% crystal violet. After washing, membranes were dried and bound dye was eluted with 10% acetic acid. The optical density of recovered eluate was read spectrophotometrically at 600 nm.

Tumor growth in mice and quantification of blood vessel density

1×10^6 BxPC-3 or SMMU-1 cells were injected s.c. into the backs of 6–8-weeks-old female BALB/cABom nude mice (M&B, Ry, Denmark). When tumor nodules appeared, the mice started to receive subcutaneous injections proximal to the tumor of 20 μg (BxPC-3) or 50 μg (SMMU-1) of wild-type GST-HABD, GST-HABD^{R41AR78SY79S} (GST-3MUT) or GST in 100 μl PBS. The treatment was repeated every second day. The tumor volume was measured and calculated using the formula $(\text{width}^2 \times \text{length}) \times 0.52$ (O'Reilly *et al*., 1997). At the end of the experiments, the mice were killed and tumors were dissected and analysed for weight.

For immunohistochemical analysis, dissected tumors were fixed in 4% paraformaldehyde and embedded into paraffin. Tissue sections (5 μm-thick) were stained for blood vessels using goat anti-mouse PECAM-1 polyclonal antibody diluted 1:50 (M-20; Santa Cruz Biotechnology, Santa Cruz, CA, USA) followed by incubation with biotin-conjugated rabbit anti-goat secondary antibody (Jackson Immunoresearch, West Grove, PA, USA). Antibody binding was detected using Vectastain ABC Kit and 3-amino-9-ethyl carbazole (AEC) as chromophore (Vector Laboratories, Burlingame, CA, USA). For quantification of blood vessel density three tumors per treatment were selected and 700–1600 of PECAM-1-positive blood vessels from each group were counted at $\times 200$ magnification.

Chick CAM angiogenesis assay

In all, 10-day-old chick embryos were prepared as described (Brooks *et al*., 1999). For angiogenesis assay, filter discs, 5 mm in diameter, were saturated with 3 mg/ml cortisone acetate (Sigma), soaked with 100 ng/ml VEGF (Sigma), 1 μg/ml bFGF (Gibco Lifetech, Carlsbad, CA, USA) or 200 ng/ml TGFα (Sigma) in PBS and placed onto CAMs. Filter discs were then treated daily by topical addition of 10 μg of GST-HABD, GST-3MUT, GST in 25 μl PBS or vehicle alone. After 72 h, the filter discs and the surrounding CAM tissue were dissected and angiogenesis quantified in a dissection microscope. Angiogenesis was assessed in a double blind manner as the number of blood vessel branch points within the CAM area directly under the filter discs.

Cell cycle analysis

Exponentially growing cells were incubated for 48 h in the presence of 15 (CPAE) or 30 (all other cells) μg/ml GST-HABD, GST-3MUT or GST. All cells were incubated with proteins in serum containing medium with 10 mM HEPES pH 7.4. Tumor cells were incubated in 5% FCS while HUVEC and CPAE cells were grown in 10% FCS. After 48 h, cells were pulsed with 30 μg/ml bromodeoxyuridine (BrdU) for 60 min, harvested and fixed in ice-cold ethanol. Cells were then stained for BrdU with anti-BrdU mAb G3G4 (Developmental Studies Hybridoma Bank, University of Iowa, IA, USA) diluted 1:50 followed by a FITC-conjugated goat anti-mouse antibody (Jackson Immunoresearch, West Grove, PA, USA) in parallel staining with propidium iodide (PI). The cell cycle distribution was then analysed with a FACScan Flow Cytometer (Becton Dickinson, Franklin Lakes, NJ, USA) after plotting FITC-content *vs* PI as previously described (Bakhiet *et al*., 2001).

MTT cell proliferation assay

For the proliferation assay CPAE cells were plated onto 24-well culture plates (12,500 cells/well) and incubated overnight. Then complete media was replaced by 10% FCS-containing medium and the cells were incubated for 48 h in the presence of 0.1–10 μg/ml GST-HABD, GST-3MUT or GST. At the end of the treatment, 10 μl of MTT (Thiozolyl Blue, Sigma) solution (0.5% in PBS) was added to 100 μl of medium in each well. After 3 h incubation with MTT at 37°C, the medium was carefully removed and the converted MTT was extracted from cells with acidic isopropanol (0.1 N HCl in isopropanol). Absorbance of converted dye was measured using plate reader at 540 nm with background subtraction at 690 nm.

GST-HABD binding assay

Subconfluent adherent cells were washed once with ice-cold PBS containing 0.1% BSA, 0.1% NaN_3 (stain wash medium, SWM) and removed from plates by scraping. The cells were incubated for 1 h on ice with 5 μg/ml Alexa488 labeled GST-proteins in 100 μl SWM, then washed three times with ice-cold SWM and resuspended in PBS. Fluorescence was analysed by FACSort Flow Cytometer (Becton Dickinson, Franklin Lakes, New Jersey).

Statistical analysis

Statistical analysis of data was perfomed using a heteroscedastic two-tailed Student's *t*-test.

Acknowledgements
We thank Dr Anatoli Onischenko for the help with the chick CAM angiogenesis model. This work was supported by grants from the Swedish Cancer Society, the Estonian Science Foundation (3841, 5129) and Howard Hughes Medical Institute's International Research Fellowship. PK is an International Senior Research Fellow of the Wellcome Trust.

References

Ahrens T, Sleeman JP, Schempp CM, Howells N, Hofmann M, Ponta H, Herrlich P and Simon JC. (2001). *Oncogene*, **20,** 3399–3408.

Arch R, Wirth K, Hofmann M, Ponta H, Matzku S, Herrlich P and Zoller M. (1992). *Science*, **257,** 682–685.

Aruffo A, Stamenkovic I, Melnick M, Underhill CB and Seed B. (1990). *Cell*, **61,** 1303–1313.

Bajorath J, Greenfield B, Munro SB, Day AJ and Aruffo A. (1998). *J. Biol. Chem.*, **273,** 338–343.

Bakhiet M, Tjernlund A, Mousa A, Gad A, Strömblad S, Kuziel WA, Seiger A and Andersson J. (2001). *Nat. Cell. Biol.*, **3,** 150–157.

Bartolazzi A, Nocks A, Aruffo A, Spring F and Stamenkovic I. (1996). *J. Cell. Biol.*, **132,** 1199–1208.

Bennett KL, Jackson DG, Simon JC, Tanczos E, Peach R, Modrell B, Stamenkovic I, Plowman G and Aruffo A. (1995). *J. Cell. Biol.*, **128,** 687–698.

Bergers G, Brekken R, McMahon G, Vu TH, Itoh T, Tamaki K, Tanzawa K, Thorpe P, Itohara S, Werb Z and Hanahan D. (2000). *Nat. Cell. Biol.*, **2,** 737–744.

Brooks PC, Montgomery AM and Cheresh DA. (1999). *Methods Mol. Biol.*, **129,** 257–269.

Cichy J, Bals R, Potempa J, Mani A and Pure E. (2002). *J. Biol. Chem.*, **277,** 44440–44447.

Culty M, Nguyen HA and Underhill CB. (1992). *J. Cell. Biol.*, **116,** 1055–1062.

Dimitroff CJ, Lee JY, Rafii S, Fuhlbrigge RC and Sackstein R. (2001). *J. Cell. Biol.*, **153,** 1277–1286.

Griffioen AW, Coenen MJ, Damen CA, Hellwig SM, van Weering DH, Vooys W, Blijham GH and Groenewegen G. (1997). *Blood*, **90,** 1150–1159.

Guan KL and Dixon JE. (1991). *Anal. Biochem.*, **192,** 262–267.

Gunthert U, Hofmann M, Rudy W, Reber S, Zoller M, Haussmann I, Matzku S, Wenzel A, Ponta H and Herrlich P. (1991). *Cell*, **65,** 13–24.

Guo N, Krutzsch HC, Inman JK and Roberts DD. (1997). *Cancer Res.*, **57,** 1735–1742.

Guo Y, Ma J, Wang J, Che X, Narula J, Bigby M, Wu M and Sy MS. (1994). *Cancer Res.*, **54,** 1561–1565.

Hanahan D and Folkman J. (1996). *Cell*, **86,** 353–364.

Holmgren L, O'Reilly MS and Folkman J. (1995). *Nat. Med.*, **1,** 149–153.

Jalkanen S and Jalkanen M. (1992). *J. Cell. Biol.*, **116,** 817–825.

Kajita M, Itoh Y, Chiba T, Mori H, Okada A, Kinoh H and Seiki M. (2001). *J. Cell. Biol.*, **153,** 893–904.

Katoh S, McCarthy JB and Kincade PW. (1994). *J. Immunol.*, **153,** 3440–3449.

Kaya G, Rodriguez I, Jorcano JL, Vassalli P and Stamenkovic I. (1997). *Genes Dev.*, **11,** 996–1007.

Kerbel R and Folkman J. (2002). *Nat. Rev. Cancer*, **2,** 727–739.

Koch AE, Halloran MM, Haskell CJ, Shah MR and Polverini PJ. (1995). *Nature*, **376,** 517–519.

Kogerman P, Sy MS and Culp LA. (1997). *Oncogene*, **15,** 1407–1416.

Kohda D, Morton CJ, Parkar AA, Hatanaka H, Inagaki FM, Campbell ID and Day AJ. (1996). *Cell*, **86,** 767–775.

Lesley J, Hyman R and Kincade PW. (1993). *Adv. Immunol.*, **54,** 271–335.

Lokeshwar VB, Iida N and Bourguignon LY. (1996). *J. Biol. Chem.*, **271,** 23853–23864.

Mori H, Tomari T, Koshikawa N, Kajita M, Itoh Y, Sato H, Tojo H, Yana I and Seiki M. (2002). *EMBO J.*, **21,** 3949–3959.

Nguyen M, Strubel NA and Bischoff J. (1993). *Nature*, **365,** 267–269.

Okamoto I, Kawano Y, Tsuiki H, Sasaki J, Nakao M, Matsumoto M, Suga M, Ando M, Nakajima M and Saya H. (1999). *Oncogene*, **18,** 1435–1446.

Okamoto I, Tsuiki H, Kenyon LC, Godwin AK, Emlet DR, Holgado-Madruga M, Lanham IS, Joynes CJ, Vo KT, Guha A, Matsumoto M, Ushio Y, Saya H and Wong AJ. (2002). *Am. J. Pathol.*, **160,** 441–447.

O'Reilly, MS, Boehm T, Shing Y, Fukai N, Vasios G, Lane WS, Flynn E, Birkhead JR, Olsen BR and Folkman J. (1997). *Cell*, **88,** 277–285.

O'Reilly MS, Holmgren L, Chen C and Folkman J. (1996). *Nat. Med.*, **2,** 689–692.

O'Reilly MS, Holmgren L, Shing Y, Chen C, Rosenthal RA, Moses M, Lane WS, Cao Y, Sage EH and Folkman J. (1994). *Cell*, **79,** 315–328.

O'Reilly MS, Pirie-Shepherd S, Lane WS and Folkman J. (1999). *Science*, **285,** 1926–1928.

Parangi S, O'Reilly M, Christofori G, Holmgren L, Grosfeld J, Folkman J and Hanahan D. (1996). *Proc. Natl. Acad. Sci. USA*, **93,** 2002–2007.

Savani RC, Cao G, Pooler PM, Zaman A, Zhou Z and DeLisser HM. (2001). *J. Biol. Chem.*, **276,** 36770–36778.

Schmits R, Filmus J, Gerwin N, Senaldi G, Kiefer F, Kundig T, Wakeham A, Shahinian A, Catzavelos C, Rak J, Furlonger C, Zakarian A, Simard JJ, Ohashi PS, Paige CJ, Gutierrez-Ramos JC and Mak TW. (1997). *Blood*, **90,** 2217–2233.

Screaton GR, Bell MV, Jackson DG, Cornelis FB, Gerth U and Bell JI. (1992). *Proc. Natl. Acad. Sci. USA*, **89,** 12160–12164.

Sherman LS, Rizvi TA, Karyala S and Ratner N. (2000). *J. Cell. Biol.*, **150,** 1071–1084.

Stellmach V, Crawford SE, Zhou W and Bouck N. (2001). *Proc. Natl. Acad. Sci. USA*, **98,** 2593–2597.

Thomas L, Byers HR, Vink J and Stamenkovic I. (1992). *J. Cell. Biol.*, **118,** 971–977.

Trochon V, Mabilat C, Bertrand P, Legrand Y, Smadja-Joffe F, Soria C, Delpech B and Lu H. (1996). *Int. J. Cancer*, **66,** 664–668.

van der Voort R, Taher TE, Wielenga VJ, Spaargaren M, Prevo R, Smit L, David G, Hartmann G, Gherardi E and Pals ST. (1999). *J. Biol. Chem.*, **274,** 6499–6506.

Weber GF, Ashkar S, Glimcher MJ and Cantor H. (1996). *Science*, **271,** 509–512.

Yu Q and Stamenkovic I. (1999). *Genes Dev.*, **13,** 35–48.

Yu Q and Stamenkovic I. (2000). *Genes Dev.*, **14,** 163–176.

Yu Q, Toole BP and Stamenkovic I. (1997). *J. Exp. Med.*, **186,** 1985–1996.

Zhang H, Li Z, Viklund E. and Strömblad S. (2002). *J. Cell. Biol.*, **158,** 1287–1297.

PUBLICATION II

Päll T., Pink A., Kasak L., Turkina M., Anderson W., Valkna A., Kogerman P. (2011) Soluble CD44 Interacts with Intermediate Filament Protein Vimentin on Endothelial Cell Surface. PLoS ONE 6(12): e29305. doi:10.1371/journal.pone.0029305

OPEN ACCESS Freely available online PLoS one

Soluble CD44 Interacts with Intermediate Filament Protein Vimentin on Endothelial Cell Surface

Taavi Päll[1,2]*, Anne Pink[1,2], Lagle Kasak[1,2], Marina Turkina[2], Wally Anderson[2], Andres Valkna[1,2], Priit Kogerman[1,2]

1 Department of Gene Technology, Tallinn University of Technology, Tallinn, Estonia, **2** Competence Center for Cancer Research, Tallinn, Estonia

Abstract

CD44 is a cell surface glycoprotein that functions as hyaluronan receptor. Mouse and human serum contain substantial amounts of soluble CD44, generated either by shedding or alternative splicing. During inflammation and in cancer patients serum levels of soluble CD44 are significantly increased. Experimentally, soluble CD44 overexpression blocks cancer cell adhesion to HA. We have previously found that recombinant CD44 hyaluronan binding domain (CD44HABD) and its non-HA-binding mutant inhibited tumor xenograft growth, angiogenesis, and endothelial cell proliferation. These data suggested an additional target other than HA for CD44HABD. By using non-HA-binding CD44HABD Arg41Ala, Arg78Ser, and Tyr79Ser-triple mutant (CD443MUT) we have identified intermediate filament protein vimentin as a novel interaction partner of CD44. We found that vimentin is expressed on the cell surface of human umbilical vein endothelial cells (HUVEC). Endogenous CD44 and vimentin coprecipitate from HUVECs, and when overexpressed in vimentin-negative MCF-7 cells. By using deletion mutants, we found that CD44HABD and CD443MUT bind vimentin N-terminal head domain. CD443MUT binds vimentin in solution with a Kd in range of 12–37 nM, and immobilised vimentin with Kd of 74 nM. CD443MUT binds to HUVEC and recombinant vimentin displaces CD443MUT from its binding sites. CD44HABD and CD443MUT were internalized by wild-type endothelial cells, but not by lung endothelial cells isolated from vimentin knock-out mice. Together, these data suggest that vimentin provides a specific binding site for soluble CD44 on endothelial cells.

Citation: Päll T, Pink A, Kasak L, Turkina M, Anderson W, et al. (2011) Soluble CD44 Interacts with Intermediate Filament Protein Vimentin on Endothelial Cell Surface. PLoS ONE 6(12): e29305. doi:10.1371/journal.pone.0029305

Editor: Valdur Saks, Université Joseph Fourier, France

Received July 12, 2011; **Accepted** November 24, 2011; **Published** December 21, 2011

Funding: This work was supported by the European Regional Development Fund via Enterprise Estonia grants (EU28138/EU28658, EU30013) to Competence Center for Cancer Research and by Estonian Science Fund (grant 8116 to P.K.). The funders had no role in study design, data collection and analysis, decision to publish, or preparation of the manuscript.

Competing Interests: The authors have declared that no competing interests exist.

* E-mail: taavi.pall@ttu.ee

Introduction

CD44 transmembrane glycoprotein functions as hyaluronan (HA) receptor. CD44 has functions in a lymphocyte homing, mediates cell adhesion to HA and HA metabolism. CD44 is expressed on many cell types including endothelial cells (EC) and has multiple alternatively spliced isoforms. CD44 plays a significant role in tumor malignancy. High levels of CD44 expression on tumor cells is sufficient to establish metastatic behavior [1,2]. CD44 is involved in pathological angiogenesis, as its expression is elevated in tumor vasculature, and CD44 expression can be induced in cultured ECs by angiogenic growth factors [3] Furthermore, CD44 knockout mice show reduced vascularisation of tumor xenografts and Matrigel plugs [4]. In addition to cell surface expression, CD44 is present in soluble form in lymph and serum [5] or bound to extracellular matrix [6]. Soluble CD44 is generated either by alternative splicing [7] or, more importantly, by ectodomain shedding by matrix metalloproteases [8,9].The size of shed CD44 is highly heterogeneous because of glycosylations and variant exons [5,9–11]. The serum concentration of sCD44 in mice is known to range between 490 to 2100 ng/ml [5]. Studies of sCD44 in the sera of non-Hodgkin's lymphoma and breast cancer patients show that physiological sCD44 level in healthy persons is in the range of 250 to 500 ng/ml [12–14]. The serum concentration of sCD44 in healthy individuals is ~3 nM whereas it was shown to be significantly elevated in patients with advanced gastric (24 nM) or colon cancer (31 nM) [11]. Elevated serum sCD44 or sCD44v6 is a predictor of poor therapeutic outcome in non-Hodgkin's lymphoma or breast cancer patients, respectively [12,15].The source of sCD44 are lymphocytes, macrophages, ECs, and tumor cells [10,11,16]. In non-Hodgkin's lymphoma, the source of elevated sCD44 are lymphoma cells, and sCD44 levels decrease after treatment in patients with complete remission [10,17]. Endothelial and macrophage CD44 expression is increased in atheromas and CD44 shedding from EC and macrophages is stimulated by proinflammatory cytokines [16].

Tumors are surrounded by HA-rich ECM. When overexpressed in tumor cells, soluble CD44 can function as an antagonist to cell membrane CD44 and block its binding to ECM HA. Overexpression of soluble forms of CD44 inhibits HA-adhesion of mouse mammary carcinoma or melanoma cells and caused inhibition of tumor cell proliferation, and reduced tumorigenicity [18–20]. CD44 knockout in mouse breast cancer model caused increased numbers of lung metastases, which correlated with reduced invasion of CD44-expressing metastatic breast cancer cell lines into HA-containing collagen matrixes [21].

CD44 binds HA via the link module in its N-terminal domain. The link module is approximately 100 amino acids long and consists of two alpha helices and two triple-stranded antiparallel beta sheets, stabilized by two disulphide bridges [22]. The structure of CD44 HABD has an additional lobe consisting of four beta strands formed by the residues flanking the core link module [23,24]. This enlarged structure is stabilized by an additional disulphide bridge between flanking regions. Together, the human CD44 HABD structure consists amino acids 21–169. The HA-binding surface of CD44 is exclusively covered by the link module and its flanking regions do not contribute to the HA binding [23]. The critical residues in CD44 HA-binding surface directly involved in binding are Arg41, Tyr42, Arg78, and Tyr79, according to studies of human CD44 [23,25]. Glycosylation of Asn25 and Asn125 within CD44 HABD is involved in regulation of HA binding [26]. Altogether, CD44 has five N-glycosylation sites (Asn25, Asn57, Asn100, Asn110, Asn120) within its HABD. Bacterially expressed recombinant human CD44 HABD containing amino acids 20–178 binds HA comparably to glycosylated CD44-Rg fusion protein [24]. HA binding function is also retained by a recombinant human CD44HABD containing amino acids 21–132, whereas HA binding was abolished by the mutations in Arg41, Arg78, and Tyr79 [27].

Vimentin intermediate filaments comprises supporting framework within cells. Vimentin functions in intracellular vesicular transport, including β1-integrin trafficking [28], transport of lysosomal membrane proteins by binding AP-3 complex [29], and as a cytosolic reservoir for tSNARE SNAP23 [30]. Importantly, vimentin knockout cells apparently retain intact receptor-mediated endocytosis, as transferrin receptor level and distribution is normal [29,30]. Vimentin-deficient mice reproduce and develop normally [31], however, they show reduced elasticity of arteries, decreased nitric oxide production and elevated endothelin [32,33]. Vimentin is expressed on cell surface in several cell types, including TNF-α induced macrophages [34], cutaneous T-cell lymphoma [35], platelets [36], and brain microvascular endothelial cells [37]. Vimentin extracellular ligands include vitronectin/PAI-1 complex [36], and *E. coli* IbeA protein [37]. Vimentin is a antiangiogenesis target overexpressed on tumor endothelium *in vivo*. Anti-vimentin antibody treatment inhibited subcutaneous tumor xenograft growth and tumor blood vessel density in mice, suggesting that vimentin is localized to the cell surface in tumor endothelial cells [38].

CD44 and vimentin are both detectable from membrane lipid raft fractions [39–41] and from clathrin-independent pathway endocytic vesicles in fibroblasts [42]. CD44 and vimentin are upregulated during epithelial-mesenchymal transition (EMT) of cancer cells. Mammary epithelial cells undergoing EMT downregulate epithelial genes and upregulate mesenchymal genes, such as E-cadherin, N-cadherin and vimentin, respectively. Suppression of standard CD44 isoform in Snail- or TGF-β-induced human mammary epithelial cells inhibits EMT, accompanied by vimentin downregulation [43].

We have previously found that recombinant CD44 HABD 21–132, as a model for soluble CD44, inhibited human subcutaneous tumor xenograft growth in mice, angiogenesis in chick chorioallantoic membrane, and EC proliferation [27]. Surprisingly, these CD44HABD functions were independent of its HA-binding propery, as non-HA-binding mutant was similarly effective. Therefore, we proposed that CD44HABD could bind additionally to a different ligand than HA. In this study, we used CD44HABD non-HA-binding mutant as a bait in GST pull-down assay and identified vimentin as a novel CD44 interacting protein.

Results

Identification of vimentin as CD44 HABD-binding protein

To identify EC target of CD44 HABD 21–132 (CD44HABD) and its non-HA-binding mutant CD44HABD^{R41AR78SY79S} (CD443MUT), we used GST pull-down from HUVEC lysate. Silver staining of pull-down reactions separated by SDS-PAGE revealed that GST-tagged CD443MUT precipitated a 60 kD protein (Figure 1A). This protein was identified by MALDI-TOF-MS protein fingerprinting as vimentin. To confirm that CD44HABD-proteins pull down vimentin, we used anti-vimentin (V9) immunoblotting. Immunoblotting confirmed that GST-tagged CD44HABD and CD443MUT pulled down endogenous vimentin from HUVEC lysates (Figure 1B, upper panel). To determine whether CD44HABD and CD443MUT bind vimentin directly, we used recombinant vimentin in the GST pull-down assay. We found that both CD44HABD and CD443MUT were able to pull down recombinant vimentin, suggesting that CD44 interacts with vimentin directly (Figure 1B, lower panel). We next used immunoprecipitation (IP) to determine whether endogenous CD44 and vimentin associate in EC. HUVEC lysate was immunoprecipitated using anti-CD44 (MEM-263) antibody and immunoprecipitates were subsequently analyzed by immunoblotting. We found that a minor population of vimentin coimmunoprecipitated with CD44 from HUVEC lysate (Figure 1C). We also tested whether anti-vimentin antibodies coimmunoprecipitate CD44. However, we were not able to detect CD44 from anti-vimentin IPs (A.P., unpublished data). To further confirm full-length CD44 and vimentin association we overexpressed C-terminally Flag-tagged CD44 standard isoform and Myc-tagged vimentin in vimentin nonexpressing MCF-7 cells. Overexpressed vimentin was exposed to the cell surface as detected by cell surface biotinylation (Figure S1). Immunoprecipitation results showed that anti-Flag immunoprecipitated a vimentin-Myc from CD44-Flag transfected cells (Figure 1D).

Vimentin and CD443MUT in vitro binding affinity

CD443MUT interaction with recombinant full length human vimentin was further characterized by isothermal titration calorimetry (ITC) and by surface plasmon resonance (SPR). We used two different preparations of CD443MUT. ITC experiments showed that CD443MUT binds to recombinant vimentin with Kd in 12–37 nM range with stoichiometry (vimentin/CD443MUT) of ≈7 mol/mol (Table 1). SPR experiments were carried out with vimentin immobilized into measuring cell. Kinetic analysis by SPR revealed that binding of CD443MUT to immobilized vimentin is described by a two-site ligand binding model. CD443MUT bound to a high-affinity site of immobilized vimentin with Kd 74 nM and Kd for low affinity site was 15 μM (Table 2). Analysis of kinetic data using equilibrium response values resulted in 15±2 μM Kd. The stoichiometry of vimentin/CD443MUT complex in SPR experiment was measured≈6 mol/mol .

Mapping of vimentin CD44-binding region

To map CD44-binding region in vimentin, we generated truncated vimentin constructs (Figure 2A). Vimentin deletion mutant VIM1-96 contains only head domain, VIM1-245 contains head domain and alpha-helices 1A-B, and VIM97-466 mutant lacks the head domain (aa numbering according to human vimentin). VIM246-466 mutant contains C-terminal half of the protein starting from alpha-helices 2A-B. VIM407-466 contains the tail domain. Lysates of MCF-7 cells, expressing either full-length vimentin or its deletion mutants, were used in GST pull-down with CD44HABD or CD443MUT. Pull-downs were analyzed by immunoblotting using tag-specific antibodies. This analysis showed that CD44HABD and CD443MUT bound only vimentin deletion mutants containing the head domain (VIM1-96 and VIM1-245; Figure 2B). Deletion of the head domain was sufficient to abolish binding of vimentin to CD44HABD and CD443MUT(VIM97-477, VIM246-466 or VIM407-466).

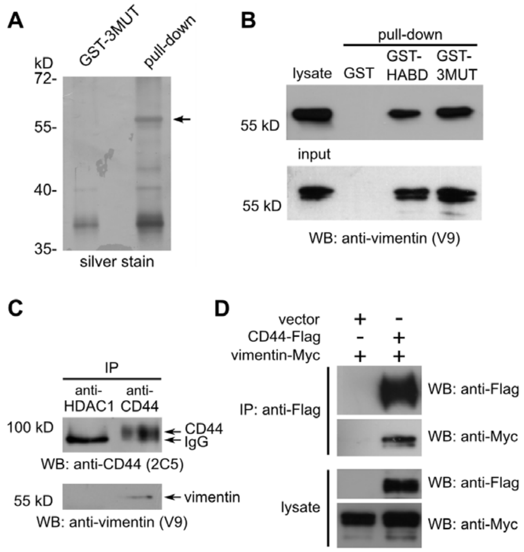

Figure 1. Identification of vimentin as CD44HABD-binding protein. (A) HUVEC lysate was used in GST pull-down to identify CD443MUT interacting proteins. Lysate was incubated with GST-CD443MUT (GST-3MUT) coated beads. Bound proteins were eluted using reduced glutathione and analyzed by SDS-PAGE and silver staining. GST-3MUT precipitated protein band (shown by arrow) was cut off from gel, trypsinolyzed and analyzed by MALDI-TOF MS. This protein was identified as vimentin. (B, upper panel) Vimentin pull-down by CD44HABD (GST-HABD) and GST-3MUT was confirmed by immunoblotting using anti-vimentin V9 antibody. (B, lower panel) GST-HABD and GST-3MUT pull-down recombinant vimentin. (C) Coimmunoprecipitation of vimentin with CD44 from HUVEC lysate. Anti-HDAC-1 antibody was used as a negative control (see Materials and methods). (D) Coimmunoprecipitation of over-expressed vimentin-Myc with CD44-Flag from MCF-7 lysates using tag-specific antibodies.
doi:10.1371/journal.pone.0029305.g001

Cell surface vimentin and CD443MUT-vimentin interaction is induced by VEGF

To detect cell surface vimentin, we performed biotinylation of cell surface proteins of adherent living HUVEC, followed by IP of vimentin from cell lysates. Biotinylated proteins were detected by immunoblotting using HRP-conjugated strepavidin. We found that anti-vimentin (V9) antibody immunoprecipitated from HUVEC lysate a 60 kD biotinylated protein. We used anti-CD44 (H4C4) antibody as positive control and found that it IPd a 100 kD biotinylated protein. These proteins correspond to expected sizes of vimentin and endothelial CD44, respectively (Figure 3A upper panel). The identity of biotinylated proteins was confirmed by immunoblotting with vimentin- or CD44-specific antibodies (Figure 3A lower panel).

Next, we decided to test whether CD443MUT cellular binding can be induced with angiogenic growth factors. To determine the effect of angiogenic stimulus on CD443MUT cellular binding we induced 6 h serum starved HUVEC 30 min with VEGF165 at 37°C. Then we incubated cells with Alexa Fluor 488-labeled CD443MUT at 4°C. CD443MUT-A488 cellular binding was quantitated using flow cytometry. We found a significant binding of CD443MUT-A488 to HUVEC compared to GST-A488 control ($P = 0.015$, $n = 3$, unpaired t-test). Under these conditions ~20% cells bound CD443MUT. VEGF treatment induced a further increase in CD443MUT cellular binding compared to non-induced cells, although this result was statistically marginally significant ($P = 0.067$, $n = 3$; Figure 3B). To confirm that VEGF induces cell surface vimentin binding sites for CD443MUT, we used cell surface biotinylation of HUVEC followed by GST pull-down with CD443MUT. For this, overnight serum starved HUVEC were induced 1 hour with VEGF or left non-induced, followed by cell surface biotinylation of live adherent cells. GST-CD443MUT or GST alone were used in pull-downs from cell-surface biotinylated HUVEC lysates. Subsecuently, precipitated proteins were detected by western blotting either by strepavidin-HRP or anti-vimentin (V9) antibody. We found that CD443MUT pulled down a 60 kD biotinylated protein from VEGF-stimulated but not from serum starved cells. This protein turned out to be vimentin since it could be detected with a vimentin-specific antibody (Figure 3C).

Vimentin displaces CD443MUT from HUVEC

To further characterize CD443MUT and vimentin interaction on HUVECs we measured the ability of vimentin to compete with ^{125}I-labeled CD443MUT for cellular binding. The results of displacement binding experiments showed that CD443MUT displaced itself from HUVEC with logEC50 -5.8 ± 0.05 M (EC50 = 1.57 μM, $n = 9$; Figure 3D). Vimentin displaced CD443MUT from HUVEC with logEC50 -5.37 ± 0.21 M (EC50 = 4.26 μM , $n = 2$) which is not significantly different from displacement by CD443MUT itself (extra sum of squares F-test, $P = 0.0711$; $F = 3.298$ (1,171)). BSA did not displace CD443MUT effectively, with logEC -3.93 ± 0.06 M (EC50 = 117 μM, $n = 4$).

CD44HABD endocytosis by HUVEC

Given that vimentin provides specific binding site for CD443MUT on EC, we decided to test whether CD443MUT is endocytosed upon binding to cell surface vimentin. We incubated HUVEC with unlabeled CD443MUT for 30 min at 37°C to allow internalization. CD443MUT was detected by immunofluorescence confocal microscopy using CD443MUT specific mouse monoclonal antibody 1A2 (Figure S2). Recombinant GST uptake

Table 1. Summary of Kd values for CD443MUT and vimentin interaction measured by ITC.

CD443MUT preparation	CD443MUT (μM)	Vimentin (μM)	Kd (M)	n[a] (mol/mol)
A	4.2	1.8	$1.2 \cdot 10{-}8 \pm 10{-}9$	9.9 ± 0.5
	1.5	0.5	$3.7 \cdot 10{-}8 \pm 10{-}9$	
B	4.2	1.8	$1.8 \cdot 10{-}8 \pm 10{-}9$	7.2 ± 0.3
	0.9	0.5	$2.3 \cdot 10{-}8 \pm 10{-}9$	

[a], stoichiometry (vimentin/CD443MUT).
doi:10.1371/journal.pone.0029305.t001

Table 2. Kinetic parameters for binding of CD443MUT to vimentin measured by SPR.

Kass1 (M^{-1} s^{-1})×10^3	Kass2 (M^{-1} s^{-1})	Kdiss1 (s^{-1})×10^{-4}	Kdiss2 (s^{-1})×10^{-3}	Kd (μM) Kdiss1/Kass1	Kd (μM) equation 1	*n* (mol/mol)
7.6±0.1	183±7	5.6±0.1	1.9±0.1	0.074	15±2	6.2

doi:10.1371/journal.pone.0029305.t002

was used as a control. The results showed that CD443MUT was readily endocytosed by HUVEC and displayed a vesicular localization pattern (Figure 4A). Next, we used CD443MUT directly conjugated to Alexa Fluor 568 for internalization assay. CD443MUT-A568 was endocytosed and distributed in HUVEC cytoplasm similarly to unlabeled CD443MUT (Figure 4B). HUVECs express vimentin at high level, and endocytosed CD443MUT-containing vesicles were surrounded by a dense network of vimentin intermediate filaments, however, there was no direct colocalization of CD443MUT with vimentin filaments (Figure 4A and B).

Next, we used a generic endocytosis marker cholera toxin B conjugated to Alexa Fluor 555 (CTxB-A555) to trace CD443MUT following endocytosis. We found that after 30 min uptake Alexa Fluor 488-labeled CD44HABD as well as -3MUT colocalized with CTxB-A555 positive structures (Figure 5A). We quantitated colocalization of CTxB with CD44HABD and CD443MUT from single slices of confocal image stacks as described in Materials and Methods. Altogether, $\sim 2.6 \cdot 10^4$ CTxB-positive vesicles were analyzed from CD44HABD- ($n = 39$) or CD443MUT-incubated cells ($n = 38$). As shown in Figure 5B, approximately 4–5% of CTxB-vesicles colocalized and showed positive correlation with CD44HABD (average Pearson's $r = 0.469$, 95% CI 0.438 to 0.498, $df = 679$, $P < 0.0001$) or CD443MUT ($r = 0.532$, 95% CI 0.503 to 0.531, $df = 608$, $P < 0.0001$). We next analyzed CD443MUT-A488 colocalization with early endosome marker EEA1 in HUVEC after 10 min uptake followed by 20 min chase. We found that CD443MUT-A488 showed extensive colocalization with EEA1-positive vesicles after 10 min incubation (Figure 5C). Quantitation of CD443MUT and EEA1 colocalization in $\sim 6.5 \cdot 10^3$ EEA1-endosomes showed that 32% of EEA1-endosomes colocalized with CD443MUT after 10 min incubation ($r = 0.311$, 95% CI 0.266 to 0.355, $df = 407$, $P < 0.0001$), whereas a fraction of EEA1-endosomes showing colocalization falled to 7% after 20 min chase ($r = 0.321$, 95% CI 0.251 to 0.388, $df = 172$, $P < 0.0001$) following the incubation (Figure 5D). The number of CD443MUT-vesicles in cells reduced during 20 min chase by ~7.5 times (Figure 5D, rightmost panel) suggesting trafficking of CD44 to late endosomal-lysosomal degradation pathway. Therefore, we next analyzed whether CD443MUT is targeted to the CD63-positive late endosomal compartment after 20 min chase following a 10 min pulse with CD443MUT-A488. However, we found that CD443MUT-A488 showed no significant accumulation within anti-CD63 staining vesicles after 20 min (Figure 5E) or 50 min chase (data not shown). Together, these results indicate that recombinant CD44HABD and CD443MUT are endocytosed and reach early endosomal compartment.

CD443MUT endocytosis is inhibited in ECs derived from vimentin-null mice

To test directly whether vimentin mediates CD443MUT internalization, we isolated lung endothelial cells from wild-type

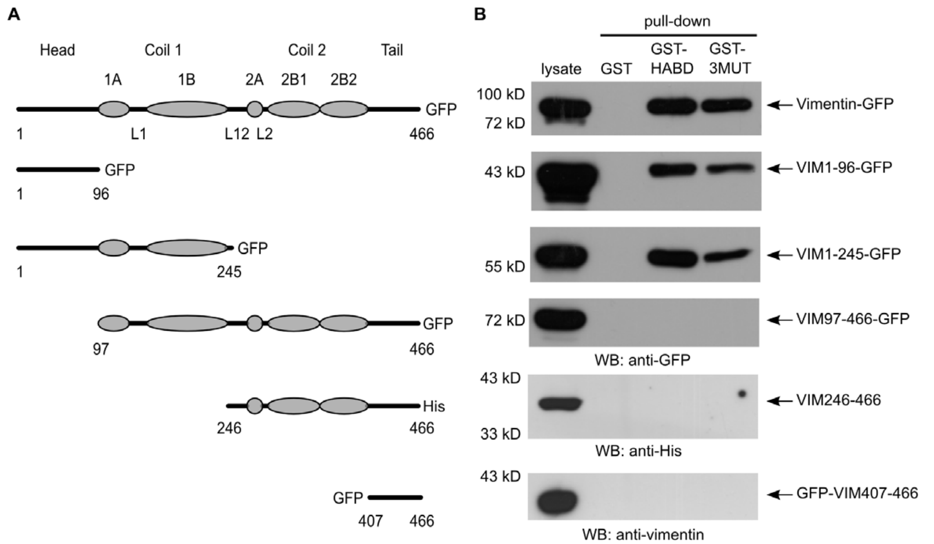

Figure 2. CD443MUT binds vimentin N-terminal head domain. (A) A diagram of vimentin sub-domains and deletion mutants used in pull-down reactions. Ellipses represent alpha-helices in coiled-coil domains and L1-L2 mark linker regions. GFP, green fluorescent protein. (B) GST pull-down reactions were performed from cell lysates transfected with full length vimentin or its deletion mutants (see Materials and methods). Eluates from pull-downs were analyzed by immunoblotting.
doi:10.1371/journal.pone.0029305.g002

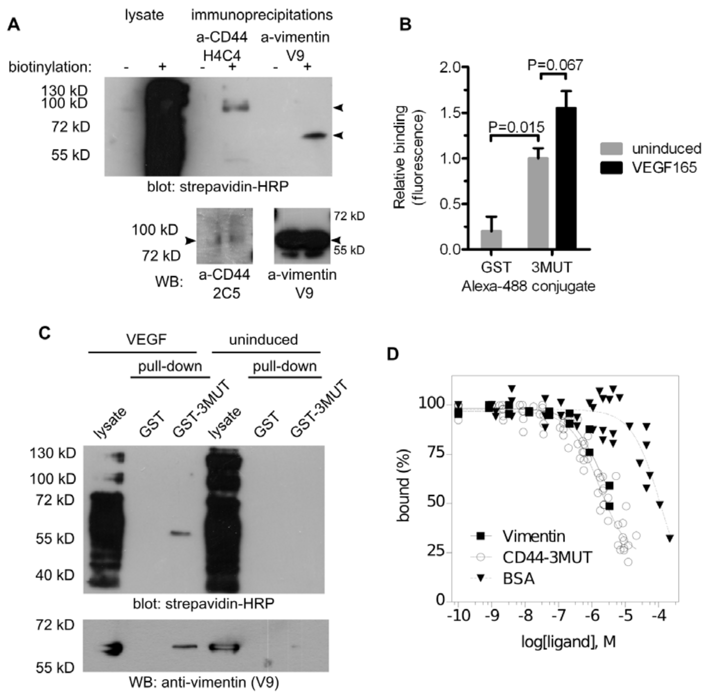

Figure 3. VEGF induces cell surface vimentin and CD443MUT cellular binding. (A) For detection of cell surface vimentin, asynchronously growing live adherent HUVEC were cell surface biotinylated and lysate was used for immunoprecipitation using anti-vimentin or anti-CD44 antibodies. Immunoprecipitated proteins were detected by immunoblotting using strepavidin-HRP (upper panel) or specific antibodies (lower panels). (B) 6 hour serum-starved HUVEC were induced for 30 min with VEGF165, followed by incubation on ice with Alexa Fluor 488-labeled CD443MUT (3MUT). GST Alexa Fluor 488 conjugate was used as negative control. Cellular binding of A488-conjugated proteins was analyzed by FACS. Bars represent average geomean of fluorescence from three experiments (mean $\pm$ SE). (C) Overnight serum-starved HUVEC were induced for 1 hour with VEGF165, followed by cell surface biotinylation. Lysate from biotinylated cells was used in pull-down using GST-3MUT. Precipitated proteins were detected by immunoblotting using strepavidin-HRP (upper panel) or anti-vimentin antibody (lower panel). (D) For displacement assay, cells were resuspended in incubation buffer in 96-well plate. CD443MUT, vimentin or BSA at different concentrations was added to the wells along with ^{125}I-labeled CD443MUT. Reactions were incubated overnight at 4°C. After incubation, reactions were stopped by filtration through glass fiber filters blocked with BSA. Filters were washed with PBS and bound radioactivity was measured using gamma counter. The curves represent global fitting of normalized radioligand binding data from two to nine experiments.
doi:10.1371/journal.pone.0029305.g003

(WT) or vimentin-null mice (Figure 6A). We characterized isolated mouse lung endothelial cells (MLEC) for endothelial-specific cell surface markers by flow cytometry (Figure 6B). FACS staining showed that PECAM-1 and CD44 were expressed on vimentin-null MLEC at levels comparable to WT cells. However, ICAM-2 expression was reduced on vimentin-null MLEC compared to WT cells. We next tested the internalization of CD443MUT-A568 by MLEC. We found that WT MLEC endocytosed CD443MUT comparably to HUVEC after 30 min uptake, whereas CD443MUT uptake by MLECs isolated from vimentin-null mice was inhibited (Figure 6C).

Discussion

We have identified vimentin as a novel CD44 binding protein. Our results – the fact that recombinant CD44HABD and CD443MUT pulled down both endogenous as well as recombinant vimentin, and the finding that vimentin displaces CD443MUT bound to HUVEC cells, suggest that CD44-vimentin interaction is a direct protein-protein interaction. To our knowledge, CD44-vimentin interaction is the first protein-protein interaction described for CD44 HABD. CD44 HABD mediates low affinity interactions with its ECM ligand HA with an *in vitro* Kd of 50 μM [23]. CD44 is a membrane glycoprotein and interacts via its glycosylated variant exons with various extracellular ligands, including fibronectin, collagen XIV, E-selectin and osteopontin [44–47]. CD44 HABD contains five N-linked glycosylation sites [48]. Our experiments, where glycosylated EC-endogenous or tumor cell over-expressed full-length CD44 immunoprecipitated vimentin correlate with our initial findings obtained with soluble recombinant CD44HABD or CD443MUT and strongly suggest that post-translationally modified CD44 can also form a complex with vimentin. However, we were not able to detect full-length CD44 in anti-vimentin antibody immunoprecipitates from HUVEC lysates, which can be explained by the fact that while HUVEC express high levels of vimentin, only a small fraction forms a complex with membrane bound CD44.

We found that CD44 HABD binds to vimentin within its head domain. Vimentin head-domain interactions include ankyrin binding at the plasma membrane [49], vimentin head-domain is also important in filament formation [50]. Our finding that CD44 binds to vimentin head domain is consistent with the proposed

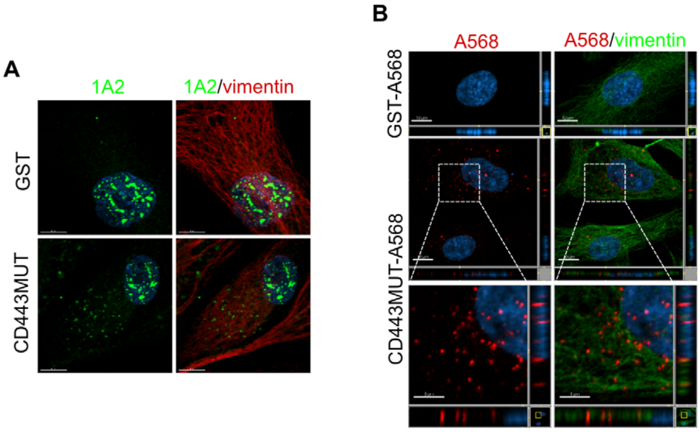

Figure 4. CD443MUT endocytosis by HUVEC. HUVEC were grown overnight on glass slides and incubated for 30 min at 37°C with 1 μM unlabeled or Alexa Fluor 568-labeled CD443MUT or GST. Cells were analyzed by confocal microscopy. (A) Uptake of unlabeled CD443MUT by HUVEC was detected with anti-CD443MUT mouse mAb 1A2 (green). Vimentin intermediate filaments were detected with rabbit polyclonal antibody (red). Nuclei were stained with Hoechst (blue). Images are maximum intensity projections, generated along the z-axis of image stack. Scale bars, 10 μm. (B) Internalization of directly Alexa Fluor 568-labeled CD443MUT by HUVEC (red). Vimentin (green) was detected with V9 mAb. Scale bars, upper and middle panels 10 μm; insets 5 μm.
doi:10.1371/journal.pone.0029305.g004

vimentin structure. Parallelly aligned dimers of vimentin assemble laterally into tetramers in a fashion whereby first halves of antiparallel coiled-coil domains overlap. Physiologically, vimentin forms a non-polar 32-meric unit-length filaments (ULF) consisting of 16 dimers or 8 tetramers [51]. The observed stoichiometries of 6–10 moles of vimentin per one mole CD443MUT probably reflects the number of head domains available on the ULF surface. The Kd values calculated from SPR data (12–37 nM) for the high affinity binding site are about 2–5 times higher than Kd-s resulting from ITC experiments (74 nM). Such experimental discrepancy can be explained either by limited dynamics of the immobilized vimentin or by sterical hindrances in the environment of the SPR chip. Currently the exact model of vimentin binding of CD44 or whether its binding site coincides with the HA binding surface, is not known. However, our data show that pharmacophores for HA-binding are not necessary for vimentin binding. Our data suggest a protein-protein interaction model which is constrained by the fact that CD44 is a type I membrane receptor and vimentin is a cytoplasmic intermediate filament protein. Nevertheless, several independent findings make this interaction spaciotemporally feasible. In addition to generation of CD44 intracellular domain resulting from shedding, full-length CD44 is also endocytosed and transported to the nucleus via NLS located in its intracellular domain [52,53]. In this process CD44 acts as scaffold for STAT3 and p300 [53]. Importantly, leptomycin B induces CD44 nuclear accumulation, suggesting a nuclear-cytoplasmic shuttling [52]. On the other hand, cell surface vimentin is a well-known phenomenon without any known function. We show that cell surface vimentin is readily detectable in primary human endothelial cells, in addition to its previously reported presence in malignant lymphocytes, activated macrophages and platelets [34–36]. Vimentin provides bacterial binding sites on the surface of human brain endothelial cells [37]. Our results suggest that vimentin might provide a binding site for soluble CD44 on EC. This is supported by our result that exogenously added vimentin can efficiently displace CD443MUT from ECs. In addition, we found that CD443MUT EC binding was enhanced by VEGF. These results were confirmed by experiments of cell surface biotinylation of starved or VEGF-induced ECs showing that CD443MUT was able to pull-down biotinylated vimentin from VEGF-treated but not from serum starved ECs. The discrepancy between the binding of CD443MUT to starved EC in cellular binding experiment and lack of any detectable biotinylated vimentin in pull-downs from starved EC could be explained by the different length of serum starvation in these experiments (6 h v. over-night, respectively). We suggest that the physiological relevance of these results is supported by findings that vimentin and CD44 are up-regulated on tumor endothelial cells, whereas vimentin has been proposed as a potential anti-angiogenesis target [3,38].

Here we show that after binding CD44HABD and its non-HA-binding triple mutant are endocytosed by ECs. A fraction of CD44HABD-proteins colocalized with generic endocytosis tracer CTxB-positive vesicles and were targeted to early endosomal structures. Importantly, we found that CD443MUT uptake was lost in vimentin knock-out endothelial cells, suggesting further that such internalization is mediated by vimentin. The number of CD443MUT-positive vesicles and early-endosomal localization decreased rapidly, most probably suggesting its targeting to lysosomal degradation. However, we were not able to detect significant accumulation of fluorescently labeled CD443MUT within late endosomal compartment.

We propose that vimentin forms a complex with full-length CD44. In this model, soluble CD44 antagonizes binding of membrane CD44 to vimentin. However, the role for soluble CD44 in tumorigenesis still remains elusive, as highly elevated soluble CD44 associates with aggressive growth and bad prognosis in cancer patients, and yet our previous results suggest that recombinant CD44 administration can inhibit tumor xenograft growth and angiogenesis [27]. We can speculate, that in cancer patients with high sCD44, tumor cells have acquired resistance to its inhibitory effects, while shedding of cell-surface bound CD44 confers significant selective advantage in tumor microenvironment. In summary, given the facts that the expression of CD44

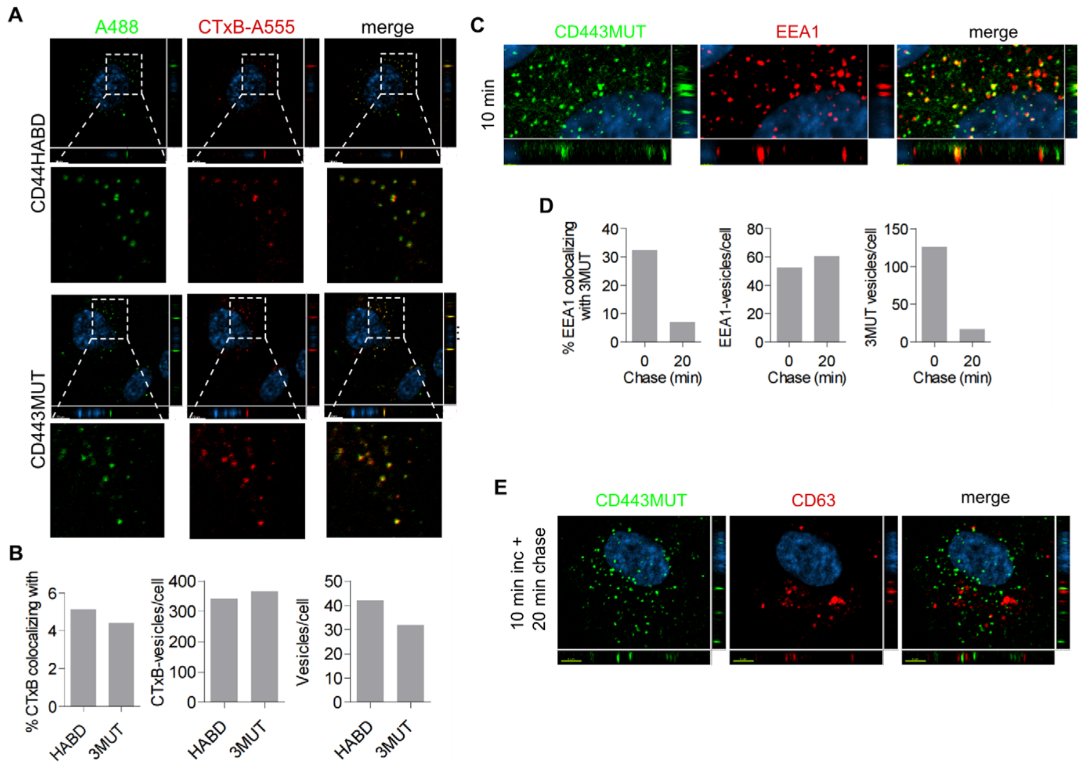

Figure 5. Analysis of endocytosed CD443MUT localization. (A) HUVEC were incubated with A488-labeled CD44HABD or CD443MUT (green) in the presence of CTxB-A555 (red) for 30 min. Nuclei were stained with Hoechst. Images show single confocal plane. Scale bars, 10 µm. (B) Colocalization analysis of CD44HABD (HABD) and CD443MUT (3MUT) with CTxB. Left, the fraction of CTxB-vesicles colocalizing with HABD (n = 39 cells) or 3MUT (n = 38 cells). Middle, the number of CTxB-vesicles per cell; right, the number of HABD- or 3MUT-containing vesicles per cell. (C–E) HUVEC were incubated with CD443MUT-A488 for 10 min after which CD443MUT-containing media was changed to 10% FBS HUVEC growth media and cells were further incubated for 20 min. Then cells were fixed and stained with anti-EEA1 or anti-CD63 antibodies. (C) Localization of 3MUT- and early endosomal marker EEA1-positive veicles after 10 min incubation in HUVEC. (D) Quantitation of EEA1-vesicles colocalizing with CD443MUT after 10 min incubation (n = 26 cells) and after 20 min chase (n = 40 cells; left). The number of EEA1- and 3MUT vesicles per cell (middle and left, respectively). (E) Localization of internalized 3MUT and late endosomal protein CD63-positive vesicles. Scale bars, 2 µm (C) and 5 µm (E).
doi:10.1371/journal.pone.0029305.g005

and vimentin correlate with EMT in cancer cells, and with tumor angiogenesis, our findings provide rationale for further functional studies on the role of these proteins in EMT and angiogenesis.

Materials and Methods

Cell lines and antibodies

HUVEC and MLEC cells were grown in M199 medium supplemented with 20% FBS, 4 mM L-glutamine, 50 µg/ml heparin and 30 µg/ml EC growth supplement (ECGS, Upstate Biotechnology, Lake Placid, NY, USA). MCF-7 cells (ATCC, Manassas, VA, USA) were grown in RPMI, supplemented with 10% FBS and 2 mM L-glutamine. Anti-vimentin (V9), anti-Myc (A-14) and anti-HDAC1 (H-11) antibodies were from Santa Cruz Biotechnology (Santa Cruz, CA, USA). Anti-vimentin rabbit polyclonal (18-272-196311) was from Genway (San Diego, CA, USA). Anti human-CD44 (2C5) was from R&D Systems (Minneapolis, MN, USA). Mouse anti-human CD44 (H4C4) was from DSHB (University of Iowa, IA, USA). Anti CD443MUT mouse mAb 1A2 (Figure S2) was generated by LabAS Ltd (Tartu, Estonia). Anti-CD44 (MEM-263) was from EXBIO Praha (Czech Republic). Anti-mouse PECAM-1 (MEC13.3), anti-mouse ICAM-2 (3C4) and anti-EEA1 mAb were from BD Pharmingen (Palo Alto, CA, USA). Rat anti-CD63/lamp-3 (R5G2) was from MBL International (Woburn, MA, USA). Anti-Flag-M2 antibody was from Sigma.

Purification of recombinant proteins and fluorescence labeling

CD44HABD and CD443MUT GST fusion-proteins were purified as described [27]. CD44HABD and CD443MUT include aa 21–132 of human CD44 protein. CD44HABD and -3MUT were expressed using pET11c vector (Novagen). Urea dissolved inclusion bodies were purified by gel filtration in Superdex-200HR 16/60 column (GE Healthcare, Uppsala, Sweden). Refolding was performed by gradient dialysis into 50 mM Tris pH 8.0, 150 mM NaCl and final dialysis into PBS. Endotoxin level was measured using the Endosafe-PTS (Charles River, L'Arbresle, France). Endotoxin values of CD443MUT batches were 22–93 EU/mg. Human vimentin was expressed using pET15b vector (Novagen). His-tagged vimentin was purified using Ni-affinity resin (Sigma)

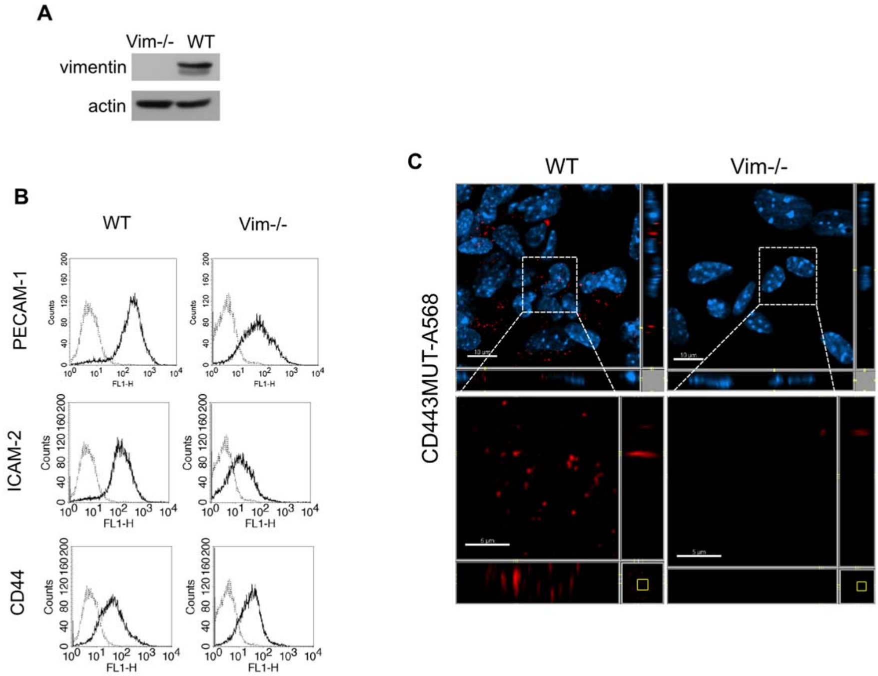

Figure 6. Vimentin dependent endocytosis of CD443MUT. MLEC were isolated either from wild-type (WT) or vimentin-null mice. (A) Immunoblot of WT of Vim−/− MLEC lysates with anti-vimentin rabbit polyclonal antibody. (B) FACS analysis of MLEC for cell surface markers with either anti-PECAM-1, anti-ICAM-2 or anti-CD44 antibodies (black lines). Gray lines, no primary antibody controls. (C) MLEC-s were incubated with CD443MUT-A568 (red) for 30 min and processed for immunofluorescence. Scale bars, upper panels 10 µm; insets 5 µm.
doi:10.1371/journal.pone.0029305.g006

under denaturing conditions. Refolding was performed by gradient dialysis into 10 mM Tris pH 8.0 with final dialysis into 10 mM phosphate buffer pH 7.4. Proteins were fluorescence-labeled using sulfo-NHS-Alexa Fluor 488 or −568 protein labeling kit (Molecular Probes, Eugene, OR, USA).

GST pull-down, immunoprecipitation and cell surface biotinylation

Adherent cells were rinsed with ice-cold PBS and lysed on ice in 50 mM Tris pH 8.0, supplemented with protease inhibitor cocktail (PIC; Roche, Mannheim, Germany). Lysate was centrifuged at 14000 rpm for 30 min at 4°C. Pellet was solubilized in 2% CHAPS, 50 mM Tris pH 8.0, 50 mM NaCl, PIC buffer and centrifuged at 14000 rpm for 10 min at 4°C. Supernatant was precleared by incubation with GST-bound glutathione-sepharose 4FF beads (Amersham Biosciences, Uppsala, Sweden). Precleared lysate was incubated overnight at 4°C with 10 µg GST, GST-tagged CD44HABD or CD443MUT immobilized onto glutathione beads. After washes with 50 mM Tris pH 8.0, 150 mM NaCl, PIC buffer, beads were eluted with 20 mM reduced glutathione in 50 mM Tris pH 8.0. Eluates were precipitated with 20% TCA, precipitate was washed with cold acetone and aspirated dry. For MALDI-TOF MS analysis of tryptic peptides, protein samples were alkylated and visualized by silver staining on SDS-PAGE.

For biotinylation, adherent cells were incubated with 1 mM EZ-Link Sulfo-NHS-LC-biotin (Pierce, Rockford, IL, USA) in PBS-0.05% NaN_3 for 30 min on ice, washed with 100 mM glycine-PBS and lysed as described above. For IP of endogenous proteins, adherent cells were rinsed with cold PBS and lysed in 50 mM Tris pH 8.0, 50 mM NaCl, 1% CHAPS, PIC buffer. Lysate was centrifuged at 14000 rpm for 30 min at 4°C. Supernatant was pre-cleared with anti-HDAC1 immobilized onto protein A/G sepharose beads (Amersham Biosciences) at 4°C. Precleared lysate was incubated with anti-HDAC1 or anti-CD44 (MEM-263) antibodies immobilized onto protein A/G beads overnight at 4°C. Beads were washed with lysis buffer and bound proteins were eluted with 0.5 M glycine (pH 2.5). Finally, pH of eluates was adjusted with 1 M Tris pH 8.0 and they were analyzed by immunoblotting using anti-CD44 (2C5) or rabbit anti-vimentin antibody. For IP of over-expressed proteins, adherent cells were rinsed in cold PBS, lysed in lysis buffer containing 40 mM Hepes pH 7.4, 120 mM NaCl, 1 mM EDTA, 0.6% CHAPS and PIC. Lysates were centrifuged at 14000 rpm for 30 min at 4°C. Supernatants were incubated with anti-Flag-M2 affinity gel (Sigma) overnight at 4°C, beads were washed with lysis buffer and bound proteins were eluted with 2× Laemmli sample buffer. Eluted protein complexes were analyzed by immunoblotting with anti-Flag-M2 or anti-Myc.

Isothermal titration calorimetry and surface plasmon resonance

ITC measurements were performed on a Nano-2G instrument (TA Instruments, New Castle, DE, USA). Experiments were performed in 50 mM Tris, 150 mM NaCl, pH 8.0 at 25°C. The main experimental parameters were: sample cell volume – 1 ml, syringe size – 250 µl, stirring rate – 250 rpm, injection volume – 10 µl, time interval between injections – 300 s. Titration data were analyzed by non-linear fitting (SigmaPlot 10). SPR measurements were performed on Biacore3000 (GE Healthcare). Vimentin was covalently coupled to CM5 chip using amine coupling kit (GE Healthcare). In association phase, CD443MUT concentrations 0.46–123 µM were injected over the chip surface. In the dissociation phase, the sensor chip surface was eluted with buffer 50 mM Tris, 150 mM NaCl, pH 8.0. The association rate constants and the dissociation rate constants were estimated using BIAevaluation software (GE Healthcare) using a parallel binding model, A+B1 ↔AB1, A+B2 ↔ AB2. K_d values were also determined from analysis of the equilibrium data using equation 1: $\Delta R = (\Delta R_{max} \cdot x)/(K_d + x) + (c \cdot x)$, where x – concentration of the injected protein, ΔR – the increase of the response value at equilibrium, ΔR_{max} – capacity of the immobilised vimentin to bind a protein (the number of binding sites), and c describes weak or non-specific interaction.

Displacement assays

Adherent cells were harvested from culture plates with 5 mM EDTA in PBS. Proteins were iodinated with ^{125}I by using Iodo-beads (Pierce). Cells were resuspended in incubation buffer 20 mM Tris-HCl pH 7.5, 5 mM $MgCl_2$, 30 mM NaCl, 3 mM $CaCl_2$ or DMEM, 25 mM HEPES, 0.1% BSA. Cell suspension was transferred into 96-well microtitre plate in 100 µl volume. Unlabeled protein at different concentrations and ^{125}I labeled protein in 20 µl volume of incubation buffer was added into wells. Reactions were incubated overnight at 4°C and stopped by filtration through GF/B filters blocked with 0.1% BSA-PBS, followed by washes with cold PBS. Filters were transfered into 5 ml vials and bound radioactivity was measured using gamma counter (PerkinElmer).

FACS analyses

For CD443MUT cellular binding, HUVEC were serum starved 6 h and then induced for 30 min at 37°C with 10 ng/ml VEGF-165 in media containing 0.5% FBS. Alexa Fluor 488-conjugated CD443MUT or GST was added into media at 25 µg/ml and cells were incubated for 1 h on ice. Cells were harvested from culture plates by scraping. After washes with 0.1% BSA-PBS, cells were fixed in 4% formaldehyde-PBS and analyzed using FACSCalibur flow cytometer (BD Biosciences).

DNA constructs and transfection

Full-length vimentin was PCR amplified from human vimentin cDNA and inserted into EcoRI/SacII site of pcDNA3.1/MycHisB vector (Invitrogen). Vimentin deletion mutants containing amino acids 1-96 (VIM1-96), 1-245 (VIM1-245), 246-466 (VIM246-466) and 97-466 (VIM97-466) were PCR amplified from human vimentin cDNA using oligonucleotide pairs containing EcoRI/NotI sites. PCR fragments were inserted into EcoRI/NotI site of pcDNA3.1/MycHisB vector. Vimentin-GFP (GFP, green fluorescent protein) constructs were created by inserting EcoRI/SacII fragment from respective vimentin-pcDNA3.1/MycHisB constructs into pEGFP-N1 vector. Vimentin deletion mutant containing aa 407-466 (VIM407-466) was PCR amplified from human vimentin cDNA and inserted into EcoRI/SalI site of pEGFP-C2 vector. For creating Flag-tagged CD44 DNA construct, full-length CD44 was PCR amplified from human standard CD44 isoform cDNA and inserted into EcoRI/NotI site of pCMV-Tag4a vector (Stratagene). MCF-7 cells were transfected using 1:2 DNA:PEI ratio. Transfected cells were grown at 37°C for 24 h. GST pull-down was performed as described above.

Mouse lung endothelial cells

Wild-type MLEC were isolated from C3H mouse strain (The Jackson Laboratory) and vimentin−/− from Vim1/Vim1 mice [31] obtained from EMMA (CNRS/CDTA, Orleans, France). Lungs from three 6–8 week old mice were dissected and finely minced with scissors on a dry culture dish. Lung pieces were put into 20 ml pre-warmed 0.2% collagenase-I (Sigma) in PBS and incubated with gentle agitation for 45 min at 37°C. Collagenase digested lung suspension was triturated through 100 µm cell strainer (BD Biosciences). Cell suspension was centrifuged 8 min 400 *g* at 4°C. Cell pellet was resuspended in 2 ml 0.1% BSA-PBS. Cells were sorted by incubation for 15 min at RT with sheep anti-rat IgG Dynabeads (Dynal, Norway) coated with rat anti-mouse CD31 (MEC13.3) and rat anti-mouse ICAM-2 (3C4) antibodies. Bead-bound cells were separated using a magnetic rack and washed five times with M199 medium containing 10% FBS. After separation, cells were plated onto dish and grown in M199 containing 10 mM HEPES, 20% FBS, 4 mM L-glutamine and supplemented with 50 µg/ml Heparin, 30 µg/ml ECGS and penicillin-streptomycin.

Internalization assay, immunofluorescence microscopy and image processing

For internalization assays, cells on 8-well slide (BD Falcon) were incubated at 37°C with CTxB-Alexa 555 (Invitrogen) and/or CD44HABD-proteins at 13 µg/ml (≈1 µM) in 0.5% FBS containing media for 10 or 30 min. After 10 min uptake, cells were washed with PBS two to three times and media was changed to 10% FBS containing M199 HUVEC growth media and slides were incubated for 20 or 50 min at 37°C. After incubations cells were washed and fixed with 4% formaldehyde-PBS on for 10 min on ice and for 10 min at RT. Cells were permeabilized using 0.1% Triton X-100 in 0.1% BSA-PBS. Antibodies were diluted in 0.1% BSA-PBS. Secondary antibody dilutions were supplemented with 10 µg/ml Hoechst 33258 (Sigma). Slides were mounted in Mowiol 4–88 (Sigma-Aldrich, St Louis, MO, USA). Confocal fluorescent imaging was performed using Zeiss LSM510 microscope with ×63/1.4 oil immersion objective in multi-channel mode (Carl Zeiss MicroImaging, Germany). Images were prepared using Imaris 6.4 software (Bitplane, Zurich, Switzerland). For quantitation of endocytosis and vesicular colocalization, single slices from the middle plane of the cell were semi-automatically selected from confocal image stacks using Fiji package (http://pacific.mpi-cbg.de/wiki/index.php/Fiji). Cell-profiler 2.0 (r10415) software was used ror image segmentation and automated analysis [54]. Endosomal outlines were identified using Otsu global treshold, then endosomal marker/tracer object outlines were used to create a mask to identify colocalizing CD44HABD- or CD443MUT objects. Within these objects correlation was measured between endocytosis marker and CD44, and objects showing positive correlation were finally counted as colocalizing. For calculation of average correlation coefficient and 95% confidence interval, individual object coefficients were transformed to z scores.

Statistical analysis of data

Data represent mean ± SE. Statistical analysis and non-linear fitting of data was performed using GraphPad Prism 5 software (San Diego, CA, USA).

Supporting Information

Figure S1 Cell-surface expression of overexpressed vimentin in MCF-7 cells. Vimentin- or empty vector transfected MCF-7 cells were subjected to cell surface biotinylation (see Materials and Methods). Lysates were immunoprecipitated with anti-vimentin antibody. Lysates and immunoprecipitates were analyzed by WB using strepavidin-HRP (upper panel) or anti-vimentin antibody (lower panel). Arrows indicate the location of full length vimentin.
(TIF)

Figure S2 Characterization of anti-CD443MUT mouse mAb 1A2. (A) ELISA analysis of serially diluted 1A2 mAb (3.1 mg/ml) of rat serum−, rat serum+CD443MUT- or CD443MUT-coated wells. PBS, no primary antibody control. (B) Microplate wells were coated with different concentrations of CD443MUT mixed with rat serum and analyzed by ELISA using 1A2 mAb at 1:400 dilution. (C) Wells were coated with CD44 peptides and analyzed by ELISA using 1A2 mAb at 1:50000 dilution. (D) Amino acid alignment of CD44HABD, CD443MUT and peptides used for epitope mapping. Amino acid numbering is according to human CD44; mutated positions are indicated in green (wild-type amino acids) or red (mutant amino acids). Bars, mean ± SD.
(TIF)

Acknowledgments

We thank Dr. Ulf Hellmann for MS analyses, Miina Lillepruun and Dr. Aivar Lõokene for calorimetry and SPR, Aili Kallastu for protein purification, and Kersti Olspert for technical assistance. We thank Dr. Emma Colucci-Guyon for vimentin-deficient mice.

Author Contributions

Conceived and designed the experiments: TP AP LK AV PK. Performed the experiments: TP AP LK MT WA. Analyzed the data: TP AP LK AV. Wrote the paper: TP AP AV.

References

1. Günthert U, Hofmann M, Rudy W, Reber S, Zöller M, et al. (1991) A new variant of glycoprotein CD44 confers metastatic potential to rat carcinoma cells. Cell 65: 13–24.
2. Kogerman P, Sy MS, Culp LA (1997) Counter-selection for over-expressed human CD44s in primary tumors versus lung metastases in a mouse fibrosarcoma model. Oncogene 15: 1407–1416.
3. Griffioen AW, Coenen MJ, Damen CA, Hellwig SM, van Weering DH, et al. (1997) CD44 is involved in tumor angiogenesis; an activation antigen on human endothelial cells. Blood 90: 1150–1159.
4. Cao G, Savani RC, Fehrenbach M, Lyons C, Zhang L, et al. (2006) Involvement of endothelial CD44 during in vivo angiogenesis. Am J Pathol 169: 325–336.
5. Katoh S, McCarthy JB, Kincade PW (1994) Characterization of soluble CD44 in the circulation of mice. Levels are affected by immune activity and tumor growth. J Immunol 153: 3440–3449.
6. Cichy J, Bals R, Potempa J, Mani A, Pure E (2002) Proteinase-mediated release of epithelial cell-associated CD44. Extracellular CD44 complexes with components of cellular matrices. J Biol Chem 277: 44440–44447.
7. Yu Q, Toole BP (1996) A new alternatively spliced exon between v9 and v10 provides a molecular basis for synthesis of soluble CD44. J Biol Chem 271: 20603–20607.
8. Okamoto I, Kawano Y, Tsuiki H, Sasaki J, Nakao M, et al. (1999) CD44 cleavage induced by a membrane-associated metalloprotease plays a critical role in tumor cell migration. Oncogene 18: 1435–1446.
9. Nakamura H, Suenaga N, Taniwaki K, Matsuki H, Yonezawa K, et al. (2004) Constitutive and induced CD44 shedding by ADAM-like proteases and membrane-type 1 matrix metalloproteinase. Cancer Res 64: 876–882.
10. Ristämaki R, Joensuu H, Grön-Virta K, Salmi M, Jalkanen S (1997) Origin and function of circulating CD44 in non-Hodgkin's lymphoma. J Immunol 158: 3000–3008.
11. Guo YJ, Liu G, Wang X, Jin D, Wu M, et al. (1994) Potential use of soluble CD44 in serum as indicator of tumor burden and metastasis in patients with gastric or colon cancer. Cancer Res 54: 422–426.
12. Mayer S, zur Hausen A, Watermann DO, Stamm S, Jäger M, et al. (2008) Increased soluble CD44 concentrations are associated with larger tumor size and lymph node metastasis in breast cancer patients. J Cancer Res Clin Oncol 134: 1229–1235.
13. Mäenpää H, Ristamäki R, Virtamo J, Franssila K, Albanes D, et al. (2000) Serum CD44 levels preceding the diagnosis of non-Hodgkin's lymphoma. Leuk Lymphoma 37: 585–592.
14. Niitsu N, Iijima K (2002) High serum soluble CD44 is correlated with a poor outcome of aggressive non-Hodgkin's lymphoma. Leuk Res 26: 241–248.
15. Ristamäki R, Joensuu H, Lappalainen K, Teerenhovi L, Jalkanen S (1997) Elevated serum CD44 level is associated with unfavorable outcome in non-Hodgkin's lymphoma. Blood 90: 4039–4045.
16. Krettek A, Sukhova GK, Schönbeck U, Libby P (2004) Enhanced expression of CD44 variants in human atheroma and abdominal aortic aneurysm: possible role for a feedback loop in endothelial cells. Am J Pathol 165: 1571–1581.
17. Ristamäki R, Joensuu H, Salmi M, Jalkanen S (1994) Serum CD44 in malignant lymphoma: an association with treatment response. Blood 84: 238–243.
18. Yu Q, Toole BP, Stamenkovic I (1997) Induction of apoptosis of metastatic mammary carcinoma cells in vivo by disruption of tumor cell surface CD44 function. J Exp Med 186: 1985–1996.
19. Ahrens T, Sleeman JP, Schempp CM, Howells N, Hofmann M, et al. (2001) Soluble CD44 inhibits melanoma tumor growth by blocking cell surface CD44 binding to hyaluronic acid. Oncogene 20: 3399–3408.
20. Peterson RM, Yu Q, Stamenkovic I, Toole BP (2000) Perturbation of hyaluronan interactions by soluble CD44 inhibits growth of murine mammary carcinoma cells in ascites. Am J Pathol 156: 2159–2167.
21. Lopez JI, Camenisch TD, Stevens MV, Sands BJ, McDonald J, et al. (2005) CD44 Attenuates Metastatic Invasion during Breast Cancer Progression. Cancer Research. pp 6755–6763.
22. Kohda D, Morton CJ, Parkar AA, Hatanaka H, Inagaki FM, et al. (1996) Solution structure of the link module: a hyaluronan-binding domain involved in extracellular matrix stability and cell migration. Cell 86: 767–775.
23. Banerji S, Wright AJ, Noble M, Mahoney DJ, Campbell ID, et al. (2007) Structures of the Cd44-hyaluronan complex provide insight into a fundamental carbohydrate-protein interaction. Nat Struct Mol Biol 14: 234–239.
24. Teriete P, Banerji S, Noble M, Blundell CD, Wright AJ, et al. (2004) Structure of the regulatory hyaluronan binding domain in the inflammatory leukocyte homing receptor CD44. Molecular Cell 13: 483–496.
25. Bajorath J, Greenfield B, Munro SB, Day AJ, Aruffo A (1998) Identification of CD44 residues important for hyaluronan binding and delineation of the binding site. J Biol Chem 273: 338–343.
26. English NM, Lesley JF, Hyman R (1998) Site-specific de-N-glycosylation of CD44 can activate hyaluronan binding, and CD44 activation states show distinct threshold densities for hyaluronan binding. Cancer Res 58: 3736–3742.
27. Päll T, Gad A, Kasak L, Drews M, Strömblad S, et al. (2004) Recombinant CD44-HABD is a novel and potent direct angiogenesis inhibitor enforcing endothelial cell-specific growth inhibition independently of hyaluronic acid binding. Oncogene 23: 7874–7881.
28. Ivaska J, Vuoriluoto K, Huovinen T, Izawa I, Inagaki M, et al. (2005) PKCepsilon-mediated phosphorylation of vimentin controls integrin recycling and motility. EMBO J 24: 3834–3845.
29. Styers ML, Salazar G, Love R, Peden AA, Kowalczyk AP, et al. (2004) The endo-lysosomal sorting machinery interacts with the intermediate filament cytoskeleton. Mol Biol Cell 15: 5369–5382.
30. Faigle W, Colucci-Guyon E, Louvard D, Amigorena S, Galli T (2000) Vimentin filaments in fibroblasts are a reservoir for SNAP23, a component of the membrane fusion machinery. Mol Biol Cell 11: 3485–3494.
31. Colucci-Guyon E, Portier MM, Dunia I, Paulin D, Pournin S, et al. (1994) Mice lacking vimentin develop and reproduce without an obvious phenotype. Cell 79: 679–694.
32. Henrion D, Terzi F, Matrougui K, Duriez M, Boulanger CM, et al. (1997) Impaired flow-induced dilation in mesenteric resistance arteries from mice lacking vimentin. J Clin Invest 100: 2909–2914.
33. Terzi F, Henrion D, Colucci-Guyon E, Federici P, Babinet C, et al. (1997) Reduction of renal mass is lethal in mice lacking vimentin. Role of endothelin-nitric oxide imbalance. J Clin Invest 100: 1520–1528.
34. Mor-Vaknin N, Punturieri A, Sitwala K, Markovitz DM (2003) Vimentin is secreted by activated macrophages. Nat Cell Biol 5: 59–63.
35. Huet D, Bagot M, Loyaux D, Capdevielle J, Conraux L, et al. (2006) SC5 mAb represents a unique tool for the detection of extracellular vimentin as a specific marker of Sezary cells. J Immunol 176: 652–659.
36. Podor TJ, Singh D, Chindemi P, Foulon DM, McKelvie R, et al. (2002) Vimentin exposed on activated platelets and platelet microparticles localizes vitronectin and plasminogen activator inhibitor complexes on their surface. J Biol Chem 277: 7529–7539.
37. Zou Y, He L, Huang S (2006) Identification of a surface protein on human brain microvascular endothelial cells as vimentin interacting with Escherichia coli invasion protein IbeA. Biochem Biophys Res Commun 351: 625–630.

38. van Beijnum JR, Dings RP, van der Linden E, Zwaans BMM, Ramaekers FCS, et al. (2006) Gene expression of tumor angiogenesis dissected: specific targeting of colon cancer angiogenic vasculature. Blood 108: 2339–2348.
39. Oliferenko S, Paiha K, Harder T, Gerke V, Schwärzler C, et al. (1999) Analysis of CD44-containing lipid rafts: Recruitment of annexin II and stabilization by the actin cytoskeleton. J Cell Biol 146: 843–854.
40. Runembert I, Queffeulou G, Federici P, Vrtovsnik F, Colucci-Guyon E, et al. (2002) Vimentin affects localization and activity of sodium-glucose cotransporter SGLT1 in membrane rafts. J Cell Sci 115: 713–724.
41. Lafourcade C, Sobo K, Kieffer-Jaquinod S, Garin J, van der Goot FG (2008) Regulation of the V-ATPase along the endocytic pathway occurs through reversible subunit association and membrane localization. PLoS One 3: e2758.
42. Howes MT, Kirkham M, Riches J, Cortese K, Walser PJ, et al. (2010) Clathrin-independent carriers form a high capacity endocytic sorting system at the leading edge of migrating cells. J Cell Biol 190: 675–691.
43. Brown RL, Reinke LM, Damerow MS, Perez D, Chodosh LA, et al. (2011) CD44 splice isoform switching in human and mouse epithelium is essential for epithelial-mesenchymal transition and breast cancer progression. J Clin Invest 121: 1064–1074.
44. Jalkanen S, Jalkanen M (1992) Lymphocyte CD44 binds the COOH-terminal heparin-binding domain of fibronectin. J Cell Biol 116: 817–825.
45. Ehnis T, Dieterich W, Bauer M, Lampe B, Schuppan D (1996) A chondroitin/dermatan sulfate form of CD44 is a receptor for collagen XIV (undulin). Exp Cell Res 229: 388–397.
46. Dimitroff CJ, Lee JY, Rafii S, Fuhlbrigge RC, Sackstein R (2001) CD44 is a major E-selectin ligand on human hematopoietic progenitor cells. J Cell Biol 153: 1277–1286.
47. Weber GF, Ashkar S, Glimcher MJ, Cantor H (1996) Receptor-ligand interaction between CD44 and osteopontin (Eta-1). Science 271: 509–512.
48. Bartolazzi A, Nocks A, Aruffo A, Spring F, Stamenkovic I (1996) Glycosylation of CD44 is implicated in CD44-mediated cell adhesion to hyaluronan. J Cell Biol 132: 1199–1208.
49. Georgatos SD, Weaver DC, Marchesi VT (1985) Site specificity in vimentin-membrane interactions: intermediate filament subunits associate with the plasma membrane via their head domains. J Cell Biol 100: 1962–1967.
50. Aziz A, Hess JF, Budamagunta MS, Voss JC, Fitzgerald PG (2010) Site-directed spin labeling and electron paramagnetic resonance determination of vimentin head domain structure. J Biol Chem 285: 15278–15285.
51. Sokolova AV, Kreplak L, Wedig T, Mücke N, Svergun DI, et al. (2006) Monitoring intermediate filament assembly by small-angle x-ray scattering reveals the molecular architecture of assembly intermediates. Proc Natl Acad Sci U S A 103: 16206–16211.
52. Janiszewska M, De Vito C, Le Bitoux M, Fusco C, Stamenkovic I (2010) Transportin regulates nuclear import of CD44. J Biol Chem 285: 30548–30557.
53. Lee J, Wang M, Chen J (2009) Acetylation and activation of STAT3 mediated by nuclear translocation of CD44. J Cell Biol 185: 949–957.
54. Carpenter AE, Jones TR, Lamprecht MR, Clarke C, Kang IH, et al. (2006) CellProfiler: image analysis software for identifying and quantifying cell phenotypes. Genome Biol 7: R100.

MANUSCRIPT

Pink A., Kallastu A., **Päll T**., Turkina M., Školnaja M., Kogerman P., Valkna A. (2013) Purification, characterization and plasma half-life of PEGylated soluble recombinant non-HA-binding CD44

Purification, characterization and plasma half-life of PEGylated soluble recombinant non-HA-binding CD44

Anne Pink[a,b], Aili Kallastu[b], Taavi Päll[a,b], Marina Turkina[b], Marianna Školnaja[b], Priit Kogerman[a,b] and Andres Valkna[a,b,*]

[a] Tallinn University of Technology, Department of Gene Technology, Akadeemia tee 15, 12618 Tallinn, Estonia;

[b] Competence Centre for Cancer Research, Akadeemia tee 15, 12618 Tallinn, Estonia;

* corresponding author. E-mail address: andres.valkna@ttu.ee. Fax: +372 6204336

PATENT

Kogerman P., **Päll T**., Strömblad S. (2010) Drug for treating states related to the inhibition of angiogenesis and/or endothelial cell proliferation. US Patent No: 8,192,744

US008192744B2

(12) **United States Patent**
Stromblad et al.

(10) **Patent No.: US 8,192,744 B2**
(45) **Date of Patent: Jun. 5, 2012**

(54) **DRUG FOR TREATING STATES RELATED TO THE INHIBITION OF ANGIOGENESIS AND/OR ENDOTHELIAL CELL PROLIFERATION**

(75) Inventors: **Staffan Stromblad**, Huddinge (SE); **Taavi Pall**, Tabasalu (EE); **Priit Kogerman**, Tabasalu (EE)

(73) Assignee: **IBCC Holding AS**, Tallinn (EE)

(*) Notice: Subject to any disclaimer, the term of this patent is extended or adjusted under 35 U.S.C. 154(b) by 0 days.

(21) Appl. No.: **12/660,886**

(22) Filed: **Mar. 5, 2010**

(65) **Prior Publication Data**

US 2011/0009310 A1 Jan. 13, 2011

Related U.S. Application Data

(63) Continuation-in-part of application No. 10/487,620, filed as application No. PCT/SE02/15431 on Aug. 26, 2002, now abandoned.

(51) **Int. Cl.**
A61K 38/16 (2006.01)
A61K 39/00 (2006.01)

(52) **U.S. Cl.** **424/184.1**; 424/185.1; 514/21.2

(58) **Field of Classification Search** .... None
See application file for complete search history.

(56) **References Cited**

FOREIGN PATENT DOCUMENTS

WO WO/2003/018044 * 6/2003

OTHER PUBLICATIONS

Pall et al. Recombinant CD44-HABD is a novel and potent direct angiogenesis inhibitor enforcing endothelial cell-specific growth inhibition independently of hyaluronic acid binding. Oncogene (2004) 23, 7874-7881.*

Bajorath, J. et al. 1998. Identification of CD44 Residues Important to Hyaluronan Binding and Delineation . . . J. Biol. Chem. 273(1) 338-343.

Bartolazzi, A. et al. 1994. Interaction between CD44 and Hyaluronate is directly implicated in the regulation.. J. Exp. Med. 180:53-66.

Gao, C.A.,et al. 1981. Metastasis suppression by the standard CD44 isoform does not require the binding . . . Cancer Rws. 58:2350-2352.

Brown, T. et al. 1991. Human Keratinosytes express a New CD44 Core protein (CD44E) as . . . The J. of Cell Biol. 113(1):207-221.

Auerbach , R. et al. 2003 Angiogenesis Assays: A critical overview. Clinical Chemistry 49(1): 32-40.

Yu, G and Stamenkovic, I. 1999. Localization of matrix metalloproteinase 9 to the cell surface . . . Genes & Development 13:35-48.

* cited by examiner

Primary Examiner — Maher Haddad
(74) *Attorney, Agent, or Firm* — Gearhart Law, LLC

(57) **ABSTRACT**

Soluble recombinant CD44 hyaluronic acid binding domain (CD44HABD) inhibits angiogenesis in vivo in chick and mouse and thereby inhibits human tumor growth of various origins. The anti-angiogenic effect of CD44-HABD is independent of hyaluronic acid (HA) binding, since non-HA-binding mutants of CD44HABD still maintain anti-angiogenic properties. The invention discloses soluble non glycosylated CD44 recombinant proteins as a novel class of angiogenesis inhibitors based on targeting of vascular cell surface receptor. A method of block of angiogenesis and treatment of human tumors using recombinant CD44 proteins as well as their analogues is disclosed. As a further embodiment of the invention, methods for screening for new drug targets using CD44 recombinant proteins and their analogues are presented.

14 Claims, 17 Drawing Sheets

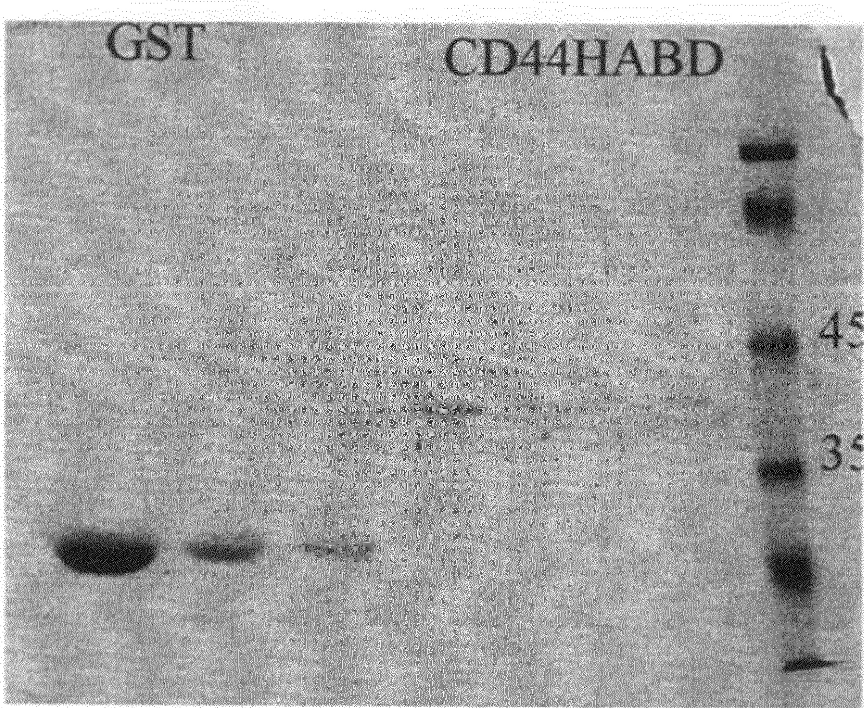

FIG.1

a

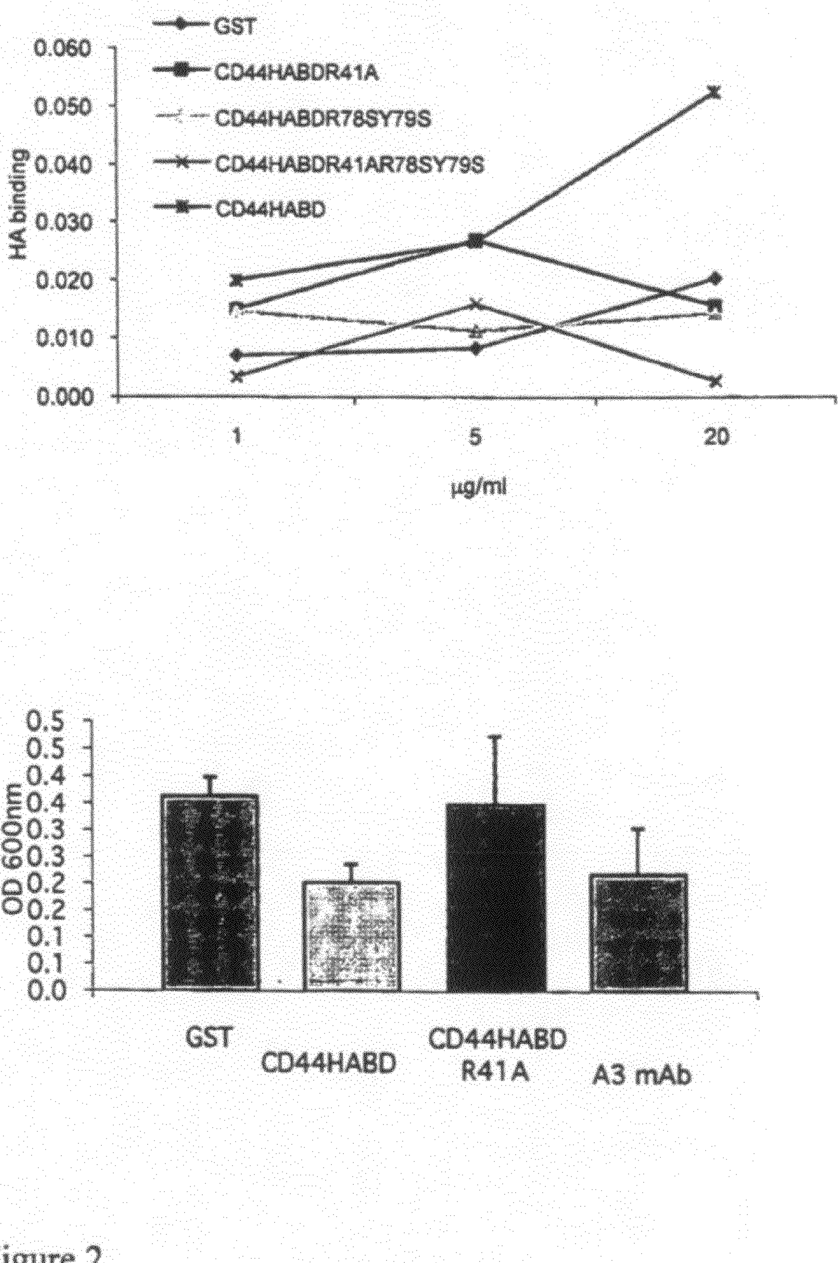

GST
CD44HABDR41A
CD44HABDR78SY79S
CD44HABDR41AR78SY79S
CD44HABD
HA binding
0.060
0.050
0.040
0.030
0.020
0.010
0.000
1
5
20
µg/ml
b
OD 600nm
0.5
0.5
0.4
0.4
0.3
0.3
0.2
0.2
0.1
0.1
0.0
GST
CD44HABD
CD44HABD R41A
A3 mAb

Figure 2

a

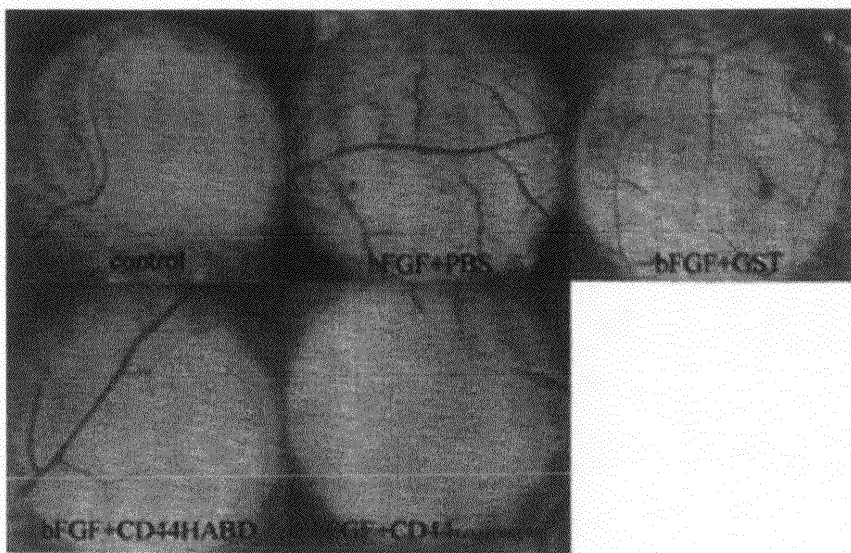

Fig. 3A

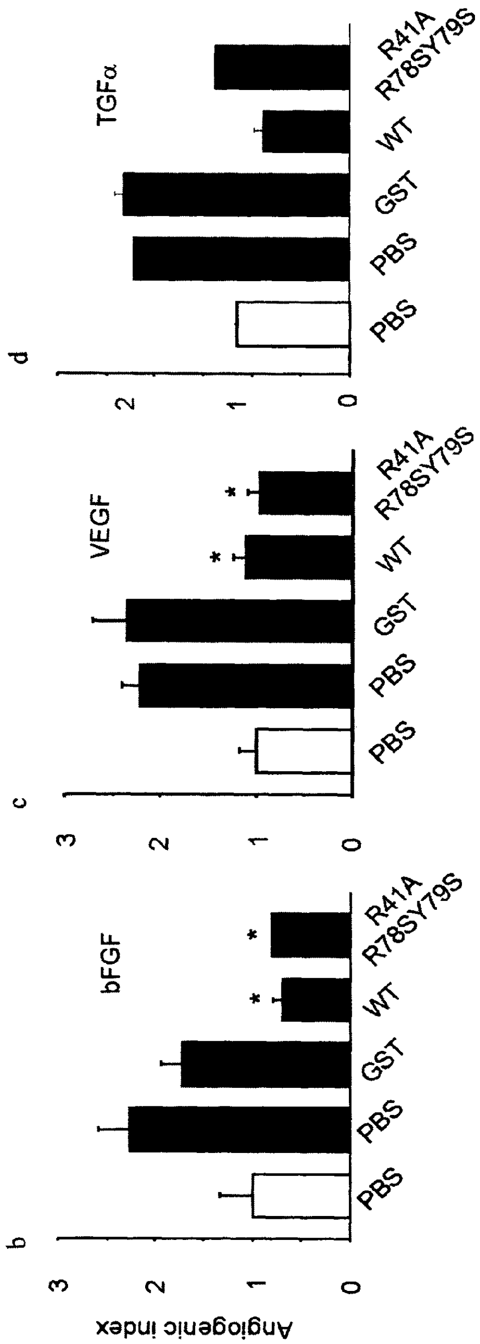
b
bFGF
Angiogenic index
0
1
2
3
PBS
PBS
GST
WT
R41A R78SY79S
*
*
c
VEGF
0
1
2
3
PBS
PBS
GST
WT
R41A R78SY79S
*
*
d
TGFα
0
1
2
PBS
PBS
GST
WT
R41A R78SY79S

FIG. 3 B-D

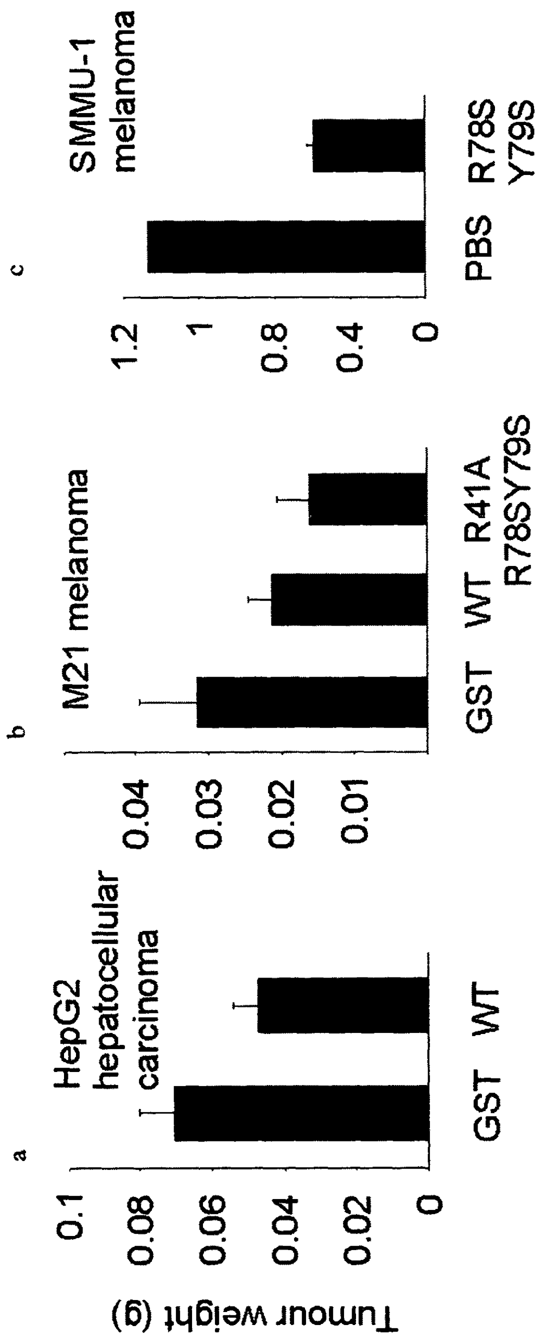
a
HepG2 hepatocellular carcinoma
Tumour weight (g)
0.1
0.08
0.06
0.04
0.02
0
GST
WT
b
M21 melanoma
0.04
0.03
0.02
0.01
GST
WT
R41A R78SY79S
c
SMMU-1 melanoma
1.2
1
0.8
0.4
0
PBS
R78S Y79S

FIG. 4

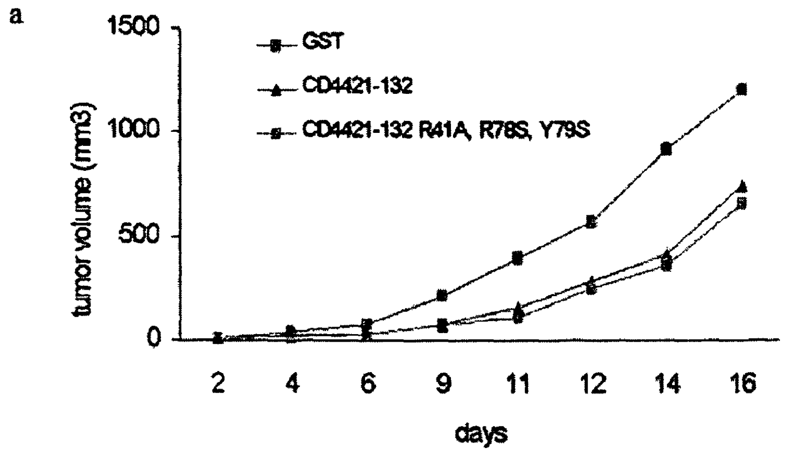
a
1500
1000
500
0
tumor volume (mm3)
GST
CD4421-132
CD4421-132 R41A, R78S, Y79S
2
4
6
9
11
12
14
16
days

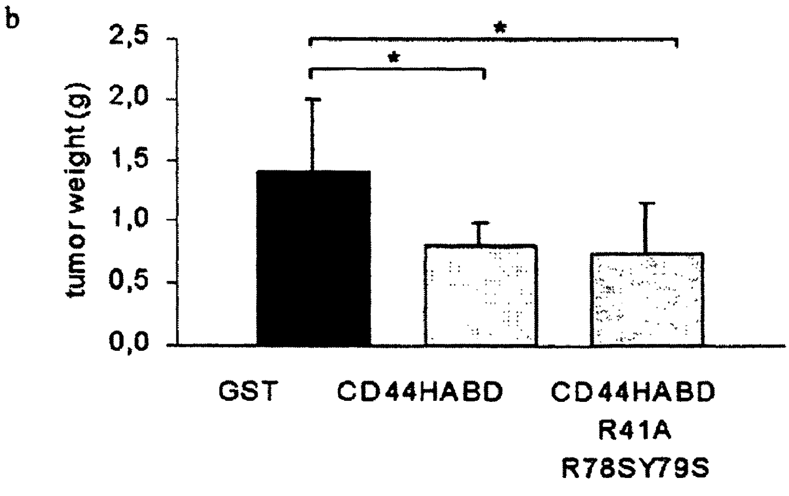
b
2,5
2,0
1,5
1,0
0,5
0,0
tumor weight (g)
*
*
GST
CD44HABD
CD44HABD
R41A
R78SY79S

FIG. 5 A-B

c

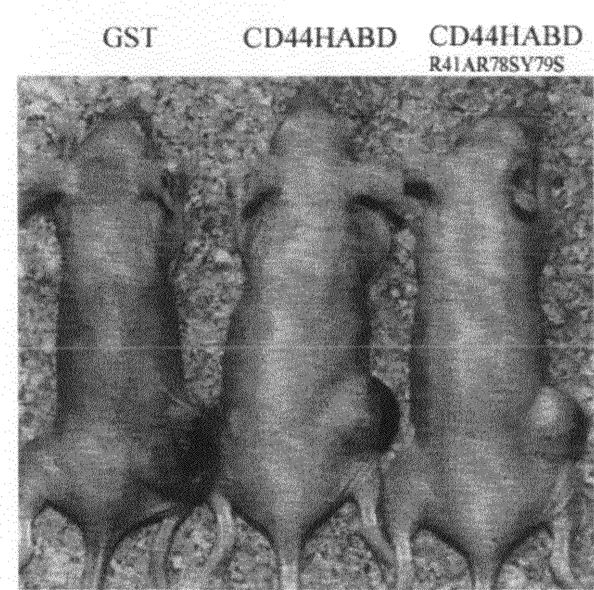
GST
CD44HABD
CD44HABD
R41AR78SY79S

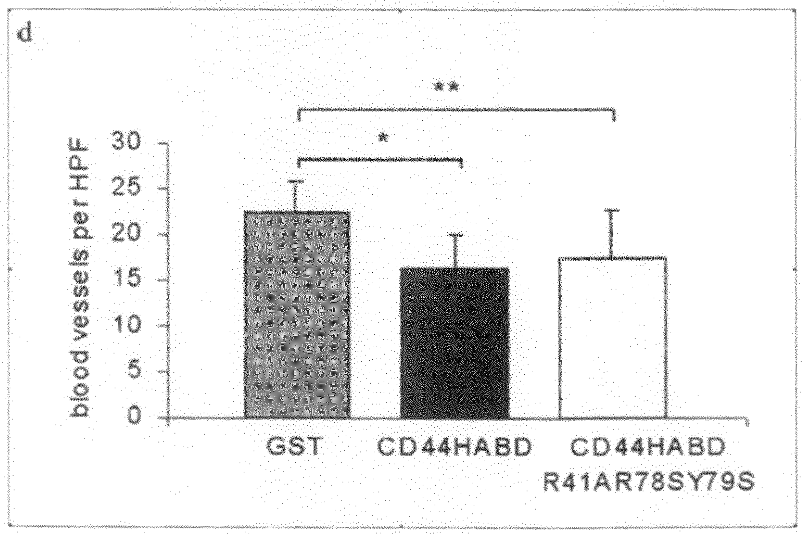
d
**
*
blood vessels per HPF
30
25
20
15
10
5
0
GST
CD44HABD
CD44HABD
R41AR78SY79S

FIG. 5 C-D

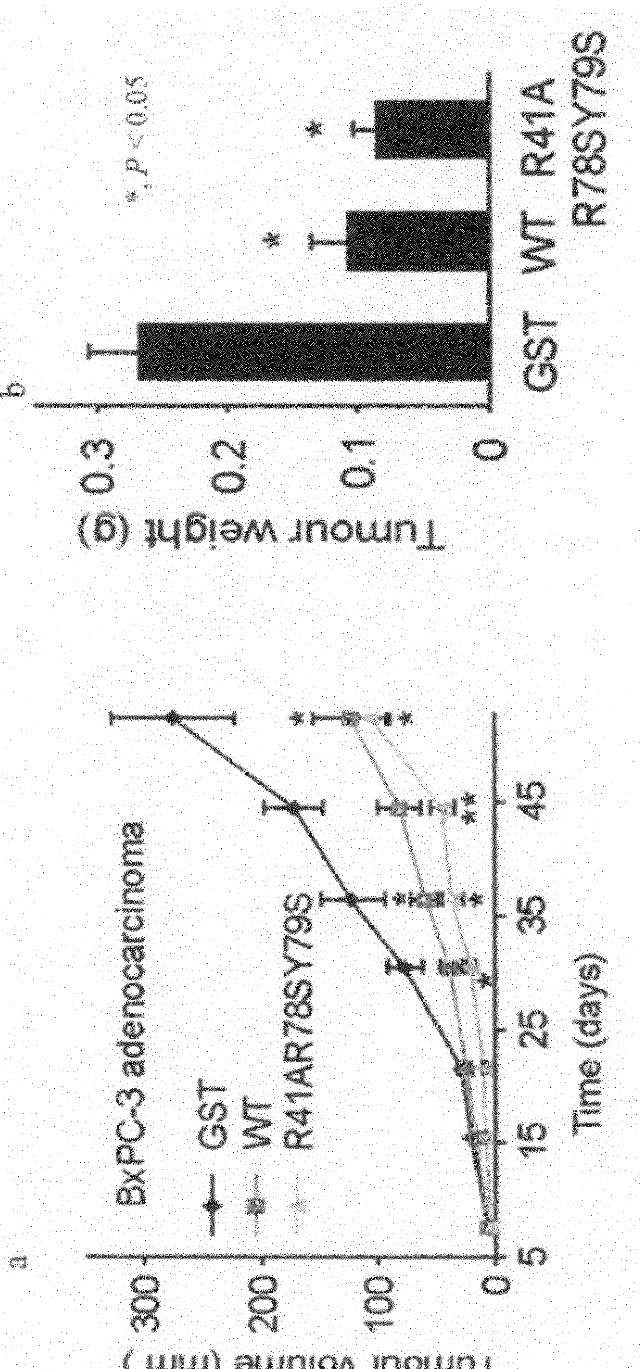
a
BxPC-3 adenocarcinoma
GST
WT
R41AR78SY79S
Tumour volume (mm3)
300
200
100
0
5
15
25
35
45
Time (days)
b
*, P < 0.05
Tumour weight (g)
0.3
0.2
0.1
0
GST
WT
R41A
R78SY79S

FIG. 6

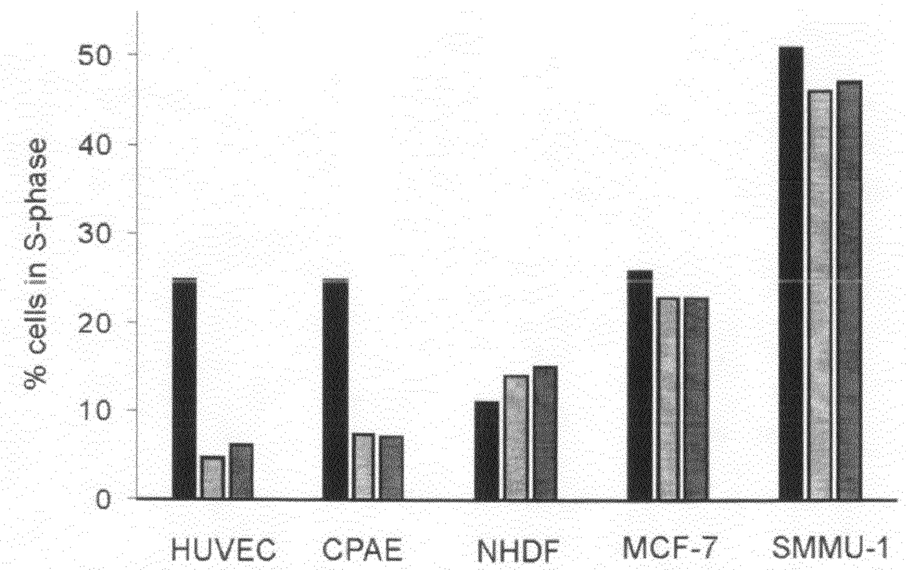

FIG. 7

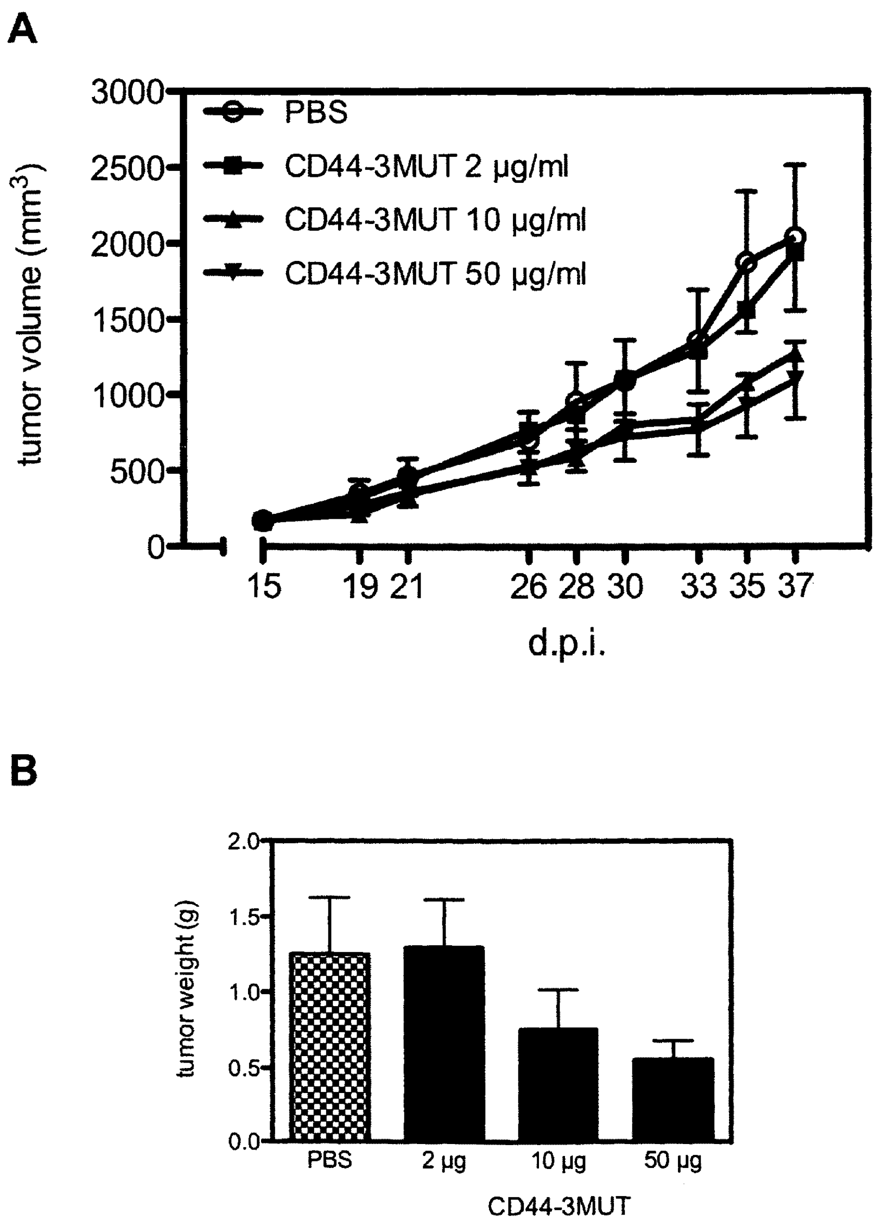
A
3000
2500
2000
1500
1000
500
0
tumor volume (mm3)
PBS
CD44-3MUT 2 µg/ml
CD44-3MUT 10 µg/ml
CD44-3MUT 50 µg/ml
15
19 21
26 28 30
33 35 37
d.p.i.
B
2.0
1.5
1.0
0.5
0.0
tumor weight (g)
PBS
2 µg
10 µg
50 µg
CD44-3MUT

FIG. 8

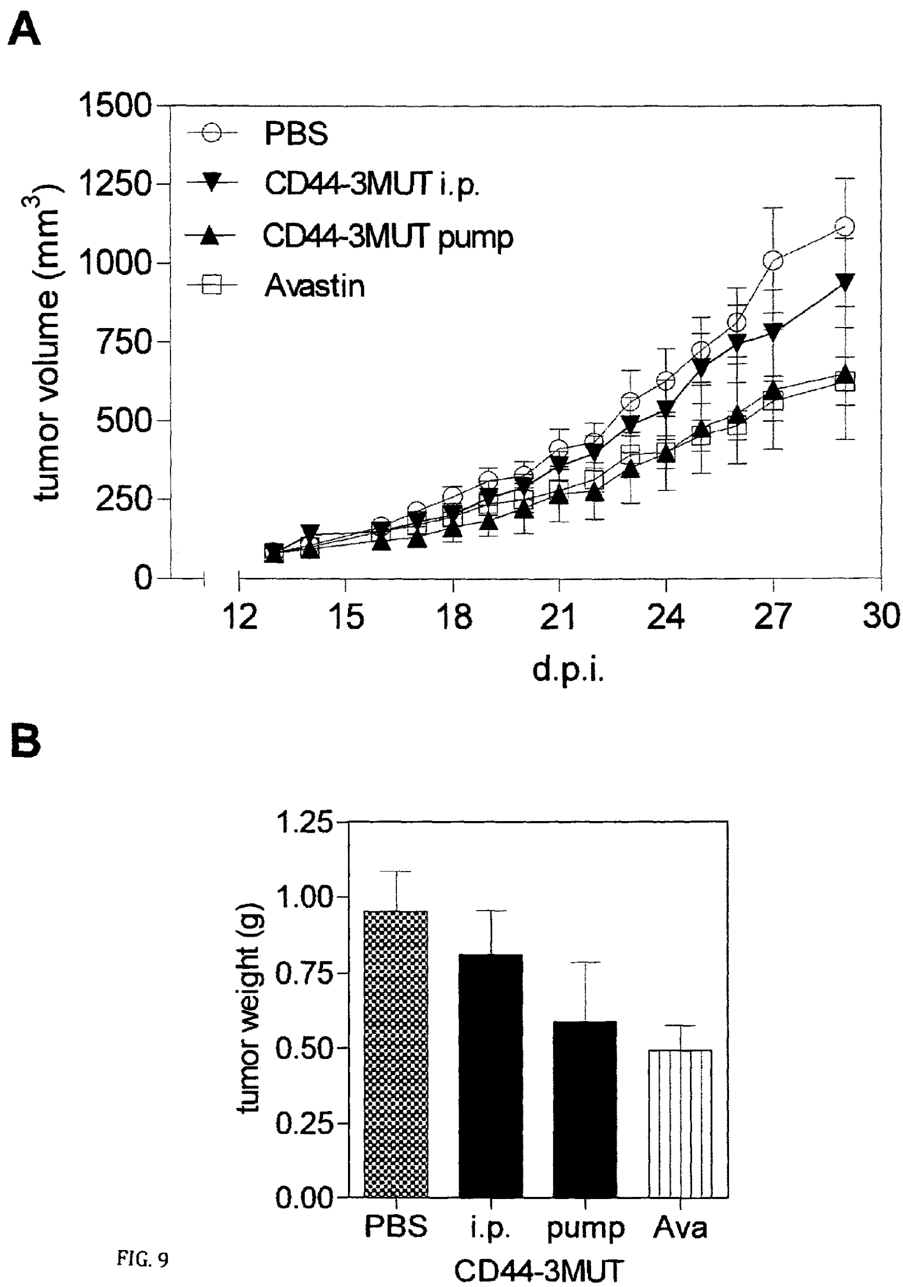
A
1500
1250
1000
750
500
250
0
tumor volume (mm3)
PBS
CD44-3MUT i.p.
CD44-3MUT pump
Avastin
12
15
18
21
24
27
30
d.p.i.
B
1.25
1.00
0.75
0.50
0.25
0.00
tumor weight (g)
PBS
i.p.
pump
Ava
CD44-3MUT

FIG. 9

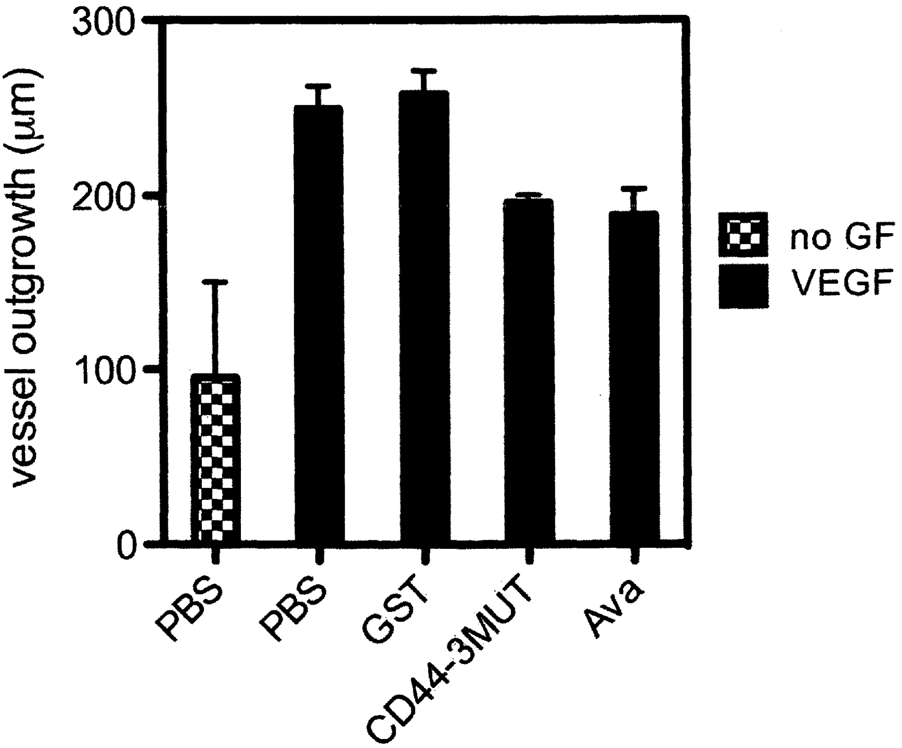

300
200
100
0
vessel outgrowth (μm)
no GF
VEGF
PBS
PBS
GST
CD44-3MUT
Ava

FIG. 10

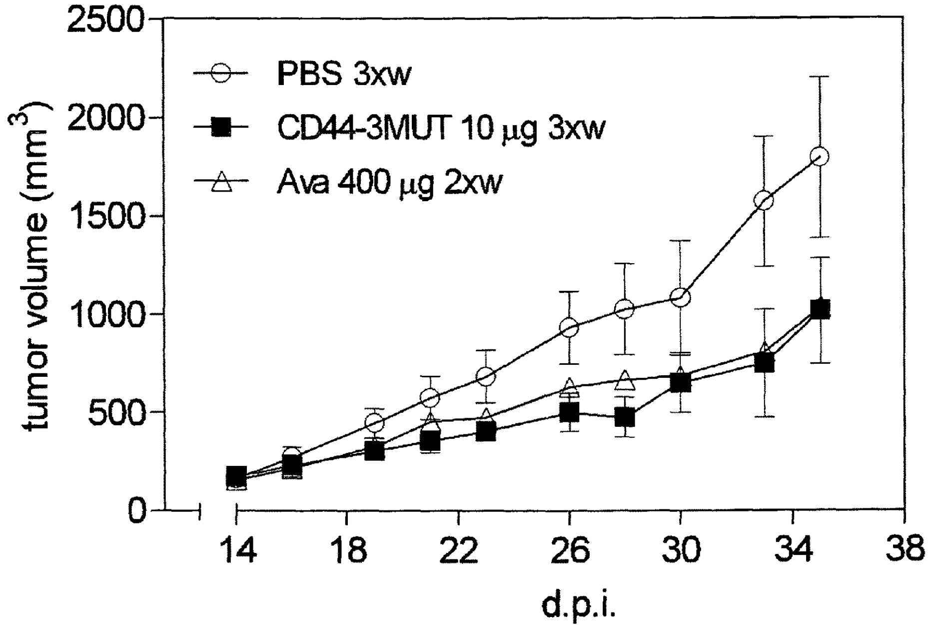

PBS 3xw
CD44-3MUT 10 μg 3xw
Ava 400 μg 2xw
tumor volume (mm3)
2500
2000
1500
1000
500
0
14
18
22
26
30
34
38
d.p.i.

FIG.11

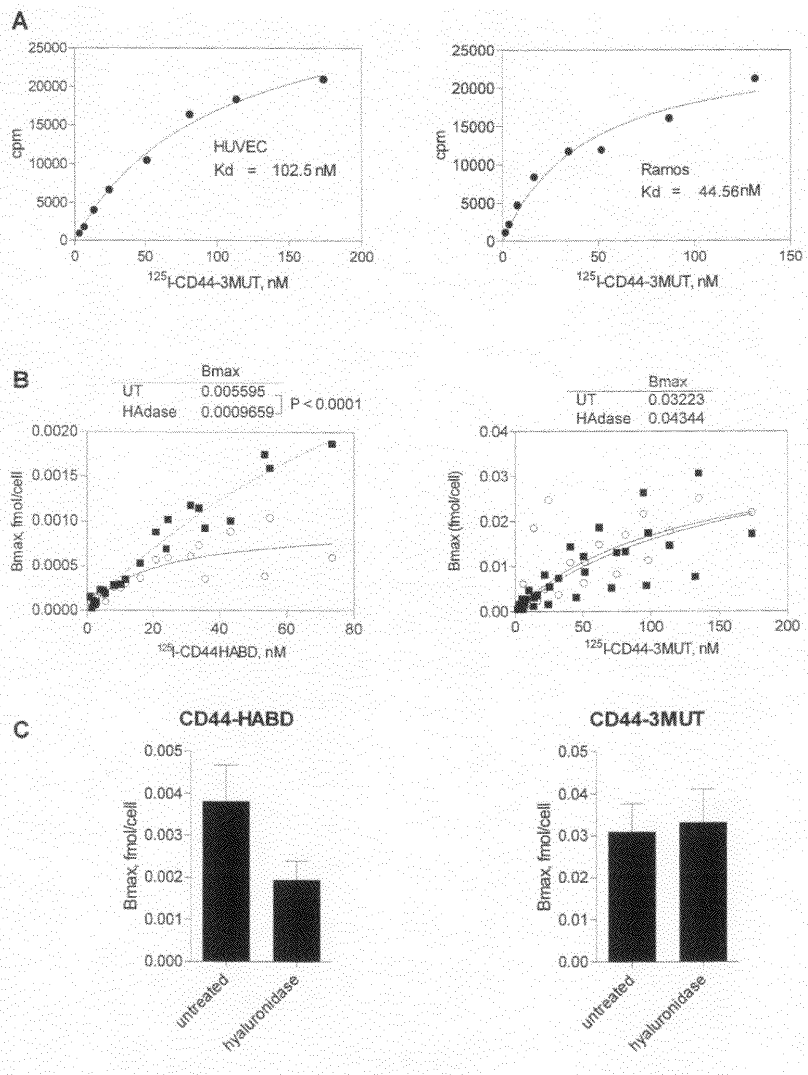
A
HUVEC
Kd = 102.5 nM
cpm
^{125}I-CD44-3MUT, nM
Ramos
Kd = 44.56nM
cpm
^{125}I-CD44-3MUT, nM
B
Bmax
UT 0.005595
HAdase 0.0009659
P < 0.0001
Bmax, fmol/cell
^{125}I-CD44HABD, nM
Bmax
UT 0.03223
HAdase 0.04344
Bmax (fmol/cell)
^{125}I-CD44-3MUT, nM
HAdase
UT
C
CD44-HABD
Bmax, fmol/cell
untreated
hyaluronidase
CD44-3MUT
Bmax, fmol/cell
untreated
hyaluronidase

FIG.12

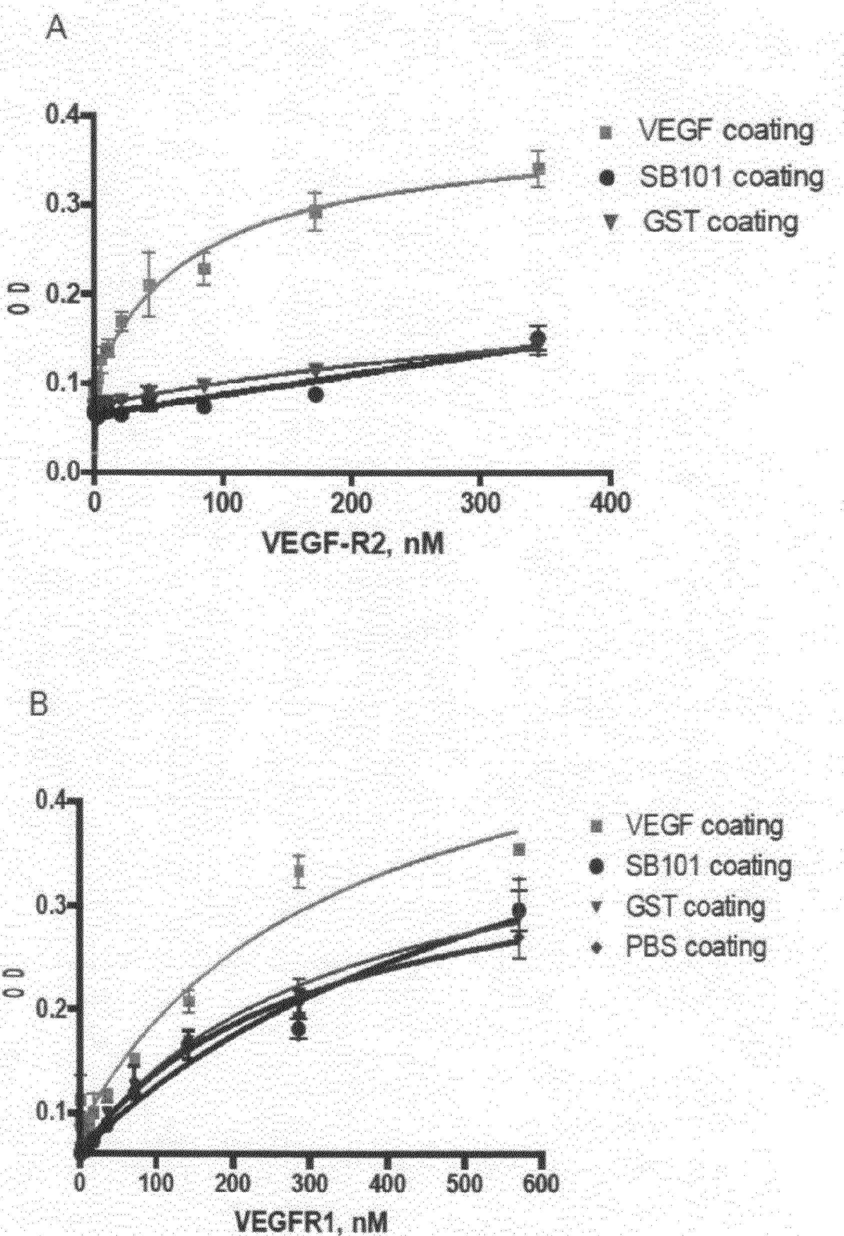
A
0.4
0.3
0.2
0.1
0.0
OD
0
100
200
300
400
VEGF-R2, nM
VEGF coating
SB101 coating
GST coating
B
0.4
0.3
0.2
0.1
OD
0
100
200
300
400
500
600
VEGFR1, nM
VEGF coating
SB101 coating
GST coating
PBS coating

FIG. 13

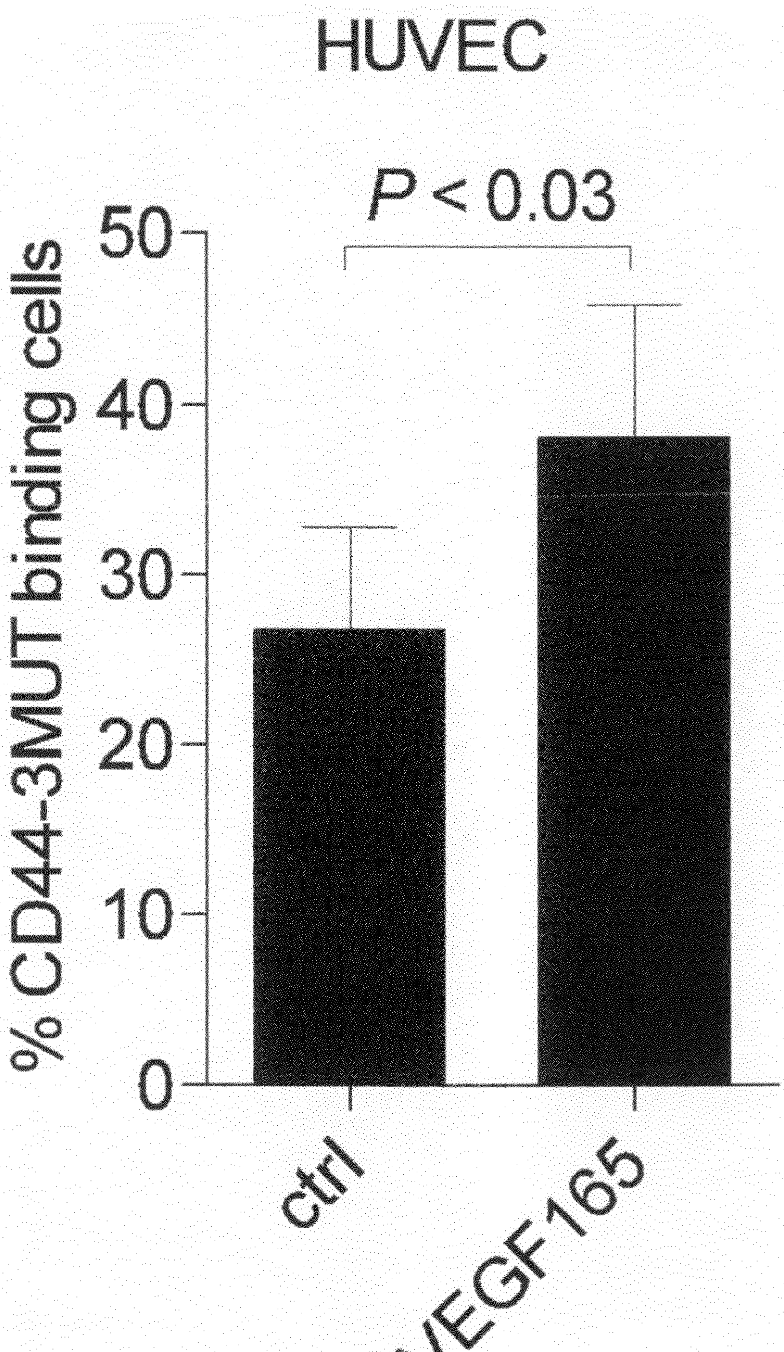
HUVEC
P < 0.03
% CD44-3MUT binding cells
50
40
30
20
10
0
ctrl
VEGF165

FIG. 14

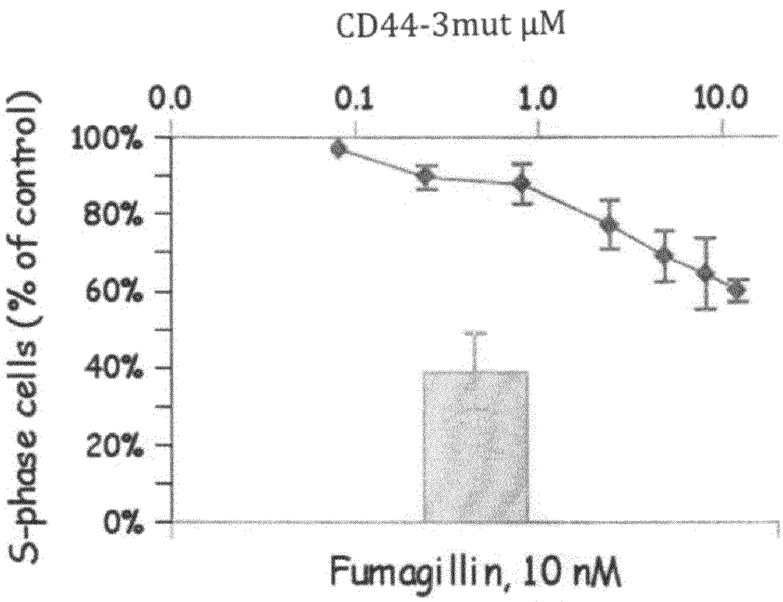
CD44-3mut μM
0.0
0.1
1.0
10.0
100%
80%
60%
40%
20%
0%
S-phase cells (% of control)
Fumagillin, 10 nM

Fig. 15

DRUG FOR TREATING STATES RELATED TO THE INHIBITION OF ANGIOGENESIS AND/OR ENDOTHELIAL CELL PROLIFERATION

PRIORITY

This application is a continuation-in-part of the U.S. patent application Ser. No. 10/487,620 filed on May 24, 2004, now abandoned the priority of which is claimed, and which is a national application of PCT/SE02/015431, filed on Aug. 26, 2002 and published as WO2003/018044 on Mar. 6, 2003, the priority of which is also claimed.

SEQUENCE LISTING

This application contains sequence data provided on a computer readable diskette and as a paper version. The paper version of the sequence data is identical to the data provided on the diskette.

TECHNICAL FIELD

The invention refers to the use of a molecule comprising the CD44-hyaluronic acid binding domain for a drug and manufacturing the drug. Furthermore, the invention relates to a method for screening for substances binding to the molecule comprising the CD44-hyaluronic acid binding domain.

TECHNICAL BACKGROUND

The formation of new blood vessels by angiogenesis is a central event in many different pathological states, including ocular diseases causing blindness, such as macular degeneration, diabetic retinopathy and states of retinal hypoxia, states of chronic inflammation, such as rheumatoid arthritis, in psoriasis, atherosclerosis, restenosis, as well as in cancer growth and metastasis. In addition, hemangioma is caused by uncontrolled proliferation of endothelial cells. Given that many of these diseases are of a chronic nature and presently lack satisfactory cure, search for treatments and drugs against these diseases is very important. According to current paradigm all solid tumors need to induce angiogenesis to cover their metabolic needs and grow over millimeter size. Therefore a possibility to inhibit tumor growth by reducing the neovascularization within tumor tissue would be most useful as adjuvant therapy for cancer cure. To this end, an agent blocking angiogenesis has the potential to constitute a medicament for all these common angiogenesis- (and/or endothelial cell-) dependent diseases.

One interesting target for drugs against diseases of this kind has been CD44 (Naot et al., Adv Cancer Res 1997; 71 :241-319). CD44 is a cell surface receptor for the large glycosaminoglycan of the extracellular matrix hyaluronic acid (HA) (Aruffo et al., Cell 1990; 61:1303-13). CD44 plays a role in various cellular and physiological functions, including adhesion to and migration on HA, HA degradation and tumor metastasis. The CD44 receptor shows a complex pattern of alternative splicing in its variable region of the extracellular domain (Screaton et al., PNAS 1992; 89: 12160-4). CD44 is able to bind matrix metalloproteinase-9 (MMP-9) and can thereby localize MMP-9 to the cellular membrane, which may in part explain its activity in promoting tumor cell invasion and metastasis (Yu, 1999).

Among patent references disclosing CD44 and its connection to diseases described above may U.S. Pat. Nos. 6,025,138, 5,902,795, 6,150,162, 6,001,356, 5,990,299 and U.S. Pat. No. 5,951,982 be mentioned.

WO94/09811 describes the use of CD44 in treating inflammation or detecting cancer metastasis of hematopoietic origin. Use of CD44 for inhibiting solid tumor growth or angiogenesis is not disclosed. WO 99/45942 discloses the use of HA-binding proteins and peptides including CD44 to inhibit cancer and angiogenesis-dependent diseases. CD44 is mentioned as one example of a long list of HA-binding proteins. In both publications the use of CD44 is limited to its ability to bind hyaluronic acid.

Ahrens et al. (Oncogene 2001; 20; 3399-3408) discloses that soluble CD44 inhibits melanoma tumor growth by blocking the binding of tumor cell surface CD44 to hyaluronic acid. Thus, this work teaches a hyaluronic acid binding dependent mechanism for the CD44 effect directly on melanoma tumor cell growth.

Alpaugh et al. (Exp. Cell Res. 261, 150-158 (2000)) discloses myoepithelial-specific CD44 and its antiangiogenic properties. This study deals with HA-binding properties of CD44.

Bajorath (PROTEINS: Structure, Function, and Genetics 39: 103-111 (2000)) discloses CD44 and its binding to HA, cell adhesion and CD44-signalling. Moreover, CD44 mutagenesis experiments are disclosed involving among others the well-established non-HA-binding mutations R41A and R78S, and their impact on CD44-binding to HA.

Bartolazzi et al. (1994) discloses an experiment where mammalian cell expressed CD44HRg-molecule inhibits tumor growth in nude mice. A mutant molecule CD44-R41A-Rg, not mediating cell attachment to hyaluronate, also expressed from mammalian cell did not have similar effect.

Thus, the prior art discloses the potential use of CD44 to specify that any effects are dependent on HA-CD44-interaction. Consequently, all utility ascribed this far to CD44-derived peptides is directly dependent on their ability to bind hyaluronic acid.

Given that hyaluronic acid is widely expressed in the body at high levels, a treatment based on inhibition of this extracellular component result in a high risk for unwanted side effects outside of the tumor. Furthermore, because of the high total amounts of HA in the body, such strategy will require high doses of HA-blocking recombinant proteins, thus even further increasing the risk for side effects.

Accordingly, a need exists for finding novel drugs for treating tumors, as well as novel pathways for the relation between CD44 and tumor growth, in order to provide new drug targets, which avoid the side effects described above.

There is also a clear need for a drug that could be administered in substantially smaller doses than substances having primary effect on CD44-HA binding function.

In addition, there is a need to develop novel inhibitors of angiogenesis, as these constitute potential medicaments not only for cancer, but also for an array of common diseases as disclosed above. To this end, it is important to elucidate the relation between CD44 and angiogenesis, in particular the potential direct effects of CD44 on the vasculature and on the various diseases that are dependent on new blood vessel formation.

SUMMARY OF THE INVENTION

Kogerman et al. (Oncogene 1997; 15: 1407-16) found that mouse fibrosarcoma cells stably expressing human CD44 standard isoform (hCD44s) had lost their hCD44s expression in large subcutaneous tumors. When hCD44s negative cells from these primary tumors were reintroduced subcutaneously into new mice for second round of tumor growth, then resulting tumors had significantly shorter latency times than hCD44s positive tumors.

The observed longer latency times for hCD44s expressing tumors lead the inventors to realize that the inhibitory effect of hCD44s over expression in subcutaneous tumor growth is connected to inhibition of tumor angiogenesis. Induction of angiogenesis is essential for growth and persistence of solid tumors and their metastases. In the absence of angiogenesis, tumors cannot grow beyond a minimal size and remain dormant in the form of micrometastases (Holmgren et al., Nat Med 1995; 1: 149-53). The inventors disclose here that recombinant soluble human CD44 hyaluronic acid binding (CD44HABD) domain inhibits angiogenesis in vivo in chick and endothelial cell proliferation in vitro, and thereby blocks human tumor growth in chick and mice. The inventors describe a novel type of angiogenesis inhibitor, as they found that recombinant cell surface receptor CD44 inhibits angiogenesis and tumor growth in vivo and endothelial cell proliferation in vitro. Furthermore, the inventors have created mutant forms of CD44 that are surprisingly also capable of inhibiting angiogenesis. The mutant forms were found to inhibit tumor growth in vivo and the effect is dose-dependent. The advantage with these mutants of CD44 is that they do not bind HA, demonstrating that the mechanism for inhibition of angiogenesis is unexpectedly independent of binding to HA. Importantly, use of mutant CD44 for systemic administration as a medicament will be more specific for angiogenesis, since it will not be bound up by HA in the body, and can therefore be used at lower doses and has less risk of causing unwanted side effects.

Accordingly, the invention relates to the use of a molecule comprising a non-HA-binding variant of the CD44-hyaluronic acid binding domain, as well as analogues and recombinant variants thereof, including the specified mutants, for treating states related to the inhibition of angiogenesis and manufacturing of a medicament for treating such states. Moreover, the invention relates to a method for screening for molecules binding to the CD44-hyaluronic acid-binding domain, thereby being potential targets for inhibiting angiogenesis and for cell proliferation. Further, the invention relates to a kit for carrying out the screening method, as well as the molecules found by the method. Also, the invention relates to a molecule comprising a non-HA-binding variant of the CD44-hyaluronic acid binding domain, as well as analogues, recombinant and mutated variants thereof for targeting of endothelial cells.

According to this disclosure, drugs for treating states related to angiogenesis, such as various cancerous states, can be easily provided, taking advantage of the novel mechanisms presented herein. Furthermore, through the method of screening, other molecules may be found, which affect cell proliferation and/or angiogenesis.

SHORT DESCRIPTION OF THE DRAWINGS

FIG. **1** shows a SDS PAGE of recombinant GST and GST-CD44 proteins. The gel was stained with Coomassie Brilliant Blue. Molecular weight markers are shown on the right.

FIG. **2** shows that recombinant CD44HABD binds to hyaluronic acid. a, wild type CD44HABD, but not R41A, R78SY79S or R41AR78SY79S HA non-binding mutants, binds to immobilized HA. b, CD44HABD inhibits human aortic endothelial cell migration towards HA, whereas R41A HA-non-binding mutant has no effect. A3, monoclonal antibody to CD44, that blocks HA binding, and also inhibit endothelial cell migration.

FIG. **3** shows that recombinant human CD44HABD blocks angiogenesis in vivo in chick chorio-allantoic membrane. a, Filter discs and associated CAM from typical angiogenesis experiment where angiogenesis was induced with bFGF. b-d, Angiogenesis was assessed as number of blood vessel branch points; mean angiogenic index+/−SEM. *(P<0.05), significant results.

FIG. **4** shows that recombinant CD44HABD inhibits melanoma (SMMU-1, M21) and hepatocellular carcinoma (HepG2) growth in chick CAM.

FIG. **5** shows that recombinant CD44HABD inhibits CD44 negative melanoma growth. a, Growth curve of s.c. SMMU-1 tumors in nude mice treated with CD44HABD, CD44HABD^{R41AR78SY79S} or GST as control, n=8 per group. b, Tumor weights at day 16, where the black line represents the median value. c, Representative photographs of mice at day 16, treated as indicated. d, Blood vessel density at tumor border per high power field (HPF). *(P<0.005), **(0.05) significant results.

FIG. **6**. CD44-HABD fusion proteins inhibit the growth of human pancreatic cancer cells in nude mice. BxPC-3 pancreatic adenocarcinoma (a) tumors in nude mice treated with GST-CD44HABD (solid rectangular), GST-CD44HABD^{R41AR785Y79S} (solid triangle) or GST (diamond-solid) as control (n=6-7). b, average BxPC-3 tumor weights at the end of experiment. Values in graphs and bars represent mean+/−s.e.m. Asterisk indicates P<0.05.

FIG. **7**. Recombinant CD44HABD blocks specifically endothelial cell cycle. The proportion of cells in S-phase when treated with GST (black), GST-CD44HABD (pale gray) or GST-CD44HABD^{R41AR78SY79S} (gray).) HUVEC, human vascular endothelial cells; CPAE, cow pulmonary arteria endothelial cells; NHDF, normal human dermal fibroblasts; MCF-7, human breast carcinoma cells.

FIG. **8**. shows tumor growth assay with Hep3b human hepatoma cells in nude mice. Hep3b cells (3.5×10^6) were injected subcutaneously into Foxn1 athymic nude mice. Intraperitoneal treatment with drugs started on day 14 post inoculation when the average tumor volume reached 150 mm^3. CD44-3MUT and PBS (phosphate buffered saline) were administered thrice a week. Tumor length (L) and width (W) were measured throughout the study. Tumor volumes were calculated using formula $V=L*W^2/2$. Final weight of dissected tumors was measured. Panel A, growth curves of tumors treated with different doses of CD44-3MUT. Panel B, average tumor weights at the end of experiment. Error bars indicate SEM.

FIG. **9** Tumor growth assay with Hep3b human hepatoma cells in nude mice. Hep3b cells (5×10^6 cells) were injected subcutaneously into Foxn1 athymic nude mice. 14 days after inoculation, the average tumor volume reached 85 mm^3, mice were grouped into 4 groups. In one group CD44-3MUT was administrated 1 μg/mouse after every 12 hours by intraperitoneal injection. Another three groups of mice were anesthetized and 100 μl osmotic-pumps were implanted into intraperitoneal cavity through the midline abdominal incision. Before implantation pumps were filled with treatment solutions: PBS; Avastin (AVA) 400 μg/pump (approximate drug release from pump is 28.6 μg/day); CD44-3MUT 150 μg/pump (drug release 1.07 μg/day). Tumor length (L) and width (W) were measured throughout the study. Tumor volumes were calculated using formula $V=L*W^2/2$. Final weight of dissected tumors was measured. Panel A, growth curves of tumors treated with different administration methods of CD44-3MUT. Panel B, average tumor weights at the end of experiment. Error bars indicate SEM. Experiments have been performed by Celecure as blind experiments.

FIG. **10** Angiogenesis assay with chick aortic fragments. Aortic fragments were dissected from 14-day old chick embryo and embedded into collagen-I matrix containing VEGF and respective proteins. After 48 h of incubation photomicrographs were taken from aortic rings and blood vessel outgrowth was quantified on images by measuring vessel length from tip to aortic tissue. CD44-3MUT inhibits significantly VEGF-induced blood vessel growth (p=0.002, one-way ANOVA, n=4 independent experiments).

FIG. **11** Tumor growth assay with Hep3b human hepatoma cells in nude mice. Hep3b cells (3.5×10^6) were injected subcutaneously into Foxn1 athymic nude mice. Intraperitoneal treatment with drugs started on day 14 post inoculation when average tumor volume reached 150 mm^3. CD44-3MUT was injected in the dose 10 μg per animal (0.4 mg/kg) thrice a week and Avastin dosing was used 400 μg per animal twice a week.

FIG. **12** Saturation binding of iodine-125 labeled CD44-3MUT. Cells were incubated 1 h with different concentrations of 125-I labeled CD44-3MUT. Bound radioactivity was quantified by a γ-counter. (A) Binding curves of representative experiment of HUVEC endothelial cells (left) and Ramos lymphoma cells (right). Kd-s were calculated using non-linear fit of specific binding. (B) Enzymatic degradation of hyaluronan reduces significantly CD44-HABD cellular binding (left panel), whereas CD44-3MUT binding remained unchanged. Curve was fitted to global specific binding data using non-lin fit. Statistical analysis was performed using extra sum of squares F-test. (C) Bmax of CD44-HABD and CD44-3MUT on HUVEC. Bars show mean±SE (n=3). Abbreviations: UT, untreated; Hadase, hyaluronidase; 3MUT, CD44-3MUT; HABD, CD44-HABD.

FIG. **13** Test of CD44-3MUT binding to VEGF receptors. Modified ELISA tests to evaluate the binding of VEGFR2 (panel A) and VEGFR1 (panel B) to immobilized CD44-3MUT. ELISA plate wells were coated with VEGF, as positive control and GST (Glutathione-S-transferase), PBS or CD44-3MUT. Nonspecific binding was blocked with 2.5% non-fat dry milk solution. VEGFR1 and VEGFR2 were added into the coated wells and incubated for 1 h at RT. VEGFR binding was detected with anti-VEGFR antibodies

FIG. **14** CD44-3MUT binding to growth factor treated endothelial cells. Serum starved HUVEC were induced 30 min with VEGF165, followed by incubation with directly fluorescence-labeled CD44-3MUT at 4° C. CD44-3MUT binding by HUVEC was analyzed by FACS. Bars represent percentage of cells binding CD44-3MUT (mean±SE, n=5). Statistical analysis was done using two-tailed paired t-test.

FIG. **15** Cell proliferation assay of HUVE cells. CD44-3MUT inhibits endothelial cell proliferation in dose-dependent fashion. Exponentially growing HUVE cell populations were treated with respective proteins for 24 h. Cells were double-stained with propidium iodide and BrdU and analyzed by FACS.

DEFINITIONS

The "hyaluronic acid binding domain" is hereafter referred to as HABD.

By a "non-HA-binding variant" of HABD is meant a variant that is modified by way of mutation or in any other way, so that it at least partly has lost its ability to bind to HA, but still has the capacity to inhibit angiogenesis and/or endothelial cell proliferation.

"Molecule" means here the smallest particle of a substance that retains the chemical and physical properties of the substance and is composed of two or more atoms; a group of like or different atoms held together by chemical forces.

Accordingly "Administering soluble human CD44HABD molecule" does not include injecting cells. The pharmaceutical composition could be adapted to oral or parenteral use, and could be administered to the patient as tablets, capsules, suppositories, solutions, suspensions or the like.

$CD44HABD^{R41AR78SY79S}$ refers to a non HA binding triple mutant of the CD44HABD and is synonymous to CD44-3MUT. The molecule is according to SEQ ID NO:12.

By "analogues and recombinant variants" of a molecule comprising the CD44HABD, are meant molecules, such as fusion proteins, comprising the CD44HABD, thereby at least partly exerting essentially the properties of the CD44HABD.

By "states related to the inhibition of angiogenesis and/or endothelial cell proliferation" are meant such states and diseases, which may be treated or affected by an inhibition of the angiogenesis and/or endothelial cell proliferation.

By "a binding partner" for a molecule comprising the CD44HABD is meant a molecule having affinity for CD44HABD or mutants thereof.

By "a receptor molecule, or a part of a receptor molecule" is meant a molecule acting as a receptor, or being part of a receptor.

By "a modified variant" is in the context of the invention meant any modification to a normal wt-molecule, such as deletions, insertions, substitutions, analogs, fragments or recombinant variants thereof.

DETAILED DESCRIPTION OF THE INVENTION

WO94/09811 describes the use of CD44 in treating inflammation or detecting cancer metastasis. The authors show that CD44 is upregulated in inflammatory conditions and CD44 peptides are capable of inhibiting T-cell activation. No data or claims are presented on inhibition of metastasis by CD44 and no claims are made towards use of CD44 for inhibiting tumor growth or angiogenesis. WO 99/45942 discloses the use of HA-binding proteins and peptides including CD44 to inhibit cancer and angiogenesis-dependent diseases. This publication uses metastatin, a 38 kDa fragment of the cartilage link protein as well as a HA-binding peptide derived from this fragment to inhibit pulmonary metastasis of B 16 mouse melanoma and Lewis lung carcinoma. In the case of the HA-binding peptide, growth of B16 melanoma on chicken CAM and endothelial cell migration on HA have been inhibited. In both publications the use of HA-binding peptides is directly related to their ability to bind hyaluronic acid.

CD44 was previously implicated to promote angiogenesis by a mechanism dependent on its ability to bind matrix metalloproteinase-9 (MMP-9) (Yu and Stamenkovic, Genes Dev 1999; 13: 35-48; Yu and Stamenkovic, Genes Dev 2000; 14: 163-76). Over expression of soluble CD44 (sCD44v6-10) in murine TA3 mammary carcinoma cells inhibited the binding of MMP-9 to the tumor cell surface and thereby blocked tumor growth and vascularization (Yu and Stamenkovic 2000). MMP-9 was previously demonstrated to be involved in angiogenesis during development and in tumors (Vu et al., Cell 1998; 93: 411-22; Bergers et al., Nat Cell Biol 2000; 2: 737-44; Coussens et al., Cell 2000; 103: 481-90). CD44-MMP-9 complex is also implicated in activation of latent TGFβ since tubulogenesis in vitro was inhibited by block of TGFβ. (Yu and Stamenkovic, 2000).

The mutants of CD44-HABD used in this disclosure show very different affinities towards MMP-9 but independent of that, surprisingly they inhibit angiogenesis equally well. This makes it unlikely that MMP-9 binding is critical for the inhibition of angiogenesis as disclosed in the present invention. In addition, this disclosure describes a mechanism for CD44 that directly inhibits angiogenesis. Furthermore, the disclosure demonstrates a mechanism for CD44 that has a distinct target in normal endothelial cells, as compared to the previously proposed mechanism disrupting CD44-binding of MMP-9 at transformed tumor cell surfaces. Gao et al. (Cancer Res 1998; 58: 2350-2) show that metastatic ability, but not tumorigenicity of rat Dunning AT3.1 prostate cancer cells is independent of HA binding, as over expression of rat CD44 standard isoform and R44A non-HA-binding mutant both reduced dramatically formation of metastatic lung colonies but not local tumor growth. This suggests that other CD44 binding partners distinct from HA must be involved in metastasis. A number of CD44-binding proteins have been described including HGF, bFGF, fibronectin, osteopontin, selectin to name a few. However, the binding of several of these proteins is dependent on the post-translational modifications of CD44 and/or the inclusion of alternative exons in CD44 that are not present in our recombinant fusion proteins. Also, many of these CD44-binding proteins are present in large amount in the body, making CD44-derivatives binding to any of these less useful as a drug, because of a high risk of side effects. In addition, none of the previously described proteins are unique for targeting vascular cells, neither do they block a pathway required specifically for the growth of endothelial cells. Accordingly, the pathway we suggest in this disclosure has not been described before. This disclosure discloses a method for identifying the binding partner of CD44 and the pathway that is relevant for the inhibition of angiogenesis and endothelial cell growth.

In a first aspect the invention relates to the use of a molecule comprising a non-HA-binding variant of the CD44HABD, as well as analogues, recombinant and mutated variants thereof, for the manufacturing of a medicament for treating states related to the inhibition of angiogenesis and/or endothelial cell proliferation.

In one embodiment, the CD44-HABD comprises at least one mutation, thereby rendering it non-HA-binding.

In a preferred embodiment, the mutation(s) is (are) chosen from F34A, F34Y, K38R, K38S, R41A, Y42F, Y42S, R46S, E48S, K54S, Q65S, K68S, R78K, R78S, Y79F, Y79S, N100A, N100R, N101S, Y105F, Y105S, S112R, Y114F, F119A, F119Y. Preferably, the mutations are chosen from one or more of R41A, R78S, Y79S. Also, deletion mutations resulting in any fragment of CD44 from 3 to 110 amino acids in length are potentially useful for the purposes of the invention. However, the skilled person easily realizes that any mutation to wild-type HA-binding CD44, which makes the CD44-HABD, or fragments thereof, at least partly non-HA-binding, such as one or more deletions, substitutions or additions, may be introduced in the CD44-HABD part, as long as the desired properties are achieved.

The CD44-HABD is a protein covering amino acids 21-132 of intact human CD44 molecule, or has high degree of homology to this region of human CD44. The chicken CD44-HABD is the most dissimilar HABD that has been isolated by the inventors, having a sequence homology of 55% to human HABD at the amino acid level. Thus, a high degree of sequence homology means at least approximately 55% amino acid homology, desirably at least 65% homology, and most desirably at least 75% homology.

According to a preferred embodiment the C44-HABD protein and its non HA binding mutations are produced in bacterial cell culture and thereby the protein is non-glycosylated form.

Furthermore, the molecule according to the invention refers to a deleted or in any other way changed or mutated form of the CD44-HABD protein, whereby the changed form exhibits essentially the same properties as the original CD44-HABD-protein, or the herein specified CD44-HABD-mutants, as measured by any one of the methods described here.

In a preferred embodiment, the molecule comprising the non-HA-binding variant of the CD44HABD is chosen from the group comprising: human CD44HABD (SEQ ID NO: 2), dog CD44HABD (SEQ ID NO: 4), chick CD44HABD (SEQ ID NO: 6), human CD44HABD^{R41A} (SEQ ID NO: 8), human CD44HABD^{R78SY79S} (SEQ ID NO: 10), and CD44HABD^{R41AR78SY79S} (SEQ ID NO: 12), the sequences above further comprising at least one modification thereby making them non-HA-binding. Other variants are also possible, such as CD44HABD^{R78S}, CD44HABD^{Y79S}, as well as GST-CD44HABD-fusion proteins having the R41A, R78S or the. Y79S mutations.

CD44HABD^{R41A}, CD44HABD^{R78SY79S} and CD44HABD^{R41AR78SY79S} are preferred examples of mutated variants of CD44-HABD, wherein the letters/figures in superscript indicates the position and type of mutation.

GST-CD44HABD is a fusion protein of a GST-part and CD44HABD. Other possible fusion proteins may be chosen from the group comprising IgG, IgM, IgA, His, HA, FLAG, c-myc, EGFP. GST is a short for glutathione-S-transferase, being used as a tag for the purpose of being able to purify the fusion protein on a GST-binding column, as well as for the purpose of detection. GST occurs naturally as a 26 kDa protein (Parker, M. W. et al., J. Mol. Biol. 213, 221 (1990); Ji, X. et al., Biochemistry, 31, 10169 (1992); Maru, Y. et al., J. Biol. Chem. 271, 15353 (1996).).

Accordingly, in another embodiment, the recombinant variant is a fusion protein having a GST part and a CD44-HABD part, wherein the CD44-HABD-part is in a wild-type form or in a mutated form. Other tags than GST are also fully possible.

Preferably, the CD44-HABD has a homology to the sequence SEQ ID NO: 2 of at least 55%, more preferably at least 65%, even more preferably at least 75%. Most preferably, the CD44-HABD is a modified variant (non-HA-binding gene product) of the sequence SEQ ID NO: 1.

The invention may be used for all states related to the inhibition of angiogenesis and/or endothelial cell proliferation. States and diseases to be treated may be chosen from the following non limiting group: ocular diseases causing blindness, or impaired vision, such as macular degeneration, diabetic retinopathy and states of retinal hypoxia, states of chronic inflammation, such as rheumatoid arthritis, in psoriasis, atherosclerosis, restenosis, as well as in cancer growth and metastasis, as well as all forms of cancer diseases and tumors, such as a cancer of breast, prostate, colon, lung, skin, liver, brain, ovary, testis, skeleton, epithelium, endothelium, pancreas, kidney, muscle, adrenal gland, intestines, endocrine glands, oral cavities, head and neck, or other solid tissue origin, or being any form of leukemia, as well as in hemangioma. For instance, the invention may be used for mouse, rat, chick, dog, horse, cat, bovine animals and for all long-lived species in a normal zoo. Preferably, the invention is used for humans.

In still another aspect, the invention refers to a recombinant molecule comprising a GST-part and a CD44HABD part. The CD44HABD part may for example be mutated with one or more of the following mutations: F34A, F34Y, K38R, K38S, R41A, Y42F, Y42S, R46S, E48S, K54S, Q65S, K68S, R78K, R78S, Y79F, Y79S, N100A, N100R, N101S, Y105F, Y105S, S112R, Y114F, F119A, F119Y. Preferably, the mutations are chosen from one or more of R41A, R78S, Y79S. However, the skilled person easily realizes that any mutation to wild-type HA-binding CD44, which makes the CD44-HABD, or fragment thereof, at least partly non-HA-binding, such as one or more deletions, substitutions or additions, may be introduced in the CD44-HABD part, as long as the desired properties are achieved.

In a preferred embodiment, the CD44-HABD-part comprises a non-HA-binding variant of the CD44-HABD of any one of the amino acid sequences SEQ ID NO: 2, SEQ ID NO:4, SEQ ID NO:6, SEQ ID NO:8, SEQ ID NO:10, SEQ ID NO:12, the sequences above further comprising at least one modification thereby making them non-HA-binding.

In the most preferred embodiment, CD44HABD comprises at least three consecutive amino acids of the amino acids 23-132 of CD44. Basically, all fragments from 3-110 amino acids in size are potentially efficient, for example amino acids 23-25, 24-26, 25-27, etc., amino acids 23-26, 24-27, etc., 23-27, etc., 23-28, etc. Thus, all combinations of consecutive amino acids up to 110 amino acids of the original molecule are possible for the purposes of the invention, as the skilled man easily realizes, as long as they show the desired properties, as tested by the methods illustrated in the example section of this application

In another embodiment, the CD44HABD part is encoded by a sequence having at least 55% homology, preferably 65% homology, more preferably 75% homology, most preferably being any one of the nucleotide sequences: SEQ ID NO:1, SEQ ID NO:3, SEQ ID NO:5, SEQ ID NO:7, SEQ ID NO:9, SEQ ID NO:11, whereby the nucleotide sequences are in a modified form (non-HA-binding gene product or peptide).

In another aspect, the invention refers to a pharmaceutical composition in order to inhibit angiogenesis and/or endothelial cell proliferation, characterized in that it comprises at least one molecule comprising the CD44HABD, as well as analogues, recombinant and mutated variants thereof, in mixture or otherwise together with at least one pharmaceutically acceptable carrier or excipient.

The pharmaceutical compositions are prepared in a manner known to a person skilled in the pharmaceutical art. The carrier or the excipient could be a solid, semi-solid or liquid material that could serve as a vehicle or medium for the active ingredient. Suitable carriers or excipients are known in the art. The pharmaceutical composition could be adapted to oral or parenteral use and could be administered to the patient as tablets, capsules, suppositories, solutions, suspensions or the like.

The pharmaceutical compositions could be administered orally, e.g. with an inert diluent or with an edible carrier. They could be enclosed in gelatin capsules or be compressed to tablets. For oral therapeutic administration the compounds according to the invention could be incorporated with excipients and used as tablets, lozenges, capsules, elixirs, suspensions, syrups, wafers, chewing gums and the like. These preparations should contain at least 4% by weight of the compounds according to the invention, the active ingredient, but could be varied according to the special form and could, suitably, be 4-70% by weight of the unit. The amount of the active ingredient that is contained in compositions is so high that a unit dosage form suitable for administration is obtained.

The tablets, pills, capsules, lozenges and the like could also contain at least one of the following adjuvants: binders such as microcrystalline cellulose, gum tragacanth or gelatin, excipients such as starch or lactose, disintegrating agents such as alginic acid, Primogel, corn starch, and the like, lubricants such as magnesium stearate or Sterotex, glidants such as colloidal silica dioxide, and sweetening agents such as saccharose or saccharin could be added or flavorings such as peppermint, methyl salicylate or orange flavoring. When the unit dosage form is a capsule it could contain in addition of the type above a liquid carrier such as polyethylene glycol or a fatty oil. Other unit dosage forms could contain other different materials that modify the physical form of the unit dosage form, e.g. as coatings. Accordingly, tablets or pills could be coated with sugar, shellac or other enteric coating agents. Syrup could in addition to the active ingredient contain saccharose as a sweetening agent and some preservatives, dyes and flavoring agents. Materials that are used for preparation of these different compositions should be pharmaceutically pure and non-toxic in the amounts used.

For parenteral administration the compounds according to the invention could be incorporated in a solution or suspension. Parenteral administration refers to the administration not through the alimentary canal but rather by injection through some other route, as subcutaneous, intramuscular, intraorbital, intracapsular, intraspinal, infrasternal, intravenous, intranasal, intrapulmonary, through the urinary tract, through the lactiferous tract in cattle, into an organ such as bone marrow, etc. Bone marrow may also be treated in vitro. These preparations could contain at least 0.1% by weight of an active compound according to the invention but could be varied to be approximately 0.1-50% thereof by weight. The amount of the active ingredient that is contained in such compositions is so high that a suitable dosage is obtained. The solutions or suspensions could also comprise at least one of the following adjuvants: sterile diluents such as water for injection, saline, fixed oils, polyethylene glycols, glycerol, propylene glycol or other synthetic solvents, antibacterial agents such as benzyl alcohol or methyl paraben, antioxidants such as ascorbic acid or sodium bisulfite, chelating agents such as ethylene diamine tetra-acetic acid, buffers such as acetates, citrates or phosphates, and agents for adjustment of the tonicity such as sodium chloride or dextrose. The parenteral preparation could be enclosed in ampoules, disposable syringes or multiple dosage vessels made of glass or plastic. For topical administration the compounds according to the invention could be incorporated in a solution, suspension, or ointment. These preparations could contain at least 0.1% by weight of an active compound according to the invention but could be varied to be approximately 0.1-50% thereof by weight. The amount of the active ingredient that is contained in such compositions is so high that a suitable dosage is obtained. The administration could be facilitated by applying touch, pressure, massage or heat, warms, or infrared light on the skin, which leads to enhanced skin permeability. Hirvonen et al., Nat Biotechnology 1996; 14: 1710-13 describes how to enhance the transport of a drug via the skin using the driving force of an applied electric field. Preferably, iontophoresis is affected at a slightly basic pH.

In yet another aspect, the invention relates to a method for the treatment of a cancerous tumor or any other disease related to angiogenesis and/or endothelial cell proliferation in a subject, comprising administrating a pharmaceutical dose of a molecule comprising the CD44HABD, as well as analogues, recombinant and mutated variants thereof.

By a subject is meant any mammal, including humans. A human subject is preferred.

In another embodiment, the invention may be used for treating other diseases and disorders characterized by excessive formation of blood vessels and/or uncontrolled endothelial cell proliferation. These include, but are not limited to, adult blindness, or impaired vision, caused by diabetic retinopathy or macular degeneration, psoriasis and various states of chronical inflammation and hemangioma.

CD44HABD or a fragment thereof can be obtained by any method of recombinant expression or chemical synthesis known in the art. According to most preferred embodiment it is expressed in bacterial cells as described in example 1. It can be cloned into baculovirus vectors and expressed in insect cells. Bacterially expressed proteins lack any posttranslational modifications and accordingly the putative N-linked glycosylation sites of CD44HABD are nonglycosylated in the recombinant protein. The proteins of this disclosure can however be also expressed in mammalian cells or in any other expression system, but in such case the recombinant protein would need to be modified to remove the glycosylation. The affinity tag can be added to the protein product and the protein can be purified using affinity chromatography with the selected tag. The affinity tags are well known in the art and include, but are not limited to, GST-tag, His-tag, S-tag, T7-tag, V5-tag, E2-tag, c-myc-tag, HA-tag, FLAG-tag. The protein may be expressed without any tag and be purified by immunoaffinity, ion exchange or gel filtration chromatography or a combination thereof. Furthermore, non-glycosylated CD44HABD, fragments thereof, or its analogues can be obtained by known methods of chemical synthesis including but not limited to solid-phase peptide synthesis. CD44HABD obtained by any of the described methods is included in the present invention.

In still another aspect, the invention relates to a method for screening for a binding partner for a molecule comprising the CD44HABD as well as analogues, mutants and recombinant variants thereof, comprising the steps of:

a) providing the molecule comprising the CD44HABD, or fragments thereof;

b) contacting a potential binding partner to said molecule; and

c) determining the effect of said molecule on said potential binding partner.

Potential methods for screening comprise: (I) a) Incubation of CD44/HABD, CD44HABD analogues or mutants thereof with cells, cell lysates, cellular fractions, tissues, organisms, animals or parts of organisms or animals.

b) Purification and detection of CD44HABD binding partners (e.g. by affinity columns, gel electrophoreses, and any detection using antibodies or protein staining or isotopes or other means of detecting CD44HABD or tags connected to CD44HABD.

c) Identification of CD44HABD binding partners by localization in gel electrophoresis (e.g. 2D electrophoresis), use of mass spectroscopy, sequencing, antibodies or other means of identification.

d) Determining the effect of CD44HABD on identified binding partners or determining the effect of other interacting agents of said potential binding partner in vitro or in vivo.

e) Using an identified CD44HABD-binding partner to design novel inhibitors of cell proliferation and/or angiogenesis.

(II) a) Using CD44HABD as a bait for genetic screening of DNA, cDNA, phage, peptide, protein, cell or organism libraries or screening of synthetic peptide, protein, polysaccharide, lipid, heparan sulphate or proteoglycan libraries using CD44HABD, analogues or mutants thereof as a bait,

b) Detection of CD44HABD binding partners by selection markers.

c) Identification of CD44HABD binding partners by sequencing, hybridization, restriction analysis, antibodies or by step-wise elimination within a library or by other means of identification.

d) Determining the effect of CD44HABD on identified binding partner or determining the effect of other interacting agents of said potential binding partner in vitro or in vivo.

e) Using an identified CD44HABD-binding partner to design novel inhibitors of cell proliferation and/or angiogenesis.

Moreover, the screening method of the invention may also be used for determining the effect of other activators or functional blocking agents of said potential binding partners.

Furthermore, a CD44HABD-mutant, or fragment, may be used for the screening. This may provide a more specific search for finding anti-angiogenic molecules.

In one embodiment, the potential binding partner is chosen from the group comprising: proteins, glycoproteins, proteoglycans, heparan sulphates, lipids, glycans, glycosides and saccharides.

In another embodiment, the potential binding partner is a receptor molecule, or a part of a receptor molecule or a molecule binding to a cell surface receptor molecule or a molecule located at the cell surface without being a receptor molecule.

In yet another embodiment, the potential binding partner is an extracellular molecule, being localized in the extracellular matrix, tissue sinuses, lymph- or blood vessels.

In yet another aspect, the invention relates to a binding partner for a molecule comprising the CD44HABD found by the method described above. The said binding partner, being a molecule promoting or inhibiting angiogenesis and therefore a potential target for the development of novel inhibitors of angiogenesis, e.g. a cell surface receptor that normally confers pro-angiogenic signaling, including a receptor for soluble angiogenic factors, such as growth factor receptor (e.g. VEGF-receptor family, FGF-receptor family, EGF-receptor family, PDGF-receptor family), receptor for the extracellular matrix (e.g. integrins, syndecans, proteoglycans), cell-cell-adhesion receptor (e.g. Cadherins, Ig-like superfamily, selectins). The receptor transduces pro-angiogenic signals into endothelial cells or block anti-angiogenic signaling or promote anti-angiogenic signaling in endothelial cells. Activation of this receptor to signal occurs by binding to an extracellular ligand or by activation targeting the cytoplasmic domain of the receptor by intracellular signaling events. Alternatively, the receptor at the cell surface acts as a carrier that transports and directs its ligand to an intracellular receptor (e.g. nuclear receptor), both which are examples of potential binding partners that may be identified by the claimed screening methods and may be utilized as anti-angiogenic targets.

In still another aspect, the invention refers to a kit for carrying out the method described above comprising, in separate vials, the molecule, or the genetic information, comprising the CD44HABD, analogues or mutants or parts thereof, and the potential binding partner, or parts thereof.

In yet another aspect the invention refers to the use of a molecule comprising the CD44HABD-, as well as analogues, recombinant and mutated variants or fragments thereof for targeting of endothelial cells. Since the CD44HABD-molecule of the invention has shown the capacity to bind endothelial cells, it may be used to target such cells.

In one embodiment, the molecule further comprises a moiety showing chemotherapeutic and gene therapy properties. Hereby, the CD44-HABD-molecule of the invention, in a modified variant, may be used as an anti-tumor drug towards endothelial cells. As the skilled person in the art realizes, the function that is coupled to the CD44-HABD-molecule of the invention may also have other properties than anti-tumoral such as anti-endothelial cell proliferation and/or migration, pro-apoptotic or disrupting essential functions of endothelial cells or other vascular cells. However, a moiety having anti-tumoral properties is one preferred embodiment.

By "showing chemotherapeutic properties" is meant that the molecule having this property has the capacity to inhibit the growth and/or kill the cells it is targeted for, as measured by use of in vitro tissue culture of cells or tissues, in vitro screening of enzymatic activity, e.g. kinase, phosphatase, glycosylation, acetylation, proteolysis, linker ligation or any other enzymatic activities, proton transfer, in vitro or in vivo screening of ion pump function, and/or in vivo or in vitro screening of cell growth, apoptosis, or other means of cell death, tumor progression, metastasis, invasion, angiogenesis and/or tissue homeostasis.

The moiety showing chemotherapeutic and/or gene therapy properties may for example be chosen from different viruses for gene therapy, various chemotherapeutics, which would be known by the skilled person of the art, naked DNA coupled to HABD, mutants, or fragments thereof, as well as other DNA-carriers, including but not limited to lipids, peptides and proteins.

For example, Arap et al. (Science, 1998, 279: 377-380), Ellerby et al. (Nature Medicine, 1999,5; 9:1032-1038), and Trepel et al. (Human Gene Therapy, 2000, 11:1971-1981) discloses the coupling of a doxorubicin molecule (cytostatica), the coupling of an apoptosis-inducing peptide, and the coupling of a virus, respectively, for targeting of endothelial cells.

The coupling of a virus is an example on how an endothelial-targeting molecule can be used for gene therapy.

Accordingly, in yet another embodiment, the invention relates to a molecule comprising the CD44HABD, as well as analogues, recombinant and mutated variants or fragments thereof, and a moiety showing chemotherapeutic and/or gene therapeutic properties.

In still another embodiment, the invention relates to a molecule of the invention coupled to a moiety having chemotherapeutic properties as defined above, for medical use.

The invention will now be described with reference to the following examples, which are intended for illustrative purposes only, and do not limit the scope of the invention in any way.

EXAMPLES

Example 1

Construction and Purification of Wild-Type and Mutant Human CD44HABD as Non-Glycosylated GST Fusion Protein

Human CD44 standard isoform cDNA (Stamenkovic et al., EMBO J 1991; 10: 343-8) was used to PCR amplify the hyaluronic acid binding domain, covering amino acids 21-132 (SEQ ID NO: 2), with the oligonucleotides 5'CGCGAATTCCAGATCGATTTGAATATG 3' (SEQ ID NO: 13) (containing internal EcoR1 cleavage site) and 5'CGCGAGCTCCTTCTAACATGTAGTCAG 3' (SEQ ID NO: 14) (containing internal Sac1 cleavage site). The resulting PCR amplification product was cloned into a pGEX-KG vector (Guan and Dixon, Anal Biochem 1991; 192: 262-7). Generation of CD44HABD hyaluronic acid non-binding mutant was performed by site-directed mutagenesis according to the manufacurer's protocol (Quickchange.RTM., Stratagene). Mutagenic oligo pairs:

```
For R41A
                                    (SEQ ID NO: 15)
(5'GAGAAAAATGGTGCCTACAGCATCTCTCGG-3'
and
                                    (SEQ ID NO: 16)
5'AGATGCTGTAGGCACCATTTTTCTCCACG-3',
For R78SY79S
                                    (SEQ ID NO: 17)
(5'GACCTGCAGCTCTGGGTTCATAG 3',
and
                                    (SEQ ID NO: 18)
5'ATGAACCCAGAGCTGCAGGTCTC 3'
```

were used for introduction of R41A and R78S, Y79S mutations respectively into wild type CD44HABD.

Chicken CAM and dog liver RNA were purified from the respective tissues using RNAqueous kit from Ambion (Austin Tex.) according to manufacturers specifications. CDNAs encoding chicken and dog CD44HABD were obtained by RT-PCR with primers specific to nucleotides 63-81 (SEQ ID NO: 4) and 359-330 (SEQ ID NO:6) of CD44 from the respective species. The primer pairs were as follows:

```
For chicken:
5'-CAGAGACACAATTCAATATA-3',    (SEQ ID NO: 19)
and

5'-TTGGCTCACATGCTTTG-3'        (SEQ ID NO: 20)

Fr dog:
5'-CGCAGATCGATTTGAACATA-3',    (SEQ ID NO: 21)
and

5'-CCGATGTACAATCCTCTTC-3'.     (SEQ ID NO: 22)
```

The cDNAs corresponding to SEQ ID NO: 3 (dog) and SEQ ID NO: 5 (chicken) were cloned into bacterial expression vector pET15b (Novagen) that expresses proteins in *E. coli* as fusions with His-tag. Wild type and R41A, R78S, Y79S mutant GST-CD44HABD expression was induced in *E. coli* BL21 strain at 27° C. with 1 mM IPTG at OD_{600}=0.7 and purified using glutathione agarose beads (Sigma) according to manufacture's protocol. The resulting protein was essentially pure as detected by Coomassie Brilliant Blue staining of the preparation separated by SDS polyacrylamide electrophoresis (FIG. **1**). Chicken and dog CD44HABD were purified using the HICAM Resin (Sigma) according to manufacturer's protocol. The resulting protein was also essentially pure and free of contaminants as judged by Coomassie Brilliant Blue staining of SDS-polyacrylamide gels.

As is indicated already above, bacterially expressed proteins lack any posttranslational modifications and accordingly the putative N-linked glycosylation sites of CD44HABD are non-glycosylated in the recombinant protein as produced under this example and used in all the following examples.

Example 2

Recombinant Wild-Type but not Mutant CD44HABD can Bind Hyaluronic Acid (HA) in Dose-Dependent manner and can Inhibit Haptotaxis of Human Aortic Endothelial Cells (HAEC) Towards HA

High molecular weight hyaluronic acid at 1 mg ml^{-1} (Sigma) in PBS was used to coat Maxisorp (Nunc) plates overnight at room temperature (RT). Wells were washed with PBS and blocked with 2% BSA for 2 h at RT. Purified proteins diluted in PBS were added to the wells and incubated 1 h at RT. After three times washing with PBS-T, mouse anti GST antibody B-14 (Santa Cruz Biotechnology) was incubated 1 h at RT before further washing and 1 h incubation at RT with HRP-conjugated goat anti mouse secondary antibody (Dako). HA binding was visualized by with OPD chromogenic substrate (Sigma) and absorbance was read at 450 nm. As shown in FIG. **2**A, wild type but not mutant CD44 fusion proteins bind HA in a concentration dependent manner.

Human aortic endothelial cells (HAEC) were obtained from Clonetics and grown in EBM-2 media (Clonetics) supplemented with 10% FCS, 2 μg ml^{-1} mouse EGF (Sigma) and 50 μg ml^{-1} gentamycin. Cell migration assay was performed in Transwell migration chambers (pore size 8 mm; Costar). Lower compartment of chambers contained 1 μg ml^{-1} high molecular weight hyaluronic acid (Sigma). CD44HABD, CD44HABD^{R41A} or GST (10 μg ml^{-1}) was added to the lower compartment. For antibody inhibition assay, cells were preincubated 30 min with 10 μg ml^{-1} anti CD44 mAb A3 (Guo et al., 1993, 1994). Aortic endothelial cells were added to the upper compartment of the Transwell chamber and allowed to migrate to the underside of the membrane for 2.5 h. The migrated cells were fixed and stained with 0.5% crystal violet. After washing membranes were dried and bound dye was eluted with 10% acetic acid. Optical density of recovered elute was spectrophotometrically read at 600 nm. The results shown in FIG. **2**B demonstrate that wild type CD44HABD but not respective non-HA-binding R41A mutant, inhibited human aortic endothelial cell migration towards HA whereas migration was also inhibited by antibody that specifically blocks CD44 binding to HA (A3).

Example 3

Recombinant CD44 Fusion Proteins Block Angiogenesis in Chick Cam Independent on HA-Binding

10-day-old chick embryos were prepared as described in [Brooks et al., J Clin Invest 1995; 96: 1815-22]. For angiogenesis assay, filter discs soaked with 100 ng ml^{-1} VEGF (Sigma), 100 ng ml^{-1} TGFα (Sigma) or 1 μg ml^{-1} bFGF (Gibco Lifetech) were placed on CAMs, followed by daily ectopical addition of 10 μg of CD44HABD, CD44HABD^{R41AR78SY79S} or GST and PBS as controls (n=6 per group). After 72 h, filter discs and the surrounding CAM tissue were dissected and angiogenesis quantified in a dissection microscope. Angiogenesis was assessed as the number of blood vessel branch points within the CAM area directly under the filter discs.

GST-CD44HABD and GST-CD44HABD^{R41AR78SY79S} but not GST treatment completely abolished the angiogenic effect of VEGF, bFGF or TGFα (FIG. **3***a-d*), indicating that soluble CD44HABD blocks angiogenesis induced by three distinct angiogenic factors and this inhibition is independent on HA binding since HA non-binding mutants were equally effective in inhibiting angiogenesis.

Example 4

Recombinant CD44HABD Proteins Block the Growth of Different Tumor Cell Lines on Chick Cam Independent of HA-Binding Capacity

SMMU-1 human melanoma cells were originally isolated from primary tumor and is CD44-negative (Guo et al., Cancer Res 1994; 54: 1561-5). HepG2 human hepato-cellular carcinoma was grown in RPMI1640 containing 10% fetal bovine serum and 50 mg ml^{-1} ginomycin. SMMU-1-cells and M21 cells were grown in DMEM containing 10% fetal bovine serum and 50 μg ml^{-1} gentamycin. The cells were detached from the plates by trypsinization and 1 million cells were seeded onto the CAMS of 10-day old chicken embryos. The tumors were treated every two days with 10 μg of the fusion protein of either human or chicken origin in 100 μl of PBS or with vehicle alone. 7 days later the tumors were resected and the wet mass was determined. As shown in FIG. **4** the tumor growth of all tested tumor cell lines was inhibited significantly by HA-binding wild type as well as by HA-nonbinding mutated CD44HADB.

Example 5

Recombinant CD44 Fusion Proteins Inhibit Tumor Growth in Nude Mice Independent of HA-Binding Capacity

1×10^6 SMMU-1 cells were injected subcutaneously into backs of 6-week old female BALB/cABom nude mice (M&B). Next day mice were injected subcutaneously proximal to the tumor with 2.4 mg kg^{-1} of body weight of GST-CD44HABD, GST-CD44HABD^{R41AR78SY79S} or GST alone in 100 μl PBS. The treatment was repeated every second day and animals were sacrificed after two weeks, tumors dissected and analyzed for weight and prepared for tissue analysis. Subcutaneous treatment of mice with CD44HABD or non-HA-binding mutant CD44HABD^{R41AR78SY79S} significantly reduced tumor growth when compared to GST-treated controls (FIG. **5***a, c*, P<0.05 at all time points). At day 16, when mice were sacrificed, CD44HABD and CD44HABD^{R41AR78SY79S} treated mice had in average 45% smaller tumor burden (47% and 43% respectively) than GST-treated mice (FIG. **5***b*).

For immunohistochemical analysis, 4 μm thick tissue sections were cut from formalin fixed and paraffin embedded SMMU-1 tumors of similar size. Blood vessel staining on tissue sections was performed using goat anti-mouse PECAM-1 (Santa Cruz Biotech) primary antibody and primary antibody binding was detected by alkaline phosphatase conjugated anti-goat secondary antibodies and developed using Vectastain kit (Vector Laboratories). Immunohistochemical analysis of tumors by staining for PECAM-1 positive blood vessels showed that CD44HABD and CD44HABD^{R41AR78SY79} treated tumors were also less vascularized at the tumor border (FIG. **5***d*).

Example 6

Recombinant Non-Glycosylated CD44HABD^{R41AR78SY79} (CD44-3MUT) Affects on Xenograted Human Tumors

Hep3b cells (3.5×10^6) were injected subcutaneously into Foxn1 athymic nude mice. Intraperitoneal treatment with drugs started on day 14 post inoculation when the average tumor volume reached 150 mm^3. Administration of 10 μg of CD44-3MUT 3 times a week decreases tumor growth significantly. Results on are shown in FIG. **9**. (FIG. **1** OF THE REPORT) Administration of CD44-3MUT in the range of 2-50 μg/mouse (0.1-2.5 mg/kg) inhibits tumor growth in dose-dependent manner.

We have also shown that CD44-3MUT effect on tumor growth is dose-dependent regardless of the method of administration. FIG. **9** shows the results when the protein was administered intraperitoneal but there were no significant differences when the administration was intravenous (results not shown).

Taken into account that CD44-3MUT is a protein of small size that has relatively short clearance kinetics we have also used constant drug administration using intraperitoneal micro-osmotic pumps over the period of 14 days. Such administration routine gives consistent level of CD44-3MUT and might improve the anti-angiogenic and anti-tumour efficacy. We have shown that CD44-3MUT administrated using micro-osmotic pump giving the dose of 1 μg/mouse/day inhibits tumor growth significantly and more effectively than the same dose administrated intraperitoneally (FIG. **10**).

Example 7

CD44HABD^{R41AR78SY79} (CD44-3MUT) Affects the Growth of Blood Vessels as Tested in Ex Vivo Chick Aortic Assay

The inhibitory effect of CD44-3MUT to the growth of blood vessels was confirmed also in ex vivo chick aortic ring assay. Results are shown in FIG. **11**. In this system, aortic rings cultured in collagen gel give rise to micro vascular networks composed of branching endothelial channels. By using intact vascular explants, it reproduces more accurately the environment in which angiogenesis takes place than those with isolated endothelial cells. The growth of blood vessels from chicken embryo aortic ring embedded into collagen-I gel was induced by VEGF according to the used method (Auerbach et al., 2003; Clinical Chem. 49:1; 32-40) and test proteins were added directly into the growth matrix. Significant reduction of VEGF induced angiogenesis after CD44-3MUT treatment was observed.

Example 8

CD44-HABD Fusion Proteins Inhibit the Growth of Human Pancreatic Cancer also in Nude Mice Independent of HA-Binding Capacity

1×10^6 BxPC-3 (ATCC, Manassas, Va.) cells were injected subcutaneously into backs of 6-8 week old female BALB/cABom nude mice (M&B, Ry, Denmark). When tumor nodules appeared mice started to receive by subcutaneous injections proximal to the tumor 20 μg (BxPC-3) or 50 μg (SMMU-1) of GST-CD44HABD, GST-CD44HABD^{R41AR78SY79S} or GST in 100 μl PBS. The treatment was repeated in every second day and animals were sacrificed when most of control tumors reached 25 mm in diameter. Tumor volume was calculated using formula (Width$^2\times$Length)$\times$0.52. At the end of experiment tumors were dissected out, analyzed for weight and prepared for tissue analysis. BxPC-3 cells gave rise to slowly growing tumors. The GST-treated controls reached the average weight of 0.267+/−0.042 g at day 52 when mice were sacrificed (FIG. **2***d-g*). The treatment of mice with GST-CD44HABD or GST-CD44HABD^{R41AR78SY79S} significantly inhibited BxPC-3 tumor growth reducing the average tumor weight by 60% (0.108+/−0.028 g) and 70% (0.085+/−0.017 g) compared to control, respectively ($P<0.05$; $n=6$). Results are shown in FIG. **6**.

Example 9

CD44-3MUT Treatment is as Efficient as Anti-VEGF Therapy

We have also compared the effects of CD44-3MUT and anti-VEGF antibody (Avastin, bevacizumab, Roche). Avastin is an approved angiogenesis inhibitor. It is, in combination with intravenous 5-fluorouracil-based chemotherapy, indicated for first- or second-line treatment of patients with metastatic carcinoma of the colon or rectum. In combination with carboplatin and paclitaxel, is indicated for first-line treatment of patients with unrespectable, locally advanced, recurrent or metastatic non-squamous, non-small cell lung cancer. In combination with paclitaxel Avastin is indicated for the treatment of patients who have not received chemotherapy for metastatic HER2-negative breast cancer.

It has been shown in animal model that Avastin inhibits grafted human tumor growth in mice also as a monotherapy. We compared Avastin efficacy with efficacy of CD44-3MUT. The experimental conditions were similar to those shown in Example 6. As is shown in FIG. **12** CD44-3MUT treatment gives similar effect compared to anti-VEGF therapy.

Example 9

Recombinant CD44HABD Inhibits Specifically Endothelial Cell Proliferation In Vitro and Blocks Endothelial Cell Cycle

For cell cycle analysis exponentially growing primary human vascular endothelial cells (HUVEC), cow pulmonary arterial endothelial (CPAE) cells, primary human fibroblasts (NHDF), MCF-7 or SMMU1 cells were incubated 48 h in the presence of 30 μg ml^{-1} GST-CD44HABD, GST-CD44HABD^{R41AR78SY79S}, GST or PBS. Cells were pulsed with 30 μg ml^{-1} bromodeoxyuridine (BrdU) for 60 min, harvested and fixed in ice-cold ethanol. Cells were then stained for BrdU with anti-BrdU mAb G3G4 (Developmental Studies Hybridoma Bank, University of Iowa, Iowa) diluted 1:50 followed by fluorescein isothiocyanate-conjugated goat anti-mouse antibody (Jackson Immunoresearch, West Grove, Pa.) in parallel with staining with propidium iodide. The cell cycle distribution was then analyzed with a FACScan Flow Cytometer (Becton Dickinson, Franklin Lakes, N.J.).

Human vascular endothelial cells and cow pulmonary arterial endothelial cells exposed to GST-CD44HABD or GST-CD44HABD$^{R41AR78SY79-S}$ displayed a markedly reduced amount of cells in S-phase (5% and 6%, respectively) as compared to control treated cells (25%; FIG. **7**D). Furthermore, CD44HABD had no significant effect on the cell cycle of primary human fibroblasts (NHDF) or on any of the tumor cells tested, suggesting that cell cycle inhibition by CD44HABD is specific for endothelial cells.

Example 10

Characterization of CD44-3MUT (CD44HABD^{R41AR78SY79S})

We tested cellular binding of CD44-3MUT on different endothelial, lymphoid and tumor cell lines to characterize it's cell-type specificity and to obtain an estimate of it's equilibrium dissociation constant (Kd) and maximum number of binding sites (Bmax).

For binding assays we used Hep3B human hepatocellular carcinoma, MCF-7 human breast adenocarcinoma, COS-1 African green monkey kidney fibroblasts, cow pulmonary artery endothelial cells (CPAE), human umbilical vein endothelial cells (HUVEC), RAMOS and RAJI human Burkitt's lymphoma cells, and THP-1 human monocytic leukemia cell lines. Saturation binding experiments were done by incubating cells with different concentrations of 125I-labeled CD44-3MUT. Nonspecific binding was defined by the addition of excess nonradioactive CD44-3MUT into reaction. To test whether cellular binding of CD44-3MUT is mediated via hyaluronic acid, we treated cells in some experiments with hyaluronidase to destroy possible binding sites. Bound radioactivity was quantified using γ-counter. Specific and nonspecific binding was analyzed using simultaneous nonlinear curve fitting function in GraphPad Prism 4/5 software.

We found that HUVEC binds 125I-CD44-3MUT with average Kd 146±72 nM and Bmax 0.028±0.019 fmol/cell (n=15; mean±SD). Ramos lymphoma cells bound 125I-CD44-3MUT with average Kd 54±22 nM (FIG. **13**A, Table 1). We tested also wild type 125I-CD44-HABD binding to HUVEC treated with hyaluronidase or left untreated. 125I-CD44-HABD bound to HUVEC with average Kd 82±28 nM (n=3) (FIG. **13**B,C). Whereas hyaluronidase treatment of HUVEC had no significant effect on 125I-CD44-3MUT binding yielding Kd 188±38 nM and Bmax 0.039±0.022 fmol/cell (n=4) (FIGS. **13**B and C). Interestingly, CD44-3MUT has up to 10 times more binding sites on HUVEC than wt CD44-HABD.

TABLE 1

125I-CD44-3MUT cellular binding

	Kd, nM	Bmax, fmol/cell	n[b]	cells origin
Ramos	54 ± 22[a]	0.0198 ± 0.0054	2	Burkitt's lymphoma cells
Raji	140 ± 9	0.0175 ± 6.2E−05	2	Burkitt's lymphoma cells
THP-1	93 ± 19	0.0226 ± 0.0133	5	human myelocytic leukemia
HUVEC	146 ± 72	0.028 ± 0.019	15	human umbilical vein endithelial cells
PC-3	171 ± 62	0.0192 ± 0.0023	2	human prostate adenocarcinoma
COS-1	176 ± 74	0.0305 ± 0.021	5	green monkey kidney fibroblasts
CPAE	185	0.08	1	cow pulmonary artery endothelial cells
MCF-7	422 ± 379	0.095 ± 0.097	2	human breast adenocarcinoma
Hep3B	966 ± 764	0.265 ± 0.19	4	human hepatocellular carcinoma

[a]values shown as mean ± SD.
[b]number of experiments

In addition to HUVEC and Ramos, 125I-CD44-SMUT binds with comparable affinity to other tested cell lines including Raji lymphoma, THP-1 monocytic leukemia, PC-3 prostate carcinoma, COS-1 monkey fibroblasts and CPAE cow aortic endothelial cells (Table 1). Binding to MCF-7 breast carcinoma cells is saturable but with lower affinity, Kd 422±379 nM. 125I-CD44-3MUT binding to Hep3B hepatic carcinoma remained virtually unsaturated.

These results suggest that there is a specific binding site for CD44-3MUT protein on the surface of cells of different origin.

Example 11

CD44-3MUT Does not Bind to VEGF Receptors In Vitro

Results of Example 3 above, show that CD44-3MUT inhibits angiogenesis induced by different growth factors (TGF-alfa, bFGF and VEGF) in chick CAM, suggesting the CD44-3MUT target in angiogenesis inhibition is downstream of these signaling pathways, i.e. CD44-3MUT is not blocking growth factor binding to their receptors. To test the hypothesis we directly measured CD44-3MUT binding to VEGF receptors. VEGF signaling pathway is a well exploited mechanism targeted by many different anti-cancer drugs (e.g. Avastin). We have developed a modified ELISA test (to detect CD44-3MUT binding specificity to isolated recombinant receptors VEGFR1 and VEGFR2). Obtained results indicate that CD44-3MUT does not bind to VEGF receptors in vitro, as does VEGF itself in our assay (FIG. **14**) Therefore the anti-angiogenic effect of CD44-3MUT is most probably not due to direct interference with VEFG-related signal transduction.

Example 12

CD44-3MUT Binds to Activated/Growth Factor Induced Endothelial Cells

Next we examined whether the activation of endothelial cells by VEGF has effect on CD44-3MUT cellular binding. For this, we serum starved HUVEC for 6 h followed by indction with 10 ng/ml VEGF for 30 min. After induction HUVEC were incubated with fluorescence-labeled CD44-3MUT at 4 C. Results show that treatment of endothelial cells with VEGF increases significantly CD44-3MUT bound HUVEC-cells from 26.8%-6.1 to 38%=/−7.9 (P=0.028, two tailed paired t-test, FIG. **15**). This experiment shows that CD44-3MUT binds preferably to activated/growth factor induced endothelial cells, indicating that in physiological context CD44-3MUT will be probably targeted to sites where endothelial cell proliferation and/or migration takes place or where endothelial permeability is changed (e.g. angiogenesis, wound healing, inflammation).

Example 13

CD44-3MUT Inhibits Endothelial Cell Proliferation in a Dose-Dependent Fashion

Exponentially growing HUVE cell populations were treated with respective proteins for 24 h. Cells were double-stained with propidium iodide and BrdU and analyzed by FACS. Results showing that CD44-3MUT treatment inhibits endothelial cell proliferation in a dose-responsive way are depicted in FIG. **16**.

SEQUENCE LISTING

<160> NUMBER OF SEQ ID NOS: 24

<210> SEQ ID NO 1
<211> LENGTH: 336
<212> TYPE: DNA
<213> ORGANISM: Homo sapiens

<400> SEQUENCE: 1

```
cagatcgatt tgaatataac ctgccgcttt gcaggtgtat tccacgtgga gaaaaatggt     60

cgctacagca tctctcggac ggaggccgct gacctctgca aggctttcaa tagcaccttg    120

cccacaatgg cccagatgga gaaagctctg agcatcggat ttgagacctg caggtatggg    180

ttcatagaag ggcatgtggt gattccccgg atccacccca actccatctg tgcagcaaac    240

aacacagggg tgtacatcct cacatacaac acctcccagt atgacacata ttgcttcaat    300

gcttcagctc cacctgaaga agattgtaca tcagtc                              336
```

<210> SEQ ID NO 2
<211> LENGTH: 112
<212> TYPE: PRT
<213> ORGANISM: Homo sapiens
<220> FEATURE:
<221> NAME/KEY: PEPTIDE
<222> LOCATION: (1)..(112)
<223> OTHER INFORMATION: CD44 HABD

<400> SEQUENCE: 2

```
Gly Ile Asp Leu Asn Met Thr Cys Arg Phe Ala Gly Val Phe His Val
1               5                   10                  15

Glu Lys Asn Gly Arg Tyr Ser Ile Ser Arg Thr Glu Ala Ala Asp Leu
            20                  25                  30

Cys Lys Ala Phe Asn Ser Thr Leu Pro Thr Met Ala Gln Met Glu Lys
        35                  40                  45

Ala Leu Ser Ile Gly Phe Glu Thr Cys Arg Tyr Gly Phe Ile Glu Gly
    50                  55                  60

His Val Val Ile Pro Arg Ile His Pro Asn Ser Ile Cys Ala Ala Asn
65                  70                  75                  80

Asn Thr Gly Val Tyr Ile Leu Thr Ser Asn Thr Ser Gln Tyr Asp Thr
                85                  90                  95

Tyr Cys Phe Asn Ala Ser Ala Pro Pro Glu Glu Asp Cys Thr Ser Val
            100                 105                 110
```

<210> SEQ ID NO 3
<211> LENGTH: 336
<212> TYPE: DNA
<213> ORGANISM: Canis familiaris

<400> SEQUENCE: 3

```
cgcagatcga tttgaacata acctgccgct acgcaggtgt gttccatgtg gagaaaaacg     60

gtcgctacag catctccagg acggcggctg ccgacctctg caaggctttc aacagcaccc    120

tgcccaccat ggcccagatg gagcgagccc tgagcgtggg ctttgagacc tgcaggtacg    180

ggttcataga aggacatgtg gtgatccccc gtatccaacc caatgctatt tgtgctgcaa    240

accatacagg ggtgtacatc ctcatatcca acacctccca gtacgacacg tattgcttca    300

atgcttcagc tccacctgaa gaggattgta catcgg                              336
```

<210> SEQ ID NO 4
<211> LENGTH: 112

<212> TYPE: PRT
<213> ORGANISM: Canis familiaris
<220> FEATURE:
<221> NAME/KEY: PEPTIDE
<222> LOCATION: (1)..(112)
<223> OTHER INFORMATION: CD44 HABD

<400> SEQUENCE: 4

```
Gln Ile Asp Leu Asn Ile Thr Cys Arg Tyr Ala Gly Val Phe His Val
1               5                   10                  15

Glu Lys Asn Gly Arg Tyr Ser Ile Ser Arg Thr Ala Ala Ala Asp Leu
            20                  25                  30

Cys Lys Ala Phe Asn Ser Thr Leu Pro Thr Met Ala Gln Met Glu Arg
        35                  40                  45

Ala Leu Ser Val Gly Phe Glu Thr Cys Arg Tyr Gly Phe Ile Glu Gly
    50                  55                  60

His Val Val Ile Pro Arg Ile Gln Pro Asn Ala Ile Cys Ala Ala Asn
65                  70                  75                  80

His Thr Gly Val Tyr Ile Leu Ile Ser Asn Thr Ser Gln Tyr Asp Thr
                85                  90                  95

Tyr Cys Phe Asn Ala Ser Ala Pro Pro Glu Glu Asp Cys Thr Ser Val
            100                 105                 110
```

<210> SEQ ID NO 5
<211> LENGTH: 339
<212> TYPE: DNA
<213> ORGANISM: gallus gallus

<400> SEQUENCE: 5

```
cagagacaca attcaatata acttgcagat atggaggagt gtttcatgtg gagaaaaatg     60

gtcgctacag tctcacacga gctgaagcaa ttgagctctg tagagctctc aatagtacct    120

tggcaacact ggagcaattt gaaagagctc atgcacttgg atttgaaacg tgcaggtatg    180

gttttatagt ggggcatatt gttatcccac gaatcaatcc atatcatctt tgtgcagcaa    240

atcatacagg catttacaaa ctttcagcaa atacaactgg ccggtatgat gcatattgtt    300

acaatgcaac agaaacgagg agcaaagcat gtgagccaa                           339
```

<210> SEQ ID NO 6
<211> LENGTH: 112
<212> TYPE: PRT
<213> ORGANISM: Gallus gallus
<220> FEATURE:
<221> NAME/KEY: PEPTIDE
<222> LOCATION: (1)..(112)
<223> OTHER INFORMATION: CD44HABD

<400> SEQUENCE: 6

```
Glu Thr Gln Phe Asn Ile Thr Cys Arg Tyr Gly Gly Val Phe His Val
1               5                   10                  15

Glu Lys Asn Gly Arg Tyr Ser Leu Thr Arg Ala Glu Ala Ile Glu Leu
            20                  25                  30

Cys Arg Ala Leu Asn Ser Thr Leu Ala Thr Leu Val Gln Phe Glu Arg
        35                  40                  45

Ala His Ala Leu Gly Phe Glu Thr Cys Arg Tyr Gly Phe Ile Val Gly
    50                  55                  60

His Ile Val Ile Pro Arg Ile Asn Pro Tyr His Leu Cys Ala Ala Asn
65                  70                  75                  80

His Thr Gly Ile Tyr Lys Leu Ser Ala Asn Thr Thr Gly Arg Tyr Asp
                85                  90                  95
```

-continued

Ala Tyr Cys Tyr Asn Ala Thr Glu Thr Arg Ser Lys Ala Cys Glu Pro
            100   105   110

<210> SEQ ID NO 7
<211> LENGTH: 336
<212> TYPE: DNA
<213> ORGANISM: Homo sapiens

<400> SEQUENCE: 7

cagatcgatt tgaatataac ctgccgcttt gcaggtgtat tccacgtgga gaaaaatggt 60

gcctacagca tctctcggac ggaggccgct gacctctgca aggctttcaa tagcaccttg 120

cccacaatgg cccagatgga gaaagctctg agcatcggat ttgagacctg caggtatggg 180

ttcatagaag ggcatgtggt gattccccgg atccacccca actccatctg tgcagcaaac 240

aacacagggg tgtacatcct cacatacaac acctcccagt atgacacata ttgcttcaat 300

gcttcagctc cacctgaaga agattgtaca tcagtc 336

<210> SEQ ID NO 8
<211> LENGTH: 112
<212> TYPE: PRT
<213> ORGANISM: Homo sapiens
<220> FEATURE:
<221> NAME/KEY: PEPTIDE
<222> LOCATION: (1)..(112)
<223> OTHER INFORMATION: CD44 HABD mutant

<400> SEQUENCE: 8

Gln Ile Asp Leu Asn Met Thr Cys Arg Phe Ala Gly Val Phe His Val
1   5   10   15

Glu Lys Asn Gly Ala Tyr Ser Ile Ser Arg Thr Glu Ala Ala Asp Leu
            20   25   30

Cys Lys Ala Phe Asn Ser Thr Leu Pro Thr Met Ala Gln Met Glu Lys
        35   40   45

Ala Leu Ser Ile Gly Phe Glu Thr Cys Arg Tyr Gly Phe Ile Glu Gly
    50   55   60

His Val Val Ile Pro Arg Ile His Pro Asn Ser Ile Cys Ala Ala Asn
65   70   75   80

Asn Thr Gly Val Tyr Ile Leu Thr Ser Asn Thr Ser Gln Tyr Asp Thr
                85   90   95

Tyr Cys Phe Asn Ala Ser Ala Pro Pro Glu Glu Asp Cys Thr Ser Val
            100   105   110

<210> SEQ ID NO 9
<211> LENGTH: 336
<212> TYPE: DNA
<213> ORGANISM: homo sapiens

<400> SEQUENCE: 9

cagatcgatt tgaatataac ctgccgcttt gcaggtgtat tccacgtgga gaaaaatggt 60

cgctacagca tctctcggac ggaggccgct gacctctgca aggctttcaa tagcaccttg 120

cccacaatgg cccagatgga gaaagctctg agcatcggat ttgagacctg cagctctggg 180

ttcatagaag ggcatgtggt gattccccgg atccacccca actccatctg tgcagcaaac 240

aacacagggg tgtacatcct cacatacaac acctcccagt atgacacata ttgcttcaat 300

gcttcagctc cacctgaaga agattgtaca tcagtc 336

<210> SEQ ID NO 10
<211> LENGTH: 112
<212> TYPE: PRT

-continued

```
<213> ORGANISM: Homo sapiens
<220> FEATURE:
<221> NAME/KEY: PEPTIDE
<222> LOCATION: (1)..(112)
<223> OTHER INFORMATION: CD44 HABD mutant

<400> SEQUENCE: 10

Gln Ile Asp Leu Asn Met Thr Cys Arg Phe Ala Gly Val Phe His Val
1               5                   10                  15

Glu Lys Asn Gly Arg Tyr Ser Ile Ser Arg Thr Glu Ala Ala Asp Leu
            20                  25                  30

Cys Lys Ala Phe Asn Ser Thr Leu Pro Thr Met Ala Gln Met Glu Lys
        35                  40                  45

Ala Leu Ser Ile Gly Phe Glu Thr Cys Ser Ser Gly Phe Ile Glu Gly
    50                  55                  60

His Val Val Ile Pro Arg Ile His Pro Asn Ser Ile Cys Ala Ala Asn
65                  70                  75                  80

Asn Thr Gly Val Tyr Ile Leu Thr Ser Asn Thr Ser Gln Tyr Asp Thr
                85                  90                  95

Tyr Cys Phe Asn Ala Ser Ala Pro Pro Glu Glu Asp Cys Thr Ser Val
            100                 105                 110


<210> SEQ ID NO 11
<211> LENGTH: 336
<212> TYPE: DNA
<213> ORGANISM: Homo sapiens

<400> SEQUENCE: 11

cagatcgatt tgaatataac ctgccgcttt gcaggtgtat tccacgtgga gaaaaatggt     60

gcctacagca tctctcggac ggaggccgct gacctctgca aggctttcaa tagcaccttg    120

cccacaatgg cccagatgga gaaagctctg agcatcggat ttgagacctg cagctctggg    180

ttcatagaag ggcatgtggt gattccccgg atccacccca actccatctg tgcagcaaac    240

aacacagggg tgtacatcct cacatacaac acctcccagt atgacacata ttgcttcaat    300

gcttcagctc cacctgaaga agattgtaca tcagtc                              336


<210> SEQ ID NO 12
<211> LENGTH: 112
<212> TYPE: PRT
<213> ORGANISM: Homo sapiens
<220> FEATURE:
<221> NAME/KEY: PEPTIDE
<222> LOCATION: (1)..(112)
<223> OTHER INFORMATION: CD44 3-MUT

<400> SEQUENCE: 12

Gln Ile Asp Leu Asn Met Thr Cys Arg Phe Ala Gly Val Phe His Val
1               5                   10                  15

Glu Lys Asn Gly Ala Tyr Ser Ile Ser Arg Thr Glu Ala Ala Asp Leu
            20                  25                  30

Cys Lys Ala Phe Asn Ser Thr Leu Pro Thr Met Ala Gln Met Glu Lys
        35                  40                  45

Ala Leu Ser Ile Gly Phe Glu Thr Cys Ser Ser Gly Phe Ile Glu Gly
    50                  55                  60

His Val Val Ile Pro Arg Ile His Pro Asn Ser Ile Cys Ala Ala Asn
65                  70                  75                  80

Asn Thr Gly Val Tyr Ile Leu Thr Ser Asn Thr Ser Gln Tyr Asp Thr
                85                  90                  95

Tyr Cys Phe Asn Ala Ser Ala Pro Pro Glu Glu Asp Cys Thr Ser Val
```

-continued

100 105 110

<210> SEQ ID NO 13
<211> LENGTH: 27
<212> TYPE: DNA
<213> ORGANISM: artificial
<220> FEATURE:
<223> OTHER INFORMATION: chemically synthesized
<220> FEATURE:
<221> NAME/KEY: misc_feature
<222> LOCATION: (1)..(27)
<223> OTHER INFORMATION: primer

<400> SEQUENCE: 13

cgcgaattcc agatcgattt gaatatg 27

<210> SEQ ID NO 14
<211> LENGTH: 27
<212> TYPE: DNA
<213> ORGANISM: artificial
<220> FEATURE:
<223> OTHER INFORMATION: chemically synthesized
<220> FEATURE:
<221> NAME/KEY: CDS
<222> LOCATION: (1)..(27)
<223> OTHER INFORMATION: primer

<400> SEQUENCE: 14

cgc gag ctc ctt cta aca tgt agt cag 27
Arg Glu Leu Leu Leu Thr Cys Ser Gln
1 5

<210> SEQ ID NO 15
<211> LENGTH: 9
<212> TYPE: PRT
<213> ORGANISM: artificial
<220> FEATURE:
<223> OTHER INFORMATION: Synthetic Construct

<400> SEQUENCE: 15

Arg Glu Leu Leu Leu Thr Cys Ser Gln
1 5

<210> SEQ ID NO 16
<211> LENGTH: 30
<212> TYPE: DNA
<213> ORGANISM: artificial
<220> FEATURE:
<223> OTHER INFORMATION: chemically synthesized
<220> FEATURE:
<221> NAME/KEY: misc_feature
<222> LOCATION: (1)..(30)
<223> OTHER INFORMATION: primer

<400> SEQUENCE: 16

gagaaaaatg gtgcctacag catctctcgg 30

<210> SEQ ID NO 17
<211> LENGTH: 29
<212> TYPE: DNA
<213> ORGANISM: artificial
<220> FEATURE:
<223> OTHER INFORMATION: chemically synthesized
<220> FEATURE:
<221> NAME/KEY: misc_feature
<222> LOCATION: (1)..(29)
<220> FEATURE:
<221> NAME/KEY: misc_feature
<222> LOCATION: (1)..(29)
<223> OTHER INFORMATION: primer

```
<400> SEQUENCE: 17

agatgctgta ggcaccattt ttctccacg                                         29


<210> SEQ ID NO 18
<211> LENGTH: 23
<212> TYPE: DNA
<213> ORGANISM: artificial
<220> FEATURE:
<223> OTHER INFORMATION: chemically synthesized
<220> FEATURE:
<221> NAME/KEY: misc_feature
<222> LOCATION: (1)..(23)
<223> OTHER INFORMATION: primer

<400> SEQUENCE: 18

gacctgcagc tctgggttca tag                                               23


<210> SEQ ID NO 19
<211> LENGTH: 23
<212> TYPE: DNA
<213> ORGANISM: artificial
<220> FEATURE:
<223> OTHER INFORMATION: chemically synthesized
<220> FEATURE:
<221> NAME/KEY: misc_feature
<222> LOCATION: (1)..(23)
<223> OTHER INFORMATION: primer

<400> SEQUENCE: 19

atgaacccag agctgcaggt ctc                                               23


<210> SEQ ID NO 20
<211> LENGTH: 20
<212> TYPE: DNA
<213> ORGANISM: artificial
<220> FEATURE:
<223> OTHER INFORMATION: chemically synthesized
<220> FEATURE:
<221> NAME/KEY: misc_feature
<222> LOCATION: (1)..(20)
<223> OTHER INFORMATION: primer

<400> SEQUENCE: 20

cagagacaca attcaatata                                                   20


<210> SEQ ID NO 21
<211> LENGTH: 17
<212> TYPE: DNA
<213> ORGANISM: artificial
<220> FEATURE:
<223> OTHER INFORMATION: chemically synthesized
<220> FEATURE:
<221> NAME/KEY: misc_feature
<222> LOCATION: (1)..(17)
<223> OTHER INFORMATION: primer

<400> SEQUENCE: 21

ttggctcaca tgctttg                                                      17


<210> SEQ ID NO 22
<211> LENGTH: 20
<212> TYPE: DNA
<213> ORGANISM: artificial
<220> FEATURE:
<223> OTHER INFORMATION: chemically synthesized
<220> FEATURE:
<221> NAME/KEY: misc_feature
<222> LOCATION: (1)..(20)
<223> OTHER INFORMATION: primer
```

```
<400> SEQUENCE: 22

cgcagatcga tttgaacata                                                  20


<210> SEQ ID NO 23
<211> LENGTH: 19
<212> TYPE: DNA
<213> ORGANISM: artificial
<220> FEATURE:
<223> OTHER INFORMATION: chemically synthesized
<220> FEATURE:
<221> NAME/KEY: misc_feature
<222> LOCATION: (1)..(19)
<223> OTHER INFORMATION: primer

<400> SEQUENCE: 23

ccgatgtaca atcctcttc                                                   19


<210> SEQ ID NO 24
<211> LENGTH: 111
<212> TYPE: PRT
<213> ORGANISM: Homo sapiens
<220> FEATURE:
<221> NAME/KEY: PEPTIDE
<222> LOCATION: (1)..(111)
<223> OTHER INFORMATION: CD44 3MUT

<400> SEQUENCE: 24

Gln Ile Asp Leu Asn Met Thr Cys Arg Phe Ala Gly Val Phe His Val
1               5                   10                  15

Glu Leu Asn Gly Ala Tyr Ser Ile Ser Arg Thr Glu Ala Ala Asp Leu
            20                  25                  30

Cys Lys Ala Phe Asn Ser Thr Leu Pro Thr Met Ala Gln Met Glu Lys
        35                  40                  45

Ala Leu Ser Ile Gly Phe Glu Thr Cys Ser Ser Gly Phe Ile Glu Gly
    50                  55                  60

His Val Val Ile Pro Arg Ile His Pro Asn Ser Ile Cys Ala Ala Asn
65                  70                  75                  80

Asn Thr Gly Val Tyr Ile Leu Thr Ser Asn Thr Ser Gln Tyr Asp Thr
                85                  90                  95

Tyr Cys Phe Asn Ala Ser Pro Pro Glu Glu Asp Cys Thr Ser Val
            100                 105                 110
```

What is claimed is:

1. A method for treating states related to the inhibition of angiogenesis and/or endothelial cell proliferation, the method consisting the steps of:

a. expressing non-HA binding variant of CD44-hyaluronic acid binding domain in bacterial cells;

b. purifying the resulting non-glycosylated protein;

c. administering the purified non-glycosylated non-HA-binding variant of CD44-hyaluronic acid binding domain (CD44-HABD) to a patient.

2. The method according to claim **1**, wherein the non-HA binding variant of CD44-HABD has an amino acid sequence selected from the group consisting of SEQ ID NO: 8, SEQ ID NO:10 and SEQ ID NO:12.

3. The method according to claim **1**, wherein the non-HA-binding variant of CD44-hyaluronic acid binding domain (CD44-HABD) is further connected to a fusion protein partner part.

4. The method of claim **1**, wherein the state to be treated is selected from the group consisting of ocular diseases causing blindness or impaired vision, states of chronic inflammation, psoriasis, atherosclerosis, restenosis, cancer growth and metastasis, all forms of cancer diseases and tumors and hemangioma.

5. A method to target endothelial cells by providing a molecule comprising a non-HA binding variant of CD44-hyaluronic acid binding domain expressed in bacterial cells.

6. The method according to claim **5**, wherein the non-HA binding variant of CD44-HABD has an amino acid sequence selected from the group consisting of SEQ ID NO: 8, SEQ ID NO:10 and SEQ ID NO:12.

7. The method according to claim **6**, wherein the molecule further comprises a moiety having chemotherapeutical and/or gene therapeutic properties.

8. The method of claim **1**, wherein the mode of action of the non-HA-binding variant of CD44-hyaluronic acid binding domain (CD44-HABD) is independent of hyaluronic acid.

9. The method of claim **5**, wherein endothelial cell proliferation is inhibited.

10. The method of claim **1**, wherein tumor growth is inhibited.

11. The method of claim **1**, wherein effective amount of the non-HA-binding variant of CD44-hyaluronic acid binding domain is 0.1 -2.5 mg/kg.

12. The method of claim **1**, wherein the molecule is administered orally or parentally.

13. The method of claim **1**, wherein the bacterial cell is *E.coli.*

14. The method of claim **5**, wherein the bacterial cell is *E.coli.*

* * * * *

ACKNOWLEDGEMENTS

This project was conceived and started in Karolinska Institutet, Stockholm, by Priit Kogerman and then moved along myself and my supervisor to Tallinn, to be developed under the roof of different organizations – National Institute of Chemical Physics and Biophysics (KBFI), Tallinn University of Technology, Celecure AS and Competence Center for Cancer Research AS.

I would like thank current and former members of Celecure and Competence Center for Cancer Research project team: Anne Pink, Aili Kallastu, Marianna Školnaja, Marina Turkina, Kati Mädo, Anne Meikas, Annemari Linno and Riin Saarmäe and finally CCCR project leader Andres Valkna.

I am deeply greatful to people from Prof. Priit Kogerman's Tumour Biology group in TUT Department of Gene Technology, biggest thanks to Lagle Kasak and Wally Anderson – for significant contribution to the project, Indrek Tammiste, Alla Piirsoo, Piret Tiigimägi, Robert Tsanev, Piret Michelson, Illar Pata, Pille Pata, Jaak Nairismägi, Kersti Olspert, Lembi Kogerman and Monica Drews. I would like to thank Annica Gad and Staffan Strömblad from Karolinska Institutet.

Warmest thanks my dear Kaie and my daughter Kirke Mari.

SUMMARY

CD44 protein is principal cell surface receptor for HA. CD44 is involved via its HA binding property in lymphocyte rolling on endothelial lining of blood vessels. In tumorigenesis, CD44 high expression in tumor cells contributes to tumor metastasis and associates with worse prognosis in several types of cancer. Nevertheless, in micrometastases, CD44 expression rather inhibits growth and is being transiently downregulated. This finding was compatible with tumor angiogenesis paradigm, stating that tumors cannot growth over 1 mm size in the absence of angiogenesis. Therapeutically this can be exploited to control tumor growth. The current study was undertaken to test hypothesis that CD44 has antiangiogenic function in tumor microenvironment and that soluble HA binding domain of CD44 can be used to control pathological angiogenesis and tumor growth. To this end we purified recombinant CD44 HABD protein and its non-HA binding mutant as control. We tested CD44 HABD proteins in chick CAM angiogesis model and found that, indeed, angiogenesis was suppressed in response to CD44-HABD treatment. However, quite contrary to our original hypothesis, this effect was not dependent on HA binding property of CD44, as the CD44-protein with the mutated HA binding site (CD44-3MUT) was equally effective in this assay. Further tests of these proteins effect in tumor xenograft model in mice showed that they were also able to suppress sc tumor growth and confirmed that such result was not dependent on HA binding by CD44. Cellular mechanism of antiangiogenic effect by CD44-HABD and CD44-3MUT is based on inhibition of endothelial cell proliferation. CD44 proteins bind to endothelial cells via direct interaction with cell-surface exposed intermediate filament protein vimentin and become endocytosed. Soluble CD44 is physiologically present in circulation and its concentration is increased during inflammatory reactions. In Cd44 knockout mice the response and duration to vasoactive challenge is significantly increased, suggesting that endothelium is less restricted when stimulated. The molecular mechanism of this phenomenon is currently not clear. However, we propose that the physiological role of soluble CD44 might include balancing of endothelial cell responses to stimulation. Whether this holds true and by which extent this function is mediated by vimentin remains to be elucidated. Further, we hypothesize that recombinant soluble CD44 specific binding and endocytosis by endothelial cells regulates plasma membrane dynamics and/or availability of growth factor receptors, resulting in suppressed endothelial proliferation and angiogenesis.

KOKKUVÕTE

CD44 valk on peamine rakupinna hüaluroonhappe retseptor ja sellest lähtuvalt on üheks tema funktsiooniks võimaldada lümfotsüütide veeremist veresoonte seinal. CD44-le on iseloomulik geeni kümnest alternatiivsest eksonist pärit valgujärjestuste lisamine rakuvälisesse domeeni. Alternatiivsed eksonid annavad CD44-le struktuurse ja funktsionaalse mitmekesisuse, selliseid eksoneid sisaldavaid CD44 valke nimetatakse *variaabliteks isovormideks*. Funktsionaalne mitmekesisus on tingitud alternatiivsetele eksonitele lisatavatest suhkrujääkidest, mis näiteks seovad kasvufaktoreid ja seeläbi vahendavad kasvufaktorite esitlemist nende retseptoritele või sisaldavad erilisi suhkrujärjestusi, millele saavad seostuda lümfotsüütide adhesiooniretseptorid selektiinid. CD44 valgu vormi, mis ei sisalda alternatiivseid eksoneid, nimetatakse *standardseks isovormiks*. Standardse CD44 valgu rohkus kasvajarakkude pinnal soodustab kasvaja metastaaside teket ja on mitme vähivormi puhul seotud haiguse halvema prognoosiga. Siiski, meie varasemad katsetulemused näitasid, et mikrometastaasides standardse CD44 ekspressioon pärsitakse ajutiselt. Seetõttu järeldasime, et mikrometastaasides standardne CD44 pigem pidurdab nende kasvu. See leid on kooskõlas kasvaja angiogeneesi paradigmaga, mille kohaselt tahked kasvajad ei saa areneda üle 1 mm suuruse ilma angiogeneesi ehk veresoonte kasvu initsieerimata. Terapeutiliselt kasutatakse seda ära, et pidurdada vähkkasvaja suurenemist ja siirete moodustmist. Käesolev uuring viidi läbi testimaks hüpoteesi, et CD44 hüaluroonhappe retseptor omab angiogeneesi alla suruvat toimet kasvaja mikrokeskkonnas ja et rekombinantset CD44 hüaluroonhapet siduvat domääni saab kasutada patoloogilise angiogeneesi ja vähi kasvu pidurdamiseks. Sellel eesmärgil tootsime me rekombinantse CD44-HABD valgu ja kontrolliks selle hüaluroonhapet mittesiduva mutantse vormi (CD44-3MUT). Me testisime neid CD44-HABD valke kana embrüo lootemembraani angiogeneesi katses ja leidsime, et tõepoolest, need valgud surusid angiogeneesi alla. Kuid vastupidiselt meie algsele hüpoteesile ei sõltunud see efekt hüaluroonhappe sidumise funktsioonist, sest muteeritud hüaluroonhappe sidumiskohaga valk toimis sama tõhusalt. Edasised katsed nende valkudega kasvaja ksenografti mudelitega hiirtes näitasid, et nad suutsid pidurdada ka vähi kasvu. Lisaks kinnitasid ka ksenografti mudeli tulemused, et efekt ei sõltunud hüaluroonhappe sidumise funktsioonist. Angiogeneesi vastase efekti rakuline mehhanism põhineb arvatavasti endoteelirakkude jagunemise pärssimisel. CD44 valgud seostusid endoteelirakkudele ja endotsüteeriti. Me identifitseerisime valgu, mis vahendab lahustuva CD44 rakkudele seostumist ja endotsütoosi, milleks osutus raku tsütoskeleti vahepealsete filamentide valk vimentiin. Vimentiini olulisusele lahustuvate CD44 valkude rakku sisenemisel viitab ka see, et vimentiini *knockout* hiirtest eraldatud endoteelirakkudel oli lahustuva CD44 endotsütoos pärsitud. Lisaks on teiste uurimisgruppide poolt näidatud, et vimentiin on spetsiifiliselt üles reguleeritud jagunevates vähi veresoontes. Lahustuv CD44 valk esineb vereringes füsioloogiliselt ning tema hulk veres tõuseb näiteks krooniliste põletike korral. Cd44 geeni *knockout* hiirte veresooned vastavad märksa suurema amplituudiga veresooni stimuleerivatele signaalidele, viidates CD44 pidurdavale rollile vaskulaarse aktiivsuse kontrollis. Kokkuvõttes me oletame, et meie poolt kasutatav rekombinantse lahustuva CD44 seostumine ja endotsütoos endoteelirakkude poolt mõjutab raku membraanis näiteks veresoonte kasvufaktorite retseptorite kättesaadavust stimuleerimisele.

CURRICULUM VITAE

Personal data

Name:	Taavi Päll
Date and place of birth:	5. January 1974, Tartu, Estonia
Address:	Competence Centre for Cancer Research, Akadeemia tee 15 12618, Tallinn
Phone:	+372 620 4362
Email:	taavi.pall@vtak.ee
Skype:	tapa741

Education

1999 – 2013	Tallinn University of Technology, Department of Gene Technology, PhD student
1999 – 2002	Karolinska Institutet, Stockholm, Sweden, Department of Microbiology, Pathology and Immunology, visiting student
1996 – 1998	University of Tartu, Institute of Molecular and Cell Biology, MSc
1992 – 1996	University of Tartu, Faculty of Biology and Geography, BSc
1992	Tartu Secondary School No. 12

Professional employment

2008 – ...	sen. researcher, Competence Centre for Cancer Research, Tallinn, Estonia
2005 – 2011	researcher, Tallinn University of Technology, Department of Gene Technology
2005 – 2008	project manager, Competence Centre for Cancer Research
1999 – 2005	researcher, National Institute of Physics and Biophysics, Tallinn, Estonia

Supervised theses

Marianna Školnaja, 2013, MSc, "Pharmacokinetic characterization of CD44-protein based drug candidates"

Anne Pink, 2007, MSc, "Discovery and characterization of interaction between CD44 Hyaluronan binding domain and vimentin"

Wally Anderson, 2007, MSc, "The effects of CD44-based angiogenesis inhibitor on endothelial cell signaling pathways"

Anne Pink, 2005, BSc, "Mapping of matrix metalloproteinase 9 CD44 binding domain"

Wally Anderson, 2003, BSc, "Matrix metalloproteinase 9 binds CD44 hyaluronan binding domain"

Publications

1. Päll, Taavi (2013). Vimentin Mechanisms on Endothelial Migration . Ramon Andrade de Mello (Oncology Portuguese Institute of Porto Francisco Gentil, Department of Medic (Editor). Vimentin Concepts and Molecular Mechanisms (81 - 96). Nova Science Publishers

2. Päll, Taavi; Pink, Anne; Kasak, Lagle; Turkina, Marina; Anderson, Wally; Valkna, Andres; Kogerman, Priit (2011). Soluble CD44 Interacts with Intermediate Filament Protein Vimentin on Endothelial Cell Surface. PLoS ONE, 6(12), e29305

3. Päll, T.; Gad, A.; Kasak, L.; Drews, M.; Strömblad, S.; Kogerman, P (2004). Recombinant CD44-HABD is a novel and potent direct angiogenesis inhibitor enforcing endothelial cell-specific growth inhibition independently of hyaluronic acid binding. Oncogene, 23(47), 7874 - 7881.

Patents

1. Drug for treating states related to the inhibition of angiogenesis and/or endothelial cell proliferation; Owner: Celecure AS; Authors: Priit Kogerman, Taavi Päll, Staffan Strömblad; Priority number: US12/660/886; Priority date: 05.03.2010
2. Novel inhibitor of angiogenesis; Owner: Celecure AS; Authors: Taavi Päll, Wally Anderson, Lagle Kasak, Anne Pink, Aire Allikas, Andres Valkna; Priority number: US60/949518; Priority date: 13.07.2007
3. New angiogenesis inhibitors based on soluble CD44 receptor hyaluronic acid binding domain (New Drug); Owner: Celecure AS, Angitia AB; Authors: Priit Kogerman, Taavi Päll, Staffan Strömblad; Priority number: SE20010002823; US20010314971P; Priority date: 24.08.2001

ELULOOKIRJELDUS

Isikuandmed

Name:	Taavi Päll
Sünniaeg ja -koht:	5. jaanuar 1974, Tartu
Aadress:	Vähiuuringute Tehnoloogia Arenduskeskus, Akadeemia tee 15 12618, Tallinn
Telefon:	+372 620 4362
E-post:	taavi.pall@vtak.ee
Skype:	tapa741

Hariduskäik

1999 – 2013	Tallinna Tehnikaülikool, Geenitehnoloogia instituut, doktorant
1999 – 2002	Karolinska Institutet, Stockholm, Rootsi, Department of Microbiology, Pathology and Immunology, külalistudeng
1996 – 1998	Tartu Ülikool, Molekulaar- ja rakubioloogia instituut, MSc
1992 – 1996	Tartu Ülikool, Bioloogia-geograafia teaduskond, BSc
1992	Tartu 12. Keskkool

Teenistuskäik

2008 – ...	vanemteadur, Vähiuuringute Tehnoloogia Arenduskeskus, Tallinn
2005 – 2011	teadur, Tallinna Tehnikaülikool, Geenitehnoloogia instituut
2005 – 2008	projektijuhi abi, Vähiuuringute Tehnoloogia Arenduskeskus
1999 – 2005	teadur, Keemilise ja Bioloogilise Füüsika Instituut, Tallinn

Juhendamisel kaitstud lõputööd

Marianna Školnaja, 2013, MSc, "CD44-valgul põhinevate ravimikandidaatide farmakokineetiliste parameetrite määramine"
Anne Pink, 2007, MSc, "CD44 hüaluroonhapet siduva domeeni ja vimentiini interaktsiooni tuvastamine ning iseloomustamine"
Wally Anderson,2007, MSc, "CD44 valgul põhineva angiogeneesi inhibiitori toime endoteelirakkude signaaliradadele"
Anne Pink, 2005, BSc, "Maatriks metalloproteaas-9 CD44 retseptorile seonduva domeeni kaardistamine"
Wally Anderson, 2003, BSc, "MMP-9 seondub CD44 hüaluroonhapet siduvale domäänile"

Publikatsioonid

1. Päll, Taavi (2013). Vimentin Mechanisms on Endothelial Migration . Ramon Andrade de Mello (Oncology Portuguese Institute of Porto Francisco Gentil, Department of Medic (Toim.). Vimentin Concepts and Molecular Mechanisms (81 - 96). Nova Science Publishers

2. Päll, Taavi; Pink, Anne; Kasak, Lagle; Turkina, Marina; Anderson, Wally; Valkna, Andres; Kogerman, Priit (2011). Soluble CD44 Interacts with Intermediate Filament Protein Vimentin on Endothelial Cell Surface. PLoS ONE, 6(12), e29305

3. Päll, T.; Gad, A.; Kasak, L.; Drews, M.; Strömblad, S.; Kogerman, P (2004). Recombinant CD44-HABD is a novel and potent direct angiogenesis inhibitor enforcing endothelial cell-specific growth inhibition independently of hyaluronic acid binding. Oncogene, 23(47), 7874 - 7881.

Patentsed leiutised

1. Drug for treating states related to the inhibition of angiogenesis and/or endothelial cell proliferation; Omanik: Celecure AS; Autorid: Priit Kogerman, Taavi Päll, Staffan Strömblad; Prioriteedinumber: US12/660/886; Prioriteedikuupäev: 05.03.2010
2. Novel inhibitor of angiogenesis; Omanik: Celecure AS; Autorid: Taavi Päll, Wally Anderson, Lagle Kasak, Anne Pink, Aire Allikas, Andres Valkna; Prioriteedinumber: US60/949518; Prioriteedikuupäev: 13.07.2007
3. New angiogenesis inhibitors based on soluble CD44 receptor hyaluronic acid binding domain (New Drug); Omanik: Celecure AS, Angitia AB; Autorid: Priit Kogerman, Taavi Päll, Staffan Strömblad; Prioriteedinumber: SE20010002823; US20010314971P; Prioriteedikuupäev: 24.08.2001

DISSERTATIONS DEFENDED AT TALLINN UNIVERSITY OF TECHNOLOGY ON NATURAL AND EXACT SCIENCES

1. Olav Kongas. Nonlinear Dynamics in Modeling Cardiac Arrhytmias. 1998.
2. Kalju Vanatalu. Optimization of Processes of Microbial Biosynthesis of Isotopically Labeled Biomolecules and Their Complexes. 1999.
3. Ahto Buldas. An Algebraic Approach to the Structure of Graphs. 1999.
4. Monika Drews. A Metabolic Study of Insect Cells in Batch and Continuous Culture: Application of Chemostat and Turbidostat to the Production of Recombinant Proteins. 1999.
5. Eola Valdre. Endothelial-Specific Regulation of Vessel Formation: Role of Receptor Tyrosine Kinases. 2000.
6. Kalju Lott. Doping and Defect Thermodynamic Equilibrium in ZnS. 2000.
7. Reet Koljak. Novel Fatty Acid Dioxygenases from the Corals Plexaura homomalla and Gersemia fruticosa. 2001.
8. Anne Paju. Asymmetric oxidation of Prochiral and Racemic Ketones by Using Sharpless Catalyst. 2001.
9. Marko Vendelin. Cardiac Mechanoenergetics in silico. 2001.
10. Pearu Peterson. Multi-Soliton Interactions and the Inverse Problem of Wave Crest. 2001.
11. Anne Menert. Microcalorimetry of Anaerobic Digestion. 2001.
12. Toomas Tiivel. The Role of the Mitochondrial Outer Membrane in in vivo Regulation of Respiration in Normal Heart and Skeletal Muscle Cell. 2002.
13. Olle Hints. Ordovician Scolecodonts of Estonia and Neighbouring Areas: Taxonomy, Distribution, Palaeoecology, and Application. 2002.
14. Jaak Nõlvak. Chitinozoan Biostratigrapy in the Ordovician of Baltoscandia. 2002.
15. Liivi Kluge. On Algebraic Structure of Pre-Operad. 2002.
16. Jaanus Lass. Biosignal Interpretation: Study of Cardiac Arrhytmias and Electromagnetic Field Effects on Human Nervous System. 2002.
17. Janek Peterson. Synthesis, Structural Characterization and Modification of PAMAM Dendrimers. 2002.
18. Merike Vaher. Room Temperature Ionic Liquids as Background Electrolyte Additives in Capillary Electrophoresis. 2002.
19. Valdek Mikli. Electron Microscopy and Image Analysis Study of Powdered Hardmetal Materials and Optoelectronic Thin Films. 2003.
20. Mart Viljus. The Microstructure and Properties of Fine-Grained Cermets. 2003.
21. Signe Kask. Identification and Characterization of Dairy-Related Lactobacillus. 2003.
22. Tiiu-Mai Laht. Influence of Microstructure of the Curd on Enzymatic and Microbiological Processes in Swiss-Type Cheese. 2003.

23. Anne Kuusksalu. 2-5A Synthetase in the Marine Sponge Geodia cydonium. 2003.
24. Sergei Bereznev. Solar Cells Based on Polycristalline Copper-Indium Chalcogenides and Conductive Polymers. 2003.
25. Kadri Kriis. Asymmetric Synthesis of C2-Symmetric Bimorpholines and Their Application as Chiral Ligands in the Transfer Hydrogenation of Aromatic Ketones. 2004.
26. Jekaterina Reut. Polypyrrole Coatings on Conducting and Insulating Substracts. 2004.
27. Sven Nõmm. Realization and Identification of Discrete-Time Nonlinear Systems. 2004.
28. Olga Kijatkina. Deposition of Copper Indium Disulphide Films by Chemical Spray Pyrolysis. 2004.
29. Gert Tamberg. On Sampling Operators Defined by Rogosinski, Hann and Blackman Windows. 2004.
30. Monika Übner. Interaction of Humic Substances with Metal Cations. 2004.
31. Kaarel Adamberg. Growth Characteristics of Non-Starter Lactic Acid Bacteria from Cheese. 2004.
32. Imre Vallikivi. Lipase-Catalysed Reactions of Prostaglandins. 2004.
33. Merike Peld. Substituted Apatites as Sorbents for Heavy Metals. 2005.
34. Vitali Syritski. Study of Synthesis and Redox Switching of Polypyrrole and Poly(3,4-ethylenedioxythiophene) by Using in-situ Techniques. 2004.
35. Lee Põllumaa. Evaluation of Ecotoxicological Effects Related to Oil Shale Industry. 2004.
36. Riina Aav. Synthesis of 9,11-Secosterols Intermediates. 2005.
37. Andres Braunbrück. Wave Interaction in Weakly Inhomogeneous Materials. 2005.
38. Robert Kitt. Generalised Scale-Invariance in Financial Time Series. 2005.
39. Juss Pavelson. Mesoscale Physical Processes and the Related Impact on the Summer Nutrient Fields and Phytoplankton Blooms in the Western Gulf of Finland. 2005.
40. Olari Ilison. Solitons and Solitary Waves in Media with Higher Order Dispersive and Nonlinear Effects. 2005.
41. Maksim Säkki. Intermittency and Long-Range Structurization of Heart Rate. 2005.
42. Enli Kiipli. Modelling Seawater Chemistry of the East Baltic Basin in the Late Ordovician–Early Silurian. 2005.
43. Igor Golovtsov. Modification of Conductive Properties and Processability of Polyparaphenylene, Polypyrrole and polyaniline. 2005.
44. Katrin Laos. Interaction Between Furcellaran and the Globular Proteins (Bovine Serum Albumin β-Lactoglobulin). 2005.
45. Arvo Mere. Structural and Electrical Properties of Spray Deposited Copper Indium Disulphide Films for Solar Cells. 2006.
46. Sille Ehala. Development and Application of Various On- and Off-Line Analytical Methods for the Analysis of Bioactive Compounds. 2006.

47. Maria Kulp. Capillary Electrophoretic Monitoring of Biochemical Reaction Kinetics. 2006.
48. Anu Aaspõllu. Proteinases from Vipera lebetina Snake Venom Affecting Hemostasis. 2006.
49. Lyudmila Chekulayeva. Photosensitized Inactivation of Tumor Cells by Porphyrins and Chlorins. 2006.
50. Merle Uudsemaa. Quantum-Chemical Modeling of Solvated First Row Transition Metal Ions. 2006.
51. Tagli Pitsi. Nutrition Situation of Pre-School Children in Estonia from 1995 to 2004. 2006.
52. Angela Ivask. Luminescent Recombinant Sensor Bacteria for the Analysis of Bioavailable Heavy Metals. 2006.
53. Tiina Lõugas. Study on Physico-Chemical Properties and Some Bioactive Compounds of Sea Buckthorn (Hippophae rhamnoides L.). 2006.
54. Kaja Kasemets. Effect of Changing Environmental Conditions on the Fermentative Growth of Saccharomyces cerevisae S288C: Auxo-accelerostat Study. 2006.
55. Ildar Nisamedtinov. Application of 13C and Fluorescence Labeling in Metabolic Studies of Saccharomyces spp. 2006.
56. Alar Leibak. On Additive Generalisation of Voronoï's Theory of Perfect Forms over Algebraic Number Fields. 2006.
57. Andri Jagomägi. Photoluminescence of Chalcopyrite Tellurides. 2006.
58. Tõnu Martma. Application of Carbon Isotopes to the Study of the Ordovician and Silurian of the Baltic. 2006.
59. Marit Kauk. Chemical Composition of CuInSe2 Monograin Powders for Solar Cell Application. 2006.
60. Julia Kois. Electrochemical Deposition of CuInSe2 Thin Films for Photovoltaic Applications. 2006.
61. Ilona Oja Açik. Sol-Gel Deposition of Titanium Dioxide Films. 2007.
62. Tiia Anmann. Integrated and Organized Cellular Bioenergetic Systems in Heart and Brain. 2007.
63. Katrin Trummal. Purification, Characterization and Specificity Studies of Metalloproteinases from Vipera lebetina Snake Venom. 2007.
64. Gennadi Lessin. Biochemical Definition of Coastal Zone Using Numerical Modeling and Measurement Data. 2007.
65. Enno Pais. Inverse problems to determine non-homogeneous degenerate memory kernels in heat flow. 2007.
66. Maria Borissova. Capillary Electrophoresis on Alkylimidazolium Salts. 2007.
67. Karin Valmsen. Prostaglandin Synthesis in the Coral Plexaura homomalla: Control of Prostaglandin Stereochemistry at Carbon 15 by Cyclooxygenases. 2007.
68. Kristjan Piirimäe. Long-Term Changes of Nutrient Fluxes in the Drainage Basin of the Gulf of Finland – Application of the PolFlow Model. 2007.

69. Tatjana Dedova. Chemical Spray Pyrolysis Deposition of Zinc Sulfide Thin Films and Zinc Oxide Nanostructured Layers. 2007.
70. Katrin Tomson. Production of Labelled Recombinant Proteins in Fed-Batch Systems in Escherichia coli. 2007.
71. Cecilia Sarmiento. Suppressors of RNA Silencing in Plants. 2008.
72. Vilja Mardla. Inhibition of Platelet Aggregation with Combination of Antiplatelet Agents. 2008.
73. Maie Bachmann. Effect of Modulated Microwave Radiation on Human Resting Electroencephalographic Signal. 2008.
74. Dan Hüvonen. Terahertz Spectroscopy of Low-Dimensional Spin Systems. 2008.
75. Ly Villo. Stereoselective Chemoenzymatic Synthesis of Deoxy Sugar Esters Involving Candida antarctica Lipase B. 2008.
76. Johan Anton. Technology of Integrated Photoelasticity for Residual Stress Measurement in Glass Articles of Axisymmetric Shape. 2008.
77. Olga Volobujeva. SEM Study of Selenization of Different Thin Metallic Films. 2008.
78. Artur Jõgi. Synthesis of 4'-Substituted 2,3'-dideoxynucleoside Analogues. 2008.
79. Mario Kadastik. Doubly Charged Higgs Boson Decays and Implications on Neutrino Physics. 2008.
80. Fernando Pérez-Caballero. Carbon Aerogels from 5-Methylresorcinol-Formaldehyde Gels. 2008.
81. Sirje Vaask. The Comparability, Reproducibility and Validity of Estonian Food Consumption Surveys. 2008.
82. Anna Menaker. Electrosynthesized Conducting Polymers, Polypyrrole and Poly(3,4-ethylenedioxythiophene), for Molecular Imprinting. 2009.
83. Lauri Ilison. Solitons and Solitary Waves in Hierarchical Korteweg-de Vries Type Systems. 2009.
84. Kaia Ernits. Study of In2S3 and ZnS Thin Films Deposited by Ultrasonic Spray Pyrolysis and Chemical Deposition. 2009.
85. Veljo Sinivee. Portable Spectrometer for Ionizing Radiation "Gammamapper". 2009.
86. Jüri Virkepu. On Lagrange Formalism for Lie Theory and Operadic Harmonic Oscillator in Low Dimensions. 2009.
87. Marko Piirsoo. Deciphering Molecular Basis of Schwann Cell Development. 2009.
88. Kati Helmja. Determination of Phenolic Compounds and Their Antioxidative Capability in Plant Extracts. 2010.
89. Merike Sõmera. Sobemoviruses: Genomic Organization, Potential for Recombination and Necessity of P1 in Systemic Infection. 2010.
90. Kristjan Laes. Preparation and Impedance Spectroscopy of Hybrid Structures Based on CuIn3Se5 Photoabsorber. 2010.
91. Kristin Lippur. Asymmetric Synthesis of 2,2'-Bimorpholine and its 5,5'-Substituted Derivatives. 2010.

92. Merike Luman. Dialysis Dose and Nutrition Assessment by an Optical Method. 2010.
93. Mihhail Berezovski. Numerical Simulation of Wave Propagation in Heterogeneous and Microstructured Materials. 2010.
94. Tamara Aid-Pavlidis. Structure and Regulation of BDNF Gene. 2010.
95. Olga Bragina. The Role of Sonic Hedgehog Pathway in Neuro- and Tumorigenesis. 2010.
96. Merle Randrüüt. Wave Propagation in Microstructured Solids: Solitary and Periodic Waves. 2010.
97. Marju Laars. Asymmetric Organocatalytic Michael and Aldol Reactions Mediated by Cyclic Amines. 2010.
98. Maarja Grossberg. Optical Properties of Multinary Semiconductor Compounds for Photovoltaic Applications. 2010.
99. Alla Maloverjan. Vertebrate Homologues of Drosophila Fused Kinase and Their Role in Sonic Hedgehog Signalling Pathway. 2010.
100. Priit Pruunsild. Neuronal Activity-Dependent Transcription Factors and Regulation of Human BDNF Gene. 2010.
101. Tatjana Knjazeva. New Approaches in Capillary Electrophoresis for Separation and Study of Proteins. 2011.
102. Atanas Katerski. Chemical Composition of Sprayed Copper Indium Disulfide Films for Nanostructured Solar Cells. 2011.
103. Kristi Timmo. Formation of Properties of CuInSe2 and Cu2ZnSn(S,Se)4 Monograin Powders Synthesized in Molten KI. 2011.
104. Kert Tamm. Wave Propagation and Interaction in Mindlin-Type Microstructured Solids: Numerical Simulation. 2011.
105. Adrian Popp. Ordovician Proetid Trilobites in Baltoscandia and Germany. 2011.
106. Ove Pärn. Sea Ice Deformation Events in the Gulf of Finland and This Impact on Shipping. 2011.
107. Germo Väli. Numerical Experiments on Matter Transport in the Baltic Sea. 2011.
108. Andrus Seiman. Point-of-Care Analyser Based on Capillary Electrophoresis. 2011.
109. Olga Katargina. Tick-Borne Pathogens Circulating in Estonia (Tick-Borne Encephalitis Virus, Anaplasma phagocytophilum, Babesia Species): Their Prevalence and Genetic Characterization. 2011.
110. Ingrid Sumeri. The Study of Probiotic Bacteria in Human Gastrointestinal Tract Simulator. 2011.
111. Kairit Zovo. Functional Characterization of Cellular Copper Proteome. 2011.
112. Natalja Makarytsheva. Analysis of Organic Species in Sediments and Soil by High Performance Separation Methods. 2011.
113. Monika Mortimer. Evaluation of the Biological Effects of Engineered Nanoparticles on Unicellular Pro- and Eukaryotic Organisms. 2011.
114. Kersti Tepp. Molecular System Bioenergetics of Cardiac Cells: Quantitative Analysis of Structure-Function Relationship. 2011.

115. Anna-Liisa Peikolainen. Organic Aerogels Based on 5-Methylresorcinol. 2011.
116. Leeli Amon. Palaeoecological Reconstruction of Late-Glacial Vegetation Dynamics in Eastern Baltic Area: A View Based on Plant Macrofossil Analysis. 2011.
117. Tanel Peets. Dispersion Analysis of Wave Motion in Microstructured Solids. 2011.
118. Liina Kaupmees. Selenization of Molybdenum as Contact Material in Solar Cells. 2011.
119. Allan Olspert. Properties of VPg and Coat Protein of Sobemoviruses. 2011.
120. Kadri Koppel. Food Category Appraisal Using Sensory Methods. 2011.
121. Jelena Gorbatšova. Development of Methods for CE Analysis of Plant Phenolics and Vitamins. 2011.
122. Karin Viipsi. Impact of EDTA and Humic Substances on the Removal of Cd and Zn from Aqueous Solutions by Apatite. 2012.
123. David Schryer. Metabolic Flux Analysis of Compartmentalized Systems Using Dynamic Isotopologue Modeling. 2012.
124. Ardo Illaste. Analysis of Molecular Movements in Cardiac Myocytes. 2012.
125. Indrek Reile. 3-Alkylcyclopentane-1,2-Diones in Asymmetric Oxidation and Alkylation Reactions. 2012.
126. Tatjana Tamberg. Some Classes of Finite 2-Groups and Their Endomorphism Semigroups. 2012.
127. Taavi Liblik. Variability of Thermohaline Structure in the Gulf of Finland in Summer. 2012.
128. Priidik Lagemaa. Operational Forecasting in Estonian Marine Waters. 2012.
129. Andrei Errapart. Photoelastic Tomography in Linear and Non-linear Approximation. 2012.
130. Külliki Krabbi. Biochemical Diagnosis of Classical Galactosemia and Mucopolysaccharidoses in Estonia. 2012.
131. Kristel Kaseleht. Identification of Aroma Compounds in Food using SPME-GC/MS and GC-Olfactometry. 2012.
132. Kristel Kodar. Immunoglobulin G Glycosylation Profiling in Patients with Gastric Cancer. 2012.
133. Kai Rosin. Solar Radiation and Wind as Agents of the Formation of the Radiation Regime in Water Bodies. 2012.
134. Ann Tiiman. Interactions of Alzheimer‘s Amyloid-Beta Peptides with Zn(II) and Cu(II) Ions. 2012.
135. Olga Gavrilova. Application and Elaboration of Accounting Approaches for Sustainable Development. 2012.
136. Olesja Bondarenko. Development of Bacterial Biosensors and Human Stem Cell-Based In Vitro Assays for the Toxicological Profiling of Synthetic Nanoparticles. 2012.
137. Katri Muska. Study of Composition and Thermal Treatments of Quaternary Compounds for Monograin Layer Solar Cells. 2012.

138. Ranno Nahku. Validation of Critical Factors for the Quantitative Characterization of Bacterial Physiology in Accelerostat Cultures. 2012.
139. Petri-Jaan Lahtvee. Quantitative Omics-level Analysis of Growth Rate Dependent Energy Metabolism in Lactococcus lactis. 2012.
140. Kerti Orumets. Molecular Mechanisms Controlling Intracellular Glutathione Levels in Baker's Yeast Saccharomyces cerevisiae and its Random Mutagenized Glutathione Over-Accumulating Isolate. 2012.
141. Loreida Timberg. Spice-Cured Sprats Ripening, Sensory Parameters Development, and Quality Indicators. 2012.
142. Anna Mihhalevski. Rye Sourdough Fermentation and Bread Stability. 2012.
143. Liisa Arike. Quantitative Proteomics of Escherichia coli: From Relative to Absolute Scale. 2012.
144. Kairi Otto. Deposition of In2S3 Thin Films by Chemical Spray Pyrolysis. 2012.
145. Mari Sepp. Functions of the Basic Helix-Loop-Helix Transcription Factor TCF4 in Health and Disease. 2012.
146. Anna Suhhova. Detection of the Effect of Weak Stressors on Human Resting Electroencephalographic Signal. 2012.
147. Aram Kazarjan. Development and Production of Extruded Food and Feed Products Containing Probiotic Microorganisms. 2012.
148. Rivo Uiboupin. Application of Remote Sensing Methods for the Investigation of Spatio-Temporal Variability of Sea Surface Temperature and Chlorophyll Fields in the Gulf of Finland. 2013.
149. Tiina Kriščiunaite. A Study of Milk Coagulability. 2013.
150. Tuuli Levandi. Comparative Study of Cereal Varieties by Analytical Separation Methods and Chemometrics. 2013.
151. Natalja Kabanova. Development of a Microcalorimetric Method for the Study of Fermentation Processes. 2013.
152. Himani Khanduri. Magnetic Properties of Functional Oxides. 2013.
153. Julia Smirnova. Investigation of Properties and Reaction Mechanisms of Redox-Active Proteins by ESI MS. 2013.
154. Mervi Sepp. Estimation of Diffusion Restrictions in Cardiomyocytes Using Kinetic Measurements. 2013.
155. Kersti Jääger. Differentiation and Heterogeneity of Mesenchymal Stem Cells. 2013.
156. Victor Alari. Multi-Scale Wind Wave modeling in the Baltic Sea. 2013.